Elisabetta Coppi

Purines as Transmitter Molecules

Electrophysiological Studies on Purinergic Signalling
in Different Cell Systems

Progetto grafico di Alberto Pizarro Fernández

Printed in Italy

A Marco,
per la sua pazienza

Contents

Abbreviations

AD	anoxic depolarization
ADA	adenosine deaminase
ABC	ATP-binding cassette
aCSF	artificial cerebral spinal fluid
ADP	adenosine 5' diphosphate
AFM	atomic force microscopy
AK	adenosine kinase
AMP	adenosine 5' monophosphate
AOPCP	ß-methylene-adenosine diphosphate
Ap4A	diadenosine-tetraphosphate
AR 132	N^6-methyl-2-phenylethynyladenosine
ARC67085	2-propylthio-β,γ-dichloromethylene-D-ATP
AR-C69931MX	N^6-(2-methylthioethyl)-2-(3,3,3-trifluoropropylthio)-β,γ-dichloromethylene ATP
ARL 67156	6-N,N-diethyl-D-β,γ-dibromomethylene ATP
ATL-146	4-{3-[6-Amino-9-(5-ethylcarbamoyl-3,4-dihydroxy-tetrahydro-furan-2-yl)-9H-purin-2-yl]-prop-2-ynyl}-cyclohexanecarboxylic acid
ATP	adenosine 5' triphosphate
ATPγS	adenosine 5'-O-(3-thiotriphosphate)
AUC	area under the curve
αβ-meATP	αβ-methylen ATP
BBG	Brilliant Blue G
BK	Big (conductance) potassium channels
BzATP	2,3-O- (4-benzoylbenzoyl)-ATP
5-Br-UDP	5-bromo-UDP
cAMP	cyclic adenosine monophosphate
CCPA	2-Chloro-N^6-cyclopentyladenosine
CFTR	cystic fibrosis transmembrane conductance regulator
CGS 15943	9-chloro-2-(2-furyl)(1,2,4)triazolo(1,5-c)quinazolin-5-amine
CGS 21680	2-p-(2-carboxyethyl)phenethylamino-5'-N-ethylcarboxamidoadenosine hydrochloride
CHO	Chinese hamster ovary
C.L.	confidential limits
Cl-IB-MECA	1-[2-chloro-6[[(3-iodophenyl)methyl]amino]-9H-purin-9-yl]-1-deoxy-N-methyl-ß-D-ribofuranuronamide
C_m	membrane capacitance
CNS	central nervous system
CNT	concentrative nucleoside transporter
CPA	N6-Cyclopentyladenosine
CP 66713	4-amino [1, 2, 4] triazolo [4, 3a] quinoxaline
CSC	8-(3-chlorostyryl)caffeine

CysLT	cysteinyl-leukotriene
DC	direct current
DPCPX	8-cyclopentyl-1,3-dipropylxanthine
DRGN	dorsal root ganglion neuron
ECoG	cortical electrogram
EGTA	ethylene glycol-bis(β-aminoethylether)N,N,N',N'-tetracetic acid
ENT	equilibrative nucleoside transporter
e5'-NT	extracellular 5'-nucleotidase
GABA	γ-amino-butyric acid
GAP-43	growth-associated protein-43
GIRK	G protein-coupled inwardly rectifying potassium channels
GPCR	G protein-coupled receptors
GRK	GPCR related kinases
fEPSP	field excitatory post-synaptic potential
FGF	fibroblast growth factor
[^{18}F]CPFPX	[^{18}F]8-cyclopentyl-3-(3-fluoropropyl)-1-propylxanthine
HEK cells	human embryonic kidney cells
hMSCs	human mesenchymal stem cells
HSP70	heat shock protein 70
HSP90	heat shock protein 90
IB-MECA	1-deoxy-1-[6-[[(3-iodophenyl)-methyl]amino]-9H-purin-9-yl]-N-methyl-beta-D-ribofuranuronamide
IK	Intermediate (conductance) potassium channels
I_{KCa}	Ca^{2+}-activated K^+ current
I_{KDR}	delayed rectifier K^+ current
IL-1β	interleukin-1β
IMDM	Iscove's modified Dulbecco's medium
INS37217	P^1-(uridine 5')-P^4-(2'-deoxycytidine-5')tetraphosphate
IOS	intrinsic optical signal
ISI	inter-spike interval
KCNQ	canali K+
KGlu	potassium gluconate
KN-62	(1-[N,O-bis(5-isoquinolinesulfonyl)-N-methyl-L-tyrosyl]-4-phenylpiperazine)
KN-04	(N-[1-[N-methyl-p-(5-isoquinolinesulfonyl)benzyl]-2-(4-phenylpiperazine)ethyl]-5-isoquinolinesulfonamide)
KW-6002	(E)-1,3-diethyl-8-(3,4-dimethoxystyryl)-7-methyl-3,7-dihydro-1H-purine-2,6-dione
LPS	lipopolysaccharide
LTD$_4$	leukotriene D4
LTP	long term potentiation
LUF5835	2-amino-4-(3-hydroxyphenyl)-6-(1H-imidazol-2-ylmethylsulfanyl)pyridine-3,5-dicarbonitrile
mAHP	medium afterhyperpolarization potential
mEPSC	miniature excitatory postsynaptic currents
mGluR	metabotropic glutamate receptor
MRE 2029F20	N-benzo[1,3]dioxol-5-yl-2-[5-(2,6-dioxo-1,3-dipropyl-2,3,6,7-tetrahydro-1H-purin-8-yl)-1-methyl-1H-pyrazol-3-yloxy]-acetamide
MRS 1220	9-chloro-2-(2-furyl) [1,2,4]triazolo[1,5-c]quinazolin-5-phenylacetamide
MRS 1523	5-propyl-2-ethyl-4-propyl-3-(ethylsulfanylcarbonyl)-6-phenylpyridine-5-carboxylate
MRS 1706	N-(4-acetylphenyl)-2-[4-(2,3,6,7-tetrahydro-2,6-dioxo-1,3-dipropyl-1H-purin-8-yl) phenoxy]acetamide

MRS 1754	1,3-dipropyl-8-[4-[((4-cyanophenyl)carbamoylmethyl)oxy]phenyl]xanthine
MRS 2179	2'-deoxy-N^6-methyladenosine 3',5'-bisphosphate tetraammonium salt
MRS2211	6-(2'-chloro-5'-nitro-azophenyl)-pyridoxal-α5-phosphate
MRS2279	2-chloro-N^6-methyl-(N)-methanocarba-2'-deoxyadenosine 3',5'-bisphosphate
MRS 2365	(N)-methanocarba-2-methylthio-ADP
MRS2500	2-iodo-N^6-methyl-(N)-methanocarba-2'-deoxyadenosine 3',5'-bisphosphate
MRS2567	1,2-di-(4-isothiocyanatophenyl)ethane;
MRS 2578	1,4-di-[(3-isothiocyanato phenyl)-thioureido]butane
NANC	non-adrenergic non-cholinergic
NBMPR	nitrobenzylthioinosine
NECA	5'-N-ethylcarboxamidoadenosine
NF023	8-(benzamido)naphthalene-1,3,5-trisulphonic acid
NGF	neuronal growth factor
NMDA	N-methyl-D-aspartate
NR1	NMDA receptor subunit 1
NO	Azote monoxyde
NR2A	NMDA receptor subunit 2A
NR2B	NMDA receptor subunit 2B
NMDG	N-methyl-D-glucamine
NTPDase	nucleoside triphosphate diphosphohydrolase
5'-NT	5'-nucleotidase
OGD	oxygen-glucose deprivation
PBS	phosphate buffer solution
PCR	polymerase chain reaction
PKA	protein kinase A
PKC	protein kinase C
PLA_2	phospholipase A_2
PLC	phospholipase C
PLD	phospholipase D
PNS	peripheral nervous system
PPADS	pyridoxalphosphate-6-azophenyl-2',4'-disulfonic acid tetrasodium salt
P/S	penicillin/streptomycin
PSB-601	8-[4-(4-benzylpiperazide-1-sulfonyl)phenyl]-1-propylxanthine
PSVT	paroxysmal supraventricular tachycardia
RB2	reactive blue 2
R_s	series resistance
R_m	membrane resistance
RT-PCR	reverse transcriptase polymerase chain reaction
SAH	S-adenosylhomocystein
SAHH	S-adenosylhomocysteine hydrolase
sAHP	slow afterhyperpolarization potential
SCH 58261	7-(2-phenylethyl)-5-amino-2-(2-furyl)-pyrazolo-[4,3-e]-1,2,4-triazolol[1,5-c]pyrimidine
SD	spreading depression
s.e.	standard error
SK	Small (conductance) potassium channels
Suramin	8-(3-benzamido-4-methylbenzamido)naphthalene-1,3,5-trisulfonic acid
TEA	tetraethyl ammonium
TM	transmembrane domain
TNP-ATP	2'-3'-O-(2,4,6-trinitrophenyl)-ATP
TTX	tetrodotoxin
TRP	transient receptor potential

UDP	uridine 5' diphosphate
UTP	uridine 5' triphosphate
UTPγS	uridine-(O-3-thiotriphosphate)
VDACL	volume -dependent large-conductance anion channels
VIP	vasoactive intestinal polypeptide
VR1	vanilloid receptor 1
VT 72	N^6-methoxy-2-phenylethynyladenosine
VT 158	N^6-methoxy-2-phenylethynyl-5'-N-methylcarboxamidoadenosine,
VT 160	N^6-methoxy-2-(2-pyridinyl)-ethynyl-5'-N-methylcarboxamidoadenosine
VT 163	N^6-methoxy-2-p-acetylphenylethynyl-5'-N-methylcarboxamidoadenosine
VUF 5574	N-(2-methoxyphenyl)-N'-(2-(3-pyridyl)quinazolin-4-yl)urea
WSAB	5-[[(4-pyridyl)amino]carbonyl]amino-8-methyl-2-(2-furyl)-pyrazolo[4,3-e]1 ,2,4-triazolo[1,5-c]pyrimidine hydrochloride
ZM 241385	4-(-2-[7-amino-2-{2-furyl}{1,2,4}triazolo{2,3-a}{1,3,5}triazin-5-yl-amino]ethyl)phenol

Introduction

1. Historical overview

The physiological role of adenosine triphosphate (ATP) has been historically linked to cell metabolism since ATP is a ubiquitous intracellular energy source in a number of enzymatic processes. However, in recent years, ATP has emerged as one of the most versatile molecules of biological systems, being implicated in a variety of cell processes, from platelet aggregation to neurotransmission.

The fact that high-energy phosphate bond containing molecules, such as ATP, which plays such a key role in all aspects of cell function, may also act as an extracellular chemical messenger, was initially met with considerable scepticism. The first evidence about a role for ATP acting at the extracellular level came from the cardiovascular field, with pioneer studies in the '30s demonstrating potent actions of extracellular ATP and adenosine on the heart and coronary blood vessels (Drury *et al.*, 1929). Such effects (negative chronotropic effect on the heart, dilatation of coronary vessels, muscular weakness, ataxia, sleepiness) were very complex and hard to interpreter, involving both peripheral and central mechanisms (for a general overview see: Green *et al.*, 1950).

Additional work was made in the '70s, when a new branch of neurotransmission, other than the classical adrenergic and cholinergic pathways, was discovered in the autonomic nervous system. This kind of neurotransmission, initially called non-adrenergic non-cholinergic (NANC), was firstly described in the guinea-pig taenia coli (Burnstock *et al.*, 1963) as an inhibitory action of an unknown substance in the contractile activity of this intestinal muscle. Later studies described similar NANC effects in different smooth muscles of the digestive and urinary apparata, with both excitatory and inhibitory effects being described (Martinson 1965). Various substances have been initially suggested to mediate NANC neurotransmission (VIP, substance P, NO) but ATP emerged as the most likely candidate since exogenous application of purine derivatives mimicked NANC effects (Burnstock *et al.*, 1970) and a release of ATP was found after stimulation of NANC fibres (Su *et al.*, 1971). From these studies, the term 'purinergic signalling' was firstly introduced in the scientific literature by Burnstock (Burnstock 1972).

At about the same period, the idea that nerve terminals could release more than one neurotransmitter was gaining support, particularly in the autonomic nervous system (Burnstock 1976). This concept seemed to be particularly appropriate to support the hypothesis of purinergic transmission, in fact in those years several studies demonstrated that ATP was co-released with acetylcholine in the bladder (Burnstock *et al.*, 1978) and with noradrenaline in the taenia coli (Su *et al.*, 1971) and in the vas deferens (Westfall *et al.*, 1978).

An implicit concept for sustaining the hypothesis of purinergic neurotransmission proposed in the '70s was the existence of purinergic receptors. The first evidence in this direction suggested the existence of two different subfamilies of such 'purinoceptors', identified as P1 and P2 receptors, selective for adenosine and ATP respectively (Burnstock 1978). This distinction helped clarifying the incredible variety and complexity of purine-mediated effects observed till then and the ubiquitous presence of ecto-ATPases, enzymes catalysing extracellular nucleotides degradation. The presence of these enzyme on cell membranes incredibly complicated the scenario by forming ADP, AMP and adenosine from extracellular ATP (Zimmermann et $al.$, 1998), so that some of the actions of ATP were directly due to P2 receptor activation, whereas others were due to the indirect action of adenosine on P1 receptors.

Both P1 and P2 subfamilies where later recognised to be further divided into different subtypes. P1 receptors were initially distinguished into two classes (A_1 and A_2 receptors) on the basis of their excitatory or inhibitory actions on adenylyl cyclase (van Calker et $al.$, 1979). Later work defined four different subtypes of P1 receptors: A_1, A_{2A}, A_{2B} and A_3 (Fredholm et $al.$, 2001). P2 receptors appeared to be more heterogeneous, with P2T, P2Z and P2U subtypes being proposed from different authors (Gordon 1986; O'Connor et $al.$, 1991). Definitive classification came from Abbracchio and Burnstock (Abbracchio et $al.$, 1994) who proposed that P2 purinoceptors should belong to two major families: P2X ligand-gated ion channel receptors and P2Y G-protein-coupled receptors. Cloning experiments supported this classification and helped subdividing P2 receptors into 7 P2X and 8 P2Y subtypes (King et $al.$, 2002; North 2002).

To date, it is well recognised that purinergic signalling plays a fundamental role in several biological systems, from invertebrates to mammals, and purinergic-mediated effects including both short-term (neurotransmission, endothelial-mediated vasodilatation, platelet aggregation) and long-term (cell proliferation, differentiation, migration and death) phenomenon have been demonstrated.

2. Synthesis, release and catabolism of ATP

The synthesis of ATP, whose molecular structure is shown in figure 1, comprises three independent metabolic pathways. The adenine ring (synthesized from the nucleic acid cycle) and the ribosium molecule (synthesized from glucide metabolism) lead to the formation of the nucleoside adenosine (figure 2), whose metabolism is described in the next section. Successive nucleoside phosphorylations by the enzyme adenylate kinase leads to the synthesis of adenosine mono-, di- and triphosphate (AMP, ADP and ATP) respectively. These enzymatic reactions are characterized by great activation energy, obtained from the oxidation cycle of tricarboxylic acids (citric cycle) of the Krebs cycle, during oxidative phosphorylation (aerobic oxidation) in mitochondria (for a review see: Kalckar 1969). A small amount of ATP is also synthesized in the cytosol during the breakdown of glucose to lactic acid (anaerobic glycolysis).

The ATP, so generated, is mainly used for a number of metabolic processes, from energy supply to phosphate donor in phosphorylation processes, allowing cell survival and contributing to the fine tuned equilibrium of intracellular ATP, ADP, AMP and adenosine that constitute the 'purine pool' of the living cell. Only a small fraction of the intracellular amount of ATP is devolved to purinergic transmission by various mechanisms of release. The intracellular ATP levels are usually kept in the mM range (1-2 mM), whereas extracellular concentrations of adenine nucleotides are scarce, generally

fluctuating in the low nanomolar range, (Melani *et al.*, 2005; Phillis *et al.*, 1993). In fact, nucleosides and nucleotides are hydrophilic molecules whose size and charge impede them from crossing the plasma membrane by simple diffusion (Chaudry 1982; Glynn 1968). For this reason, specialised transport systems are required for their movement into or out of cells.
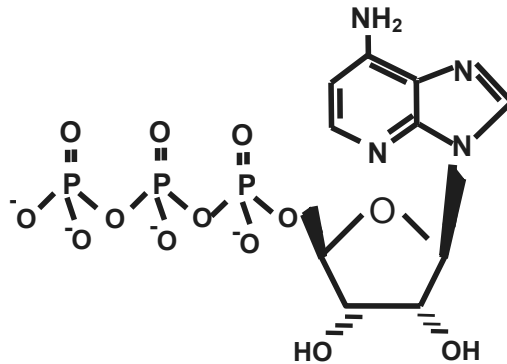
Figure 1. Molecular structure of ATP.

When the 'purinergic hypothesis' was firstly formulated, it was generally assumed that the main source of ATP acting on purinoceptors was damaged or dying cells (Bodin *et al.*, 2001). However, it is now recognized that ATP is released from many cells in a physiological or pathophysiological way in response to specific stimuli by numerous mechanisms, including vesicular exocytosis, voltage-dependent anion channels and connexin hemichannels.

2.1 Vesicular release of ATP

It has been known for a long time that some secretory vesicles of the autonomic nervous system terminals contain, in addition to catecholamine or acetylcholine, large quantities of ATP (Douglas *et al.*, 1966; Dowdall *et al.*, 1974). At first, it was thought that the principal role of ATP present in synaptic vesicles was associated with the supply of energy needed for the storage and the membrane transport of neurotransmitters, or with the process of vesicular exocytosis (Johnson 1987). However, the kinetics of ATP and neurotransmitter release were shown to be of the same magnitude, suggesting that ATP was likely released as a neurotransmitter itself (Silinsky 1975; Zimmermann *et al.*, 1976). For instance, stimulation of the frog motor nerve at the neuromuscular junction implied that ATP was released synchronously together with acetylcholine with a brief latency characteristic of quantal release from synaptic vesicles (Silinsky *et al.*, 1996).

The vesicular release of ATP is typical (even if not exclusive) of neuronal cells, and is triggered by specific stimuli. For example, it is mediated by K^+-induced membrane depolarization (White 1978) in a TTX-sensitive (Kasakov *et al.*, 1988) and Ca^{2+}-dependent way (White *et al.*, 1982). Electrical stimulation of nerve terminals is also able to induce the vesicular release of ATP. It has been demonstrated that brief, high-frequency burst stimulations (100 Hz for 50 ms duration every 2 s for 1 min: to mimic long term potentiation: LTP) of rat hippocampal CA1 pyramidal cells induces a more than nine fold increase in the basal ATP outflow, reaching a maximum 1 minute af-

ter stimulation onset (Cunha *et al.*, 1996). The same authors demonstrated that a prolonged, low-frequency train of stimulations (5 Hz, 900 pulses, to mimic long term depression: LTD) does not produce similar effects on ATP release. These observations suggested a potential role of ATP during intense synaptic activity or synaptic plasticity phenomena, in particular LTP, and this hypothesis has been largely confirmed in the following years (Fujii 2004; Wieraszko 1996).

2.2 Anion channel-mediated release of ATP

Experimental evidence indicates that, in some cases, ATP is released in a non-secretory fashion (Ferguson 1999). Since ATP cannot cross the cell membrane, it has to be assumed that a carrier membrane protein is involved. It is known that most ATP molecules exist in anionic form (ATP^{4-}) at physiological pH, and that a number of Cl^- channels exhibit significant permeability to large organic anions (Strange *et al.*, 1996). Therefore, the possibility exists that some anion channels can also conduct ATP.

Firstly, the cystic fibrosis transmembrane conductance regulator (CFTR) has been reported as a possible candidate for this mechanism. CFTR is a member of the ATP-binding cassette (ABC) protein family, a group of membrane ATPases which can transport various substrates (inorganic anions, amino acids, polysaccharides, sugars and peptides) against their concentration gradient (Saurin *et al.*, 1999). These membrane proteins are cAMP-dependent Cl^- channels which have a fundamental role in promoting osmotic secretion of liquids into the lumen of airways epithelia, and whose impairment causes cystic fibrosis disease. It has been firstly demonstrated that CFTR may also function as an ATP-permeable channel, providing an efficacious mechanism of ATP release in the extracellular space (Reisin *et al.*, 1994). However, the concept that some ABC proteins can transport or release ATP by acting as an ATP channel (the so called "CFTR=ATP channel hypothesis") has been later confuted in a number of studies (Grygorczyk *et al.*, 1996; Li *et al.*, 1996). An alternative explanation for the anion channel-associated efflux of ATP came from studies of swelling-induced ATP release in a murine mammary cell line (C127i). In these cells, hypotonic-induced cellular swelling activates volume- and voltage-dependent large-conductance anion channels (VDACL Cl^- channels) which exhibit significant permeability to large organic anions, such as glutamate and ATP. Patch-clamp studies clearly demonstrated that these Cl^- channels are also permeable to ATP, with a P_{ATP}/P_{Cl} ratio of 0.08–0.1 (Sabirov *et al.*, 2001), which is comparable to the value previously reported for CFTR-expressing cells (P_{ATP}/P_{Cl}=0.1-0.2: Cantiello *et al.*, 1998). These works also clarified why the swelling-induced ATP efflux was inhibited by extracellularly applied Gd^{3+}, which blocks VDACL but not CFTR channels.

2.3 Connexin hemichannel-mediated ATP release

Connexins are membrane proteins assembled in hexamers on the plasma membrane to form a 'connexon'. This structure is a half of a gap junction, which forms a whole gap junction when tied together with an analogous connexon domain on the plasma membrane of an adjacent cell. The main role of gap junctions is electrical coupling between adjacent cells through the so called 'electrical synapse', but they are also permeable to ions and small molecules, such as Ca^{2+}, fluorescent dyes and cAMP. In fact, fluorescent dye fluxes between cells in intact tissues have been used to ascertain the presence of gap junctions on adjacent cells. However, in addition to docking with connexins hexam-

ers in neighbouring cells, connexons may form 'hemichannels' that exist independently within an individual cell. In this case, connexons serve as transmembrane channels linking the cytoplasmic compartment to the extracellular space and providing a pathway for the release of small-sized molecules (Hofer *et al.*, 1998; Zampighi *et al.*, 1999).

The evidence that connexin hemichannels are also permeable to ATP came from studies on primary cultures of mouse astrocytes. Astrocytes, like multiple other cell types, are capable of widespread intercellular communication via propagated increases in intracellular Ca^{2+} concentration in a variety of circumstances, such as mechanical stimuli (Charles *et al.*, 1991). Initial studies identified gap junctions as a pathway for intercellular Ca^{2+} wave propagation, supposing a direct passage of Ca^{2+} ions from one cell to the other (Charles *et al.*, 1992). More recent studies demonstrated that an extracellular signalling pathway, involving ATP release and purinergic receptor activation, is required. In fact, in a recent study (Stout *et al.*, 2002), mechanically-stimulated ATP release in astrocytes was enhanced by the connexin hemichannel activator quinine and by low extracellular Ca^{2+} (a manoeuvre known to induce the opening of hemichannels). In addition, Ca^{2+} waves were blocked by the ATP degradator apyrase and by the selective antagonist of P2 receptors, PPADS (Stout *et al.*, 2002). Successive studies in different kinds of cells (corneal endothelial cells: Gomes *et al.*, 2005a; inner ear: Zhao *et al.*, 2005; human mesenchymal stem cells: Kawano *et al.*, 2006) definitely demonstrated that Ca^{2+} wave propagation is mediated by extracellular ATP released through connexin hemichannels and successive P2 receptor activation. This mechanism engages ATP in a number of developmental processes mediated by intercellular propagation of Ca^{2+} waves, such as neural progenitor stem cell proliferation in the subventricular zone (Weissman *et al.*, 2004) or in the retinal pigmented epithelium (Pearson *et al.*, 2005).

The cessation of ATP signalling is thinly regulated by enzymatic degradation of extracellular nucleotides through membrane-bound ecto-ATPases and ecto-5'nucleotidases. These enzymes, widely expressed by several cell lines, are able to hydrolyze extracellular purines with a very high efficacy, for example the time to eliminate a single quantum of released ATP by ecto-ATPases has been estimated to be between 50 and 100 ms.

Several metabolic pathways are responsible for ATP catabolism. The first step of the reaction is catalyzed by ecto-ATPases, or ecto-nucleoside triphosphate diphosphohydrolases (NTPDases), that hydrolyze a single phosphate group from ATP and ADP leading respectively to ADP and AMP formation. This class of enzymes comprise different isoforms: NTPDase1, 2, 3 (and possibly 8: Sesti *et al.*, 2003) are membrane-bound enzymes responsible for ATP catabolism at extracellular level, whereas NTPDase4,5,6 are soluble cytoplasmic isoforms that dephosphorylate intracellular nucleotides (Zimmermann 2000). NTPDase1 hydrolyzes ATP and ADP equally well, while NTPDase2 and 3 present high and moderate ATP preference, respectively (Muller *et al.*, 2006). Selective inhibitors of these enzymes, such as the ATP analogue ARL 67156 (Crack *et al.*, 1995), have been recently developed since an excellent strategy to potentiate ATP signalling is just inhibiting its catabolism, which also allows the experimenter to distinguish ATP-mediated from adenosine-elicited effects. More selective and potent ecto-ATPase inhibitors have been recently developed by Müller and co-workers (Müller *et al.*, 2006). This class of compounds, polyoxotungstate derivatives, includes different kinds of molecules which can selectively inhibit NTPDase 1, 2, 3, or all of them, with high affinity (K_i in the low micromolar range) without directly binding to P2 receptors. A variant of NTPDase enzymes in ATP catabolism is the ecto-apyrase, which removes two phosphate groups at once from an ATP molecule leading to the formation of AMP and pyrophosphate (PPi).

Successive steps of dephosphorylation are mediated by ecto-5'nucleotidases (e5'-NTs) that finally convert AMP to adenosine (for a general overview see: Zimmermann 1996). Also this class of enzymes possesses soluble cytosolic isoforms responsible for degradation of intracellular purines. E5'-NT are competitively inhibited by the nucleotide analogue AOPCP, that is commonly used to block adenosine formation from extracellular ATP. It should be noted that this compound does not prevent ATP degradation but leads to the accumulation of extracellular ADP, which is itself an agonist at some P2 receptors. Anyway, AOPCP is a useful tool for separating P2 from P1-mediated actions. NTPDase activity is enhanced by either Ca^{2+} or Mg^{2+}, whereas e5'-NT is inhibited by extracellular ATP and ADP.

All these enzymes can catalyze the hydrolysis of purines with a very high efficacy, but they also possesses a lower affinity for a variety of other nucleotides, such as pyrimidines (UTP, UDP, UMP), that may function as substrates as well (Zimmermann 1996).

Several studies (James et al., 1993; Torres et al., 1990; Zimmermann 1986) demonstrated that the extracellular rate of ATP and ADP hydrolysis (operated by NTP-Dases1,2,3 and apyrase) is higher than that of AMP hydrolysis (catalyzed by e5'-NT). In fact, it has been reported that the $T_{1/2}$ for ATP conversion to adenosine is approximately 200 ms, and the last step in this pathway (transformation of AMP to adenosine by e5'NT) seems to be the rate-limiting step (Dunwiddie et al., 1997b). Thus, ATP half-life in the extracellular space is very short, in the range of a few ms, whereas AMP is a more long-lived molecule.

3. Synthesis, release and catabolism of adenosine.

The synthesis of adenosine is strictly linked to ATP metabolism, since ADP, AMP and adenosine are all products of ATP breakdown.

As shown in figure 2, intracellular adenosine is generated from AMP by intracellularly localized 5'-nucleotidases (5'-NTs; a family of numerous enzyme isoforms) (Schubert et al., 1979) and from S-adenosylhomocysteine (SAH) by cytoplasmic S-adenosylhomocysteine hydrolase (SAHH) (Broch et al., 1980). Adenosine catabolism is due to the enzymes adenosine deaminase (ADA) and adenosine kinase (AK), which lead to the formation of inosine and AMP, respectively (for a review see: Borowiec et al., 2006).

Adenosine synthesis from AMP is strictly dependent on the energy balance of the cell. In fact, 5'-NT is inhibited by ATP itself and possesses a high affinity for the substrate AMP. For this reason, when the cell is supporting a high metabolic activity with a great breakdown of ATP and production of its catabolite AMP, the enzyme 5'-NT is in the ideal conditions to work, encountering a high concentration of the substrate (AMP) and a low level of the inhibitor (ATP) (Meghji et al., 1993). As a consequence, adenosine synthesis is greatly enhanced during periods of elevated metabolic activity or low energy supply, such as epileptic seizures or hypoxic and ischemic conditions. In agreement with these observations is the fact that adenosine appears to play a pivotal role in balancing energy supply with energy demand in cell systems and has been termed a 'retaliatory metabolite'.

Adenosine formation from SAH is only relevant in peripheral tissues (for example in the heart), whereas the low level of the enzyme SAHH in the central nervous system (CNS) is responsible for the small contribute of this reaction to the final intracellular concentration of adenosine (Latini et al., 1995).
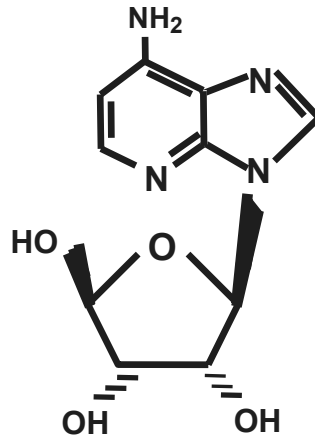
Figure 2. Molecular structure of adenosine.

As already mentioned for ATP, adenosine itself is a hydrophilic molecule that cannot cross the plasma membrane. There are two pathways by which adenosine can gain access to the extracellular compartment: it can be released through specific membrane transporters, or it can be synthesized directly in the extracellular milieu from ATP catabolism operated by membrane ecto-nucleotidases and ecto-ATPases. A third possibility would be the exocytotic release of adenosine. However, partly due to technical reasons, the presence of adenosine in vesicles has yet to be proven.

3.1 Adenosine release

Bi-directional nucleoside transporters contribute to the fine-tuning of extracellular concentrations of adenosine in the vicinity of adenosine receptors. Two classes of such molecules have been described: equilibrative nucleosides transporters (ENTs) and concentrative nucleosides transporters (CNTs). The first class consists of facilitated diffusion of adenosine on the basis of its concentration gradient, without energy consumption, and is selectively blocked by nitrobenzylthioinosine (NBMPR) and dipyridamole. The second class of adenosine transporters takes advantage of the Na^+ concentration gradient across the cell membrane to transport adenosine against its concentration gradient. This mechanism is called Na^+-dependent concentrative nucleoside transport (for a general review see: Griffith *et al.*, 1996).

The fact that nucleoside transport inhibitors, for example dipyridamole (Phillis *et al.*, 1979) or low temperature (Dunwiddie *et al.*, 2000), generally potentiate the actions of extracellular adenosine demonstrates their predominant reuptake function. In fact, the main role of both classes of nucleoside transporters is to rapidly clear adenosine once generated into the extracellular milieu (Baldwin *et al.*, 2004; Kong *et al.*, 2004).

It has been demonstrated that hypoxic conditions down-regulate dipyridamole-sensitive adenosine transporters (ENT1/2) thus increasing adenosine half-life in the extracellular space (Eltzschig *et al.*, 2005). This mechanism may contribute to the enhancement of extracellular adenosine concentrations, in concert with its augmented synthesis operated by intracellular 5'-NT previously described, during hypoxic-ischemic conditions.

3.2 Synthesis of adenosine at extracellular level

Adenosine synthesis can take place directly at the extracellular level, through the hydrolysis of extracellular ATP operated by NTPDases and e5'-NTs, as already described. Hence, these enzymes have a dual function in modulating purinergic neurotransmission: i) they rapidly interrupt ATP-mediated signalling by degrading extracellular nucleotides; ii) they synthesise extracellular adenosine, which activates P1 receptors. The increased adenosine concentrations reported in the extracellular space during pathological conditions and cell damage are likely due to increased release from the intracellular compartment, but may also arise from conversion of extracellular ATP to adenosine by NTPDases and e5'-NTs. In this regard, it has been suggested that the close spatial correlation between adenosine P1 receptors and e5'-NTs suggests that the adenosine formed from ATP at the extracellular level may be of greater physiological relevance than the released nucleotide itself (Cunha *et al.*, 1998). However, how much the released ATP contributes to the adenosine concentration in the extracellular milieu still needs to be clarified.

A schematic illustration of adenosine and ATP metabolic pathways is depicted in figure 3.

Figure 3. Metabolic pathways of purines nucleotides and nucleosides and the different mechanisms of release.

Purinergic receptors

Purinergic receptors are subdivided into P1 and P2 receptors on the basis of their agonist profile: P1 receptors are activated by the adenine nucleoside (adenosine) while P2 receptors are activated by purine and pyrimidine nucleotides (ATP, ADP, UTP and UDP) (for a general review see: Ralevic and Burnstock 1998).

1. P1 receptors

Molecular cloning and pharmacological studies have identified four subtypes of adenosine P1 receptors: A_1, A_{2A}, A_{2B} and A_3 receptors (Fredholm *et al.*, 2001). All of them have already been cloned at least from rat, mouse and human. Structural data report a close similarity between adenosine receptors of the same subtype among mammalian species, excepte for A_3 receptors. This subtype is the most recently discovered one, being cloned only in the last 15 years (Zhou *et al.*, 1992), and presents the largest variability. For instance, almost 30% difference in the amino acid sequence is found between humans and rats (Fredholm *et al.*, 2001).

All P1 receptors are metabotropic GPCR. Hence, A_1 and A_3 subtypes are associated with G_i activation, adenylyl cyclase inhibition and decrease of intracellular cAMP levels, while A_{2A} and A_{2B} receptors are linked to G_s proteins that activate the same enzyme increasing cAMP concentration in the cytosol. However, adenosine receptors have also been reported to couple to other G-proteins than G_s modulating different second messenger systems (see table 1). For instance, in addition to their effects on adenylate cyclase (and contrary to adenosine A_{2A} receptors) adenosine A_1, A_{2B} and A_3 receptors are also characterized by their stimulatory effect on phospholipase C (PLC) (Abbracchio *et al.*, 1995a; Feoktistov *et al.*, 1997). Furthermore, A_1 and A_3 receptors can also activate phospholipase D (PLD) (Fredholm *et al.*, 2001). Several types of Ca^{2+} and K^+ channels are also activated (either by a direct G protein-channel interaction or by second messenger systems) after adenosine receptor stimulation, such as the inward rectifier GIRK channel Kir3.0 that is positively modulated by adenosine A_1 receptor activation (Takigawa *et al.*, 2002).

A_1 and A_{2A} receptors present a particularly high affinity for the endogenous ligand, being activated by nanomolar concentrations of adenosine. On the other hand, the affinity values of A_{2B} and A_3 receptors for adenosine in binding experiments are higher than 1 μM (Fredholm *et al.*, 2001). For this reason, A_{2B} and A_3 subtypes are also called "low affinity receptors". Under physiological conditions, extracellular adenosine concentrations are estimated to be in the range of 30 to 200 nM (see: Latini *et al.*, 2001). These levels are sufficient to activate A_1 and A_{2A} subtypes, but not "low affinity" A_{2B} and

A_3 receptors, which require higher concentrations of adenosine to be activated. Such concentrations are only reached under pathological conditions, such as during hypoxia or ischemia *in vivo* (Pedata *et al.*, 2001) and *in vitro* (Latini *et al.*, 1999b). Contrary to A_1 and A_{2A} subtypes, both human and rat A_3 receptors are quickly desensitised by a few minutes of agonist exposure (Palmer *et al.*, 1995; Trincavelli *et al.*, 2002a; Trincavelli *et al.*, 2002b).

Table 1. Characteristics and distribution of adenosine receptor subtypes in the CNS

Receptor subtypes	G-protein	G-protein coupling effect	Adenosine affinity	Distribution
A_1	$G_{i\,1/2/3}$	$\downarrow$ cAMP	3-30 nM	High levels in cortex, hippocampus, cerebellum. Intermediate levels in striatum and thalamus
		$\uparrow$ PLC, IP_3/DAG		
		$\uparrow$ Arachidonato, PLA_2		
		$\uparrow$ PLD		
	G_o			
A_{2A}	G_s	$\uparrow$ cAMP	1-20 nM	High levels in striatum, nucleus accumbens and olfactory tubercle. Low levels in cortex and hippocampus
	G_{olf}	$\uparrow$ cAMP		
	$G_{15/16}$	$\uparrow$ IP_3		
A_{2B}	G_s	$\uparrow$ cAMP	5-20 μM	Low level
	$G_{q/11}$	$\uparrow$ PLC, IP_3/DAG, $\uparrow$ PLD		
A_3	$G_{i2/3}$	$\downarrow$ cAMP	>1 μM	Widespread distribution. Higher levels in rat hippocampus and cerebellum.
	$G_{q/11}$	$\uparrow$ PLC, IP_3/DAG $\uparrow$ PLD		

Taken from: Fredholm et al., 2001; von Lubitz 1999.

2. Pharmacology of P1 receptors

Since adenosine receptors have been studied for a long time, there are several useful pharmacological tools available at present. Numerous adenosine analogues have been developed that selectively bind one of the four different subtypes of P1 receptors. In human, rat and mouse tissues, the A_1 full agonist CCPA (and to a lesser extent CPA) and the antagonist DPCPX are highly selective compounds active at nanomolar concentrations. Allosteric enhancers for this receptor subtype (such as PD81723 and analogues) are also available and increase the agonist binding and its effects (Bruns *et al.*, 1990; van der Klein *et al.*, 1999).

NECA was long considered to be a selective A_2 agonist but it has been largely demonstrated that it is an unselective agonist at all P1 receptors, only slightly preferring

A_{2A} subtypes (Fredholm *et al.*, 2001). However, based on evidence that 2-substitution of NECA molecule increased selectivity, CGS 21680 was developed as an A_{2A} selective agonist (Hutchison *et al.*, 1989). This compound is less potent and selective in humans than in rats (Kull *et al.*, 1999), but it has been replaced by another recently developed A_{2A} agonist, ATL-146, which is 50 fold more potent than CGS 21680 at the human receptor (Rieger *et al.*, 2001). Among the numerous A_{2A} antagonists, the most selective so far are SCH 58261 and the structurally related ZM 241385 (Poucher *et al.*, 1995).

Potent A_{2B} agonists with affinity values in the low nanomolar range have been lacking till recently, when a new class of non-adenosine compounds (pyridine derivatives) has been synthesised by Beukers and colleagues (Beukers *et al.*, 2004). Among them, LUF5835 is a full agonist with an EC_{50} of 10 nM at human A_{2B} receptor expressed in CHO cells. Unfortunately, its selectivity towards A_1 and A_{2A} receptors is not adequate to discriminate between them in native tissues. The situation is somewhat more favourable for antagonists, as some potent and relatively selective compounds have been found among anilide derivatives of xanthines with K_i values in the low nanomolar range, such as MRS 1754 (Ji *et al.*, 2001), that is over 200-fold selective for A_{2B} versus all other P1 receptors (Kim *et al.*, 2000). Another useful compound is MRE 2029F20, that acts as an inverse agonist to block A_{2B} receptors (Varani *et al.*, 2005). Finally, the more recently synthesised A_{2B} antagonist is PSB-601 (Yan *et al.*, 2006), a sulfophenylxanthine exhibits a K_i value of 3.6 nM for the human A_{2B} receptor combined with high selectivity versus the other human adenosine receptor subtypes (575-fold versus A_1, 134-fold versus A_{2A}, and >278-fold versus A_3).

An emblematic feature of the adenosine A_3 receptor, the most recently discovered one, is its insensitivity to the antagonistic actions of methylxanthines, such as caffeine and theophylline, the traditional blockers of adenosine receptors (Fredholm 1995). Hence, most A_3 antagonists are dihydropyridines, pyridines and flavonoids (Baraldi *et al.*, 2000). Another class of highly selective compounds are isoquinoline and quinazoline derivatives, such as VUF5574 that presents a K_i value of 4 nM versus human A_3 receptors but not versus the rat isoform (Muijlwijk-Koezen *et al.*, 2000). In this regard, it is worth noticing that significant species differences in the affinity of adenosine A_3 receptor antagonists have been noted, as expected from the high structural inter-species variability already mentioned. The affinity values of several A_3 blockers are typically more than 100-fold greater on human than rat receptors, as described for MRS 1220. The unique rat-selective compound is the A_3 agonist MRS 1523. In contrast, the affinity of the most widely used A_3 agonist, Cl-IB-MECA, does not vary beyond an order of magnitude between the species examined, at least among mammals. The high affinity (low nanomolar range) and selectivity (more than 100-fold versus A_1 and A_{2A} receptors) of this compound towards A_3 receptors turns it into the most used pharmacological tool for investigating A_3-mediated effects (Jeong *et al.*, 2003).

3. Distribution of P1 receptors.

Receptor distribution provides helpful information on whether the endogenous agonist will exert significant effects in the intact organism. Thus, in this case, the rather low levels of adenosine present under basal physiological conditions and the 3-fold difference in receptor affinity for the agonist between the four P1 subtypes might suggest adenosine acts as a tonic modulator of normal cell functions or whether its role only becomes relevant during pathological conditions. As reported in table 1, the highest levels of adenosine A_1 receptors are present in the CNS (Dixon *et al.*, 1996) with well

known regional distributions (Schindler *et al.*, 2001) that will be examined in detail. High levels are also found in adrenal glands, eye and atria. Intermediate levels are also found in skeletal muscles, liver, kidney, adipose tissue, gastrointestinal smooth muscles and bronchi. Lung and pancreas present low level of A_1 receptor expression (Fredholm *et al.*, 2001).

A_{2A} receptors are highly present in spleen, thymus, immune cells (leukocytes and granulocytes) and platelets. Lower levels are also found in the heart, lung and blood vessels. A_{2B} subtype is particularly abundant in the gastrointestinal tract, mainly in caecum, colon and urinary bladder. Other regions are lung, blood vessels and adipose tissue.

The A_3 subtype is mainly found in rat testis (Meyerhof *et al.*, 1991) and mast cells, in accordance with the fact that for a long time the unique role assigned to this receptor have been mast cell degranulation and histamine release. Intermediate levels are also found in the lung, spleen, thyroid and liver (Linden *et al.*, 1993; Salvatore *et al.*, 1993). Low levels of A_3 receptors are found in the brain (Dixon *et al.*, 1996), as described below.

3.1 Central Nervous System (CNS)

There is much information on the distribution of the A_1 and A_{2A} receptors in the brain because excellent pharmacological tools, including radioligands, are available to exactly localise protein expression on cell membranes. In the case of A_{2B} and A_3 data are less impressive, and mostly related on the expression of the corresponding mRNAs that do not provide any information about the sub cellular districts of receptor distribution. It is true that mRNA expression and protein distribution often co localize, but occasionally do not exactly match. For example, in several brain regions, mRNA expression cannot be obviously detected even in areas where immunostaining for the receptor protein is observed. This is frequently due to the specialised expression of receptor proteins at nerve terminals, the protein synthesis taking place in the cell soma sometimes quite remote from the presynaptic region.

As already mentioned, the highest levels of A_1 receptor expression are found in the CNS, suggesting a particularly important role of adenosine in brain functions. Recently, by using [^{18}F]8-cyclopentyl-3-(3-fluoropropyl)-1-propylxanthine ([^{18}F]CPFPX) and PET imaging, A_1 receptors were quantified in the human CNS (Meyer *et al.*, 2005). The highest expression of A_1 receptors has been found in the cortex, hippocampus, cerebellum and dorsal horn of the spinal cord; intermediate levels in basal ganglia structures including the striatum (mRNA encoding A_1 receptors is present in large striatal cholinergic interneurones: (Dixon *et al.*, 1996) globus pallidus, subthalamic nucleus and thalamus (Fredholm *et al.*, 2001). An abundant expression of the adenosine A_1 receptor protein also occurs in the trigeminal ganglia, a finding supporting a role of this receptor in pain regulation (Schindler *et al.*, 2001). Neuronal A_1 receptors are localized both pre- and postsynaptically (Deckert *et al.*, 1988). In the hippocampus, a brain area in which A_1 receptors are abundant, subcellular analysis of nerve terminals revealed that A_1 receptor immunoreactivity is strategically located in the active zone of presynaptic terminals, as expected on the basis of the ability of A_1 receptor agonists to depress neurotransmitter release. It has also been demonstrated that A_1 receptor immunoreactivity is evident at postsynaptic sites together with NMDA receptor subunits NR1, NR2A and NR2B and with N-and P/Q-type calcium channel immunoreactivity, emphasizing the importance of A_1 receptors in the control of dendritic integration (Rebola *et al.*, 2003). A_1 receptors

can be found also extrasynaptically on dendrites (Rivkees *et al.*, 1995) and on the axonal fibres of the hippocampus (Swanson *et al.*, 1995). Activation of A_1 receptors along the axon may be a powerful extrasynaptic mechanism by which adenosine alters axonal electric transmission to inhibit neurotransmitter release (Swanson *et al.*, 1995).

A_{2A} receptors are principally located in the basal ganglia: in the caudate-putamen, nucleus accumbens and olfactory tubercle (Jarvis *et al.*, 1989; Rosin *et al.*, 1998). In particular, this receptor subtype is expressed on striatopallidal GABAergic-enkephalin neurones (where it co-localises with dopamine D_2 receptors), but not on GABAergic-dynorphin striatal neurones (Fredholm *et al.*, 2003). In the striatum the A_{2A} receptor gene is found to a lesser extent also in large striatal cholinergic interneurones (Dixon *et al.*, 1996). A minor density of A_{2A} receptor mRNA has been identified also in hippocampus and cortex (Cunha *et al.*, 1994; Dixon *et al.*, 1996). Besides postsynaptically, A_{2A} receptors are also located presynaptically on different GABAergic, cholinergic, glutamatergic neurone types, although to a lesser extent (Hettinger *et al.*, 2001; Rosin *et al.*, 2003). In recent years, particular interest has been dedicated to study receptor dimerization, either in homomeric and heteromeric structures, since this phenomenon seems to frequently occur in numerous cell types and can modify the pharmacological profile of receptors and their functional role. Various lines of evidence indicate that such an interaction occurs in the striatum between A_{2A} adenosine and D_2 dopamine receptors, which usually co-localize in this brain region. This heterodimerization inhibits D2 receptor functions (Ferrè *et al.*, 1991), leading to co-aggregation and co-internalization of both proteins as a result of long-term exposure to A_{2A} or D_2 agonists (Hillion *et al.*, 2002).

Both A_1 and A_{2A} receptors are expressed in the brain not only in neurones but also on microglial cells (Fiebich *et al.*, 1996), astrocytes (Biber *et al.*, 1999; Lee *et al.*, 2003), blood cells and vasculature (Phillis 2004).

The distribution of A_{2B} and A_3 adenosine receptors in the CNS has been difficult to determine since central levels of mRNAs encoding these two adenosine receptors are extremely low, even below the detection limits of *in situ* hybridisation techniques. The more sensitive RT-PCR method was then successfully applied to this issue (Dixon *et al.*, 1996).

A_{2B} receptors are ubiquitously distributed in the brain and their mRNA has been detected in all rat cerebral areas studied (Dixon *et al.*, 1996; von Lubitz 1999). Up to now, it has been difficult to relate A_{2B} receptors to specific physiological responses because of the paucity of A_{2B} selective agonists or antagonists.

The expression level of A_3 adenosine receptor in the brain is generally lower than that of the other subtypes (Ji *et al.*, 1994) and is highly species-dependent (Fredholm *et al.*, 2000; Fredholm *et al.*, 2001). A_3 receptors are found in both neuronal and non-neuronal elements, i.e. astrocytes, microglia, and vasculature of the cerebral tissue (Zhao *et al.*, 1997) with widespread distribution. However, in the rat, a significant expression of A_3 receptors is found in cerebellum and hippocampus (De M *et al.*, 1993; Dixon *et al.*, 1996) where they are mainly expressed at the presynaptic level (Lopes *et al.*, 2003).

4. P2 receptors

Extracellular P2 receptors are divided into two main classes based on whether they are ligand-gated ion channels (P2X) or G-protein coupled receptors (P2Y) (for a review see: Ralevic and Burnstock 1998).

The lack of highly-selective agents or reliable radioligand binding assays for the characterization of P2 receptors, in comparison to the relatively more defined adenosine receptor field, has led to difficulty in discriminating between the different P2X and P2Y receptor subtypes. Only recently, advantage has been taken from new highly selective molecules and markers able to discern at least between some of the different P2 receptor subtypes, such as $P2Y_1$ (Houston *et al.*, 2006), $P2X_7$ (Romagnoli *et al.*, 2004) and $P2X_3$ and $P2X_{2/3}$ (Jarvis *et al.*, 2004).

5. P2X receptors

In the mid '90s, seven different genes encoding P2X receptors ($P2X_{1-7}$) were identified in vertebrates (Brake *et al.*, 1994; Valera *et al.*, 1994). They encode for seven different subunits of P2X receptors that share 40-50% identity in amino acid sequences (for a review see: North *et al.*, 2000). Each subunit (composed of between 379 to 595 amino acids residues) comprises two hydrophobic transmembrane domains, separated by a large extracellular loop (about 280 amino acids) containing the ligand-binding region (Jiang *et al.*, 2000b). Both -NH2 and -COOH termini are cytoplasmic (Brake *et al.*, 1994). A striking feature among $P2X_{1-7}$ subunits is the presence of 10 conserved cysteine residues in the extracellular loop that could be oxidized to form disulfide bonds contributing to the tertiary structure of the protein (Ennion *et al.*, 2002). In addition, all P2X subunits contain consensus sequences for *N*-linked glycosylation processes (Asn-X-Ser/Thr) that are essential for receptor trafficking to the cell surface (Torres *et al.*, 1998a).

From the described structure it seemed unlikely that the two transmembrane domains (TM) of a single P2X subunit would be able to form an ion-conducting pore on their own and suggested that subunits associate to form multimeric channels. In fact, it has been confirmed that the assembly of three or six subunits (as homomers or heteromers) builds up a functional nucleotide receptor channel (Lewis *et al.*, 1995). No crystal structure of P2X receptors is available at present, but recent studies using atomic force microscopy (AFM) and electron microscopy of purified $P2X_2$ receptors gave us the first pictures of the receptors (Barrera *et al.*, 2005). On the basis of this and other studies (Mio *et al.*, 2005: see also figure 3) the 'trimeric hypothesis', which is also consistent with a model of three ATP molecules binding to describe channel opening reported in previous works (Bean 1990; Bean *et al.*, 1990; Ding *et al.*, 1999), is prevailing.

A schematic example of the molecular structure of a single subunit and of trimeric assembly of P2X receptors is shown in figure 4.

Once the multimeric conformation of P2X receptors was confirmed, studies of coimmunoprecipitation with epitope-tagged subunits transfected in HEK293 cells showed that $P2X_2/P2X_3$, $P2X_4/P2X_6$ and $P2X_1/P2X_5$ may co-assemble to form heteromers (Torres *et al.*, 1998b). Recent investigations employing different recombinant systems gave evidence for several novel P2X receptor phenotypes: $P2X_{1/2}$ (Brown *et al.*, 2002b), $P2X_{1/4}$ (Nicke *et al.*, 2005) and $P2X_{2/6}$ (King *et al.*, 2000). In contrast, $P2X_7$ has the unique characteristic to be only found in homomeric structures (Torres *et al.*, 1999), while $P2X_6$ receptors appear only to assemble in heteromeric channels, with no described functional homomeric structures being described (Soto *et al.*, 1996).

The permeability of some P2X receptors presents peculiar characteristics since it changes during prolonged agonist application. In fact, some P2X receptors show pore dilation during prolonged agonist exposure as evidenced by a progressive increase in

their permeability to large organic cations, including NMDG, Tris, and TEA (Virginio *et al.*, 1999). Such phenomenon, described for $P2X_2$, $P2X_{2/3}$, $P2X_4$ and, most of all, for $P2X_7$ receptors, is probably due to the existence of several open conformation states (Stojilkovic *et al.*, 2005). The $P2X_2$ dilated pore reverts to its closed state within 2 s after agonist removal (Virginio *et al.*, 1999). On the contrary, permeabilization induced by prolonged $P2X_7$ receptor stimulation seems to be an irreversible process, usually followed by membrane blebbing and cell death (Klapperstuck *et al.*, 2000). For this reason, the $P2X_7$ subtype was named 'cytolytic P2Z receptor' when firstly described in macrophages and lymphocytes (Surprenant *et al.*, 1996). The mechanism of pore formation during prolonged agonist exposure is still unclear, and options vary between decreased filter selectivity of existing channels (Smart *et al.*, 2002) to formation of oligomers and rearrangement of receptors into new molecular complexes (Kim *et al.*, 2001).
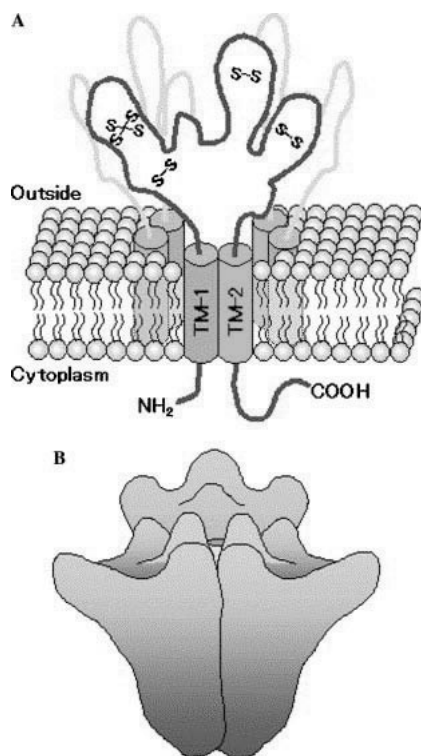
Figure 4. Structural model of the $P2X_2$ receptor. A. Membrane topology of the $P2X_2$ receptor. Each subunit is proposed to have two transmembrane domains (TM-1 and TM-2) with a cysteine rich large extracellular domain. Three subunits are combined to form a functional channel. The marks of S–S indicate putative disulfide bonds. B. Schematic drawing of the $P2X_2$ receptor model. Three subunits form an inverted three-sided pyramidal structure with a crown-shaped outer surface. Taken from: Mio et al., 2005.

Electrophysiological and pharmacological properties of P2X ligand gated cation channels are strictly dependent on the subunit composition of the receptor. Studies on recombinant homomeric P2X receptors have been used to characterise the general profile of single homomeric assemblies to avoid complications arising from expression of

and association with different subunits encountered in native tissues (North 2002). The typical P2X-mediated current evoked at a resting membrane potential ($\sim$ -60 mV) is an inward Na^+ and Ca^{2+} current with single-channel conductances in the range of 18-50 pS (North 2002) and 27 pS (Poletto Chaves *et al.*, 2006). The reversal potential is around 0 mV (typical of non-specific cation permeable channels) and, at positive potentials, an outward current prevails that is mainly due to the outflow of K^+ ions. The total current-voltage (I-V) plot of the majority of P2X receptors is characterized by a marked inward-rectification, but linear I-V relationships have also been described (especially for P2X$_7$ receptors), depending on different subunit composition and cell expression systems (Evans *et al.*, 1996).

Another parameter commonly used to distinguish the different P2X receptor subunits is the rate of deactivation (the kinetics of current decay evoked by washout of the agonist) and desensitization (the current decay evoked by prolonged agonist application) (Stojilkovic *et al.*, 2005). P2X$_1$ and P2X$_3$ are called 'fast desensitizing P2X receptors' because they undergo rapid desensitization, on the order of hundreds of milliseconds, with an extremely slow recovery time course ($\geq$ 5 min) (Rettinger *et al.*, 2003). On the other hand, P2X$_2$, P2X$_4$ and P2X$_{2/3}$ are called 'slow desensitizing P2X receptors' since they show relatively sustained responses to 1–2 s applications of the agonist (Roberts *et al.*, 2006). Other heteromeric channels comprise responses with both fast and slow components, while P2X$_7$ receptors do not show desensitization at all (Ralevic *et al.*, 1998). The deactivation rate is equally fast (on the order of a few ms) for all P2X receptors, except for those undergoing pore dilation after prolonged agonist exposure (P2X$_{2,4,7}$) as already described. The recombinant P2X$_6$ subunit is poorly expressed in heterologous systems and probably does not form functional homomeric channels in vivo (Torres *et al.*, 1999). For this reason it is also called a "silent subunit" (North 2002).

These properties are summarized in figure 5.

Many P2X-mediated currents are influenced by extracellular pH and divalent cation concentration. For example, Zn^{2+}, Mg^{2+} and Ca^{2+} can enhance or decrease the agonist-activated current of different P2X receptor assemblies, depending on their subunit composition (North 2002). These properties are summarized in table 2.
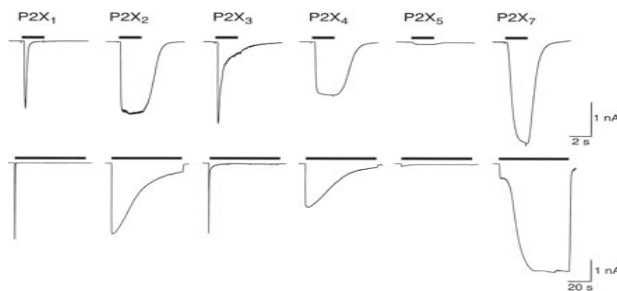
Figure 5. Fast (top) and slow (bottom) desensitization compared for homomeric rat P2X receptors transfected in HEK293 cells 48 h before whole cell recordings. Note the different time scale between upper and lower panels. Fast desensitization is observed only with P2X$_1$ and P2X$_3$: brief applications (2 s duration) of ATP (30 μM, except 1 mM for P2X$_7$). Slow desensitization is observed for P2X$_2$ and P2X$_4$: more prolonged applications (60 s duration) of ATP (30 μM, except 1 mM for P2X$_7$). Taken from: North 2002.

Table 2: Properties of P2X-mediated currents.

Receptor	Ca^{2+}	Mg^{2+}	Zn^{2+}	Cu^+	H^+	Desensitization	Pore dilation
$P2X_1$	No effect >100 mM	—	—	—	Decrease $pK_a \approx 6.3$	Fast	No
$P2X_2$	Decrease 5 mM	—	Increase 20 μM	Increase 16 μM	Increase $pK_a \approx 7.3$	Slow	Yes
$P2X_3$	Decrease 90 mM	—	—	—	Decrease $pK_a \approx 6.0$	Fast	No
$P2X_4$	—	—	Increase 2 μM	No effect to 50 μM	Decrease $pK_a \approx 7.0$	Slow	Yes
$P2X_5$	Decrease	—	Increase	—	No effect	Slow	No
$P2X_6$	—	—	—	—	—	Slow	No
$P2X_7$	Decrease 3 mM	Decrease 500 μM	Decrease 10 μM	Decrease 0.5 μM	Decrease $pK_a \approx 6.1$	Slow	Yes, irre-versible
$P2X_{2/3}$	Decrease 15 mM	—	—	—	Increase $pK_a \approx 7.3$	Slow	—
$P2X_{1/5}$	No effect	—	—	—	Decrease	Fast / slow	No
$P2X_{4/6}$	—	—	Increase	—	—	Slow	—

Values reported in each column are the concentrations that decrease by 50% (pKa in the case of hydrogen) or cause 50% of the maximal increase in response to ATP. Taken from: Roberts et al., 2006. The last two columns show the desensitization and permeation characteristics of P2X-mediated currents, and are taken from North et al., 2000. A dash signifies that these conditions have not been studied for that receptor.

Upon activation by extracellular ATP, a channel comprised of P2X receptor sub-units opens and allows cations to move across the plasma membrane, resulting in changes in the electrical potential of the cell that, in turn, propagates a signal. This flux of ions across the plasma membrane has important signalling functions, especially in impulse propagation in the nervous system and in muscle contractility, where the activation of P2X receptors also generates global Ca^{2+} fluxes (Ca^{2+} permeates the channel pore) by depolarizing cells and facilitating voltage-sensitive Ca^{2+} influx (He *et al.*, 2003; Koshimizu *et al.*, 2000). In fact, P2X receptor activation causes the accumulation of Ca^{2+} ions in the cytoplasm, which is responsible for activating numerous signalling molecules with a slower time course (Erb *et al.*, 2006). In non-excitable cells, Ca^{2+} influx through the pore represents the main mechanism by which P2X receptors modulate cellular functions, such as secretion (Stojilkovic *et al.*, 2005). Thus, generally speaking, Ca^{2+} influx through the plasma membrane channels and its diffusion within the cell provides an effective mechanism by which P2X receptors control numerous cellular functions in different cellular compartments, and can even be used to detect the presence of such receptors on the cell surface (He *et al.*, 2003).

6. Pharmacology of P2X receptors

6.1 Agonists

All P2X receptors are endogenously activated by adenine nucleotides. Homomeric P2X receptors expressed in recombinant systems differ in their sensitivity to the endogenous agonist ATP, with EC_{50}s in the order: $P2X_1 = P2X_3 < P2X_2 < P2X_4 = P2X_5 < P2X_6 << P2X_7$ (Stojilkovic et $al.$, 2005).

Table 3: Agonist sensitivities of cloned P2X receptors.

Receptor	ATP	ADP	αβmeATP	βγmeATP	2meSATP	BzATP
$P2X_1$	1	30 80%	1-3 100%	10 40%	1>> 100%>>	3 60%
$P2X_2$	10	≈300 100%	>100 <5%	>300 <10%	3>> 100%>>	30 60%
$P2X_3$	1	≈50 >80%	1 100%	>300 —	0.3>> 100%>>	— —
$P2X_4$	10	>>100 —	>>100 <10%	— —	10–100>> 30–80%>>	— —
$P2X_5$	10	≈300 >80%	>>100 —	— —	10>> —>>	>500
$P2X_7$	100	>>300 —	>>300 —	>100 —	10>> 80%>>	3 300%
$P2X_{2/3}$	1	—	1	—	—>>	—
$P2X_{1/5}$	1	10	5	—	—>>	—
$P2X_{4/6}$	10	—	30	—	—>>	—

Table 3. The upper of the two values in each cell is the concentration (μM) eliciting 50% of maximal response (EC_{50}) to that agonist; the lower value is the maximal response evoked by that agonist as a fraction of the maximal response evoked by ATP. There are differences among EC_{50} reported for agonists that range up to 10-fold. Values reported are measured in the presence of 1–2 mM Ca^{2+} and Mg^{2+} and refer to rat receptors. Taken from North et al., 2000 and represent approximate averages of the published value. A dash signifies that these conditions have not been studied for that receptor.

$P2X_1$ and $P2X_3$ exhibit high sensitivity to αβ-meATP, which is retained in heteromeric configurations. For this reason αβ-meATP sensitivity is usually taken as an index of $P2X_1$ and $P2X_3$ subunit expression in native systems (Khakh et $al.$, 2001). In addition, if the αβ-meATP-activated current undergoes rapid desensitization, it is an indication of homomeric $P2X_1$ or $P2X_3$ expression, whereas if the αβ-meATP-activated current does not inactivate the channels are likely a heteromeric $P2X_{2-3}$ structure.

The $P2X_7$ subtype is sensitive to the endogenous agonist only at concentrations higher that 100 μM (North et $al.$, 2000). However, it is potently activated by the selective $P2X_7$ agonist benzoylbenzoyl ATP (BzATP). Since $P2X_7$ receptors only coassemble in homomeric structures, their expression in native tissues is easily identified by their sensitivity to this drug.

These properties are summarized in table 3.

6.2 Antagonists

PPADS, suramin and Reactive Blue 2 (RB2) are the most commonly used non-selective antagonists at P2X receptors. These substances are able to counteract the activation of a number of P2X receptors, but show no selectivity within the P2X family or towards heteromeric assemblies of different subunits. In addition, the recombinant homomeric P2X$_4$ is almost insensitive to these substances (Wang *et al.*, 1996) being actually potentiated by suramin, RB2, and, depending on the concentration, also by PPADS (Townsend-Nicholson *et al.*, 1999).

Table 4: Antagonist affinities at cloned P2X receptors.

	Suramin	NF023	PPADS	TNP-ATP
P2X$_1$	1 µM	200 nM	1 µM	6 nM
P2X$_2$	10 µM	100 nM	1 µM	1 µM
P2X$_3$	3 µM	1 µM	1 µM	1 nM
P2X$_4$	>300 µM	>100 µM	>300 µM	15 µM
P2X$_5$	4 µM	—	3 µM	—
P2X$_7$	500 µM	—	50 µM	>30 µM
P2X$_{2/3}$	—	1 µM	5 µM	7 nM
P2X$_{1/5}$	—	—	—	200 nM

Table 4. Values are expressed as concentration causing 50% inhibition (IC$_{50}$) of the ionic current evoked by ATP. Concentrations of ATP vary, but a submaximal concentration has been chosen where possible. A dash signifies that these conditions have not been studied for that receptor. Taken from: North et al., 2000.

The recombinant homomeric P2X$_1$ and P2X$_3$ and heteromeric P2X$_{2/3}$ receptors are readily distinguishable because they are blocked by the suramin analogue NF023 and by nanomolar levels of the nucleotide analogue TNP-ATP (North *et al.*, 2000). In addition, a new compound is now available commercially that selectively blocks P2X$_1$ receptors: the suramin analogue NF449. This compound has an IC$_{50}$ value of 0.3 nM, for the rat P2X$_1$ homomeric receptor, and 0.7 nM for the rat heteromeric P2X$_{1-5}$ receptor (Rettinger *et al.*, 2005), whereas it blocks rat P2X$_2$, P2X$_3$, P2X$_{2-3}$ and P2X$_4$ receptors only in the micromolar range.

The most useful blocker for P2X$_7$ receptors is Brilliant Blue G (BBG), which is highly selective for this subtype at nanomolar concentrations (Jiang *et al.*, 2000a). KN-62 and KN-04 also potently block human P2X$_7$ channels in tens of nanomolar concentration range, but not rat P2X$_7$ receptors (Chessell *et al.*, 1998). These properties are summarized in table 4.

It should be mentioned that the pharmacological profile of P2X receptors reported in the present work is based on studies carried out on recombinant systems expressing homomeric or heteromeric P2X cloned subunits transfected in oocytes or other cell types. In native systems, where the expression and coassembly of P2X subunits is usually largely unknown, the pharmacology of P2X receptors may present significant variations.

The molecular structure of some P2X antagonists is shown in figure 6.

Reactive Blue 2   **PPADS**   **Suramin**

TNP-ATP   **KN-62**   **Brilliant Blue G**
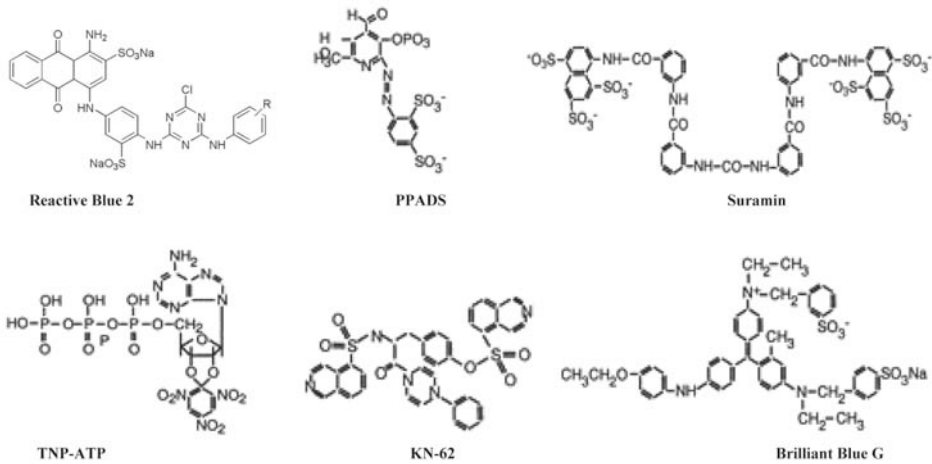
7. P2Y receptors

P2Y receptors belong to the superfamily of G protein-coupled receptors (GPCRs) (Barnard *et al.*, 1994). Within the last 15 years, at least eight different mammalian P2Y receptors (P2Y$_{1,2,4,6,11-14}$) have been cloned and functionally defined (Jacobson *et al.*, 2002), which display 19–55% sequence identity at the protein level. The family of P2Y receptors is rapidly expanding since, among the about 150 orphan GPCRs encoded by our genome (for which the ligand specificity has not yet been identified) there are some receptors structurally related to the P2Y family, especially in the TM6 and TM7 regions (Abbracchio *et al.*, 2006). In fact, a detailed pharmacological characterization of some of them revealed a purine/pyrimidine agonist profile, as has recently happened for GPR105 that has now been included in the P2Y family and re-named P2Y$_{14}$ (Abbracchio *et al.*, 2003). The youngest member of the P2Y family is the recently deorphanized GPR17 receptor (Ciana *et al.*, 2006), which presents a unique pharmacological profile since it possesses a dual ligand specificity. It is sensitive not only to purinergic compounds (UDP-linked sugars such as UDP-glucose or UDP-galactose are preferred agonists), but also to ligands for the cysteinyl-leukotriene receptor family (CysLT1 and CysLT2), such as LTD$_4$ and LTC$_4$. This results confirms not only the already proposed cross-talk between purinergic and CysLT receptor system (Ballerini *et al.*, 2005), but also the fact that some GPCRs may present a dual agonist profile, as previously hypothesized by Mellor and colleagues (Mellor *et al.*, 2001).

P2Y receptors present the typical structure of GPCRs, with seven hydrophobic transmembrane domains, an extracellular –NH$_2$ terminus containing several potential *N*-linked glycosylation sites, and an intracellular -COOH terminus containing consensus binding/phosphorylation sites for protein kinases (Erb *et al.*, 2006) that modulate receptor activities (figure 7).

Individual P2Y receptor subtypes have been linked to one or more of the four subfamilies of heterotrimeric G proteins (G$_s$, G$_{i/o}$, G$_{q/11}$, and G$_{12/13}$). It is generally accepted that P2Y$_{1,2,4,6}$ all couple via G$_q$-proteins to stimulate PLC which in turn leads to an increase in inositol phosphates and mobilization of Ca^{2+} from intracellular stores. Conversely, P2Y$_{12,13,14}$ all couple via G$_i$ proteins resulting in the inhibition of adenylate cy-
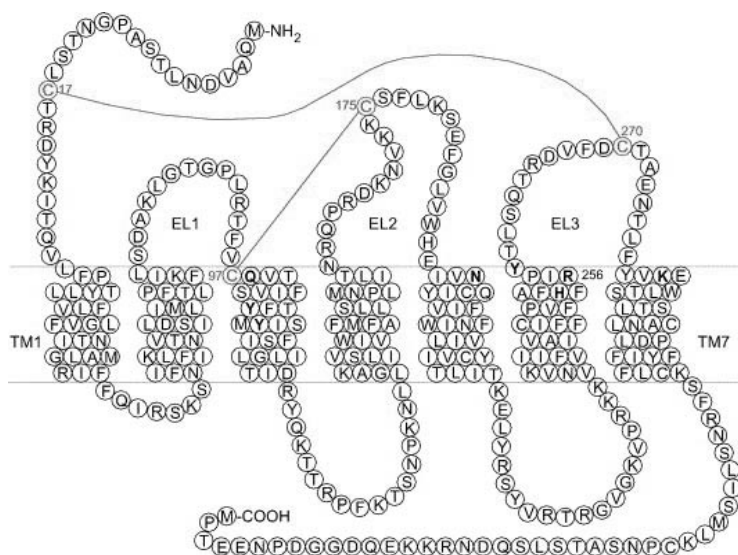
Figure 7. Molecular structure of P2Y receptors. Predicted secondary structure of the human P2Y$_{12}$ receptor. TM: transmembrane region. EL: extracellular loop. Lines represent predicted disulfide bridges. Taken from: von Kugelgen 2006.

clase followed by a decrease in intracellular cAMP levels (von Kugelgen 2006). P2Y$_{11}$ is unique since it can activate both pathways, with an agonist-specific signalling cascade. In fact, is has been clearly demonstrated that P2Y$_{11}$ receptor activation by ATP can stimulate adenylyl cyclase leading to a rise in cAMP but, simultaneously, can also activate PLC to induce the formation of IP$_3$ and the mobilization of intracellular Ca^{2+}, while UTP can only induce intracellular Ca^{2+} rise by a G$_0$-activated and PLC-independent cascade (White *et al.*, 2003). Coupling of an individual P2Y receptor subtype to multiple G proteins and signalling pathways may suggest that receptor activation leads to the induction of more than one conformational state that enables associations with different Gα subunits (Abbracchio *et al.*, 2006). Recent studies have shown that P2Y receptors can also couple to the activation of monomeric G proteins, such as Rac and RhoA (Soulet *et al.*, 2004). These data are summarized in table 5.

Table 5: P2Y receptor subtypes and G-protein coupling.

Receptor	Preferred agonist (human)	G protein	Main effector systems
P2Y$_1$	ADP	G$_{q/11}$	PLC (+), Ca^{2+} release
P2Y$_2$	ATP, UTP	G$_{q/11}$	PLC (+), Ca^{2+} release
	ATP, UTP	G$_o$	PLC (+), Ca^{2+} release
	ATP, UTP	G$_{12}$	RhoA (+)
P2Y$_4$	UTP	G$_{q/11}$	PLC (+), Ca^{2+} release
	UTP	G$_o$	PLC (+), Ca^{2+} release
P2Y$_6$	UDP	G$_{q/11}$	PLC (+), Ca^{2+} release

Receptor	Preferred agonist (human)	G protein	Main effector systems
P2Y$_{11}$	ATP	G$_{q/11}$	PLC (+), Ca^{2+} release
	ATP	G$_s$	AC (+), increased cAMP
	UTP	G$_o$	PLC-independent Ca^{2+} release
P2Y$_{12}$	ADP	G$_i$	AC (−), ↓ cAMP
	ADP	G$_{12/13}$?	RhoA (+)
P2Y$_{13}$	ADP	G$_{i/o}$	AC (−), ↓ cAMP, PLC (+), Ca^{2+} release
P2Y$_{14}$	UDP-glucose	G$_{i/o}$	PLC (+), Ca^{2+} release

G protein coupling and principal second messenger systems associated with P2Y receptor stimulation. Taken from: Erb et al., 2006.

A prolonged agonist-induced activation of GPCRs also initiates receptor desensitization, which diminishes GPCR responsiveness, leading to receptor internalization. Agonist-dependent GPCR desensitization is generally mediated by a family of GPCR kinases (GRK 1-7), which phosphorylate residues in intracellular domains of the receptor. This process seems to not be present in all P2Y receptors, but has already been described in P2Y$_2$ (Flores *et al.*, 2005), P2Y$_{12}$ (Hardy *et al.*, 2005) subtypes. P2Y$_1$ receptors also desensitize but with a different mechanism, probably involving protein kinase C (PKC) activation (Hardy *et al.*, 2005).

8. Pharmacology of P2Y receptors

8.1 Agonists

A recent update in P2Y pharmacology (Abbracchio *et al.*, 2006) distinguished four major groups of P2Y receptors, on the basis of the endogenous agonist preferred:
1. Adenine nucleotide-preferring receptors mainly responding to ATP and (mostly) ADP. This group includes human and rodent P2Y$_1$, P2Y$_{12}$, P2Y$_{13}$, with the human receptors preferring ADP over ATP (Gachet 2005; Marteau *et al.*, 2003; Palmer *et al.*, 1998).
2. Uracilic nucleotide-preferring receptors. This group includes human P2Y$_4$ and P2Y$_6$ responding to either UTP or UDP.
3. Receptors of mixed selectivity, responding to both purine and pyrimidine nucleotides: human and rodent P2Y$_2$ and P2Y$_{11}$, plus rodent P2Y$_4$ (whereas human P2Y$_4$ receptor is blocked by ATP: Kennedy *et al.*, 2000).
4. Receptors responding solely to sugar nucleotides UDP-glucose and UDP-galactose: P2Y$_{14}$ and the recently deorphanized GPR17 (Ciana *et al.*, 2006).

Synthetic agonists able to discriminate between all the different P2Y receptor subtypes are still lacking. However, considerable progress has been made in recent years with the adenine nucleotide-preferring receptors P2Y$_1$, P2Y$_{12}$ and P2Y$_{13}$, for which ADPβS has been the first preferred agonist synthesized (P2Y$_1$: EC$_{50}$=96 nM and P2Y$_{12}$: EC$_{50}$=82 nM: Jacobson *et al.*, 2002; P2Y$_{13}$: EC$_{50}$=42 nM: Communi *et al.*, 2001).

Alkylthio-substituted molecules in position 2 of the adenine ring, such as 2-MeSADP, are even more selective agonists at $P2Y_1$, $P2Y_{12}$ and $P2Y_{13}$ receptors, with EC_{50} values in the range of 1-6 nM (Jacobson *et al.*, 2002; Marteau *et al.*, 2003). The corresponding triphosphated molecule, 2-MeSATP, is less potent and selective towards $P2Y_1$ receptors since it also activates some P2X receptors (King, 1998). The most potent agonists known for the human $P2Y_1$ receptor is the newly synthesized MRS 2365, an ADP-derivative with modifications of both the ribose moiety and the adenine ring. with an EC_{50} of 0.4 nM (Chhatriwala *et al.*, 2004). In addition, this is the unique $P2Y_1$ agonist that is inactive at human $P2Y_{12}$ and $P2Y_{13}$ receptors (Chhatriwala *et al.*, 2004). Thiophosphate-containing adenine nucleotides, such as ???? and ATPγS, present a high stability toward 5-NT' and ecto-ATPase degradation and are more potent than ATP in activating the $P2Y_{11}$ receptor.

Among uracil derivatives (see figure 8), UTP and ATP are equipotent agonists at $P2Y_2$ and $P2Y_4$ receptors, with the exception of the human $P2Y_4$ that is blocked, instead of activated, by extracellular ATP (Herold *et al.*, 2004). Uridine β-thiodiphosphate (UDPβS) and γ-thiodiphosphate (UDPγS) are selective agonists at $P2Y_6$ and $P2Y_2$/$P2Y_4$ receptors, respectively (Malmsjo *et al.*, 2000).
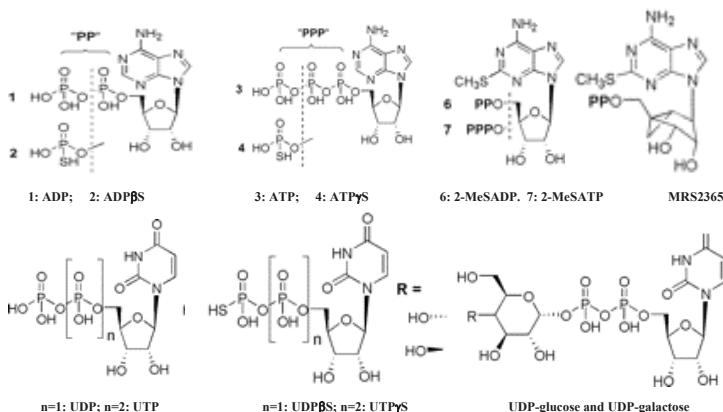
Figure. 8. Structures of adenine-derived and uracil-derived nucleotide agonists of P2Y receptors.

8.2 Antagonists

The classical P2 antagonists are suramin, PPADS and RB2. However, these molecules block not only several P2Y receptors, but also many P2X subtypes (as already mentioned) and even some unrelated proteins, such as 5'-NT (Chen *et al.*, 1996), NMDA receptors (Peoples *et al.*, 1998) and ion channels (Galietta *et al.*, 1997). Nevertheless, these compounds have been commonly used to study P2Y-mediated actions. Suramin and its derivatives are relatively non-selective and non-competitive antagonists at P2Y receptors, with a well characterized activity at the $P2Y_2$ (IC50=48 μM: Muller 2002) $P2Y_{11}$ (Communi *et al.*, 1999) and $P2Y_{13}$ receptors (Marteau *et al.*, 2003) in the micromolar range. RB2 effectively blocks $P2Y_1$ receptors (Jacobson *et al.*, 2002) and rat, but not human, $P2Y_4$ receptors at high concentrations (100 μM: Kennedy *et al.*, 2000), but high potency and selectivity have not been achieved (Brown *et al.*, 2002a; Jacobson *et*

al., 2002). PPADS, and its derivatives, competitively antagonizes $P2Y_1$ receptors and non-competitively block $P2Y_{13}$ receptors (Marteau *et al.*, 2003) at micromolar concentrations (Lambrecht *et al.*, 2002), but its action is not fully reversible (Ralevic *et al.*, 1998).

Only recently, a new generation of high affinity and selective P2Y competitive antagonists has been introduced. These compounds are able to selectively discriminate among different receptor subtypes. The first notable molecule synthesized was MRS 2179, with an IC_{50} value of 300 nM at $P2Y_1$ receptors (Nandanan *et al.*, 1999). Its 2-Chloro analogue, MRS 2216, is an even more potent agonist at this receptor, with an IC_{50} of 100 nM (Brown *et al.*, 2000). Subsequent molecular modifications lead to the newly synthesized $P2Y_1$ antagonists MRS 2279 and MRS 2500, that have particularly high affinity (IC_{50} under the nanomolar range: Ohno *et al.*, 2004) and selectivity (inactive at $P2Y_{2,4,6,11,12,13}$ and $P2X_{2,3,4,7}$: Boyer *et al.*, 2002; Marteau *et al.*, 2003) towards this receptor subtype. Only weak antagonism by MRS 2279 on rat $P2X_1$ receptor has been reported (Brown *et al.*, 2000). [33P]MRS 2179, [33P]MRS 2279 and [33P]MRS 2500 were prepared and shown to be very useful tools as radioligand probes to detect and quantify $P2Y_1$ expression in native systems and tissues (Baurand *et al.*, 2001; Waldo *et al.*, 2002). An interesting compound is AR-C69931MX (cangrelor), another ATP-derivative, that, on the contrary, does not bind to the $P2Y_1$ receptor subtype but is able to selectively block $P2Y_{12}$ and $P2Y_{13}$ receptors (Marteau *et al.*, 2003).

Among uridine-preferring P2Y subtypes, a new family of selective $P2Y_6$ antagonists, the aryl diisothiocyanate derivatives, have been recently developed. These compounds, among which MRS 2578 has the highest affinity values for rat and human receptors (IC_{50} in the nanomolar range), are promising compounds for the identification of $P2Y_6$-mediated responses. Limitations in using these compounds include pharmacological irreversibility, low stability and solubility in aqueous medium.

The molecular structure of some P2Y antagonists is shown in figure 9, whereas a summary of P2Y receptor pharmacology is reported in table 6.

Table 6 summarizes recent data about P2Y receptor distribution and pharmacological profile.

18: MRS 2179;   19: MRS 2216   **21: MRS 2279;   22: MRS 2500**
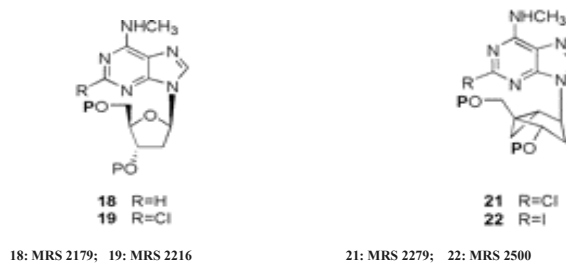
Figure 9. Structures of nucleotide-based antagonists of P2Y receptors.

9. Distribution of P2 receptors

P2 receptors are widely distributed in a large variety of tissues with varying profiles for different subtypes, as summarized in table 6. In the lung, $P2X_4$ (Bo *et al.*, 2003) and uridine-preferring $P2Y_{2,4,6}$ receptors (Bergner *et al.*, 2002; Kishore *et al.*, 2000) are most

Table 6. Summary about P2Y-receptors pharmacological profile and distribution.

	P2Y$_1$	P2Y$_2$	P2Y$_4$	P2Y$_6$	P2Y$_{11}$	P2Y$_{12}$	P2Y$_{13}$	
Tissue distribution	Wide including platelets, heart, skeletal muscle, neuronal tissues, digestive tract	Wide including lung, heart, skeletal muscle, spleen, kidney	Placenta, lung, vascular smooth muscle, brain, liver	Wide including lung, heart, aorta, spleen, placenta, thymus, intestine, brain	Spleen, intestine, immunocytes	Platelets, neural tissues	Spleen, leucocytes, bone marrow, liver, brain	Placenta, adipose tissue, intestine, brain, spleen
Preferred agonists at human receptor[c]	(N)-mc-2-MeSADP >2MeSADP >ADP =ADPβS >ATP	UTP=ATP> INS37217 >Ap4A >ATPγS	UTP> UTPγS	UDP= 5Br-UDP >>UTP >2-MeSADP	ARC67085≥ ATPγS =BzATP >ATP≥(UTP)ᵃ>2MeSATP	2-MeSADP >ADP >>(N)-mc-2-MeSADP	2-MeSADP ≥ADP >ADPβS	UDP-glu >UDP-gal
Preferred agonists at rat receptor[c]	2-MeSADP =2-MeSATP >ADP	UTP=ATP >CTP>GTP	UTP=ATP=ITP =Ap4A	UDP>UTP >ADP >2-MeSATP		2-MeSADP >ADP >ATP	ADP >2-MeSADP >ATP	UDP-glu
Suramin	5.5ᵃ	4.3ᵇ	–(300 µM)	↓27% (100 µM)	6.1	5.5	↓80% (10 µM)	
PPADS	4.9–5.4ᵃ	–(30 µM)	↓30% (100 µM)	↓69% (100 µM)	–(100 µM)	–(100 µM)	↓50% (10 µM)	
RB2	6.1ᵃ	↓80% (100 µM)	↓33% (100 µM)	6.0ᵃ	↓80% (100 µM)	↓100% (30 µM)	↓80% (10 µM)	
MRS 2179	6.8ᵃ	–(30 µM)	–(30 µM)	–(30 µM)	–(30 µM)	–(10 µM)	–(100 µM)	
MRS 2279	8.1	–(30 µM)	–(30 µM)	–(30 µM)				
MRS 2500	8.8					–(100 µM)		
MRS 2567	–(10 µM)	–(10 µM)	–(10 µM)	↓95% (10 µM)	–(10 µM)			
Cangrelor (AR-C69931MX)						8.7	↓80% (0.01 µM)	
MRS 2211	<5					–(10 µM)	6.3	

ᵃ Apparent pK$_B$ value. ᵇ Slope different from unity. Taken from: von Kugelgen 2006.

highly expressed, whereas in the ciliated airway epithelium $P2X_{4,5,7}$ and $P2Y_{1,2,6}$ prevail (Picher *et al.*, 2003; Zhang *et al.*, 2003). Smooth muscles of digestive tract and urinary system are particularly rich in P2 receptors and the first evidence for the "purinergic signalling" hypothesis came from studies on these tissues (Burnstock *et al.*, 1963). The stomach smooth muscle is rich in $P2X_7$ and $P2Y_{1,2}$ receptors (Bo *et al.*, 2003; Curro *et al.*, 1998; Jenkinson *et al.*, 2000; Otsuguro *et al.*, 1996) and in the small intestine and colon also $P2X_5$ and $P2Y_6$ are also found (Bo *et al.*, 2003; Ota *et al.*, 1994). In the kidney glomerular cells almost all P2 receptor subtypes are present (Bo *et al.*, 2003), except $P2X_{1,2}$ that are found in the distal convoluted tubules (Bo *et al.*, 2003). In the urinary bladder all P2X except for $P2X_7$ subunits are expressed (Bo *et al.*, 2003), whereas only $P2Y_1$ transcript is present among metabotropic nucleotide receptors (Obara *et al.*, 1998). The vas deferens, where ATP-mediated contractile activity has been largely characterized, is also rich in $P2X_{1,2,4,7}$ receptors (Lee *et al.*, 2000), but the presence of P2Y transcripts has not yet been described in this region. Immune cells present a particularly intense staining for purinergic nucleotide receptors, in accordance with the important role of ATP in mediating immune cell functions (Di Virgilio *et al.*, 1996). $P2X_7$ (Falzoni *et al.*, 1995; Li *et al.*, 2002) are typically expressed on monocytes and macrophages, together with $P2Y_{1,2,4,11,12}$ subtypes (Bowler *et al.*, 2003; Di Virgilio *et al.*, 1996). Neutrophils (Jin *et al.*, 1998), eosinophils (Mohanty *et al.*, 2001), lymphocytes (Wang *et al.*, 2004) and dendritic cells (Xiang *et al.*, 2006b) also present $P2X_{1,4,5}$ subunits. Megakaryocytic cells and platelets are known for their $P2Y_{12}$-mediated aggregation, but they also express $P2X_1$ and $P2Y_1$ receptors (Greco *et al.*, 2001; Hechler *et al.*, 2001; Leon *et al.*, 1997). In the heart, all P2X except $P2X_7$ subunits are expressed (Bogdanov *et al.*, 1998; Hansen *et al.*, 1999a), whereas, among P2Y subtypes, only $P2Y_{1,2,4,6}$ are found in myocytes (Webb *et al.*, 1996). In the vasculature, P2 receptors present a wide distribution with distinct subtypes revealed in different regions (Bo *et al.*, 2003; Hansen *et al.*, 1999b). For example, endothelial cells mainly express $P2X_{4,5}$ and $P2Y_{1,2,11}$ receptors (Wang *et al.*, 2002) whereas vascular smooth muscle cells express $P2X_{1,2,4}$ (Nori *et al.*, 1998) and $P2Y_{2,6}$ subtypes (Wang *et al.*, 2002).

Particularly relevant to the present work is the neuronal localization of P2 receptors that will be adescribed independently for P2X and P2Y subtypes in the next two sessions.

9.1 Neuronal localization of P2X receptors

The distribution of P2X receptors in the CNS ranges from abundant to discrete. Thus, $P2X_2$, $P2X_4$, and $P2X_6$ mRNAs or proteins have been detected throughout the brain and spinal cord, as well as in sensory and autonomic ganglia (Norenberg *et al.*, 2000a). $P2X_1$ receptors were initially believed to be absent in the brain (Valera *et al.*, 1994). However, later on, it turned out that $P2X_1$ mRNA is localised in the cerebral cortex, striatum, hippocampus and cerebellum, where $P2X_1$ subunit proteins have also been detected (Kidd *et al.*, 1995). Outside the brain, $P2X_1$ was found in the dorsal and ventral horns of the spinal cord, sensory ganglia (trigeminal, nodose and dorsal root ganglia), sensory systems (spiral ganglion in the cochlea of the inner ear) and autonomic sympathetic ganglia (superior cervical and coeliac ganglia: Collo *et al.*, 1996; Xiang *et al.*, 1998).

The $P2X_3$ receptor is believed to mostly occur in capsaicin-sensitive sensory neurones involved in nociception (Chen *et al.*, 1995; Lewis *et al.*, 1995; Vulchanova *et al.*, 1996). In fact, $P2X_3$ protein or its mRNA was found in cell bodies of sensory neurones, and in their central termination fields (dorsal horn of the spinal cord, nucleus of the

solitary tract), as well as in their peripheral endings, e.g. in taste buds of the tongue and the spiral ganglion of the inner ear (Vulchanova *et al.*, 1997). However, exceptions exist: in the adult rat nervous system, $P2X_3$ was also found in the hypothalamic supraoptic nucleus, as well as in autonomic sympathetic ganglia (Shibuya *et al.*, 1999).

$P2X_5$ also shows a restricted localisation in the CNS. $P2X_5$ mRNA was found only in the mesencephalic nucleus of the trigeminal nerve and in motoneurones of the spinal cord ventral horn (Collo *et al.*, 1996). In the peripheral nervous system, $P2X_5$ mRNA, $P2X_5$ protein, or both were identified in sensory ganglia and the spiral ganglion of the inner ear (Xiang *et al.*, 1999), whereas sympathetic ganglia such as superior cervical and coeliac ganglia did not express $P2X_5$ proteins (Xiang *et al.*, 1998).

It is generally believed that the $P2X_7$ receptor is not expressed in neuronal cells although it was originally cloned from superior cervical ganglia and brain tissue (Buell *et al.*, 1996). In accordance, recent data indicate that this receptor subtype is mainly expressed by glial cells (astrocytes, oligodendrocytes and microglia) where it regulates their activation during neuroinflamatory responses (Gendron *et al.*, 2003). More recently, detailed analysis has shown that $P2X_7$ receptors are also expressed by some peculiar neuronal cell types, such as rat spiral ganglion neurons of the inner ear and rat retinal ganglion cells (Brandle *et al.*, 1998 and 1999). Immunohistochemistry and electron microscopy techniques revealed a preferential localization of neuronal $P2X_7$ receptor protein targeted to presynaptic terminals in the CNS, throughout the spinal cord and medulla oblongata (Deuchars *et al.*, 2001), suggesting a role for $P2X_7$ receptors in modulating neurotransmitter release.

9.2 Neuronal localization of P2Y receptors

Most of the known subtypes of P2Y receptors are expressed in the central nervous system. Quantitative RT-PCR revealed that $P2Y_1$ and $P2Y_{11}$ mRNA is present in the human brain in large quantities when compared with other tissues whereas, in the same study, only low to moderate levels of $P2Y_2$, $P2Y_4$, and $P2Y_6$ were detectable (Moore *et al.*, 2001). In immunohistochemical staining of human brain slices, a striking neuronal localization of $P2Y_1$ receptors was confirmed in human and rat brain in areas such as the cerebral and cerebellar cortex, hippocampus, basal ganglia (striatum) and midbrain (Moore *et al.*, 2000). In contrast, *in situ* hybridizations of human (Hollopeter *et al.*, 2001) and rat (Sasaki *et al.*, 2003) brain sections revealed mainly a glial localization of the $P2Y_{12}$ receptor. Also $P2Y_{13}$ mRNA was detected in various regions of the human brain, such as cerebellum, hippocampus, substantia nigra, and thalamus (Communi *et al.*, 2001). In the peripheral nervous system, mRNA for all P2Y receptor subtypes except $P2Y_{11}$ and $P2Y_{14}$ has been found in sympathetic neurons (Lechner *et al.*, 2004; Norenberg *et al.*, 2000b). Sensory neurons, in contrast, were shown to express only $P2Y_{1,2,4,6}$ (Ruan *et al.*, 2003). In the intramural parasympathetic ganglia of the cat urinary bladder, the presence of $P2Y_{1,2,4,6}$, and $P2Y_{12}$ was revealed by immunohistochemistry (Ruan *et al.*, 2006). In the enteric nervous system of guinea pigs, evidence for the expression of $P2Y_1$ (Hu *et al.*, 2003), $P2Y_2$, $P2Y_6$, and $P2Y_{12}$ receptors (Xiang *et al.*, 2005 and 2006a) has been obtained. However, there is no evidence for a neuronal localization of $P2Y_{14}$ subtype, and the respective mRNA was only found in rat cortical astrocytes (Fumagalli *et al.*, 2003), where UDP-glucose also elicited a rise in intracellular Ca^{2+}. As already described for A_{2A} and D_2, also $P2Y_1$ receptors can assemble to form heterodimers with other metabotropic receptors. In particular, convincing evidences demonstrate an association between A_1 and $P2Y_1$ isoform both in co-transfect-

ed HEK293T cells (Yoshioka *et al.*, 2001; Yoshioka *et al.*, 2002b) and in native rat brain slices (cerebellum, hippocampus and cortex: (Yoshioka *et al.*, 2002a). The dimerized $A_1/P2Y_1$ receptor presents hybrid pharmacological features across P1 and P2 subtypes: it can be activated by both adenosine and ADP-related agonists (Yoshioka *et al.*, 2001) and it is blocked by DPCPX and MRS 2179 (Yoshioka *et al.*, 2002b). Such heteromeric association reinforces the already close correlation between adenosine and ATP-ergic systems, but a precise implication of this phenomenon in neuronal functions is still unknown (for a review see: Nakata *et al.*, 2004 and 2005).

Effects of extracellular purines

In virtually all peripheral tissues, extracellularly released nucleotides or nucleosides play important roles in a large number of physiological processes. In addition, the rapid breakdown of extracellular ATP to adenosine is responsible for a close interplay between ATP-ergic and adenosinergic systems whose clear dissection presents numerous experimental problems (Hussl *et al.*, 2006).

In general, the time course of P1 adenosine and P2Y adenine mediated responses is usually slower than those mediated by P2X receptor activation since they involve second messenger systems and/or ionic conductance modulation by G protein coupling (Ralevic and Burnstock 1998). Therefore, ATP likely acts as a fast neurotransmitter where P2X receptors are expressed; this action can be followed by slower effects mediated by P2Y and, after conversion to adenosine, by P1 receptors.

1. Role of P1 receptors

P1 receptors exert important pathophysiological roles in a variety of tissue, from the cardiovascular system to the brain. At systemic level, adenosine acts as a negative chronotropic, inotropic and dromotropic modulator on heart functions by activating A_1 receptors. These effects are mainly due to the attenuation of the stimulatory actions of catecholamines on the heart functions carried on by A_1 adenosine receptor activation (Fraser *et al.*, 2003; Zablocki *et al.*, 2004). The marked inhibitory effects of adenosine on the heart led to the introduction of A_1 agonists in Phase II clinical trials to slow heart rate during atrial fibrillation (see Selodeson, Aderis Pharmaceuitcals: Ellenbogen *et al.*, 2005) and in Phase III for paroxysmal supraventricular tachycardia (PSVT) with successful results (see Adenocard, Astellas Pharma: Vranic *et al.*, 2006).

In contrast, the hypotensive effects exerted by adenosine in the periphery are attributed to A_{2A} receptor activation, causing vasodilatation of blood vessels (Schindler *et al.*, 2005) and led, in the '60s-'70s, A_{2A} agonists to be tested in clinical trials as antihypertensive drugs. In addition, A_{2A} receptor stimulation also inhibits platelet aggregation (Varani *et al.*, 2000) and exhibits marked anti-inflammatory activities by inhibiting T-cell activation and proliferation, by reducing pro-inflammatory cytokine production and enhancing anti-inflammatory cytokine levels (Erdmann *et al.*, 2005; Lappas *et al.*, 2005).

Less is known about the roles of A_{2B} and A_3 receptors in the periphery. One of the first described biological effects of adenosine A_3 receptor stimulation was degranulation of mast cells (Ramkumar *et al.*, 1993), suggesting a pro-inflammatory role of this receptor subtype. This hypothesis has been confirmed by subsequent studies dem-

onstrating that A_3 receptor activation facilitates antigen-dependent histamine release from mast cells (Salvatore *et al.*, 2000). In addition, it has a demonstrated irritant effect in asthmatic lung mediated by A_3 receptor stimulation (Holgate 2005), probably partnered, in eliciting this effect, by A_{2B} receptor stimulation, that also mediates bronchoconstriction (Holgate 2005). For this reason, mixed A_{2B} and A_3 antagonists have been proposed as candidates for the treatment of asthma (Press *et al.*, 2005).

1.1 P1 receptors and neurotransmission.

The role of adenosine as a neuromodulator has long been known. In fact, many P1-mediated modulatory actions on presynaptic neurotransmitter release or postsynaptic neuronal excitability have been described. Most of the actions played by adenosine under physiological conditions are mediated by A1 and A_{2A} receptors. At the central level, adenosine exerts a number of actions: it acts as an endogenous anticonvulsant but also affects the control of motility, pain, sleep, cognition and memory. Actually, the overall stimulating effects of caffeine (the most consumed drug in the world) on arousal, concentration and motility are mainly due to its antagonism on adenosine receptors. Furthermore, adenosine has an important tonic modulation of the affective state (Florio *et al.*, 1998a, 1998b) thus influencing social interaction and aggressive behaviour.

Under physiological conditions, adenosine exerts a tonic inhibition of synaptic transmission both *in vitro* or *in vivo* by stimulating A_1 receptors, as demonstrated in several brain regions such as the hippocampus, striatum and olfactory cortex (Latini *et al.*, 2001; von Lubitz 1999). These mechanisms were studied in brain regions with a high concentration of A_1 receptors, such as the hippocampus. The inhibitory effect of adenosine A_1 receptor stimulation has a pre- and postsynaptic component. Activation of the presynaptic A_1 receptors reduces Ca^{2+} influx through the preferential inhibition of N-type and, probably, Q-type channels (Wu *et al.*, 1994; Yawo *et al.*, 1993). Inhibition of presynaptic calcium currents decreases transmitter release (Prince *et al.*, 1992) and adenosine, by stimulation of A_1 receptors, has been found to inhibit the release of virtually all classical neurotransmitters: glutamate, acetylcholine, dopamine, noradrenaline and serotonin (see in Fredholm *et al.*, 1988). In particular, a powerful suppression of glutamate release from presynaptic terminals has been described in the hippocampus (Burke *et al.*, 1988, Corradetti *et al.*, 1984), where adenosine A_1 receptor activation reduces the number of quanta released (but not the size of individual quanta nor the postsynaptic glutamate receptor sensitivity) in the Schaffer collateral-commissural pathway (Lupica *et al.*, 1992). The postsynaptic effect of A_1 receptors consists of a direct hyperpolarization of neurones via activation of GIRK channels (Kir 3.2 and 3.4 channels: potassium inward rectifiers) at the postsynaptic site (Takigawa *et al.*, 1999; Takigawa *et al.*, 2002). In some brain regions, such as the hippocampus, the endogenous adenosine that is present in the extracellular space under physiological conditions exerts a tonic inhibition of excitatory neurotransmission by the activation of both pre- and post-synaptic A_1 receptors. Exogenous application of the selective A_1 antagonist DPCPX causes a 15% increase of synaptic potential amplitude in *in vitro* brain slices (Latini *et al.*, 1999b). This is an expected result in a brain region where extracellular adenosine concentration is found to be around 10-50 nM (Latini *et al.*, 1998 and 1999b) and A_1 receptors, whose affinity for adenosine is in the low nanomolar range, are highly expressed. These data are confirmed by the fact that, in slices taken from homozygous A_1 receptor knockout mice, no evidence was found for an endogenous inhibitory action of adenosine in the Schaffer collateral pathway in the CA1 region of the hippocam-

pus or at the mossy fibre synapses in the CA3 region (Moore *et al.*, 2003). In addition, no inhibition of synaptic transmission was elicited by the application of exogenous adenosine (Johansson *et al.*, 2001).

Opposite effects from A_1-mediated synaptic inhibition are elicited by A_{2A} receptor activation, that has been shown to mediate excitatory actions in the nervous system (Latini *et al.*, 1996; Pedata *et al.*, 1984; Sebastiao *et al.*, 1996; Spignoli *et al.*, 1984). Electrophysiological investigations into the role of A_{2A} receptors in synaptic function under physiological conditions have shown that they increase synaptic neurotransmission. For example, in the hippocampus *in vitro*, A_{2A} receptor stimulation results in a Ca^{2+}-dependent release of acetylcholine (Cunha *et al.*, 1995; Spignoli *et al.*, 1984). Furthermore, the application of CGS 21680, a selective A_{2A} receptor agonist, decreases the ability of A_1 receptor agonists to inhibit excitatory neurotransmission (Cunha *et al.*, 1994; O'Kane *et al.*, 1998). This effect supports the already proposed hypothesis that A_{2A} receptor stimulation increases synaptic transmission through A_1 receptor desensitization (Dixon *et al.*, 1997; Stone *et al.*, 2004). Alternatively, another current theory is that A_{2A} receptors increase excitatory amino acid release. In fact, the selective stimulation of adenosine A_{2A} receptors augment the amount of glutamate released in hippocampus and striatum of young rats (Corsi *et al.*, 1999 and 2000; Popoli *et al.*, 1995). In spite of the excitatory role in neurotransmission brought about by A_{2A} receptors, the net effect of adenosine is an inhibitory tonus on neurotransmission, in accordance with observations suggesting that activation of A_{2A} receptors requires a protracted stimulation to induce evident effects on synaptic transmission (Latini *et al.*, 1999a). It is worth noticing that the role of A_{2A} receptors in the striatum is recently gaining interest in light of their heterodimerization with D_2 dopamine receptors. The association between A_{2A} and D_2 receptors results in an antagonistic interaction which provided a rationale for evaluating A_{2A}-selective antagonists in Parkinson's disease, supported by epidemiological evidence indicating an inverse relationship between caffeine consumption and risk of developing this pathology (Ascherio *et al.*, 2001; Ross *et al.*, 2000). It was suggested that A_{2A} antagonists not only provide symptomatic relief but also decelerate dopaminergic neurone degeneration in patients (Xu *et al.*, 2005). Two different A_{2A} antagonists, istradefylleine (KW-6002) and a derivative of the anti-malarian mefloquine (V2006), are respectively in Phase III and Phase II clinical trials for Parkinson's disease at present, with promising results (Hauser *et al.*, 2003; Weiss *et al.*, 2003).

Discrepancies about the role of adenosine A_3 receptors in the CNS are present in the literature, as indicated by the fact that the activation of this receptor subtype has been associated with both excitatory and inhibitory effects, even in the same brain region. An excitatory role of A_3 receptors has been supported by evidence indicating that, in the rat hippocampus, their activation attenuates LTD and allows induction of LTP elicited by a subliminal weak-burst protocol (Costenla *et al.*, 2001). In addition, in the same brain area, A_3 receptor activation through a selective adenosine A_3 agonist has been shown to antagonizes the adenosine A_1 receptor-mediated inhibition of excitatory neurotransmission (Dunwiddie *et al.*, 1997a). However, further electrophysiological studies refused this hypothesis, since several authors demonstrated that no significant interaction between A_1 and A_3 receptors occur in the rat cortex and hippocampus (Brand *et al.*, 2001; Lopes *et al.*, 2003). Additional evidence for an excitatory role of adenosine A_3 receptors came from studies carried out in "*in vitro*" hippocampal slices. For example, A_3 receptor stimulation always attenuated the inhibition of hippocampal slice neurotransmission caused by presynaptic metabotropic glutamate receptors in a PKC-dependent manner (Macek *et al.*, 1998). In addition, whole-cell patch clamp re-

cordings in CA3 hippocampal pyramidal neurones demonstrated that A_3 receptor activation results in a significant potentiation of high threshold hippocampal Ca^{2+} currents by a PKA-dependent mechanism (Fleming *et al.*, 1997). Finally, a facilitation of epileptiform discharge onset has been observed in the presence of the selective A_3 receptor agonist Cl-IB-MECA (Laudadio *et al.*, 2004) and a reduction of such epileptic activity was observed when A_3 receptors, activated by endogenously released adenosine during seizures, were blocked by the selective antagonist MRS 1191 (Etherington *et al.*, 2004).

Contrary to previous results, an inhibitory action has been attributed to A_3 receptors by Brand and colleagues (Brand *et al.*, 2001), who demonstrated that, in rat cortical neurones, the selective activation of this adenosine receptor subtype is involved in inhibition of excitatory neurotransmission, suggesting a synergistic action with the inhibitory effect of adenosine brought about by A_1 receptor activation. Despite results obtained by A_3 receptor stimulation, evidence that selective block of A_3 receptors does not affect neurotransmission in the CA1 region of the hippocampus under normoxic conditions, indicates that endogenous adenosine at physiological concentrationa does not exert tonic activation of A_3 receptors (Dunwiddie *et al.*, 1997a; Pugliese *et al.*, 2003). This is in line with evidence that A_3 receptor activation requires micromolar levels of extracellular adenosine, which can be reached only during pathological conditions of impairment in energy supply (for example during hypoxia or ischemia: Latini *et al.*, 1998; Pearson *et al.*, 2006). For this reason, particular interest has been dedicated to investigate A_3-mediated effects during brain damage, when the activation of this receptor subtype becomes relevant. Since a section of the present research has been dedicated to study the role of A_3 receptors during ischemic insults in the brain, it is useful to focus on the role of adenosine during such cerebral insults.

1.1 P1 receptors and cerebral ischemia

Ischemic stroke is the third leading cause of death in industrialised countries, with a mortality rate of around 30%, and it is the major cause of long-lasting disabilities. It is caused by a transient or permanent reduction in cerebral blood flow due to the occlusion of a major brain artery, either by an embolus or by local thrombosis. An effective therapy for this pathology does not exists yet. Several neuroprotective drugs have been developed and successfully tested in animal stroke models, but most of them failed to be efficacious in clinical trials (De Keyser *et al.*, 1999). A typical example concerning clinical failure of experimental models is provided by the class of NMDA receptor antagonists, that, in spite of promising results in animal models (Calabresi *et al.*, 2000; Lee *et al.*, 1999) failed to provide neuroprotection in clinical studies on patients (Caplan 1998; Plum 2001).

As reported above, the extracellular adenosine concentration under physiological conditions, calculated by different experimental approaches, is usually relatively constant in a range between 30-200 nM in brain tissue (see: Latini *et al.*, 2001). Both *in vivo* and *in vitro* studies largely demonstrate that this concentration dramatically increases during cerebral ischemia (Hagberg *et al.*, 1987; Latini *et al.*, 1999b; Melani *et al.*, 1999 and 2003; Pearson *et al.*, 2006), reaching values around 3 μM, able to activate all 4 subtypes of adenosine receptors. This is principally due to the rapid and massive depletion of intracellular ATP occurring under metabolic stress conditions, such as hypoxia or ischemia, that lead to an accumulation of AMP, which in turn is degraded to adenosine. The rate of adenosine production thus exceeds its deamination to inosine or its rephosphorylation to AMP (Deussen 2000) leading to a concentration gradient from

the intra- to the extracellular space that causes adenosine to be released by the membrane transporter proteins (ENTs). Furthermore, adenine nucleotides are released into the extracellular compartment and rapidly metabolized to adenosine by NTPDases and e5'-NTs ubiquitously expressed on the cell surface (see figure 3). Therefore, extracellular adenosine concentrations greatly increase reaching micromolar values during hypoxic/ischemic conditions. *In vitro* studies demonstrated that during ischemia adenosine reaches values as high as 30 μM (Latini *et al.*, 1999b).

A neuroprotective role of extracellular adenosine during cerebral ischemia has long been recognised by different authors. In fact it is largely known that adenosine-potentiating agents, which elevate endogenous adenosine by either inhibiting its metabolism (Lin *et al.*, 1992) or preventing its reuptake (Dux *et al.*, 1990), offer protection against ischemic neuronal damage in different *in vivo* ischemia models. Furthermore, adenosine infusion into the ischemic striatum during medial cerebral artery (MCA) occlusion significantly ameliorates the neurological outcome and reduces the infarct volume after transient focal ischemia (Kitagawa *et al.*, 2002). For all these reasons, many authors have indicated adenosine and its receptors as possible targets for therapeutic implementation in the treatment of stroke. All these protective effects of adenosine during cerebral ischemia are mainly due to adenosine A_1 receptor stimulation, that causes a reduction of Ca^{2+} influx, thus inhibiting the presynaptic release of excitatory neurotransmitters (Corradetti *et al.*, 1984; Pedata *et al.*, 1993; Zetterstrom *et al.*, 1990) and in particular of glutamate, whose over-stimulation of NMDA receptors during ischemia is one of the principal mechanisms of neuronal excitotoxicity (Choi 1990). In addition, by directly increasing the K^+ and Cl^- ion conductances at postsynaptic level, adenosine stabilises the neuronal membrane potential and reduces the neuronal hyper-excitability caused by increased glutamate release during ischemia (Tominaga *et al.*, 1992). The consequent reduction in cellular metabolism and energy consumption (Tominaga *et al.*, 1992) and a moderate lowering of the body/brain temperature (Gourine *et al.*, 2004) are protective events under ischemic conditions. Accordingly, *in vitro* models demonstrated that selective A_1 receptor stimulation reduces neuronal damage following hypoxia and/or glucose deprivation in primary cortical or hippocampal cell cultures (Daval *et al.*, 1994) and brain slices (Dux *et al.*, 1992; Marcoli *et al.*, 2003; Mori *et al.*, 1992; Newman *et al.*, 1998; Tanaka *et al.*, 1997). Although data converge in demonstrating a neuroprotective effect of adenosine through A_1 receptors during ischemia, the clinical utility of selective A_1 agonists is hampered by unwanted central and peripheral effects i.e. sedation, bradycardia, hypotension (White *et al.*, 1996).

The role of A_{2A} receptors in cerebral ischemia has been recently studied. Several data support an opposite, deleterious, role of A_{2A} receptors during ischemic brain injury in comparison to adenosine A_1 receptors. In 1994, Gao and Phillis (Gao *et al.*, 1994) demonstrated for the first time that the non-selective A_{2A} receptor antagonist CGS 15943 reduces cerebral ischemic injury in the gerbil following global forebrain ischemia. Thereafter, many reports have confirmed the neuroprotective role of A_{2A} receptor antagonists in different models of ischemia. The selective A_{2A} receptor antagonist CSC, as well as the less selective antagonists CGS 15943 and CP 66713, were able to ameliorate hippocampal cell injury during global forebrain ischemia in gerbils (Phillis 1995; von Lubitz *et al.*, 1995). In agreement with these observations, hippocampal activation of A_{2A} receptors during *in vitro* oxygen and glucose deprivation (OGD) may reduce the beneficial effects mediated by A_1 receptors and, in addition, increase glutamate outflow, thus contributing to the excitotoxic damage. These mechanisms explain the protective effects of A_{2A} selective antagonists during OGD insults (Latini *et*

al., 1999a). Similarly, the selective A_{2A} receptor antagonist SCH 58261 reduced ischemic brain damage in a rat neonatal model of hypoxia/ischemia (Bona *et al.*, 1997) and in an adult rat model of focal cerebral ischemia (Melani *et al.*, 2003 and 2006; Monopoli *et al.*, 1998). Studies in genetically manipulated mice definitely confirmed the neuroprotective role of A_{2A} receptor antagonists on ischemic brain damage. In fact, in A_{2A} receptor knockout mice subjected to focal cerebral ischemia, the cerebral damage and neurological deficits were attenuated (Chen *et al.*, 1999). The beneficial effects brought about by A_{2A} antagonists are mainly attributed to the blockade of A_{2A} receptors located presynaptically on glutamatergic terminals (Hettinger *et al.*, 2001; Rosin *et al.*, 2003) thus reducing the excitotoxic damage (Marcoli *et al.*, 2003). In fact, selective activation of adenosine A_{2A} receptors has been demonstrated to promote glutamate release under normoxic and ischemic conditions (Corsi *et al.*, 1999 and 2000; O'Regan *et al.*, 1992; Popoli *et al.*, 1995; Simpson *et al.*, 1992). In addition, recent data suggest that bone marrow derived cells, injected into rat brains (Yu *et al.*, 2004), and native microglial cells (Melani *et al.*, 2006) are important targets for A_{2A} antagonist-mediated neuroprotection against ischemic damage.

Few studies, due to the paucity of A_{2B} selective agonists and antagonists, indicate a possible role for A_{2B} receptors during brain ischemic damage. In the stratum radiatum of CA1 hippocampal slices, the number and immunostaining density of immunoreactive cells for A_{2B} receptors were increased after ischemic preconditioning (Zhou *et al.*, 2004). In human astroglial cells, the selective A_{2B} receptor antagonist MRS 1706 completely prevents the elongation of astrocytic processes, a typical morphological hallmark of *in vivo* reactive astrogliosis which represents a deleterious process induced by selective stimulation of A_{2B} receptors (Trincavelli *et al.*, 2004).

Taking into account that A_3 receptors are stimulated by micromolar concentrations of adenosine (Fredholm *et al.*, 2001), we may speculate that A_3 mediated effects would become particularly important during ischemia when high levels of extracellular adenosine are reached. Unfortunately, the few studies that are present in the literature concerning the role of A_3 receptors in cerebral ischemia are rather contradictory. The effects of A_3 receptor stimulation appear to depend on drug administration (acute versus chronic), dosage and timing of treatment with respect to the onset of the ischemic insult. *In vivo* experiments show that the acute administration of a selective A_3 receptors agonist, IB-MECA, impaired post-ischemic blood flow, increased tissue necrosis and exacerbated the loss of hippocampal neurones in the gerbil model of global forebrain ischemia (von Lubitz *et al.*, 1994). However, beneficial effects were reported when the A_3 agonist was administered chronically in the same ischemia model (von Lubitz *et al.*, 1994; von Lubitz 1999). Other studies reported that treatment with IB-MECA 20 minutes after focal cerebral ischemia decreases the infarct volume, the intensity of reactive gliosis and the microglial infiltration, whereas IB-MECA administered 20 minutes prior to ischemia increases infarct volume (von Lubitz *et al.*, 2001). Previous studies in my laboratory demonstrated that in a model of *in vitro* ischemic preconditioning, the selective A_3 receptor antagonist MRS 1523 facilitates the full recovery of CA1 hippocampal neurotransmission after a severe (7-minute) oxygen glucose deprivation (OGD) insult (Pugliese et al., 2003). These data are in line with a previous demonstration that the detrimental effects of A_3 receptor activation may be due, at least in part, to the attenuation of the beneficial effects of A_1 receptors (Dunwiddie *et al.*, 1997a). Contrary to the evidence reported, it has been shown that the A_3 receptor agonist, IB-MECA, reduced the amplitude of postsynaptic potentials in the rat cortex under normal (Brand *et al.*, 2001) and hypoxic (Hentschel *et al.*, 2003) conditions. In agreement, A_3 receptor

knockout mice showed more pronounced hippocampal pyramidal neurone damage following repeated episodes of hypoxia and a decline in cognitive function compared to wild-type mice (Fedorova *et al.*, 2003). These histological and cognitive changes were reproduced in wild-type mice by repeatedly administering the selective A_3 receptor antagonist, MRS 1523 (Fedorova *et al.*, 2003).

Since information present in the literature about the role of A_3 receptors during cerebral ischemia is scarce and conflicting at present, we focused our attention on this matter in the present work. In particular, we investigated the role of this adenosine receptor subtype in a model of *in vitro* OGD by evaluating the effect of ischemic insults of different duration on hippocampal neurotransmission. In fact, ischemic episodes occurring in the mammalian CNS result in impairment of neurotransmission and, with increasing duration of ischemia, in increasingly severe tissue damage. The impairment in neurotransmission is, however, not directly correlated with cell death and is reversible if the oxygen and glucose supply is restored within a narrow time window (Latini *et al.*, 1999b; Pugliese et al., 2003). While the disappearance of synaptic activity is the earliest detectable functional sign of tissue suffering, the absence of recovery after interruption of ischemia strongly suggests irreversible neurone damage. We monitored both events to correlate protective or deleterious effects of different A_3 receptor agonists or antagonists applied during OGD of different time duration.

Another typical electrophysiological parameter usually monitored during OGD is a rapid anoxic depolarization (AD) of a sizeable population of brain cells. This event appears as a consequence of prolonged ischemic episodes and is strictly correlated with irreversible neuronal and glial damage (for a review see: Somjen 2001), also contributing to the increase in cell damage in the so called "ischemic penumbral area" (Touzani *et al.*, 2001). An individual section will be devoted to describing this crucial event commonly considered an index of irreversible neuronal ischemic damage.

2. Anoxic depolarization

A typical consequence of a cerebral hypoxic/ischemic insult is the appearance of anoxic depolarization (AD), a rapid and regenerative wave of depolarization that propagates in the brain tissue. A similar response occurs in cerebral grey matter under normoxic conditions, as a consequence of neuronal hyper-excitability (for example during epileptic discharges) and is called spreading depression (SD). These two events are strictly correlated and present the same diagnostic criterion: an accelerating, regenerative, all-or-none type depolarization spreading out from a restricted core of grey matter into the surrounding tissue (Somjen 2001).

SD was described for the first time by Aristides Leão, in 1944, who recorded a cortical electrogram (ECoG) of epileptic discharges obtained by "tetanic" stimulation in anesthetized rabbits. Leão noticed that, immediately after the induced seizure, an unexpected silencing of the ongoing normal electrical activity occurred, and hypothesised that SD and propagation of focal seizures were related phenomena generated by the same cellular elements (Leão 1944). These first observations, later confirmed by others (Van Harreveld *et al.*, 1953), have been later supported by detailed investigations demonstrating that SD is caused by a "negative slow voltage variation" in the cortical surface that was identical to the voltage shift recorded after a few minutes of blood flow deprivation in the cerebral cortex (Leão 1947). By reaching a maximal amplitude of -15 mV, this surface potential shift was astonishingly large compared with other brain waves re-

corded by ECoG and attracted the interest of a number of neurologists. Similarly, severe hypoxia or, more generally, sudden energy failure induce an SD-like response, and "spontaneous" waves of SD emanate from the border of an ischemic core and propagate into the surrounding brain areas (the "penumbra"). To date, SD and AD have been recorded in almost all brain regions, with high similarity and reproducibility among *in vivo* and *in vitro* experiments, but they are more readily provoked in some brain areas than in others. The CA1 region of the hippocampal formation is considered the most susceptible zone, closely followed by the neocortex (Somjen 2001).

Under normoxic conditions, SD can be triggered by a number of different stimuli and chemicals. Among the chemical agents, noteworthy are K^+ ions, glutamate, and acetylcholine, because these molecules are normally present in the brain, and ouabain because it reflects the reduced function of the membrane Na^+-K^+-ATPase during high energy demand or low energy supply and ultimately raises extracellular K^+ concentration, which is known to play a key role in this phenomenon. When ion-selective microelectrodes became available in the '60s, allowing to measure "real time" ion concentration changes in live tissues, it was soon reported an overflow of K^+ ions from the cortical surface during both SD (Brinley *et al.*, 1960) and AD (Vyskocil *et al.*, 1972). This K^+ overload is also accompanied by a precipitous drop in extracellular Cl^- and Na^+ levels and a passive release of organic anions from the cell cytoplasm including glutamate (Davies *et al.*, 1995). This sequence of events suggests that during AD or SD, intra- and extracellular ion concentrations equilibrate and the electrochemical gradient across the cell membrane, which is essential for living functions, is lost. This hypothesis is also supported by the nearly complete depolarization that accompanies these events (Collewijn *et al.*, 1966), typical of cells exposed to high extracellular K^+ concentrations as during SD or AD. In fact, as expressed by Grafstein in the "potassium hypothesis" of SD (Grafstein 1956), K^+ released during intense neuronal firing accumulates in the restricted interstitial space of brain tissue and depolarizes the very cells that released it, resulting in a vicious circle that leads to neuronal hyperexcitability.

Further progresses in describing SD- and AD-related phenomena were made by using intracellular sharp microelectrodes to measure resting membrane potential before, during and after the passage of SD or AD waves. This technique allowed the recording of an abrupt depolarization in cell potential, approaching zero millivolts during SD for some seconds, that was always accompanied by a 90% decrease in membrane input resistance (Collewijn *et al.*, 1966; Muller *et al.*, 2000). The "all-or-none" nature of both events was confirmed by the observation that, once started, the amplitude of membrane depolarization was independent of the severity of the triggering event (Muller *et al.*, 2000). When membrane potential recordings were made simultaneously from stratum radiatum and stratum pyramidale of CA1 hippocampal slices, cell depolarization always began earlier and was of larger amplitude and longer duration in the layer of dendritic trees than in cell somata, suggesting that the triggering region was the dendritic layer and from there the depolarization spreads to the cell bodies (Herreras *et al.*, 1993c). A detailed analysis of the time course of different AD-related events in the hippocampus demonstrated that the onset of voltage changes was usually preceded by increased neuronal excitability that produced a "shower of population spikes" reflecting synchronized firing of pyramidal neurons (Grafstein 1956; Herreras *et al.*, 1993b). This neuronal hyperactivity, also recorded during *in vivo* experiments (Rosenblueth *et al.*, 1966), was shown to be strictly related to glutamate-induced excitotoxicity, since the voltage changes produced during AD or SD were greatly reduced by NMDA receptor antagonists (Herreras *et al.*, 1993a), that are well known neuroprotective agents against

ischemia-induced damage of the brain tissue in experimental models (Calabresi *et al.*, 2000; Lee *et al.*, 1999). In addition, the exogenous application of glutamate to the cortical surface is able to induce SD (Van Harreveld 1959). Evidence indicates, however, that a much reduced but still substantial ion gradient remains across the plasma membrane during AD (Muller *et al.*, 2000).

The massive redistribution of ions between the intra- and extracellular compartment during AD and SD leads to significant changes in cell homeostasis, reflected by the prominent cell swelling that accompany both phenomena. Leão himself firstly described a transient increase in tissue electrical impedance accompanying SD (Leão *et al.*, 1953), and this was soon confirmed by others (Hoffman *et al.*, 1973; Ochs *et al.*, 1956). The major effect was the increase in tissue resistance, and was confirmed by morphological studies to be caused by swelling of cells leading to shrinkage of the interstitial space (Kow *et al.*, 1972; Van Harreveld *et al.*, 1959). Another parameter usually measured to monitor *in vitro* induced SD or AD is the intrinsic optical signal (IOS). Cell swelling produces a marked change in intracellular volume that is reliably associated with a decrease in light scattering (Aitken *et al.*, 1999), attributable to the dilution of scattering particles in the cytosol (Barer *et al.*, 1953). This sequence of events leads to a pronounced increase in the IOS of brain tissue, as reported for the first time by Snow *et al* in hippocampal slices during SD (Snow *et al.*, 1983). This new approach permitted a detailed real-time two-dimensional mapping (not reachable with microelectrodes) of SD and AD spread, simultaneously recorded with other parameters (for example membrane potential or extracellular K^+ concentration), as exemplarily reported by Obeidat and Andrew (Obeidat *et al.*, 1998). Again, in hippocampal slices, the IOS triggered by AD or SD was stronger and occurred more rapidly in the dendritic layer of stratum radiatum than in the somatic region of stratum pyramidale (Aitken *et al.*, 1998; Muller *et al.*, 1999).

In spite of the many similarities between SD and AD events, some differences have also been described. For example, depolarization in SD is "self-limiting" and is followed by complete restoration of neuronal functions as soon as neurons recover their resting membrane potential, without any "irreversible side effects" at least after sparce SD events. On the contrary, after an AD, membrane potential and neuronal functions only recover if oxygen is restored soon after the onset of depolarization (Lipton 1999) since oxidative energy (O_2 and ATP consumption) is required to restore ion gradients (Wang *et al.*, 2000). If the ischemic insult persists during AD manifestation, neuronal damage will become irreversible and only a partial recovery of brain tissue functionality can be achieved. This seems to be mainly due to the deleterious role of a protracted intracellular Ca^{2+} rise, an event typically recorded during ischemia. In this regard it may be argued that, during normoxic SD, neurons gain as much Ca^{2+} as during AD but do not encounter such irreversible damage because membrane depolarization is self-limiting and only lasts for a few seconds. In fact, it has been demonstrated that if neurones are forced to remain depolarized for extended periods after SD triggering, even in well-oxygenated tissues they do not regain function (Herreras *et al.*, 1993b; Kawasaki *et al.*, 1988). Accordingly, if Ca^{2+} is removed from the bathing solution before oxygen is withdrawn, neurons recover their functions following a period of hypoxia that otherwise would have caused irreversible damage (Siesjo, 1989). It appears that intracellular Ca^{2+} levels must remain elevated for a critical length of time to initiate the reactions that result in irreversible cell injury (Deshpande *et al.*, 1987; Morley *et al.*, 1994). It follows that any treatment that postpones the onset of AD should extend the time limit of cell recovery. This concept has been largely confirmed by both *in vivo* and *in vitro* studies

and represents the basis of the present work to investigate the effect of different drugs acting on purinergic systems during ischemia. On these basis, we monitored AD appearance in hippocampal slices as an index of irreversible tissue damage induced by *in vitro* ischemia and we investigated the role of purinergic receptors during such insults (Obeidat *et al.*, 1998).

3. Role of P2 receptors

Studies on the functional role of P2 receptors are a recent field of research in comparison to the adenosine effects. ATP- or UTP-mediated actions have been reported in a number of tissues. Early evidence, as already anticipated in the "historical overview", came from the cardiovascular system, with observations by Drury and Szent-Gyorgyi, in 1929, reporting complex chronotropic and inotropic effects mediated by extracellular ATP on Langendorf's heart model (Drury *et al.*, 1929). Subsequent evidence about ATP-mediated effects came from the gastrointestinal system, where ATP has been firstly recognised to act as a co-transmitter with either VIP and/or NO playing a role in NANC-mediated inhibition of taenia coli motility (Burnstock *et al.*, 1963) and contraction of the esophageal sphincter (Castell 1975). A few years later, the presence of both vasoconstricting P2X receptors and vasodilating P2Y receptors in pulmonary vessels was demonstrated in rats and humans (Liu *et al.*, 1989a and 1989b). In addition, in airway epithelial cells, ATP enhances the synthesis and secretion of mucins via P2 receptor activation (Davis *et al.*, 1992). Another important aspect in which ATP exerts a key role is haemostasis, where ATP, but mostly ADP, was recognised early on as one of the most potent stimulators of platelet aggregation (Gaarder *et al.*, 1961). This discovery led to the first clinical use of a P2-related drug, clopidogrel, a prodrug of an irreversible $P2Y_{12}$ antagonist, that has proved to be effective in inhibiting pro-aggregation signals via the platelet-specific $P2Y_{12}$ ADP receptor and is used in the prevention of cardiovascular events (van Giezen *et al.*, 2005). A related compound, the selective and competitive $P2Y_{12}$ antagonist cangrelor (also known as AR-C69931MX), is now in the late stage of Phase II clinical trials for haemostasis disorders with promising results (Fugate *et al.*, 2006).

It has long been known that ATP acts as an extracellular messenger in inflammatory responses. This finding encouraged the exploration of P2 antagonists as new target for anti-inflammatory drug development. Most evidence attributes a key role for $P2X_7$ in this function; in fact this receptor is highly expressed in immune cells, including microglia, macrophages, lymphocytes, and dendritic cells (Collo *et al.*, 1997), where it mediates cytotoxic responses, cytokine release, and phagocytosis-associated cell fusion. For example, it has been shown that $P2X_7$ receptor activation in macrophages and microglial cells is one of the most potent stimuli for interleukin-1β (IL-1 β) secretion in response to lipopolysaccharide (LPS) stimulation (Ferrari *et al.*, 1997) and promotes cell infiltration and chemokine release in *in vivo* tissues (Fulgenzi *et al.*, 2005). Further studies in $P2X_7$-deficient mice confirmed the involvement of this receptor in inflammatory (Solle *et al.*, 2001) and immune (Labasi *et al.*, 2002) processes.

Among the impressive variety of actions mediated by extracellular purine nucleotides, it is helpful to focus on the involvement of P2 receptors in neurotransmission under physiological and pathological conditions, since most research of this thesis has been performed in the brain using electrophysiological techniques. The role of P2 receptors has been also investigated during *in vitro* OGD; thus a describtion of the

present knowledge on ATP and degenerative events is needed. Another important field concerns the involvement of P2 receptors in mediating trophic effects related to cell development and proliferation, since part of the research was dedicated to study ATP-mediated effects in a bone-marrow stem cell lineage. For this reason, a whole paragraph will be devoted to explore each of these arguments.

3.1 P2 receptors and neurotransmission

Differently from adenosine, ATP is considered itself a neurotransmitter since it presents all the typical features of this class of molecules:
1) It is stored in vesicles at presynaptic nerve terminals and released in quanta upon specific stimulation (electrically or chemically-induced depolarization).
2) Its extracellular concentration is finely tuned and transmitter action terminated by the coordinated action of catalytic enzymes (NTPDases) acting in the order of ms.
3) It is able to activate specific receptors on the postsynaptic membrane (P2X and P2Y receptors) which may directly elicit postsynaptic currents or membrane depolarization with a modest delay (in the case of P2X-mediated EPSCs: time delay in the order of to 1-2 ms), to propagate an electrical stimulus among adjacent excitable cells for relatively "long" distances.

Investigation into P2-mediated effects on neurotransmission have been historically complicated by the neuromodulatory role of adenosine in the CNS, since extracellularly released ATP is rapidly converted to its metabolite adenosine and, in addition, P1 receptors are widely expressed in the CNS. However, in the last 15 years, the role of P2 receptors in synaptic activity has been better elucidated, thanks to novel pharmacological tools able to selectively bind to specific P2 receptors. While ionotropic P2X receptors are mainly involved in fast synaptic transmission, directly eliciting synaptic currents (Edwards *et al*, 1992; Bardoni *et al.*, 1997; Khakh, 2001 Pankratov *et al.*, 1998; 2002; 2006), metabotropic P2Y receptors rather mediate slower neuromodulatory effects, eliciting changes in neuronal excitability or neurotransmission mainly through the G protein-related modulation of ligand-gated or voltage-gated ion channels, either at pre- or postsynaptic sites of action.

P2X-receptor mediated synaptic currents were first described in the peripheral nervous system. In late '80s-early '90s, it was demonstrated that cultured rat sensory neurons (Krishtal *et al.*, 1988) and cardiac parasympathetic ganglion cells (Fieber *et al.*, 1991) and sympathetic ganglion cells (Evans *et al.*, 1992; Cloues, 1995) displayed inward currents in the presence of exogenous ATP. These ATP-elicited currents presented the typical features of P2X-mediated conductances: a tiny delay between ATP application and current onset (less than 20 ms), strong inward rectification, Na^+ and Ca^{2+} permeability, a reversal potential around 0 mV, a single-channel conductance around 20-50 pS and, obviously, a marked sensitivity to P2 antagonists (suramin and RB2). Within the CNS, the first evidence of ATP-mediated synaptic currents came a few years later from a study in the medial habenula (Edwards *et al.*, 1992a), who demonstrated that, after exclusion of glutamate, GABA and ACh-gated ionotropic receptors with selective antagonists, it was still possible to evoke inward synaptic currents, TTX- α–β-meATP and suramin-sensitive, by electrical stimulation. In the same work, the existence of endogenous ATP release was suggested by the observation that suramin alone diminished both the frequency and the amplitude of miniature excitatory postsynaptic currents

(mEPSCs) recorded in the presence of TTX. Soon after, a number of evidences strongly supported a role of ATP as a fast neurotransmitter in other brain regions: locus ceruleus (Nieber *et al.*, 1997), trigeminal mesencephalic nucleus (Khakh *et al.*, 1997), spinal cord dorsal horn (Bardoni *et al.*, 1997), hippocampal CA1 (Pankratov *et al.*, 1998) and CA3 (Mori *et al.*, 2001) regions and somato-sensory cortex (Pankratov *et al.*, 2002).

At a presynaptic level, P2X receptor activation enhances neurotransmitter release (Cunha et al., 2000). $P2X_7$ subtypes seems to be particularly important in this effect. Their stimulation enhances glutamate release from rat dorsal horn neurons in the spinal cord (Nakatsuka et al., 2001) and in the mesencephalic nucleus (Khakh *et al.*, 1998), evidence consistent with the mainly presynaptic expression of these receptors (Deuchars *et al.*, 2001; but see Sim *et al.*, 2004 for a re-examination of this role). Several data demonstrate an important role of $P2X_7$ receptors in modulating neurotransmitter release in the hippocampus, where their stimulation induces either glutamate outflow from pyramidal cells and GABA release from hippocampal interneurones (Sperlagh *et al.*, 2002). In this brain region, $P2X_7$ receptors are also expressed by astrocytes and seem to participate to the increased glutamate release (Duan *et al.*, 2003).

P2Y receptors can modulate neurotransmission mainly by G protein coupling and consequent alterations in the opening and closure of ion channels, either voltage- or ligand-gated, at both pre- and postsynaptic level. Since a considerable section of the present work was aimed to investigate the modulation of ionic conductances by P2Y receptor activation in different cell types, this subject will be described in detail, describing the present status of knowledge in the field.

Among voltage-gated channels, Ca^{2+} and K^+ conductances are the major mediators of P2Y effects. The first evidence for regulation of voltage-activated Ca^{2+} channels via P2Y receptors was obtained in adrenal chromaffin cells, where ATP and ADP application caused a pertussis toxin (PTX)-sensitive reduction of current amplitudes (Diverse-Pierluissi *et al.*, 1991; Lim *et al.*, 1997), an effect sensitive to RB2 and mediated by the inhibition of N- and P/Q-type calcium channels (Gandia *et al.*, 1993; Powell *et al.*, 2000). Similarly, in NG108-15 neuronal hybrid cells, not only adenine but also uridine nucleotides (UTP and UDP) inhibited N-type as well as L-type Ca^{2+} channels in a PTX-sensitive and insensitive manner, respectively (Filippov *et al.*, 1996). Several other cases have been subsequently reported. In general, $P2Y_{12}$ mediated effects were found to be PTX-sensitive, as expected for $G_{i/o}$ coupled receptors, and mediated by a membrane-delimited pathway, likely due to a direct interaction of the $G_{i/o}$ βγ subunit with the Ca^{2+} channel (Simon *et al.*, 2002). In contrast, the inhibition of Ca^{2+} current via $P2Y_{1,2,4}$ and $_6$ receptors included two components: a PTX-sensitive and membrane-delimited pathway, as well as a PTX-resistant second messenger-mediated mechanism (Filippov *et al.*, 1998 and 1999). The diffusible second messenger involved in the effect was found to be a product of PLCβ-dependent hydrolysis of membrane phosphatidylinositol 4,5-bisphosphate (PIP_2: Lechner *et al.*, 2005; Gamper *et al.*, 2004). Circumstances were complicated by the fact that some P2Y-mediated responses seemed to depend on the experimental procedure used. For example, some authors reported that $P2Y_4$-mediated inhibition of Ca^{2+} currents was solely observed in the perforated patch configuration, whereas almost no inhibition was recorded in the standard whole-cell mode (Filippov *et al.*, 2003) implying involvement of a diffusible second messenger. At the functional level, voltage-activated Ca^{2+} channels, in particular N- and P/Q-type channels, are located at presynaptic nerve terminals and link invading action potentials to transmembrane Ca^{2+} influx and concomitant vesicle exocytosis (Catterall *et al.*, 2003). As a consequence, the inhibition of voltage gated Ca^{2+} currents by adenine and uridine

nucleotides may be responsible for the reduction in neurotransmitter release reported in different brain regions after stimulation of P2Y receptors, such as the hippocampus (Mendoza-Fernandez *et al.*, 2000; Rodrigues *et al.*, 2005) and cortex (von Kugelgen *et al.*, 1994 and 1997). In addition, changes in Ca^{2+} influx in neurones may also affect the activity of Ca^{2+}-dependent K^+ channels, that are known to shape single action potentials and regulate firing frequency adaptation (Faber *et al.*, 2003).

However, nucleotides were not only found to exert inhibitory effects on neuronal Ca^{2+} channels. ATP, for instance, may increase Ca^{2+} currents in hippocampal neurons (Dave *et al.*, 1996), a result also reported for rat cardiac cells (Scamps *et al.*, 1994). Unfortunately, the receptor subtypes responsible for these effects are still unknown.

Some of the mechanisms underlying the regulation of voltage-activated Ca^{2+} channels via P2Y receptors are shown in figure 10.
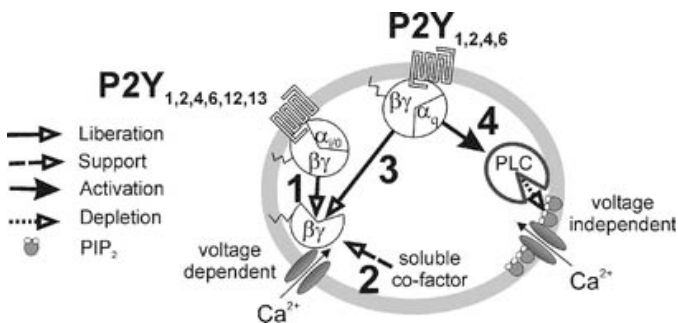
Figure 10. P2Y nucleotide receptors may use at least four different pathways to modulate neuronal Ca^{2+} channels: (1) Activation of P2Y receptors coupled to PTX-sensitive $G_{i/o}$ proteins sets βγ subunits free which directly interact with pore-forming Ca^{2+} channel proteins. (2) The same pathway sometimes also requires a soluble cofactor in addition to the membrane-associated G proteins. (3) Some P2Y receptors may also mediate such a voltage-dependent inhibition of Ca^{2+} currents via PTX-insensitive G proteins. (4) Activation of P2Y receptors linked to PTX-insensitive $G_{q/11}$ proteins initiates a signal cascade that involves diffusible second messengers and mediates inhibition of Ca^{2+} currents . For other $G_{q/11}$-coupled receptors (e.g., muscarinic or bradykinin receptors), this pathway was found to involve an activation of phospholipase C and a depletion of membrane phosphatidylinositol 4,5-bisphosphate. Taken from: Hussl et al., 2006.

Aside from voltage-gated Ca^{2+} channels, a variety of neuronal K^+ channels have been found to be modulated by extracellular nucleotides. Quite a number of different K^+ channels were reported to be modulated by various neurotransmitters, but the most intensively studied examples of K^+ channel regulation via GPCRs are inward rectifier channels (Kir belonging to Kir3, also called GIRK family) and KCNQ channels.

Concerning GIRK channels, it is known that the activation of $G_{i/o}$-linked receptors generally opens these channels (Fernandez-Fernandez *et al.*, 2001) whereas $G_{q/11}$-linked receptors usually lead to their closure (Hussl *et al.*, 2006). Many inhibitory neurotransmitters, included GABA and adenosine, cause hyperpolarizations by activating inwardly rectifying K^+ currents via receptors linked to PTX-sensitive G proteins. Accordingly, opening of GIRK channels by 2MeS-ADP in superior cervical ganglion neurons transfected with $P2Y_{12}$ receptors, that are typically coupled to $G_{i/o}$ proteins (Simon *et al.*, 2002) and a closure of GIRK channels after $P2Y_{1,2,4,6}$ receptor activation (in cells transfected with each of these receptor subtypes) in a PTX-insensitive manner has been

described (Filippov *et al.*, 2004; Mark *et al.*, 2000). Again, the latter mechanism has been attributed to PIP_2 hydrolysis and IP_3-mediated intracellular signalling pathways (Filippov *et al.*, 2004).

Among KCNQ channels, the best studied example is the M-current (I_M), that is inhibited through the activation of various GPCR coupled to $G_{q/11}$ proteins by PLCβ activation and PIP_2-IP_3-coordinated signalling (muscarinic M1-mediated closure of such a channel was the first example of this mechanism described by Brown and Adams in 1980: Brown *et al.*, 1980). Several neurotransmitters depolarize neurons by inhibiting M-type currents, an effect that is also shared by extracellular nucleotides, as demonstrated by the inhibition of I_M by UTP (Adams *et al.*, 1982) and ATP (Akasu *et al.*, 1983; Tokimasa *et al.*, 1990) in bullfrog sympathetic neurons. This was one of the first examples of a modulation of K^+ channels by nucleotides and, although the receptors involved in these effect remained unknown at that time, the inhibition of I_M by nucleotides was shown to be mediated by a G protein (Lopez *et al.*, 1989). Subsequent studies were aimed at identifying the P2Y subtype involved in I_M inhibition. Most of them recognized a UTP-preferring receptor involved in this effect: in NG108-15 hybrid cells, activation of the PLC-linked $P2Y_2$ receptor was reported to lead to an inhibition of I_M (Filippov *et al.*, 1994). Accordingly, $P2Y_6$, was found to mediate an inhibition of I_M in rat superior cervical ganglion neurons (Boehm 1998), and $P2Y_4$ in bullfrog sympathetic neurons (Meng *et al.*, 2003). In all cases, the signalling cascade underlying this effect involved an activation of PLC, generation of IP_3, and release of Ca^{2+} from intracellular stores (Bofill-Cardona *et al.*, 2000).

Another class of K^+ channels modulated by P2Y receptor activation is that of Ca^{2+}-sensitive-K^+ channels. These channels, divided into BK, SK or IK channels, are activated by increased intracellular Ca^{2+} levels either due to Ca^{+2} entry from voltage-dependent channels (L-type, N-type) or from the release of Ca^{2+} ions from intracellular stores. Since P2Y receptors mainly activate PLC-mediated intracellular Ca^{2+} release, they are a good candidate to elicit Ca^{2+}-activated K^+-channel opening. In fact, it has already been demonstrated that P2Y receptor stimulation indeed activates BK channels (in retinal Muller cells: Bringmann *et al.*, 2002; in clonal kidney cells: Hafting *et al.*, 2000) and SK channels (colon smooth muscle cells :Koh *et al.*, 1997; Zizzo *et al.*, 2006).

At a functional level, modulation of K^+ channels (GIRK, KCNQ, BK or SK) will cause changes in postsynaptic excitability rather than in neurotransmitter release, due to the preferentially dendritic and somatic expression of such proteins.

Some of the mechanisms underlying the regulation of GIRK and KCNQ channels via P2Y receptors are presented in figure 11.

Furthermore, it has been recently demonstrated that some non-selective cationic conductances can be activated by $P2Y_1$ receptor stimulation. In fact, data in the mouse hippocampus demonstrate that, in CA1 and CA3 regions, $P2Y_1$ agonists can evoke an inward cationic conductance that depolarizes GABAergic interneurones (Bowser *et al.*, 2004; Kawamura *et al.*, 2004). Similarly, in rat megakaryocytic cells, $P2Y_1$ receptor stimulation activates some non-selective cationic conductances belonging to the family of transient receptor potential channels (TRP channels) (Tolhurst *et al.*, 2005) that elicits an inward Na^+-Ca^{2+} mixed current. Both mechanisms are mediated by G_q protein-induced activation of PLC.

Finally, some ligand-gated ion channels were found to be regulated via P2Y receptors. One prominent example is the glutamatergic NMDA receptor that is also modulated by other GPCRs. Adenine and uridine nucleotides were reported to enhance currents elicited by NMDA in layer V pyramidal neurons of the rat prefrontal cortex. This

effect was firstly proposed to be mediated by P2Y$_2$ receptors (Wirkner *et al.*, 2002). However, a recent study by the same authors, demonstrated that this effect was due to the activation of P2Y$_4$ receptor expressed by astrocytes and involved the stimulation of type I mGluR (Wirkner *et al.*, 2006). In contrast, activation of P2Y$_1$ receptors inhibited currents through the NMDA receptors (Luthardt *et al.*, 2003) in the very same cells. In addition, ATP was found to inhibit NMDA receptors independently of P2Y receptors; this effect involved a direct binding of the nucleotide to the glutamate-binding site of the NR2B subunit of NMDA receptors (Ortinau *et al.*, 2003; Kloda *et al.*, 2004). Another transmitter-gated ion channel that was found to be modulated by nucleotides is the vanilloid receptor 1 (VR1) that might be relevant in peripheral sensory neurons. In rat DRG neurones, capsaicin-evoked currents through VR1 were enhanced by nucleotides (Tominaga *et al.*, 2001). This potentiation was abolished by a PKC inhibitor and mimicked by phorbol esters (PKC activators). These results indicated that a P2Y receptor linked to PKC via G$_{q/11}$ proteins was involved. Moreover, UTP was reported to be as potent an agonist as ATP, and suramin abolished the potentiation of VR1 by UTP. The authors concluded that P2Y$_2$ receptors mediated the facilitatory effects of nucleotides on VR$_1$ in mouse and rat dorsal root ganglion neurons (Moriyama *et al.*, 2003).
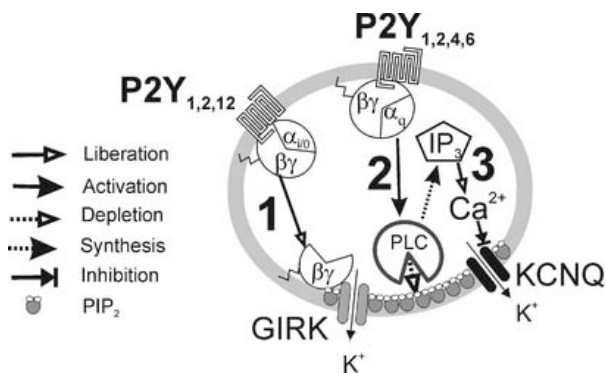
Figure 11. P2Y nucleotide receptors may use at least three different pathways to modulate the functions of GIRK and KCNQ channels: (1) Activation of P2Y receptors coupled toPTX-sensitive G$_{i/o}$ proteins sets βγ subunits free which directly interact with Kir3 proteins to activate the channels. (2) Activation of P2Y receptors linked to PTX-insensitive G$_{q/11}$ proteins leads to the activation of phospholipase C, which uses membrane phosphatidylinositol 4,5-bisphosphate (PIP$_2$) to synthesize inositol triphosphate (IP3) and diacyl glycerol. Via the depletion of PIP$_2$, GIRK channels as well as KCNQ channels are closed. (3) The accumulating IP$_3$ liberates Ca^{2+} from intracellular stores, and the increase in cytosolic Ca^{2+} inhibits KCNQ channels via calmodulin. Take from: Hussl et al., 2006.

3.2 P2 receptors and cerebral ischemia

The role of P2 receptors may become critical during pathological conditions such as ischemia, when extracellular ATP concentrations increase. Again, elucidation of the role of P2 receptors in such pathological conditions is complicated by the concomitant increase in adenosine levels, whose activation of P1 receptors has already been described. An enhanced outflow of radioactive ATP from hippocampal slices during *in*

vitro ischemic-like insults was first reported by Juranyi and co-workers (Juranyi *et al.*, 1999) and the first demonstration that ATP outflow increases *in vivo* during the induction of focal ischemia in the rat was reported by Melani and colleagues (Melani *et al.*, 2005). Evidence supports the idea that, under such pathological conditions, released ATP may exert a cytotoxic role. Intrastriatal ATP injection in rats induced, 24 hours later, a clearly lesioned area (Ryu *et al.*, 2002). The ATP-induced damage was concentration-dependent, mimicked by ATPγS and α,β meATP (but not by ADP or adenosine) and blocked by RB2, a non-specific P2 antagonist (Kharlamov *et al.*, 2002). Suramin, another non-specific P2 receptor antagonist, administered 30 minutes before occlusion of the middle cerebral artery, resulted in a significant decrease in infarct and oedema volume 6h after brain injury (Kharlamov *et al.*, 2002). In agreement, it has been demonstrated that RB2 (Melani *et al.*, 2006) and PPADS (Lammer *et al.*, 2006) improve neurological deficit and reduce the damage induced in rats in a model of focal ischemia *in vivo*. Protective effects of P2 receptor antagonists (suramin, BBG and RB2), on cell survival were also demonstrated in organotypic hippocampal slices exposed to OGD (Cavaliere *et al.*, 2001a; 2003 and 2004).

3.3 P2 receptors and trophic effects

In contrast to the toxic effects described above, P2 receptors can also exert trophic actions on cell growth and development as well as regeneration and proliferation in different tissues, including the brain (Franke *et al.*, 2006). The first indication for an ATP-mediated role came from a study on PC12 cells at the beginning of the '90s, where the authors demonstrated that ATP enhanced neuronal growth factor- (NGF)-induced neurite outgrowth, although ATP alone did not cause any neurite development. This mechanism was found to be mediated by ATP-induced Ca^{2+} influx, rather than to intracellular mobilization of the ion, and the consequent increase in cytosolic Ca^{2+} levels was the triggering signal (Aono *et al.*, 1990). Subsequent studies reported not only that the synergistic action of ATP and this trophic factor was also shared by UTP (Pooler *et al.*, 2005) and blocked by P2 antagonists (D'Ambrosi *et al.*, 2000), but also that extracellular nucleotides stimulate the synthesis and release of both NGF and fibroblast growth factor (FGF) from the same cell system (D'Ambrosi *et al.*, 2001; Huang *et al.*, 1996). Further studies demonstrated that ATP activation of $P2Y_2$ receptors enhances NGF-induced neurite outgrowth also in DRG neurones and inhibits serum-deprivation induced apoptosis by activation of the MAPKs cascade in both DRG neurones and PC12 cells (Arthur *et al.*, 2005; Arthur *et al.*, 2006). The anti-apoptotic mechanism activated by ATP in PC12 cells was demonstrated to involve the up regulation of some heat shock proteins (HSP70 and HSP90), the prevention of caspase-2 cleavage and the inhibition of cytochrome C release from mitochondria into the cytoplasm (D'Ambrosi *et al.*, 2004). P2 receptor activation was also reported to promote fibre outgrowth in the developing hippocampus (Heine *et al.*, 2006; Skladchikova *et al.*, 1999), but it remain elusive whether this effect is mediated by P2X or P2Y receptors. The unique i*n vivo* study available at present reports that injection of a stable ATP analogue, ATPγS, in the rat sciatic nerve is effective in enhancing the expression of growth-associated protein-43 (GAP-43), a marker for axonal growth, in wild-type but not $P2Y_2^{(-/-)}$ mice (Arthur *et al.*, 2005).

In the last few years, exciting results came from studies about stem cells. This field of research is receiving vast consideration among scientists since the growing knowledge of stem cell physiology and functions allows their employment as initial materi-

al for organ-engineered constructs and tissue repair. The intriguing results about the trophic roles mediated by extracellular purines and pyrimidines stimulated the investigation of similar effects also in immature, stem cell-like systems. Indeed, it has been demonstrated that various lineages of undifferentiated cells, such as haematopoietic stem cells (Lemoli *et al.*, 2004; Sak *et al.*, 2003), neuronal progenitor stem cells (Hogg *et al.*, 2004; Ryu *et al.*, 2003) and oligodendrocytes progenitors (Agresti *et al.*, 2005) respond to extracellular ATP with an increased proliferation, differentiation and/or migration by intracellular signalling cascades that are similar or synergistic to that activated by numerous growth factors. Particularly interesting data correlate these trophic effects with the occurrence of spontaneous Ca^{2+} waves that propagate among adjacent cells in a self-renewing manner. In fact, it is known that Ca^{2+}-dependent signalling pathways play crucial roles in cellular proliferation and differentiation (Clapham 1995). Such mechanism that promote periodic oscillation of intracellular Ca^{2+} seem to be triggered by a diffusible extracellular messenger spontaneously released by different kind of cells. At least in some cases ATP has been proposed to be the most likely candidate implicated in such a mechanism. In fact it was shown that a number of cultured cells, like astrocytes (Anderson *et al.*, 2004), osteoblasts (Jorgensen *et al.*, 1997; Henriksen *et al.*, 2006), fibroblasts (Gerasimovskaya *et al.*, 2002), striatal-derived cells from rat embryos (Scemes *et al.*, 2003) and endothelial cells (Gomes *et al.*, 2005a) can release ATP in an autocrine/paracrine manner, and through the activation of P2 receptors (mainly P2Y) induces the propagation of such Ca^{2+} waves. In a particularly interesting study, it was demonstrated that ATP-mediated propagation of Ca^{2+} waves through radial glial cells modulates neurogenesis in embryonic rat neocortex (Weissman *et al.*, 2004).

Aim of the study

The aim of the present study was to investigate the role of P1 and P2 purinergic receptors stimulation in different *in vitro* cell systems. In particular, this thesis is subdivided into two principal sections, differing either in methodological approaches or in the means of investigation.

1. The first section is entitled: "Role of purines in CA1 hippocampal neurotransmission under normoxic conditions and during OGD. Extracellular recordings from rat hippocampal slices."

   Within this argument of research two major points have been analysed:
   - Chapter 1: "Role of A_3 adenosine receptors during OGD."
   - Chapter 2: "Role of P2 purinergic receptors in CA1 neurotransmission under normoxic conditions and during OGD."

2. The second section is entitled: "Studies on P2 receptor modulation of membrane ionic currents by patch clamp recordings."

   Within this argument of research three major points have been analysed:
   - Chapter 3: "Role of $P2Y_1$ receptor stimulation in medium spiny neurons of rat striatal slices."
   - Chapter 4: "Role of purine nucleotides in cultured hMSCs: release of ATP and activation of P2 receptors."
   - Chapter 5: "Pharmacological characterization of the recently deorphanized GRP17 receptor transfected in 1321N1 astrocytoma cells."

Materials and methods

All animal procedures were conducted according to the European Community Guidelines for Animal Care (DL 116/92, application of the European Communities Council Directive 86/609/EEC) and approved by the Committee for Animal Care and Experimental Use of the University of Florence

1. Extracellular recordings

1.1 Acute rat hippocampal slices preparation.

Male Wistar rats (Harlan Italy; Udine Italy, 150-200 g body weight) were anesthetized with ether and decapitated with a guillotine. The hippocampi were rapidly removed and placed in ice-cold oxygenated (95% O_2 - 5% CO_2) artificial cerebral spinal fluid (aCSF) of the following composition (mM): NaCl 124, KCl 3.33, KH_2PO_4 1.25, $MgSO_4$ 1.4, $CaCl_2$ 2.5, $NaHCO_3$ 25 and D-glucose 10. Slices (400 μm nominal thicknesses) were cut using a McIlwain tissue chopper (The Mickle Lab. Engineering, Co. LTD., Gomshall, U.K.) and kept in oxygenated aCSF for at least 1 h at room temperature.

1.2 Experimental procedure

After 1 h incubation at room temperature following surgical preparation, a single slice was placed on a nylon mesh, completely submerged in a small chamber (0.8 ml) and superfused with oxygenated aCSF (30-32°C) at a constant flow rate of 1.5 ml min^{-1}. The treated solutions reached the preparation in 60 s and this delay was taken into account in our calculations. Stimulation pulses (80 μs duration, frequency; 0.066 Hz) were delivered through a bipolar nichrome electrode positioned in the stratum radiatum of the CA1 region of the hippocampus to stimulate the Schaffer collateral/commissural pathway. Evoked potentials were extracellularly recorded with glass microelectrodes shaped by a vertical pipette puller (David Kopf Instruments model 700C, Tujung, California, USA) from borosilicate capillaries (GC100F-15, outer diameter 1.0 mm, inner diameter 0.58 mm, Harvard Apparatus Ltd) filled with 150 mM NaCl. Tip resistance was 2-10 MΩ. The recording electrode was placed at the soma or at dendritic level of the CA1 region to record population spikes (PSs) or field excitatory postsynaptic potentials (fEPSPs), respectively. Responses were amplified (BM 622, Mangoni, Pisa, Italy), digitized (sample rate, 33.33 kHz), low-pass filtered in direct current (DC) mode at 10 kHz and stored for later analysis using LTP software facilities (version 2.30D, William W. Anderson 1991-2001).

The amplitude of the fEPSP was measured as the difference between the negative peak following the afferent fibre volley and the baseline value preceding the stimulus artefact. In some experiments both the amplitude and the initial slope of fEPSP were quantified, but since no appreciable difference between these two parameters was observed in control conditions, in the presence of drugs or during *in vitro* ischemia, only the measure of the amplitude was expressed in figures. The amplitude of PS was measured as the difference between the peak negativity and the averaged values of the two peak positivities following the stimulus artefact.

When a stable baseline of evoked responses was reached, time course of fEPSP or PS amplitudes was routinely measured and expressed as the percentage of the averaged values recorded 5 minutes before the application of any treatment. In some experiments, we also monitored the time course of extracellular potential preceding the stimulus artefact in DC mode. AD appearance was recorded as a negative shift in the DC voltage induced by prolonged OGD conditions. All compounds were applied by bath superfusion, a complete exchange of solutions was reached 60 s after switching the superfusion, and this delay was taken into account in our time course calculation.

1.3 Protocols used

Stimulus-response curves: at the beginning of each experiment, stimulus-response curves were obtained by gradual increase in stimulus intensity till saturation of the response. The response evoked at each stimulus intensity was measured by averaging the amplitude of three consecutive fEPSPs evoked by sweeps of the same strength. The stimulus intensity was then adjusted to produce a response whose amplitude was 40 to 50% of the maximum and was kept constant throughout the experiment. In some cases, the same stimulus-response curve was repeated during the experiment, at representative times after treatments, as indicated in the result session.

Paired pulse facilitation (PPF): to elicit PPF of the fEPSP pairs of stimuli were applied to the Schaffer collateral/commissural fibres with a 40 ms inter-pulse interval. The synaptic facilitation was quantified as the ratio (P2/P1) between the amplitude of the fEPSP elicited by the second (P2) and the first (P1) stimuli. When applied, PPF was monitored for at least 5 minutes before, during and after the application of each drug. The effects of different drugs on PPF were evaluated by measuring the P2/P1 ratio obtained before, during and 10 minutes after drug application.

1.4 OGD conditions

In vitro OGD was obtained by perfusing the slice with glucose-free aCSF gassed with nitrogen (95% N_2 - 5% CO_2). This caused a drop in pO_2 in the recording chamber from about 500 mm Hg (normoxia) to a range of 120–150 mmHg (after 2 min OGD) and of 35-75 mm Hg (after 7 minutes of OGD) (Pugliese et al., 2003), measured with an ISO2 and its associated OXEL-1 probe (WPI, Aston, U.K.). At the end of the ischemic period, slices were superfused with normal, glucose-containing, oxygenated aCSF. The effects of different OGD time duration on hippocampal slices were evaluated by monitoring the time course of fEPSP amplitude and the appearance of AD as negative shifts in the DC mode induced by OGD (Pugliese *et al.*, 2003; Pugliese *et al.*, 2006).

2-minute OGD protocol: A 2-minute OGD insult induces a partial and reversible depression of synaptic neurotransmission in the CA1 hippocampal region that started about 2 minutes after OGD application and fully reverts within 5 minutes from nor-

moxic reperfusion. This short-lasting ischemic insult does not significantly change the DC amplitude. In a typical experimental day, a control slice was submitted to 2 consecutive 2-minute OGD insults separated by 40 minutes of normoxic perfusion. The second OGD insult always produced a fEPSP depression comparable to the first one. Another slice from the same rat was then taken and submitted to the same protocol described above, but the second 2-minute OGD was carried out in the presence of different compounds, applied at least 5 minutes before, during and 5 minutes after the OGD. The effect of each drug on the OGD-induced depression of neurotransmission was obtained by comparing fEPSP depression induced by the second OGD insult versus that induced by the first OGD.

5-minute OGD protocol: A 5-minute OGD insult always induced a complete but reversible depression of synaptic neurotransmission in the CA1 hippocampal region that started about 2 minutes after OGD application and lasted for about 10 minutes. This mild ischemic insult induced a reversible decrease of DC amplitude during OGD that was < 1 mV, but a sizable AD was never recorded. In a typical experimental day, a control slice was submitted to a 5-minute OGD insult in control conditions. Since this insult always produced a maximal fEPSP depression, the effect of a 5-minute OGD insult on neurotransmission was quantified as "area under the curve" (AUC) and expressed as the time of fEPSP depression during OGD up to the recovery of the baseline potential amplitude. Then, a second slice from the same rat was taken and submitted to a 5-minute OGD insult in the presence of a different compound, applied at least 5 minutes before, during and 5 minutes after the OGD. The effect of each drug on the OGD-induced depression of neurotransmission was obtained by comparing the AUC measured in the first, control, slice with that measured in the second, treated, slice.

7-minute OGD protocol: A 7-minute OGD insult always induced a complete depression of synaptic neurotransmission in the CA1 hippocampal region that, in most cases, was not followed by a recovery of synaptic activity. This irreversible ischemic insult induced an abrupt decrease of DC amplitude with a negative shift of about 5-10 mV, interpreted as AD. In a typical experimental day, a control slice was submitted to 7 minutes of OGD. If the recovery of fEPSP amplitude after 15 minutes of reperfusion with glucose-containing and normally-oxygenated aCSF was ≤15% of the preischemic value, a second slice from the same rat was submitted to a 7-minute OGD insult in the presence of different drugs. To confirm the result obtained in the treated group, a third slice was taken from the same rat and another 7-minute OGD was performed in control conditions, to verify that no difference between slices was caused by the time gap between the experiments.

2. Patch clamp recordings

Acute rat striatal slice preparation
7 day old Sprague-Dawley rats were humanely killed by decapitation using a pair of surgical scissors (RS6930, Roboz, Germany). The skin was cut along the midline with a pair of small scissors. The skull was cut along the midline with a pair of fine scissors and the skull bones were removed using fine curved forceps. Within 60 s of decapitation the exposed brain was submerged in a 100 ml plastic weighting boat (Fisher Scientific, Loughborough, UK) containing ice-cold slicing solution continuously bubbled with a mixture of O_2 (95%) and CO_2 (5%). Then the brain was cut along the midline with a scalpel (Nº 11, Swann-Morton, Sheffield, UK) and the cerebrum was isolated

from the rostral part of the cerebellum and caudal part of the olfactory bulb. Then the brain was removed from the skull using a fine spatula. Both brain halves were allowed to cool down for 3-5 minutes in ice-cold ACSF.

For striatal slice preparation, a flat surface was cut across the dorsal side of a half brain with a scalpel. This surface was glued, using cyanoacrylate instant adhesive (Loctite UK Ltd, Watchmead, Welwyn Garden City), to the tissue block of the specimen bath of a vibroslicer (DTK 1000, Dosaka; Kyoto, Japan) with the medial side of the brain facing the cutting blade. Immediately, the specimen bath was filled with oxygenated ice-cold slicing solution until the tissue was completely covered. Slices were cut using ceramic blades (Campden Instruments Ltd, UK) at a thickness of 300 µm. Hypodermic needles (Monoject, Ballymoney, UK) were used to dissect out the striatum with the adjacent cerebral cortex from the rest of the brain slice. Slices were transferred into an incubation chamber (Edwards *et al.*, 1992b) using a plastic disposable Pasteur pipette (Scientific Laboratory Supplies Ltd, Nottingham) cut to a tip opening of 3-5 mm across. The incubation chamber contained 100 ml extracellular recording solution, with additional 1 mM $MgCl_2$ added to improve tissue viability, continuously bubbled with a mixture of O_2 (95%) and CO_2 (5%). Slices were incubated at room temperature (20 – 24 °C) for a period that ranged from 45 minutes to 8 hours before experimenting. Each slice was transferred in the same way to a recording chamber fitted to the stage of an upright microscope (Axioscope, Zeiss, Oberkochen, Germany).

3. Cell cultures

hMSCs. Human bone marrow cells were obtained from the iliac crest of marrow aspirates from healthy donors. Informed consent was obtained from all donors and the institutional ethical committee approved all procedures. Details on isolation of hMSCs have been described previously (Urbani *et al.*, 2006). Briefly, whole bone marrow aspirate was collected and small aliquots were centrifuged for 10 minutes at 700 g; the ring of white blood cells (buffy-coat) was recovered and plated in 75 cm^2 flasks ($1.6x10^5$ cells/cm^2) in growth medium (Iscove's MDM) with 50 µg/ml gentamicin, 10% FBS, 2% Ultroser° G and incubated at 37°C in a humidified atmosphere containing 95% air and 5% CO_2. On reaching confluence, the adherent cells were harvested with trypsin-EDTA for 5-10 min at 37°C, washed with PBS and 10% FBS and resuspended in complete medium (primary culture, P0). Cells were plated again at 10^4 cells/cm^2 in 100-mm dishes (P1), for the *in vitro* differentiation experiments and for determination of their growth kinetics: expansion of the cells was obtained with successive cycles of trypsinization and reseeding.

At the first passage in culture, the morphologically homogeneous population of hMSCs was analysed for the expression of cell surface molecules using flow cytometry procedures: hMSCs, recovered from flasks by trypsin-EDTA treatment, were washed in HBSS and 10% FBS and were resuspended in flow cytometry buffer consisting of CellWASH with 2% FBS. Aliquots were incubated with the following conjugated monoclonal antibodies: CD34-PE, CD45-FITC, CD14-PE, CD29-PE, CD44-FITC, CD166-PE, CD90-PE, CD73-PE, HLA-DP Q R, HLA-ABC (BD Pharmingen, San Diego, CA, USA) and CD105-PE (Ancell, Bayport, MI, USA). Non-specific fluorescence and morphologic parameters of the cells were determined by incubation of the same cell aliquot with isotype-matched mouse monoclonal antibodies. Flow cytometric acquisition was performed on a FACSort (Becton Dickinson) instrument and data were analysed

on DOT-PLOT bi-parametric diagrams using CELL QUEST software (Becton Dickinson) on a Macintosh PC. The ability of hMSCs to differentiate among osteogenic, adipogenic and chondrogenic lineages was assayed, as previously described in more detail (Urbani *et al.*, 2006) to ascertain the pluripotent differentiation potential typical of this stem cell line.

1321N1 astrocytoma cells. 1321N1 astrocytoma cells stably transfected with GPR17 were kindly provided from Department of Pharmacology, University of Milan. The cells were cultured in growth medium (DMEM) containing 10 % inactivated FBS and antibiotics (Penicillin 100U/ml/streptomycin100µg/ml-) at 37°C in a humidified atmosphere of 95 % air 5 % CO_2. When the cells had grown in culture flasks to 70%-80% confluence, they were detached with trypsin/EDTA. After centrifugation (1000 rpm for 5 minutes, RT), cells were used for patch clamp recordings.

4. Solutions

Striatal slices: for slicing procedures a modified aCSF with the following composition was used (in mM): sucrose, 206; KCl 2.5; $CaCl_2$ 1.0; $MgCl_2$ 1; NaH_2PO_4 1.25; $NaHCO_3$ 26; glucose 25; at pH 7.4 when bubbled with 95% O_2 and 5% CO_2. During whole cell recordings, slices were superfused with an extracellular aCSF solution of following composition (in mM): NaCl 125; KCl 2.5; $CaCl_2$ 1; $MgCl_2$ 1; NaH_2PO_4 1.25; $NaHCO_3$ 26; glucose 25; pH 7.4. The slicing and extracellular solutions were continuously gassed with a mixture of O_2 (95%) and CO_2 (5%) (BOC Gases, Manchester, UK). When current clamp experiments were not performed, TTX 100nM was added to the aCSF to block voltage-gated Na^+ currents. In order to keep the cell as close as possible to the physiological condition *in vivo*, patch pipettes were filled with a potassium gluconate (KGlu) pipette solution. The composition of the internal solution was (in mM): KGlu 140; EGTA 0.2; NaCl 10; $MgCl_2$ 1; adjusted to pH 7.4 with KOH. This solution was stored at -20°C in 1 ml aliquots. ATP 2 mM and GTP 0.5 mM were daily added to each aliquot in use and the solution maintained on ice before filling each pipette.

Cultured cells: The extracellular tyrode solution contained (mM): HEPES 5, glucose 10, NaCl 140, KCl 5.4, $MgCl_2$ 1.2, $CaCl_2$ 1.8. The pH was adjusted to 7.3 with NaOH. Standard pipette solution contained (mM): K-aspartate 110, KCl 20, Na_2-ATP 5, $MgCl_2$ 2, HEPES 10, Na_2-GTP 0.1, EGTA 2.75 and $CaCl_2$ 1.25. "EGTA-free" pipette solution contained K-aspartate 110, KCl 20, Na_2-ATP 5, $MgCl_2$ 2, HEPES 10, Na_2-GTP 0.1 and EGTA 0.05. "High EGTA" pipette solution contained: K-aspartate 110, KCl 20, Na_2-ATP 5, $MgCl_2$ 2, HEPES 10, Na_2-GTP 0.1, EGTA 11 and $CaCl_2$ 5. In all cases, pH was adjusted to 7.2 with KOH. In some experiments we replaced KCl with equimolar concentrations of CsCl in both the extracellular and internal pipette solution in order to eliminate membrane K^+ currents. In these cases, pH was adjusted with CsOH. For perforated-patch experiments, pipettes were back-filled with an intracellular solution containing amphotericin-B (Rae *et al.*, 1991) disolved in DMSO (30 mg/ml) and diluted to 0.12 mg/ml in standard intracellular pipette solution before recording.

5. Patch pipettes fabrication

Striatal slices. Patch pipettes were made in a vertical pipette puller (L/M-3P-A, List-Medical, Darmstadt, Germany or MF-83, Narishige, Tokyo, Japan) from thick-walled

borosilicate glass capillaries containing an internal filament (GC150F-7.5, outer diameter 1.5 mm, inner diameter 0.86 mm, Harvard Apparatus Ltd). The tip of the pipette was cleaned, smoothed and reduced by fire polishing on a microforge (MF-83, Narishige, Tokyo, Japan) to a final resistance of 6-15 MΩ. For current clamp and single channel recordings, pipettes were coated with an insulating silicone resin (Sylgard 184® Dow Corning, USA). Pipettes were back-filled with pipette solution and the level in the pipette was kept to a minimum to reduce electrical interference produced by solution creeping up the electrode or going into the suction line.

Cultured cells. Borosilicate glass electrodes (GC150T-7.5, outer diameter 1.5 mm, inner diameter 1.17 mm, Harvard Apparatus Ltd) were pulled with a Sutter Instrument (model P-87). When pipettes were filled with the intracellular solution, tip resistance was between 2 and 3.5 MΩ.

6. Experimental procedures.

Striatal slices. The cell bodies of individual neurons in brain slices were visualised under Normaski differential interference contrast optics (Yamamoto 1975; Takahashi 1978; Edwards *et al.*, 1989) using an upright microscope (Axioskop, Zeiss, Oberkochen, Germany) with an Achromat 40X water immersion objective with a numerical aperture of 0.75 and a working distance of 1.6 mm at a total magnification of 600X. Visualisation was carried out on a monochrome video monitor (VM-902K, Hitachi-Denshi, Tokyo, Japan) connected to CCD monochrome camera (RS Components, Corby, UK) mounted on top of the microscope trinocular head. Slice health was visually checked before patching and the presence of a considerable proportion of neurons with a smooth surface readily evident on the surface of the slice was used as an indicator of a good healthy slice. Individual healthy cells were identified by the smooth appearance of their surface. Striatal medium spiny neurons were identified by their location, size and morphology (Gotz *et al.*, 1997). Medium spiny neurons comprise approximately 90% of the striatal neurons (Jain *et al.*, 2001), and they are about 15 μm in diameter which is about half of the interneuron's size (Gotz *et al.*, 1997).

Patch pipettes were positioned on an electrode holder connected to the headstage of a patch clamp amplifier (Axopatch 200A, Axon Instruments, Foster City, CA, USA) and some positive pressure was applied to the inside of the pipette to generate a tiny stream of solution at the tip of the pipette that prevented the accumulation of debris at the tip and the mixing of the pipette solution inside the pipette with the external solution in the recording chamber. The patch pipette was then lowered into the recording chamber. Once in solution, the pipette resistance was measured by passing a 5 mV rectangular pulse through the input using the patch clamp amplifier. Positioning of the patch pipette was carried out under the optic field of the microscope using a micromanipulator (Suttar) and under visual control the patch pipette was lowered further down until visual contact with the slice was made. Contact between the patch pipette and the cell was visually confirmed by the formation of a characteristic dimple on the cell surface caused by flow of solution from the pipette tip. Immediately, the positive pressure was released and a small and increasing amount of gentle suction was applied to the back of the electrode. Then the cell membrane and the tip of the electrode begin to form a high resistance gigaohm seal. This configuration was then used for cell attached single channel recordings. For whole cell recordings

the patch pipette potential was held at -60 mV and suction was applied through the tubing connected to the back of the electrode holder to break the membrane and gain electrical access to the cell interior (Hamill *et al.*, 1981) and then a whole cell current can be recorded. Currents were recorded using an Axopatch 200A patch-clamp amplifier (Axon Instruments). Signals were amplified and filtered at 2 kHz (8 pole Bessel) and digitised at 20 kHz using an analogue-to-digital converter (CED micro 1401, Cambridge Electronics Design, UK).

Cultured cells. After enzymatic dissociation, cells were suspended in tyrode solution, transferred to a small chamber mounted on the platform of the inverted microscope (Olympus CKX41), and superfused at a flow rate of 2 ml min^{-1} with tyrode solution. Patching procedure was then carried on as described above, with the only difference that the patch pipette potential was held at -75 mV before suction was applied to break the membrane and gain electrical access to the cell interior. Data were acquired with an Axopatch 200B amplifier (Axon Instruments, CA, USA), low pass filtered at 10 kHz, stored and analysed with pClamp 9.2 software (Axon Instruments, CA, USA).

7. Voltage clamp protocols

Striatal slices. Series resistance (R_s) and membrane capacitance (C_m) were carefully checked and compensated throughout the experiment. Only cells showing a stable C_m and R_s before, during and after drug application were included in the analysis. In order to reduce the voltage error due to the R_s existing in whole-cell experiments, more than 75 percent of the R_s were compensated by the Axopatch-200A before starting recordings. The voltage error can be calculated by Ohm's law ($V_{err} = I\ R_s$). The average R_s before compensation from my experiments was 33 MΩ (n = 45). The holding current (I_h) was usually between +10 and – 15 pA. So originally the voltage error ($V_e = I_h R_s$) was -0.5 mV and reduced to -0.3 mV after 80% compensation. In contrast, during voltage-ramp experiments, the largest current measured at pipette potentials of +40 mV was 2000 pA, giving a R_s error of 66 mV or 13.2 mV after compensation. Therefore in these experiments R_s errors had little impact on the whole cell recordings.

Ramp protocols consisted of 1.8 s depolarization from -100 to +40 mV. 4 ramp pulses were applied at 20 s intervals. Sweeps were applied to cells by using WinWCP V3.4.6 software (available on line at http://spider.science.strath.ac.uk/ PhysPharm/ showPage.php?page Name=software_ses). All traces shown in the present work are the average of 4 consecutive ramp episodes. When the ramps recorded in control conditions were sufficiently stable (less than 10% variation) the P2Y$_1$ agonist, 2MeS-ADP, was superfused. Other ramp trials were adquired 3, 5 and 8 min after drug application. In some experiments different kinds of potassium channel blockers (TEA, iberiotoxin, apamin) were added to the superfusion in the presence of 2MeS-ADP, to evaluate if they were able to block the effect observed with the P2Y$_1$ agonist. At the end of the treatment all drugs were washed out for at least 5 minutes before another trial of ramps was recorded. Current-voltage relationships were analyzed in Excel or Prism 3.02 software after each recording. Only one whole cell recording was made in each striatal slice.

Cultured cells. Membrane resistance was measured with fast hyperpolarizing voltage pulses (from -70 to -75 mV, 40 ms duration). R_s and C_m were routinely checked and compensated during the experiment. Only cells showing a stable C_m and R_s before, during and after drug application were included in the analysis.

In order to study the effects on membrane currents evoked by the application of P2 agonists and antagonists in cultured cells (hMSCs and 1321N1 cells) we used two different protocols:

- A voltage ramp protocol, consisting of a 1500 ms depolarization (from -90 to +40 mV) from a holding potential of -75 mV, was used to evoke a wide range of overall non-specific voltage-dependent ionic currents. Each trace shown in the figures is the average of 5 consecutive episodes.
- A voltage step protocol was used to specifically generate outward currents. It consists of 16 consecutive steps (10 mV each, 1800 ms duration, -80 mV holding potential) starting from a -70 mV membrane potential to a +80 mV value. In these conditions the current amplitude was measured at the peak. A variation of this protocol was used to selectively block transient outward currents and consisted of a series of 10 consecutive depolarizing steps (10 mV each, 1800 ms duration, -40 mV holding potential) starting from -30 mV membrane potential to +60 mV. The values of currents were measured at the steady state. Only one cell was recorded from each Petri dish where cells were cultured.

8. Current clamp experiments.

Striatal slices. Current clamp recordings were performed with the WinWCP program in a TTX-free extracellular solution with sylgard-covered pipettes to reduce the noise level. After a stable whole cell configuration was reached in the voltage clamp mode with the standard procedure already described, the amplifier was switched to the "normal I-clamp" mode and, when necessary, a little negative or positive current was injected (5-10 pA) to obtain an holding potential of -70 mV. Ten steps of positive current injection (10 pA each) were imposed in control conditions, at 20 s intervals. The first step amplitude was chosen on the basis of each single cell recorded, to obtain both subthreshold and suprathreshold responses (from 2 to 50 pA). After 5 minutes application of 2MeS-ADP the same stimulation protocol was applied to the cell. If the cell was still available, a last recording was made after 5 minutes wash out.

Current clamp recordings were made by depolarizing current injection using the program WinWCP (V3.4.6) to determine the membrane current injection and to record membrane potentials. All data from each step episode were transferred to Excel to be analyzed. The frequency of action potential firing was measured as the number of action potentials/second. The amplitude of action potentials was calculated as the difference between the peak reached by the overshoot and the voltage reached by the step stimulation. The rate of depolarization and hyperpolarization of action potentials was measured as the first derivative of membrane potential over time (mV/ms). The threshold value for firing was taken as the point at which the derivative described before was ≥ 30 mV/ms. The action potential width was measured as the difference between the time of reaching the threshold during the rising phase and the time when the repolarizing potential crossed the threshold value again. The medium afterhyperpolarization potential (mAHP) was measured as the difference between the minimum potential reached after the action potential peak and the voltage reached by the step stimulation. No slow afterhyperpolarization potential (sAHP) after the end of the step was recorded in any cell investigated. The latency of the first action potential was determined as the time point where the first threshold to fire was reached. The inter-spike interval (ISI) between the first-second and the second-third action potentials were measured as the

difference between the times at the peak of the two events. Spike-frequency adaptation during repetitive firing was measured by dividing the latency between the first-second action potential and the latency between the second-third action potential. Values around 1 showed no spike frequency adaptation.

9. Measurement of ATP release from hMSCs

ATP in the cell supernatant was analyzed by the ATPLite-M Kit (Perkin-Elmer, Life and Analytical Sciences, Boston, MA, USA) according to a previously described method (Melani *et al.*, 2005). The luminescence was measured on the PerkinElmer Top-Count luminescence counter (TopCount Packard Instruments, Perkin-Elmer). In previous experiments we found that ATP levels measured in the supernatant collected after plating human astrocytoma cells (ADF1) decrease steadily over time, attaining a baseline in the low nanomolar range between 3 and 5 h thereafter and remain unchanged for up to 24 h (data not shown). High ATP release measured soon after cell plating is in agreement with previous work and is attributed to "medium change" that is a mechanical stimulation (Lazarowski *et al.*, 2000). For this reason, hMSCs were plated onto a 24-well microplate at a density of 50,000 cells/well and incubated for 24 h before ATP assay. After 24 h, a sample of extracellular medium (50 μl) was collected from each well and placed in a white 96-well microplate. The same volume of the substrate solution (50 μl) was added to each sample. Standard solutions of ATP (from 10^{-7} to 10^{-11} M) were run in parallel in the same microplate following an identical procedure to that of the samples.

The ATP values were extrapolated from the linear regression curve calculated on the basis of standard solutions and expressed in absolute values (nM).

10. Chemicals

All compounds were applied by bath superfusion by a multi-way gravity system for periods indicated in the result section. In general, antagonists were applied for 15-30 minutes and were always superfused before agonists when co-application was performed. In all cases, a stable response (at least 5 minutes) was achieved before the time points used for measurements. Enzymatic inhibitors were applied for at least 20 minutes, and results were compared with incubated slices (1h 30') to confirm that a complete block of enzymatic activity was obtained. Agonist and antagonist concentrations were calculated on the basis of K_i values reported in binding studies in the literature by using the Hill-Langmur equation or Gaddum equation as appropriate (80% receptor activation for agonists and 95% inhibition for antagonists).

DPCPX was dissolved in dimethylsulphoxide (DMSO) and stock solutions were made to obtain concentrations of DMSO lower than 0.001% in the superfusing aCSF. Control experiments, carried out in parallel, showed that this concentration of DMSO did not affect CA1 hippocampal neurotransmission.

All the A_3 adenosine receptor antagonists used in our experiments were applied 5, 10 or 20 minutes before, during OGD and 5 min after the end of ischemic episode, as indicated in the result section. The concentration used for each of the selective adenosine A_3 receptor antagonists was chosen on the basis of Ki values on rat or human A_3 receptors. MRS 1523, among all A_3 antagonists used in our experiments, is the

P1 ligands

class	Acronym	Chemical name	purchasing
A$_1$ antagonist	DPCPX	8-cyclopentyl-1,3-dipropylx-anthine	Research Biochemicals International (Natik, MA, U.S.A.)
A$_3$ antagonists	MRS 1523	3-propyl-6-ethyl-5[(ethylthio)carbonyl]-2-phe-nyl-4-propyl-3-pyridinecar-boxylate	Sigma (Milano, Italy)
	MRS 1220	N-[9-Chloro-2-(2-fura-nyl)[1,2,4]-triazolo[1,5-c]quinazolin-5-yl]benzene acetamide	Tocris (Bristol, U.K.)
	VUF 5574	(N-(2-methoxyphenyl)-N'-[2-(3-pyrindinyl)-4-quinazolinyl]-urea)	Tocris (Bristol, U.K.)
	WSAB	5-[[(4-pyridyl)amino]carbon yl]amino-8-methyl-2-(2-fu-ryl)-pyrazolo[4,3-e]1,2,4-triazolo[1,5-c]pyrimidine hydrochloride	Kindly provided by Dr. G. Spalluto, University of Trieste, Italy
class	Acronym	Chemical name	purchasing
A$_3$ agonists	Cl-IB-MECA	1-[2-chloro-6[[(3-iodophenyl)methyl]amino]-9H-purin-9-yl]-1-deoxy-N-me-thyl-ß-D-ribofuranuronamide	Tocris (Bristol, U.K.)
	AR132,	N^6-methyl-2-phenylethynylad-enosine	Kindly provided by the University of Camerino, Italy
	VT72 ,	N^6-methoxy-2-phenylethyny-ladenosine	
	VT158,	N^6-methoxy-2-phenylethynyl-5'-N-methylcarboxamidoad-enosine	
	VT160	N^6-methoxy-2-(2-pyridinyl)-ethynyl-5'-N-methylcarboxam-idoadenosine	
	VT163	N^6-methoxy-2-p-acetylphe-nylethynyl-5'-N-methylcarbox-amidoadenosine	

most potent and selective antagonist for the rat A$_3$ receptors actually available com-mercially (Ki value of 113 nM; Li *et al.*, 1998; Muller 2003). MRS 1220 is a highly po-tent antagonist at human A$_3$ receptor (Ki value of 0.65 nM) but presents a lower affin-ity for the rat isoform (Kim *et al.*, 1996). VUF 5574 is another potent ligand at human but not at rat A$_3$ receptor, showing a K$_i$ value of 4 nM and being at least 2500-fold selective versus human A$_1$ and A$_{2A}$ receptors (Muijlwijk-Koezen *et al.*, 2000). Simi-

P2 ligands

	Acronym	Chemical name	purchasing
Non-selective P2 agonists	ATP	adenosine 5' triphosphate	Sigma (Milano, Italy)
	ATPγS	adenosine 5'-O-(3-thiotriphosphate)	Sigma (Milano, Italy)
P2Y$_1$ agonist	2meS-ADP	2-(Methylthio) adenosine 5' diphosphate trisodium salt	Sigma (St. Louis, MO, USA)
P2 non-selective antagonists	Suramin		Tocris (Bristol, U.K.)
	PPADS	pyridoxalphosphate-6-azophenyl-2',4'-disulfonic acid tetrasodium salt	Tocris (Bristol, U.K.)
P2X$_7$ antagonist	BBG	Brilliant Blue G	Sigma (Milano, Italy)
P2Y$_1$ antagonist	MRS 2179	2'-deoxy-N^6-methyladenosine 3',5'-bisphosphate tetraammonium salt	Tocris (Bristol, U.K.)
NTPDase inhibitors	ARL 67156	6-N,N-diethyl-D-β,γ-dibromomethylene ATP), suramin (8-(3-benzamido-4-methylbenzamido)naphthalene-1,3,5-trisulfonic acid	Tocris (Bristol, U.K.)
	BGO 136	1-hydroxynaphthlene-3,6-disulfonic acid	Sigma (Milano, Italy)
	PV4	hexapotassium dihydrogen monoti tanoundecatungstocobaltate(II) tridecahydrate	Kindly provided from Prof. Müller, University of Bonn, Germany

larly, the recently synthesized A$_3$ antagonist WASB present a very high affinity for the human A$_3$ receptor (K$_i$ of 0.01 nM, see: Maconi *et al.*, 2002). MRS 1523, MRS 1220 and VUF 5574 were dissolved in DMSO. The hydrophilic A$_3$ antagonist WSAB was dissolved in distilled water. All the selective adenosine A$_3$ receptor agonists, Cl-IB-MECA, AR132, VT72, VT158, VT160 and VT163 were applied 5 min before, during OGD and 2 minutes after OGD (referred to as "long" application in results section) or for only 2 minutes during OGD (referred to as "short" application in results section). K$_i$ taken from radioligand and functional studies for Cl-IB-MECA are 0.33 and 11.1 nM on rat and human membranes respectively (Muller 2003). The compound has been described as highly selective for A$_3$ adenosine receptors versus A$_1$ receptors (K$_i$ of 820 nM) and A$_{2A}$ receptors (K$_i$ of 470 nM) in rat brain membranes (Kim *et al.*, 1996). When Cl-IB-MECA and the A$_3$ antagonist MRS 1523 were co-applied, the antagonist was always superfused 5 min before the combination of the two drugs. Ki values for the new A$_3$ agonists synthesized by Camerino: AR132, VT72, VT 158, VT160 and VT163, are taken from binding experiments in CHO cells stably transfected with human recombinant A$_3$ receptors. The compounds have been reported as highly selective for A$_3$ adenosine receptors *versus* A$_1$ receptors and A$_{2A}$ receptors: AR 132, A$_3$ Ki of 3.4 nM and A$_3$ selectivity *versus* A$_1$ of 500 and *versus* A$_{2A}$ of 2,500: (Volpini *et al.*, 2002); VT 72, A$_3$ Ki of 3.8 nM and A$_3$ selectivity *versus* A$_1$ of 320 and *versus* A$_{2A}$ of 1,100 (Dal Ben *et al.*, 2006; Volpini *et al.*, 2005); VT 158, A$_3$ Ki of 1.9

nM and A_3 selectivity *versus* A_1 of 4,800 and *versus* A_{2A} of 8,600 (Dal Ben *et al.*, 2006; Volpini *et al.*, 2005); VT 160, A_3 Ki of 1.1 nM and A_3 selectivity *versus* A_1 of 3,600 and *versus* A_{2A} of 16,400; VT 163: (Volpini *et al.*, 2006), A_3 Ki of 2.5 nM and A_3 selectivity *versus* A_1 of 21,500 and *versus* A_{2A} of 4,200).

Under normoxic conditions, ATP and its metabolically stable analogue ATPγS were perfused for 10 minutes, a time that allowed us to record a stable response to the compounds. Concentrations were chosen on the basis of K_i values obtained in ligand binding studies from rat membranes (see: Khakh *et al.*, 2001 for P2X receptors and: von Kugelgen 2006 for P2Y receptors). The concentration of the $P2Y_1$ selective agonist, 2MeS-ADP, was chosen on the basis of ligand binding studies from Gao and colleagues (Gao *et al.*, 2004) that reported a K_i value of 57 nM in astrocytoma cells.

The P2 purinergic antagonists suramin, PPADS, MRS 2179 and BBG were applied 10 or 15 minutes before, during, and 5 minutes after the application of P2 agonists or the induction of OGD. Suramin is a non-specific and non-competitive antagonist of P2 purinergic receptors (either P2X or P2Y). It also inhibits ecto-nucleotidases activity (Iqbal *et al.*, 2005) and affects glutamatergic and GABAergic receptor activation in rat hippocampal slices (Nakazawa *et al.*, 1995). PPADS is a non-selective antagonist at both P2Y and P2X (excluding $P2X_7$) receptors and is the compound most used to block P2 purinergic receptor activation (Lammer *et al.*, 2006; Ralevic and Burnstock, 1998). K_i values for suramin and PPADS were chosen on the basis of data in the literature (for a review see: von Kugelgen 2006). BBG is a selective $P2X_7$ receptor antagonist in the low nanomolar range, with no detectable activity on other P2X receptor subtypes at concentrations below 10 μM (Jiang *et al.*, 2000a). The concentration of the $P2Y_1$ selective antagonist MRS 2179 was chosen on the basis of Kb=177 nM reported by Moro and co-workers (Boyer *et al.*, 1998; Camaioni *et al.*, 1998; Moro *et al.*, 1998).

Ecto-ATPases (NTPDase1, 2 and 3) are responsible for the degradation of extracellular ATP (Zimmermann, 2000). In the present work, 3 different ecto-ATPase inhibitors were tested: ARL 67156, BGO 136 and PV4. ARL 67156, a commonly used ecto-ATPase inhibitor (Crack *et al.*, 1995), was superfused at a concentration of 50 μM, 20 minutes before and during ATP or ATPγS application, in accordance with previous data in the literature (Pascual *et al.*, 2005; Safiulina *et al.*, 2005). However, it has been recently shown that, at micromolar concentrations, ARL 67156 only inhibits rat NTPDase1 and 3 transiently transfected in Chinese Hamster Ovary (CHO) cells, showing negligible activity on NTPDase2 (Iqbal *et al.*, 2005). In addition, a possible interaction of this ATP analogue with some P2Y receptors have been suggested (Drakulich *et al.*, 2004). BGO 136 is a new ecto-ATPase inhibitor recently available in commerce. From the few data existing in the literature at present, this compound is described as a selective NTPDase1 and 2 blocker with Ki values in the high micromolar range (Kukulski *et al.*, 2003), being ineffective at concentrations below 5 mM (Duval *et al.*, 2003 and our unpublished observation). PV4 is a recently synthesized compound (not available commercially) that belongs to a new class of ecto-ATPase inhibitors: the polyoxotungstates (Muller *et al.*, 2006). PV4 strongly inhibits rat NTPDase1, 2 and 3 with K_i values in the nanomolar range (Muller *et al.*, 2006). Its high affinity for these enzymes renders it a useful tool (the best one available at present) to inhibit extracellular ATP catabolism without interfering with P2Y receptors, at least at 10 μM concentrations (Muller *et al.*, 2006). Since no data are available at present about the application of BGO 136 or PV4 to brain slices, for similarity with ARL 67156 we superfused these compounds 20 minutes before ATP application. In some cases hippocampal slices were preincubated

in the presence of the ecto-ATPase inhibitors 1h before starting the experiment, but since no significant difference was found with non-incubated slices, the results were pooled together.

All the P2 agonists, antagonists and NTPDase inhibitors (excepted BGO 136) were dissolved in distilled water and stock solutions at 100-10,000 times the desired final concentration, stored at -20°C and dissolved in aCSF at the final concentration immediately before slice superfusion. Since BGO 136 was applied at mM concentration, it was directly dissolved in the aCSF before slice superfusion.

GPR17 ligands

	Acronym	Chemical name	purchasing
Uridine-agonists	UDP-glucose		Kindly provided by Prof. Abbracchio, University of Milan, Italy
	UDP-galactose		
	UDP	uridine 5' diphsphate	
CysLT-agonist	LTD4		
antagonists	MRS 2179	2'-deoxy-N^6-methyladenosine 3',5'-bisphosphate tetraammonium salt	
	Montelukast		
	Pranlukast		

Toxins

Acronym			purchasing
TTX	tetrototoxin	Na$_v$ channels blocker	Alomone labs
TEA	Tetraethyl ammonium	K$_v$ channels blocked	Sigma (St. Louis, MO, USA)
Ibtx	Iberiotoxin	BK channels blocker	Sigma (St. Louis, MO, USA)
Apa	Apamin	SK channels blocker	Sigma (St. Louis, MO, USA)
PTX	Pertussis toxin	Protein G$_i$ blocker	Sigma (Milan, Italy)

When Na$_v$ channel block was required, TTX was added directly in the extracellular solution and perfused throughout the experiment. TEA was applied at a concentration of 200 µM estimated to selectively block about 80 % of BK channels (Blatz *et al.*, 1984). Apamin and iberiotoxin concentrations were chosen on the basis of previous works showing a maximal block of SK and BK channels (respectively) at 10 nM for both toxins in rat striatum (Bargas *et al.*, 1999; Nisenbaum *et al.*, 1996). PTX pre-treatment was conducted in a group of 1321N1 transfected cells, which were incubated for 18 h with PTX (100 ng/ml) before enzymatic dissociation and subsequent electrophysiological recordings.

Pipette solution component

Acronym	Chemical name	purchasing
EGTA	ethylene glycol-bis(β-aminoethyl ether)N,N,N',N'-tetracetic acid	Sigma (Milano, Italy)
Amphotericin B		Sigma (Milano, Italy)
Na$_2$-GTP	guanosine 5' triphosphate disodium salt	Sigma (Milano, Italy)
Na$_2$-ATP	adenosine 5' triphosphate disodium salt	Sigma (Milano, Italy)
Hepes	Hepes sodium salt	Sigma (Milano, Italy)

hMSCs culture medium

compound	purchasing
PBS (phosphate buffer solution)	GIBCO, Invitrogen, UK
IMDM (Iscove's Modified Dulbecco's Medium with L-glutamine and Hepes 25 mM)	EuroClone, Milan, Italy
FBS (fetal bovine serum)	HyClone, South Logan, Utah, USA
gentamicin	Schering-Plough S.p.A., Milan Italy
Ultroser° G	Pall Biosepra SA, Cergy-Saint-Christophe, France
Trypsin-EDTA (0.05% trypsin-0.02% EDTA)	(Eurobio, Courtaboeuf Cedex B, France
CellWASH (0.1% sodium azide in PBS)	Becton Dickinson, San Jose, CA, USA
	Ancell, Bayport, MI, USA

1321N1 culture medium

compound	purchasing
PBS (phosphate buffer solution)	GIBCO, Invitrogen, UK
DMEM (Dulbecco's modified Eagle's medium high glucose)	EuroClone, Milan, Italy
FBS (fetal bovine serum)	EuroClone, Milan, Italy
P/S (penicillin 100U/ml/streptomycin100µg/ml)	EuroClone, Milan, Italy
L-glutamine	EuroClone, Milan, Italy
Na-piruvate	GIBCO, Invitrogen, UK
Trypsin/EDTA	GIBCO, Invitrogen, UK
geneticin	GIBCO, Invitrogen, UK

11. Statistical analysis

Data were analyzed using Prism 3.02 software (Graphpad Software, San Diego, CA, U.S.A.) and expressed as the mean ± s.e. Data were tested for statistical significance with the paired two-tailed Student's *t* test or by analysis of variance (one-way ANOVA), as appropriate followed by Newman-Keuls multiple comparison test. Where indicated, two-tailed Mann-Whitney test was used. In all cases, a value of $P<0.05$ was considered significant.

RESULTS
Section 1

ROLE OF PURINES IN CA1 HIPPOCAMPAL NEUROTRANSMISSION
UNDER NORMOXIC CONDITIONS AND DURING OGD. EXTRACELLULAR
RECORDINGS FROM RAT HIPPOCAMPAL SLICES

Chapter 1
Role of A_3 adenosine receptors during OGD

1. Historical background

Adenosine concentration drastically rises during ischemic brain damage, reaching micromolar levels that are sufficient to activate all P1 receptors, also the "low affinity" A_3 subtype (Latini *et al.*, 2001). Even though the protective role mediated by A_1 receptor activation during such insults has been largely demonstrated, the effects of A_3 receptor stimulation are still unclear. In fact, evidence for both protective and deleterious effects due to A_3 receptor stimulation are described in the literature (for a review see: von Lubitz 1999). Likewise, controversial evidence exists about the effect of A_3 receptor stimulation on neurotransmission under normoxic conditions, as already mentioned in the introduction. In fact, both inhibitory (Brand *et al.*, 2001) and facilitatory effect (Costenla *et al.*, 2001; Dunwiddie *et al.*, 1997a; Fleming *et al.*, 1997; Laudadio *et al.*, 2004; Macek *et al.*, 1998) have been described in the brain, which might sustain , respectively, a protective or a deleterious role of A_3 receptors during ischemia.

A protective role of adenosine A_3 receptors during cerebral ischemia has been demonstrated in A_3 KO mice, that present an increased neurodegeneration in response to repeated episodes of mild hypoxia (Fedorova *et al.*, 2003). In addition, Hentschel and co-workers (Hentschel *et al.*, 2003) demonstrate that, in rat cortical neurones, the selective activation of adenosine A_3 receptors during hypoxia is involved in the inhibition of excitatory neurotransmission, suggesting that A_3 receptor stimulation contributes to the neuroprotective role of adenosine brought about by A_1 receptor activation. Similarly, at a cardiac level, most evidence indicates that A_3 receptors are involved in protection of the ischemic heart (Fredholm *et al.*, 2005).

On the other hand, a deleterious role of A_3 receptors during ischemia has also been proposed. Previous work in my laboratory demonstrated that the selective block of A_3 receptors during ischemic preconditioning limits the beneficial effects of that treatment on fEPSP recovery following a subsequent severe OGD insult in rat hippocampal slices (Pugliese *et al.*, 2003). In agreement, Von Lubitz and co-workers demonstrated that acute A_3 receptor stimulation exacerbates the damage caused by a concomitant ischemic episode *in vivo* (von Lubitz *et al.*, 1994). Nevertheless, the same study reports that chronic pre-ischemic administration of A_3 agonist elicits opposite effects, reducing cerebral damage against ischemic insults (von Lubitz *et al.*, 1994). This effect may be attributed to a desensitization of A_3 receptors. In fact, both human and rat A_3 receptors are desensitized and internalized within a few minutes after agonist exposure (Ferguson *et al.*, 2000; Palmer *et al.*, 1995 and 2000; Trincavelli *et al.*, 2000; 2002 and 2002b). Altogether, these data suggest that the outcome of A_3 receptor stimulation on synaptic transmission during hypoxic/ischemic phenomena is intricately related to the intensity and duration of receptor activation.

In the present work we used selective A_3 receptor agonists and antagonists to investigate the role of A_3 adenosine receptors on synaptic transmission, extracellularly recorded in the CA1 region of rat hippocampal slices, during brief, mild or severe OGD episodes. These insults are aimed at reproducing, *in vitro*, the consequences of blood flow interruption following cardiac arrest or occlusion of intracranial vessels.

2. Results

2.1 Experiments were performed on a total of 219 slices taken from 133 rats

2.1.1 The selective block of A_3 adenosine receptors by MRS 1523 reduces fEPSP depression evoked by a 2-minute OGD insult and induces a faster recovery of fEPSP amplitude after a 5-minute OGD.

Figure 12 shows that periods of 2 or 5 minutes of OGD induce, respectively, a partial or complete reduction of synaptic potential amplitude that was always reversible upon reperfusion with normal oxygenated aCSF. These results are in agreement with our previous studies (Latini *et al.*, 1999a and 1999b; Pugliese *et al.*, 2003).

The application of 2 minutes of OGD resulted in a partial but consistent depression of synaptic potentials, reaching a maximal inhibition of 76.3±4.2% (n=13, $P<0.001$, paired two-tailed Student's t test vs pre-ischemic baseline) a few seconds after reperfusion with normal oxygenated aCSF (figure 12A). After 2 minutes of reperfusion in normal, glucose-containing aCSF, fEPSPs progressively reappeared and reached a complete recovery within 5 minutes from the beginning of reperfusion. The application of a second 2-minute OGD insult, 40 minutes after the end of the first one, resulted in a similar depression of fEPSP amplitude (66.4±6.2%, n=13), with the same time-course. No significant difference was found by comparing synaptic potential amplitude at any time during the first and second OGD (figure 12A, $P>0.05$, paired two-tailed Student's t test). Therefore the effects of the A_3 selective antagonist MRS 1523 on fEPSPs were evaluated before and during the second 2-minute OGD insult in comparison with the first one (figure 12B). MRS 1523 (100 nM, n=10) applied 10 minutes before, during OGD and 5 minutes thereafter, did not modify the fEPSP amplitude in normoxic conditions but significantly inhibited the

fEPSP amplitude depression evoked by a 2-minute OGD (74.1±6.1% in control and 34±10% in the presence of the antagonist; $P<0.05$, paired two-tailed Student's t test , figure 12B). The effect of 100 nM MRS 1523 was maximal, since increasing the antagonist concentration to 1 μM did not potentiate the effect (data not shown).

Application of 5 minutes of OGD resulted in a complete depression of synaptic potentials within 4 minutes after OGD initiation (n=12, figure 12C). After 3.5 minutes of reperfusion in normal, glucose-containing aCSF, fEPSPs progressively reappeared and reached a complete recovery within 10 minutes of normoxic reperfusion. Since it has been demonstrated that a second 5-minute OGD episode, 50 minutes after the end of the first one, is followed by an appreciably faster recovery of fEPSPs (Latini *et al.*, 1999a and 1999b), the effect of the selective A_3 antagonist was studied in a separate group of slices. MRS 1523 (100 nM, n=7), applied 10 minutes before, during and 5 minutes after OGD application, induced a faster fEPSP recovery (AUC: 10.1±0.5 in control and 7.1±0.7 in the presence of the antagonist; $P<0.05$, one-way ANOVA, Newman-Keuls multiple comparison post-hoc test, see also figure 18C) measured from the beginning of fEPSP depression during OGD up to the recovery of synaptic potentials to the baseline value (figure 12C).
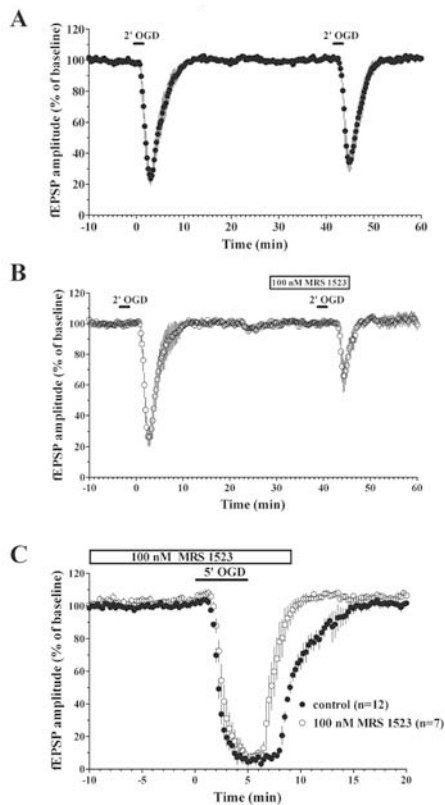
Figure 12. The selective A$_3$ adenosine receptor antagonist MRS 1523 reduces fEPSP depression induced by a 2-minute OGD episode and induces a faster fEPSP recovery after a 5-minute OGD. Data (mean ± s.e.) are expressed as percent of baseline values. **A.** Averaged time-course (n=10) of fEPSP amplitude before, during and after the application of two consecutive ischemic insults of 2 minutes duration. The second 2-minute OGD, administered 40 minutes after the end of the first period, elicited a comparable depression of synaptic potentials (P>0.05, paired Student's t test). **B.** The same protocol as before carried out in the presence of MRS 1523. MRS (100 nM) applied 10 minutes before, during and 5 minutes after the second 2-minute OGD, as indicated by the open bar. Note that, in the presence of MRS 1523, the fEPSP depression induced by OGD was significantly reduced (P<0.05, paired Student's t test) in comparison to that obtained in the absence of the drug. **C.** Time-course of fEPSP amplitude changes elicited by a 5-minute OGD insult in the absence and in the presence of 100 nM MRS 1523. The A$_3$ antagonist, applied 10 minutes before, during and 5 minutes after OGD application, induced a faster fEPSP recovery after OGD application.

2.1.2 Selective block of A$_3$ adenosine receptors prevents irreversible impairment of neurotransmission induced by a 7-minute OGD episode.

In a first series of experiments we characterised the response of synaptic excitatory transmission to 7 minutes OGD, an ischemia-like insult that in our experimental conditions has been shown to consistently produce an irreversible loss of synaptic transmission, but to be sensitive to the protective effects of ischemic preconditioning (Pugliese *et al.*, 2003).

Figure 13A illustrates the effects of 7 minutes OGD on the amplitude of synaptic responses evoked by the stimulation of CA1 stratum radiatum and recorded from the apical dendritic region of pyramidal cells. One 7-minute OGD episode induced the disappearance of the fEPSP, which did not recover after prolonged superfusion with oxygenated, glucose-containing aCSF (up to 80 minutes, n=7; not shown). The effect of 7 minutes OGD on the fEPSP was similar in 42 slices examined and the mean recovery of fEPSP amplitude, after a 7minute OGD episode, was 5±1%, n=42 (see also Figure 15).

The presence of selective adenosine A_3 receptor antagonists prevented the irreversible disappearance of synaptic potentials induced by 7 minutes of OGD. Thus, in the presence of MRS 1523 (100 nM, figure 13B), a total recovery of synaptic response was observed within 10 minutes from OGD interruption. The mean recovery of fEPSP amplitude after 7 minutes of OGD in the presence of 100 nM MRS 1523, was 83 ± 6%, (n=17, Figure 14B and 15A). Furthermore, when compared to those obtained in control conditions, in MRS 1523 treated slices the transient recovery of the fEPSP amplitude was delayed and the afferent fibre volley did not disappear at the end of the 7-minute OGD (figure 13B, trace 2, see also table 7)

Table 7. Treatment with MRS 1523 produces a delay in the effects of OGD in the CA1 region of hippocampal slices.

	Control			MRS 1523	
	(n)		(n)		
Initial fEPSP disappearance time (s)	(50/50)	177.9± 7.2	(41/41)	254.3± 10.9	P<0.0001
Transient fEPSP recovery peak time (s)	(31/50)	357 ± 17	(34/41)	480 ± 18	P<0.0001
Transient fEPSP recovery duration (s)	(31/50)	59 ± 7	(34/41)	46 ± 7	P=0.0948
Transient fEPSP recovery amplitude (%)	(31/50)	18.0 ± 3.3	(34/41)	15.5 ± 2.4	P=0.4265
Fibre volley disappearance time (s)	(34/50)	372 ± 18	(19/41)[§]	501 ± 26	P<0.0001
AD peak time (s)	(20/20)	436 ± 17	(22/33)[#]	520 ± 23	P=0.0017

Data are from slices receiving 7 or 30 minutes of OGD in control (n=50) and 7, 8, 9, 10 or 30 minutes of OGD in the presence of 100 nM MRS 1523 (n=41). Numbers in parentheses (n/n) indicate number of observations out of investigated slices. Time is calculated from OGD initiation. The amplitude of the transient fEPSP recovery is expressed as per cent of baseline fEPSP recorded before OGD application. Statistical significance was assessed with Mann-Whitney test. § Fibre volley did not disappear in any of the slices receiving a 7-minute OGD insult in the presence of MRS 1523. # AD was absent in 11 slices receiving 7 or 8 minutes of OGD in the presence of MRS 1523.
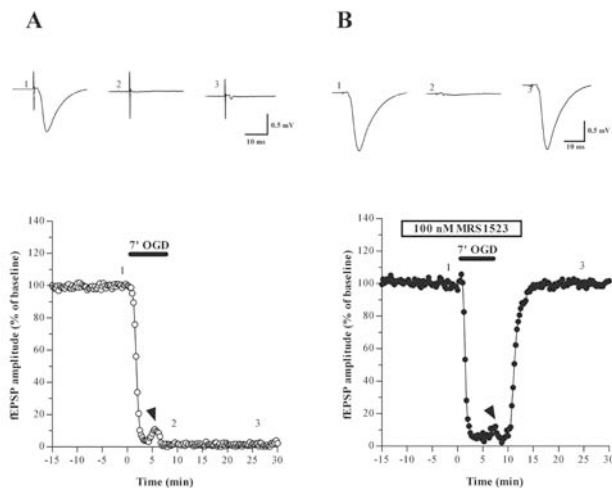
Figure 13. The A$_3$ adenosine receptor antagonist MRS 1523 protects hippocampal slices from irreversible fEPSP depression induced by 7 minutes of OGD. (A,B) Graphs: typical time courses of changes in fEPSP amplitude evoked by 7-minute OGD episodes (solid bar) in control (A) or in the presence of 100 nM MRS 1523 (B). Each point represents fEPSP amplitude expressed as percent of the mean baseline responses recorded before OGD application. Note the transient reappearance of synaptic potential during OGD (arrowheads) in A and B. Upper traces: fEPSP recordings taken at the times indicated by numbers in the corresponding graph. Note that after reperfusion in normal oxygenated aCSF, only the afferent volley recovered in controls, while a recovery of 77% was observed at the end of MRS 1523 application in normoxic conditions. A total recovery of fEPSP after 15 minutes of reperfusion in normal oxygenated aCSF was found in MRS 1523 (trace 3).

In a subset of experiments, we investigated the effects of 100 nM MRS 1523 on AD by comparing the time of peak and the magnitude of depolarising DC shifts caused by a 7-minute OGD insult in treated slices and in matched control slices from the same rats. As illustrated in figure 14A, in control conditions, 7-minute OGD episodes always caused AD, recorded as negative DC shifts, with a mean peak latency of about 6.5 minutes (390 ± 20 s) from the beginning of ischemia and a peak amplitude of 8.9 ± 0.6 mV (n=8). The duration of DC shifts was variable (range 5-15 minutes) and was always accompanied by complete and irreversible disappearance of synaptic transmission.

In the presence of MRS 1523 (100 nM, n=8), AD was virtually absent in 7 out of 8 preparations and, as shown in figure 14B, the mean recovery of potential amplitude was significantly greater than in control slices taken from the same rats (MRS 1523: 85.8 ± 13.3 %, n=8 vs control: 3.3 ± 2.5 %; $P<0.001$). Interestingly, in one experiment in which a sizeable AD (peak amplitude: -7.6 mV) was recorded, the recovery from OGD-evoked impairment in neurotransmission was only 22%. The overall effect of A$_3$ antagonism on fEPSP recovery after 7 minutes of OGD, compared with that observed in control preparations, is summarised in figure 14B. As illustrated by the frequency histogram, 39 out of 45 slices treated with any of the A$_3$ antagonists at effective concentrations (all except 0.1 nM MRS 1523), had a substantial (> 50%) recovery of fEPSP amplitude after 7-minute OGD episodes, while synaptic activity in controls (n=42) never recovered beyond 20% of responses recorded before OGD.

The protective effect of MRS 1523 on OGD-evoked irreversible depression of fEPSPs was detectable at concentrations as low as 0.1 nM and the recovery of fEPSP ampli-

tude became statistically significant with concentrations of 1-100 nM of the antagonist (figure 15A). The apparent EC_{50} value for MRS 1523 was 0.25 nM (95% C.L. 0.05-1.2 nM). However, since within the time of the antagonist application (10-20 minutes) the drug might not have reached equilibrium at the receptor level in slices, the EC_{50} value is likely to be underestimated. Similar beneficial effects on the recovery of fEPSPs from 7 minutes of OGD were exerted by the selective adenosine A_3 receptor antagonists MRS 1220, VUF 5574 and WSAB, all chemically different from MRS 1523 (Kim *et al.*, 1996; Maconi *et al.*, 2002; Muijlwijk-Koezen *et al.*, 2000). As shown in figure 15A, all A_3 antagonists prevented synaptic impairment and allowed for complete synaptic recovery within 15 minutes from OGD interruption. In addition, all compounds prevented or significantly delayed AD appearance after the 7 minute OGD insult (not shown).
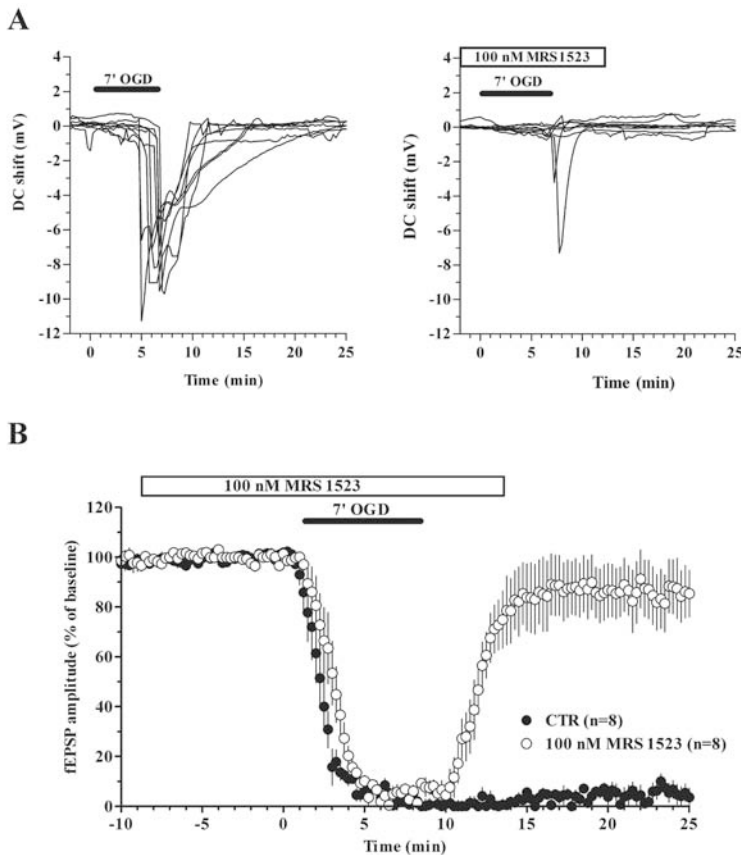
Figure 14. The A_3 adenosine receptor antagonist MRS 1523 minimises AD and protects CA1 hippocampus from irreversible fEPSP depression induced by a 7-minute OGD insult. A. AD was recorded as the negative DC shift in response to 7 minutes of OGD in control conditions (n=8) and in the presence of 100 nM MRS 1523 (open bar, n=8). MRS 1523 significantly prevented AD in 7 out of 8 slices. B. Graph shows the time-course of a 7-minute OGD effect on fEPSP amplitude, expressed as percent of baseline, in control aCSF (filled circles) and in the presence of 100 nM MRS 1523 (unfilled circles). Data are expressed as mean ± s.e. Note that in the presence of the A_3 antagonist the time-course of fEPSPs depression during OGD was significantly delayed (see table 7) in comparison to corresponding times in the absence of the drug (control slices).

2.1.3 The selective block of A_3 adenosine receptors delays the effects of prolonged OGD application on synaptic transmission.

In the experiments performed with 7 minutes of OGD, the inhibitory effect of A_3 antagonists on the development of AD seemed to be related to the significant recovery of fEPSP amplitude induced by these drugs. Furthermore, as illustrated in Figures 13 and 14, OGD episodes produced a typical sequence of neurophysiological effects that followed the initial disappearance of fEPSP and that comprised a transient recovery of fEPSP response, the disappearance of the afferent fibre volley and the development of an AD. All these phenomena were significantly delayed and/or reduced in the presence of A_3 receptor antagonists, as shown in table 7, where the effects of 100 nM MRS 1523 on OGD of different duration are summarised. The possible correlation of these effects of A_3 receptor antagonists with the recovery of the fEPSP after OGD interruption and the time window in which A_3 receptor block may play a role in limiting the deleterious effects of severe ischemia were investigated by applying OGD episodes longer than 7 minutes. To delimit the time window in which A_3 antagonists could delay the appearance of AD, we applied 30 minutes of OGD in the presence of 100 nM MRS 1523 (figure 16A). Compared to the effects observed in matched control slices, the A_3 receptor antagonist significantly increased the latency of AD peak from 7.28 minutes (437 ± 31 s) in control to 9.5 minutes (571 ± 70 s) in MRS 1523 ($P < 0.01$, Mann-Whitney test, two tailed), without significantly affecting either the average magnitude (figure 14) or the peak amplitude of AD (6.2 ± 1.2 mV, n=6 vs. 7.3 ± 0.3 mV, n=8 in control, P= 0.49, two-tailed Mann-Whitney test). No recovery of fEPSPs was recorded after interruption of the 30-minute OGD insult (not shown).

In a final set of experiments we monitored the recovery of fEPSPs while recording AD latency and amplitude following OGDs of different duration (8-10 minutes) in the presence of 100 nM MRS 1523.

As summarised in figure 16B, a significant recovery of fEPSP amplitude was obtained after OGD insults of duration up to 9 minutes. No significant recovery was observed in 5 slices after 10 minutes of OGD. On analyzing the fEPSP recovery in relation to AD appearance after OGD, it emerged that the degree of fEPSP recovery after OGD in A_3 antagonist-treated slices depended on the appearance of AD and not on the duration of OGD episodes. In fact, in the absence of AD a full recovery of fEPSP was found in most preparations receiving 7 or 8 minutes of OGD episodes and in one slice after 9 minutes OGD.

Interestingly, treatment with MRS 1523 allowed for a significantly better recovery of neurotransmission also in those slices in which AD was present, but peaked close to the end of OGD episodes (≤ 45 s) or after the interruption of OGD (25.6±5.5 % mean ± s.e., range 3-75 %, n=14 vs control 7.2±2.8 % mean ± s.e., range 0-24.5 %, n=17, $P < 0.005$, Mann-Whitney test, two-tailed). Conversely, in control slices, no considerable recovery was found even in those preparations in which AD peaked after interruption of the 7-minute OGD.

Therefore, it appears that in our experimental conditions the most relevant correlates for the degree of recovery of neurotransmission produced by A_3 receptor block during OGD was the delay in AD development, which prolonged the time-window allowed for the recovery of fEPSPs.

After evaluating the effects of the selective block of A_3 receptors activated during mild (2 or 5 minutes) and severe (7 minutes) OGD episodes by the endogenously released adenosine, we investigated the role of A_3 receptor stimulation by exogenous agonist application in the same experimental conditions.
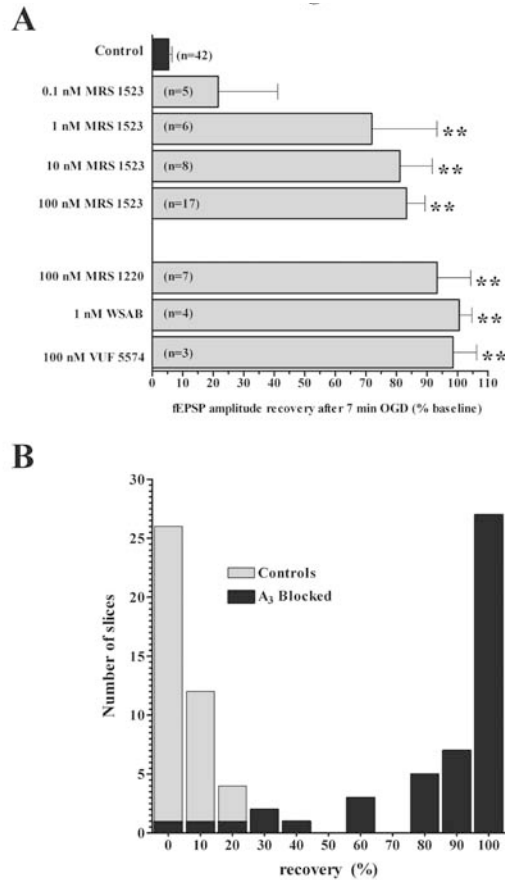
Figure 15. Effects of different selective A_3 adenosine receptor antagonists on recovery of fEPSP amplitude after a 7-minute OGD insult. A. Column bars indicate the average recovery (mean ± s.e.) of fEPSPs after 7 minute of OGD, recorded in hippocampal slices at 15 minutes reperfusion in normal, oxygenated aCSF. Asterisks indicate P<0.05, one-way ANOVA, Newman-Keuls multiple comparison post-hoc test, versus control. B. Distribution analysis of fEPSP recovery in 87 slices receiving 7-minute OGD episodes either in control or in the presence of A_3 receptor antagonists (see A, 0.1 nM MRS excluded). Bars indicate the number of cells (ordinate) that showed a given recovery of fEPSP (abscissa) from 7-minute OGD episodes in control aCSF (n=42; white bars) or in the presence of A_3 antagonists (n=45; black bars). Note that the large majority of treated slices (38 out of 45) show more than 50% recovery of fEPSPs.

2.1.4 The selective stimulation of adenosine A_3 receptors by a "long application" of Cl-IB-MECA reduces fEPSP depression evoked by a 2-minute OGD episode and induces a faster recovery of fEPSP amplitude after a 5-minute OGD.

The effect of Cl-IB-MECA (10 nM) on fEPSP amplitude after 2 minutes of OGD is shown in figure 17A. The selective A_3 agonist did not affect the amplitude of fEPSPs under normoxic conditions, but induced a significant decrease in fEPSP depression evoked by 2 minutes of OGD (72.5±4.5% in control and 39.5±7.1% in the presence of the agonist, n=13, P<0.05, paired two-tailed Student's t test). The effect of 10 nM Cl-IB-
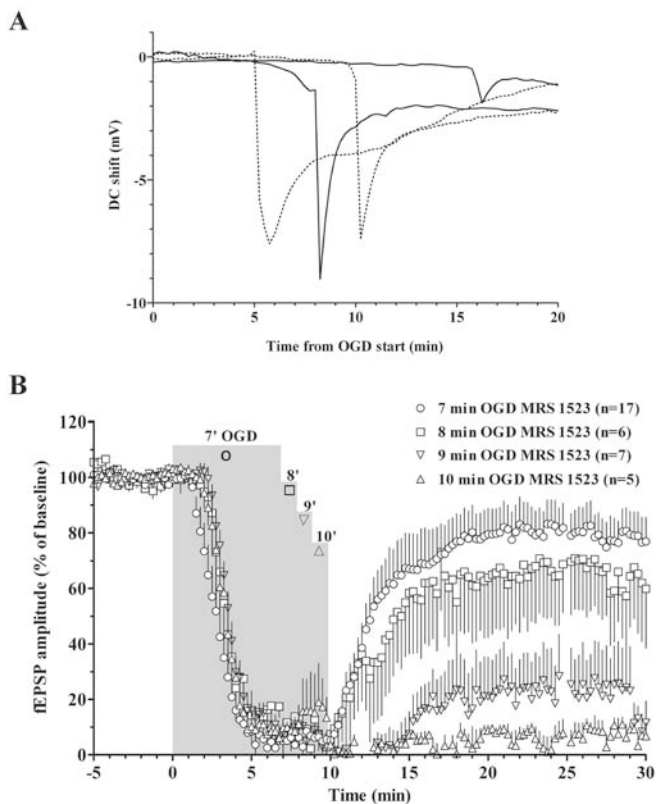
Figure 16. Treatment with MRS 1523 postpones the appearance of AD and broadens the time window for CA1 fEPSP recovery after OGD interruption. A. Time-window for OGD (30 minutes)-elicited ADs in the absence (dotted lines) or presence of 100 nM MRS 1523 (continuous lines). Traces represent ADs recorded as negative DC shifts in response to 30 minutes of OGD taken from control experiments (n=6) or in MRS 1523 (n=6). For the sake of clarity, only the earliest and the most delayed ADs observed in each group of slices are shown. Note that in MRS 1523 both the earliest and the latest ADs were delayed compared to the corresponding ADs in controls. AD magnitude, expressed as the integral of tissue depolarisation measured for 2 minutes after AD peak in MRS 1523-treated slices (3.2 ± 0.6 Vs, n=6), was not statistically different from that of controls (3.6 ± 0.7 Vs, n=8, P=0.49, Mann-Whitney, two tails). B. Time-course of fEPSP amplitude, expressed as percent of baseline level, during OGD of different time durations applied in the presence of 100 nM MRS 1523. Values are mean ± s.e.

MECA was maximal because the increase of the agonist concentration to 100 nM did not potentiate the effect (75±7% in control and 41±10% in the presence of the agonist, n=6, P<0.05, paired two-tailed Student's t test, data not shown). The effect of 10 nM Cl-IB-MECA was not antagonized by the selective A$_{2A}$ receptor antagonist ZM 241385, superfused 15 minutes before and then co-applied with Cl-IB-MECA (73±9% in control and 38±14% in the presence of 100 nM ZM 241385 in combination with Cl-IB-MECA, n=3, data not shown).

The effect of 10 nM Cl-IB-MECA during a 5-minute OGD insult is shown in figure 17B. Cl-IB-MECA did not change the fEPSP time-course before and during OGD but reduced the time of fEPSP recovery (AUC: 9.5±0.6 in control, n=10 and 7.7±0.61 in the
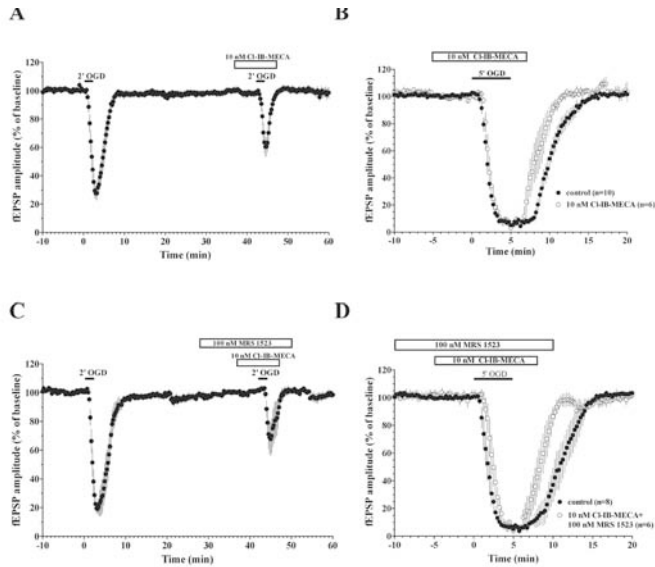
Figure 17. The selective A$_3$ adenosine receptor agonist Cl-IB-MECA, decreases fEPSP depression induced by a 2-minute OGD episode and induces a faster recovery of fEPSP amplitude after a 5-minute OGD. Time-courses of fEPSP amplitude changes elicited by different OGD insults. Data (mean ±s.e.) are expressed as percent of baseline values recorded before OGD initiation. A. 2-minute OGD insults in the absence and in the presence of Cl-IB-MECA (10 nM; n=13). The A$_3$ agonist, applied 5 minutes before, during and 2 minutes after OGD (open bar), induced a significant reduction in fEPSP depression caused by the 2-minute OGD insult (P<0.05 vs first OGD insult, paired two-tailed Student's t test). B. 5 minutes of OGD in the absence and presence of 10 nM Cl-IB-MECA. The A$_3$ agonist, applied as before, induces a faster fEPSP recovery after 5 minutes of OGD. C. 2-minute OGD insults in the absence and presence of 10 nM Cl-IB-MECA in combination with 100 nM MRS 1523 (n=7). The antagonist was always superfused alone 5 minutes before and 3 minutes after agonist application. Note that, in the presence of Cl-IB-MECA and MRS 1523, the fEPSP depression induced by a 2-minute OGD episode was significantly reduced (P<0.05 vs first OGD insult, paired two-tailed Student's *t* test). D. 5 minutes of OGD in the absence and presence of Cl-IB-MECA (10 nM) in combination with MRS 1523 (100 nM). The antagonist was applied as described before.

presence of the agonist, n=6, *P*<0.05, one-way ANOVA, Newman-Keuls multiple comparison post-hoc test, see also figure 18C).

Figures 17C and D show the effect of co-application of Cl-IB-MECA and MRS 1523 on 2 and 5 minutes of OGD, respectively. The antagonist was always superfused 5 minutes before the agonist. The effect of the co-application of the two drugs on fEPSP depression induced by a 2-minute OGD episode (81±3.3 % in control and 32.3±11.5% in the presence of the two drugs, n=7, *P*<0.05, paired two-tailed Student's *t* test, figure 17C) was not significantly different from that observed in the presence either of MRS 1523 alone (figure 12B) or Cl-IB-MECA alone (figure 17A). Similarly, the effect induced by the co-application of the two drugs on the time of fEPSP recovery after a 5-minute OGD insult (AUC: 10.6±1 in control, n=8 and 7.79±0.49 in the presence of the two drugs, n=6, *P*<0.05, one-way ANOVA, Newman-Keuls multiple comparison post-hoc test, see also figure 18C) was not different from those observed in the presence either of MRS 1523 alone (figure 12C) or Cl-IB-MECA alone (figure 17B). Thus,

we concluded that the effects of MRS 1523 and Cl-IB-MECA co-application on fEPSP inhibition induced by 2 or 5 minutes of OGD are not additive.

2.1.4 The selective stimulation of adenosine A$_3$ receptors by a "short application" of Cl-IB-MECA does not affect fEPSP depression evoked by a 2-minute OGD insult and delayed the recovery of fEPSP amplitude after a 5-minute OGD.

Since it has been demonstrated that A$_3$ adenosine receptors undergo to a rapid desensitization more evident and persistent when the agonist was applied for long times (Trincavelli *et al.*, 2002a), we chose to check a different protocol shortening the time
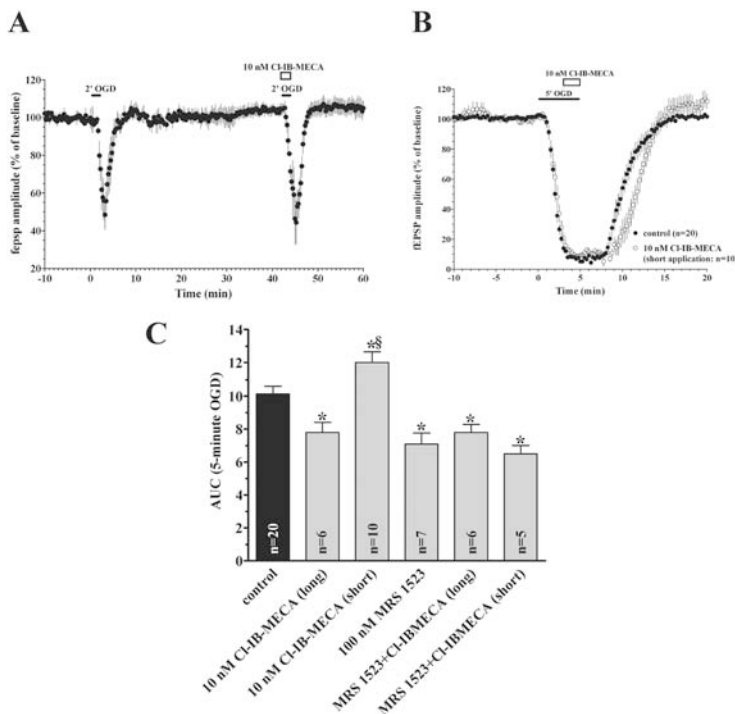
Figure 18. "Short" application Cl-IB-MECA does not modify fEPSP depression induced by a 2-minute OGD episode whereas it significantly delays fEPSP recovery after a 5-minute OGD. Data (mean ±s.e.) are expressed as percent of respective baseline values recorded before OGD application. A. Time-course of fEPSP amplitude changes elicited by 2-minute OGD episode in the absence and in the presence of Cl-IB-MECA (10 nM; n=7). The A$_3$ agonist was applied for only 2 minutes, during OGD (open bar). Note that, a "short" application of Cl-IB-MECA did not induce significant change (P>0.05, paired two-tailed Student's *t* test) in the fEPSP depression induced by 2 minutes of OGD. B. Time-course of fEPSP amplitude changes elicited by 5-minute OGD insults in the absence and in the presence of 10 nM Cl-IB-MECA. As indicated by open bar, the A$_3$ agonist was applied only for 2 minutes, at the end of the 5-minute OGD episode. Note that "short" application of Cl-IB-MECA delayed fEPSP recovery after 5 minutes of OGD. C. Columns in the graph summarize the average time of fEPSP amplitude recovery after 5-minute OGD insults in control conditions and in the presence of Cl-IB-MECA and MRS 1523, alone or in combination. * P < 0.05, one-way ANOVA followed by Newman-Keuls multiple comparison post-hoc test versus control slices; § P<0.05, one-way ANOVA followed by Newman-Keuls multiple comparison post-hoc test versus all experimental groups.

of Cl-IB-MECA application. As shown in figure 18A, Cl-IB-MECA (10 nM) applied only during the 2-minute OGD episode did not modify the outcome of fEPSP depression induced by this insult in comparison to those obtained in the absence of drug (51.6±7.7% in control and 55.6±11.8% in the presence of Cl-IB-MECA n=7, P>0.05, paired two-tailed Student's t test). Figure 18B shows that when Cl-IB-MECA was applied for 2 minutes at the end of the 5-minute OGD episode, it significantly delayed the time of fEPSP recovery (AUC: 9.7±0.4 in control, n=20 and 12.1±0.65 in the presence of the agonist, n=10, P<0.05, one-way ANOVA, Newman-Keuls multiple comparison post-hoc test, see also figure 18C). This effect was blocked in the presence of 100 nM MRS 1523 (n=5, data not shown). Similar results were obtained using different A_3 agonists: AR132 (10 nM, n=3), VT158 (5 nM, n=2) and VT 160 (5 nM, n=2). A summary of "short" and "long" application of Cl-IB-MECA during 5 minutes of OGD is illustrated in figure 18C.

2.1.5 The selective A_3 adenosine receptor agonist, Cl-IB-MECA, also protects from the irreversible depression of neurotransmission induced by a 7-minute OGD insult.

The effects of 10 nM Cl-IB-MECA on fEPSP amplitude after 7 minutes of OGD are shown in figure 19. In control slices, a 7-minute OGD insult induced an irreversible block of neurotransmission as indicated by the absence of fEPSP amplitude recovery (4.2±3.3%, n=16) when the slices were superfused in normal oxygenated aCSF. In 8 control slices in which we also measured the appearance of AD, 7-minute OGD episodes always caused AD, with a mean peak latency of about 6.6±0.3 minutes from the beginning of OGD and a peak amplitude of 7.1±0.5 mV (n=8). Cl-IB-MECA (10 nM, 5 minutes before, during and 2 minutes after OGD), did not modify fEPSP amplitude under normoxic conditions but induced a significant fEPSP recovery after 7 minutes of OGD (81.5±10.5 %, *P*<0.001, one-way ANOVA, Newman-Keuls multiple comparison post-hoc test vs control slices group, n=15, figure 19B and C). AD was absent in 5 slices out of 8 tested and it was significantly delayed in the remaining 3 slices (peak latency of 7.91± 0.54 minutes, peak amplitude 6.6± 2.0, figure 17A). Similar effects on fEPSP recovery were obtained by using different A_3 agonists, AR132 (10 nM, n=5), VT72 (10 nM, n=8), VT158 (5 nM, n=3), VT160 (5 nM, n=4) and VT163 (5 nM, n=3) (figure 19C). In addition, all the A_3 agonists tested prevented or significantly delayed AD after the 7-minute OGD episode (not shown). These data demonstrate that the effects elicited by the exogenous application of a selective A_3 receptor agonist are similar to those obtained in the presence of A_3 selective antagonists (figure 15A), thus suggesting a rapid desensitisation of this receptor subtype.

    In order to confirm that the protective effect exerted by Cl-IB-MECA on fEPSP recovery after a 7-minute OGD insult was effectively due to a desensitization of A_3 receptors, we performed a different protocol. In a separate group of slices, a 15-minute pretreatment with 10 nM Cl-IB-MECA was applied 20 minutes before the induction of a 7-minute OGD insult. As shown in figure 19D, 10 nM Cl-IB-MECA pre-treatment was enough to induce a significant fEPSP recovery after 7 minutes of OGD (103±3.6 % after Cl-IB-MECA pre-treatment, n=3, 4.1±3.6, n=3% in control) even if the compound was absent during the ischemic episode itself.
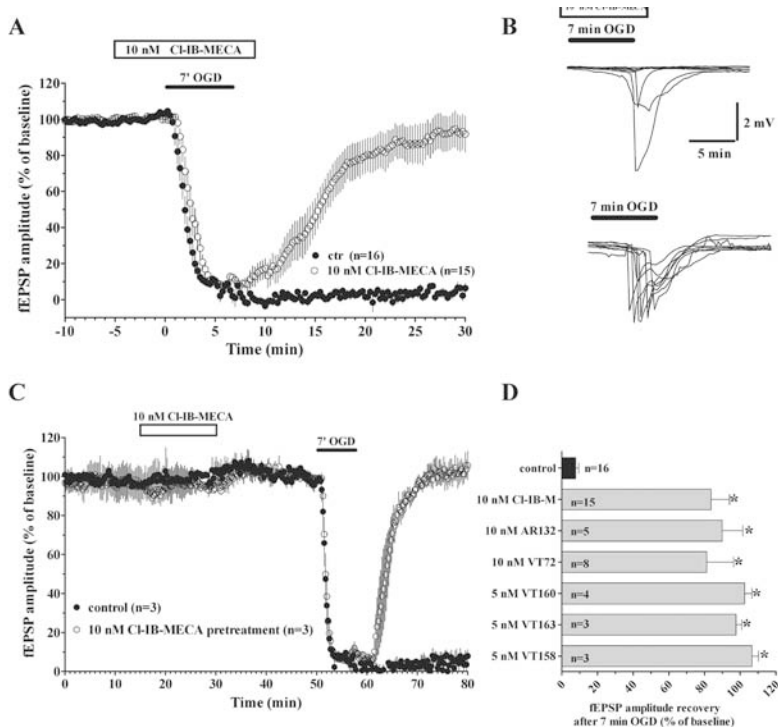
Figure 19. The selective A$_3$ adenosine agonist, Cl-IB-MECA, protects hippocampal slices from the irreversible fEPSP depression induced by a 7-minute OGD insult. Data (mean ± s.e.) are expressed as percent of baseline values recorded before OGD application. A. Time-course of fEPSP amplitude before, during and after the 7-minute OGD in the absence and in the presence of 10 nM Cl-IB-MECA. Cl-IB-MECA was applied 5 minutes before, during and 2 minutes after OGD (open bar). B. In the same slices, AD was recorded as the negative DC shift in response to 7 minutes of OGD in control conditions (n=8) and in the presence of 10 nM Cl-IB-MECA (open bar, n=8). The agonist prevented AD appearance in 5 slices and delayed it in the remaining 3 slices. C. Time-course of fEPSP amplitude in control conditions, in the presence of 10 nM Cl-IB-MECA (open bar, 15 minutes) and during the 7-minute OGD episode. OGD was applied 20 minutes after the end of Cl-IB-MECA superfusion. Note that Cl-IB-MECA does not modify fEPSP in normoxic conditions but allows a complete recovery of fEPSP amplitude after 7 minutes of OGD. D. Columns in the graph summarize the effects of different A$_3$ agonists on fEPSP recovery after 7- minute OGD insults. * $P < 0.05$, one-way ANOVA followed by Newman-Keuls multiple comparison post-hoc test versus control slices.

3. Discussion

3.1 Role of adenosine receptor antagonists in depression and disruption of CA1 hippocampal excitatory synaptic transmission during *in vitro* ischemia.

The main finding of the present work is that the selective antagonism of A_3 adenosine receptors during a severe (7-minute) OGD insult reduces the deleterious effects of ischemia on CA1 hippocampal neurotransmission and pyramidal cell survival.

In our experiments, the pre-treatment of hippocampal slices with selective A_3 adenosine receptor antagonists considerably delays the occurrence of AD and significantly protects from the irreversible disruption of excitatory neurotransmission caused by 7-minute OGD episodes. A_3 receptor antagonists exert a protective effect on OGD episodes of ≤ 9 min duration, showing that other cellular mechanisms are implicated and predominate when AD takes place after a prolonged ischemia.

We used four selective A_3 adenosine receptor antagonists with different chemical structure and lipid solubility (Jacobson *et al.*, 1997; Kim *et al.*, 1996; Li *et al.*, 1998; Maconi *et al.*, 2002; Muijlwijk-Koezen *et al.*, 2000; Muller 2003) to assess the role of A_3 receptor stimulation by endogenous adenosine released during OGD episodes. All compounds show similar protective effects on the 7-minute OGD protocol at nM concentration, ensuring specific involvement of A_3 receptors in the observed effects. MRS 1220, VUF 5574 and WSAB were reported to have higher affinity for the human A_3 receptors (Jacobson *et al.*, 1997; Kim *et al.*, 1996; Maconi *et al.*, 2002; Muijlwijk-Koezen *et al.*, 2000) and their effectiveness on native rat A_3 receptors at very low concentration may be surprising. We do not have any straightforward explanation for this phenomenon. The tissue accumulation of the lipophilic MRS 1523, MRS 1220 and VUF 5574, is an unlikely explanation since WSAB is a hydrophilic compound (Maconi *et al.*, 2002). On the other hand, receptor affinity of these compounds may also depend on specific conformations assumed by A_3 receptors in the integer cell membrane and may differ from that assessed in receptor binding experiments on disrupted membranes. Alternatively, the paucity of A_3 receptors in native tissue (Ji *et al.*, 1994; von Lubitz 1999) allows the speculation that occupancy of a substantial fraction of A_3 receptors is required for evoking cell response(s). In this case, the block of a relatively small fraction of A_3 receptors may be sufficient to greatly antagonise the effects of endogenous adenosine released during OGD (see also below).

The depression of synaptic responses caused by OGD episodes of short duration (up to 5 minutes) in the CA1 region of the hippocampus is fully reversible (Latini *et al.*, 1999b; Pugliese *et al.*, 2003). In the present work, it has been demonstrated that the selective block of A_3 receptors by the antagonist MRS 1523 reduces fEPSP inhibition caused by 2 minutes of OGD and induces a faster recovery of fEPSP amplitude after 5 minutes of OGD application. The decrease in fEPSP depression or the faster recovery of fEPSP amplitude during the selective block of A_3 receptors indicate an inhibitory role of A_3 receptors on synaptic transmission during brief OGD insults. We have previously demonstrated that depression of synaptic potentials during 2 or 5 minutes of OGD is almost completely antagonized in the presence of the selective A_1 adenosine receptor antagonist DPCPX (Latini *et al.*, 1998; 999a and 1999b). Most of the known neuroprotective effects of adenosine during ischemia both *in vivo* or *in vitro* are attrib-

uted to the depression of synaptic activity induced by the activation of A$_1$ receptors. Therefore, the decrease in synaptic depression brought about by A$_3$ adenosine receptor antagonists suggests that A$_1$ and A$_3$ receptors cooperate in inhibiting fEPSP amplitude during the first minute of OGD and share a neuroprotective role in these pathological conditions. This interpretation is in line with the observation that selective activation of A$_3$ adenosine receptors under hypoxic conditions brings about inhibition of excitatory neurotransmission in rat cortical neurons (Hentschel *et al.*, 2003) and that mice lacking A$_3$ adenosine receptors have increased neurodegeneration in response to repeated episodes of moderate hypoxia (Fedorova *et al.*, 2003).

Nevertheless, as above illustrated, the role of A$_3$ receptors is no longer beneficial during periods of severe (7-minute) OGD and drastically diverge from the A$_1$-like protective effect. In fact, unlike the A$_3$ antagonists, the selective A$_1$ receptor antagonist DPCPX impairs the recovery of synaptic potentials after a hypoxic insult (Sebastiao *et al.*, 2001). Moreover, the non-selective A$_1$ receptor antagonist theophylline increases the incidence of spreading depression (SD), the analogue of AD under normoxic conditions (Somjen 2001), and decreases the latency of SD occurrence elicited by increasing extracellular K$^+$ concentration in CA1 hippocampal slices (Kaku *et al.*, 1994). Prolonged ischemic conditions could play a pivotal role in switching the effects of A$_3$ receptor stimulation from A$_1$-like inhibition to potentiation of excitotoxic glutamate effect. The activation of PLC by adenosine A$_3$ receptors has been reported in striatal and hippocampal slices (Abbracchio *et al.*, 1995a). Rat cortical neurons exposed to *in vitro* hypoxia show an increase in PKC activation after selective A$_3$ receptor stimulation (Nieber *et al.*, 2006). Similarly to what is described in the heart, PKC-dependent activation of K$_{ATP}$ channels may enhance adenosine protection (Liang 1998) but if OGD is applied long enough to be considered severe, protracted PKC activation induced by A$_3$ receptors could account for an increase in intracellular calcium which may participate in increasing tissue excitability and thus leading to irreversible synaptic failure, as already speculated in previous work (Abbracchio *et al.*, 1999).

A constant sequence of changes in neurotransmission occurs during the application of long OGD episodes and comprises: i) the early depression of evoked fEPSPs, ii) a transient recovery of fEPSPs followed by iii) the disappearance of synaptic responses and afferent fibre volley and iv) AD. The whole sequence of events lasts about 6 min and therefore is typically recorded within the application of 7-min OGD.

Our results show that the block of A$_3$ receptor-mediated effects by selective antagonists results in a significant delay of the sequence of electrophysiological changes, including disappearance of the afferent fibre volley and AD that are considered early electrophysiological signs of tissue suffering.

The earliest event observed during OGD was the disappearance of the electrically-evoked fEPSPs that reflect the currents generated by the inflow of cations into CA1 pyramidal cell dendrites produced by activation of synaptic glutamate receptors. The predominant, although not exclusive, mechanism that accounts for the reduction in fEPSPs during the first 4-5 min of ischemia is a decrease in glutamatergic neurotransmission caused by activation of adenosine A$_1$ presynaptic receptors (Fowler 1990; Gribkoff *et al.*, 1990; Latini *et al.*, 1999a; Pedata *et al.*, 1993).

A$_3$ receptor stimulation *per se* does not produce any harmful effects in normoxic tissue. In fact neither A$_3$ receptor agonists nor adenosine disrupt CA1 neurotransmission in normally oxygenated slices (Dunwiddie *et al.*, 1997a). This implies that the main role of A$_3$ receptor activation during OGD is to hasten the processes that lead to AD and that removal of these mechanisms prolongs the period of tissue survival

to OGD, but cannot fully block the consequences of ischemia. In order to explain the mechanism by which A_3 receptors may be contributing to failure of synaptic transmission during OGD, we can postulate that stimulation of A_3 receptors by adenosine released during prolonged and severe ischemia may enhance excitatory transmission on CA1 pyramidal neurones, accounting for increased neuronal excitability and consequent lack of protection of the ischemic tissue. Stimulation of A_3 receptors in the hippocampus may in fact: i) counteract the inhibitory action of A_1 adenosine receptors on excitatory neurotransmission (Dunwiddie *et al.*, 1997a); ii) inhibit the presynaptic metabotropic glutamate receptor inhibitory function on excitatory transmission (Macek *et al.*, 1998). Furthermore, A_3 receptor-mediated stimulation of PLC could contribute to neuronal damage through mobilisation of intracellular Ca^{2+} (Abbracchio *et al.*, 1995a) and/or activation of PKC, resulting in an increase in excitability of CA1 neurones (Hu *et al.*, 1987). Consistently, our data show that the action of A_3 receptor antagonists is limited to a time window that extends survival to about 9 minutes of OGD. This time window seems to be related to the maximal delay allowed for the appearance of AD in the absence of A_3 receptor stimulation.

The generation of AD is complex and multifactorial (see Somjen 2001) and the mechanisms responsible for the delay in AD remain elusive. Interestingly, the time window of A_3 receptor-mediated effects overlaps with the delay that can be obtained by treating the slices with glutamate receptor antagonists (Somjen 2001; Tanaka *et al.*, 1997; Yamamoto *et al.*, 1997). It is appealing to suggest that removal of the A_3 receptor-mediated impairment of feedback inhibition of glutamate release exerted by specific metabotropic glutamate receptor subtypes (Macek *et al.*, 1998) may substantially decrease/delay the participation of the excitatory neurotransmitter in triggering the AD.

Our results are in contrast with those obtained in transgenic mice with a deletion of the A_3 receptor. It has been demonstrated that after repeated brief exposure to carbon monoxide, mice lacking the A_3 receptors are more vulnerable than control animals to hippocampal damage following hypoxia (Fedorova *et al.*, 2003), suggesting a neuroprotective role of A_3 receptors. The discrepancy about the functional role of A_3 receptors in the brain during hypoxia or ischemia could be due to the diversity of both the experimental conditions (hypoxia/ischemia) and pharmacological profiles of these receptors across species.

The delay of the initial depression of fEPSPs caused by A_3 antagonists indicates that A_3 receptors are activated within the first 2 minutes of OGD despite the reported low affinity of adenosine for these receptors (about 5 µM: Zhou *et al.*, 1992). However, since the estimated concentration of adenosine at the receptor level approaches 5 µM at the second minute of OGD and reaches 30-40 µM within the fifth min of OGD (Latini *et al.*, 1999b) a substantial activation of A_3 receptors may be achieved since the beginning of ischemia. According to the Hill-Langmuir equation, using the above reported values, the estimated occupancy of A_3 receptors by endogenous adenosine would approach 50% within the second min of OGD and be almost 90% at 5 min of OGD.

It is therefore conceivable that all the changes in neurophysiological parameters observed with A_3 receptor antagonists result from block of cell mechanisms activated by A_3 receptors and that their stimulation by adenosine released during OGD contributes to the development of ischemia effects from the beginning of OGD, thus hastening the deleterious effects of ischemia on neurotransmission.

A modest, transient, recovery of fEPSPs was observed in most preparations and fading of the recovery was accompanied by disappearance of the presynaptic fibre volley. This sequence of events has been ascribed to a progressive increase in the extracel-

lular K$^+$ concentration that initially produces hyperexcitability of pyramidal cells followed by a depolarizing block of neurotransmission when extracellular K$^+$ reaches 10 mM or higher concentration (Sick *et al.*, 1987). After fibre volley disappearance and in the absence of any synaptic response, the large efflux of potassium into the extracellular space combined with activation of sodium and calcium channels, triggers sustained depolarization of hippocampal cells that coincides with AD recorded in the CA1 region. Although similar to the spreading depression described by Leão (Leão 1944) and known to be harmless to the cerebral cortex under normoxic conditions, AD has been suggested to contribute to cell damage during ischemia (see Somjen 2001). Increased intracellular calcium and/or massive glutamate receptor activation are additional mechanisms that act in concert with potassium redistribution to produce AD (Tanaka *et al.*, 1997; Yamamoto *et al.*, 1997) and have been suggested to contribute to cell damage during ischemia (Somjen 2001).

3.2 Therapeutic implications for the protective role of adenosine A$_3$ receptor antagonists during prolonged ischemic conditions.

In the brain, spreading depression is a phenomenon characterised by a slow transient cellular depolarization moving at 3–4 mm/min over the surface of the cortex (Leão 1944). A large efflux of potassium into the extracellular space coincides with the shift in the DC potential. The changes in brain homeostasis are transient and do not cause visible injury in normoxic conditions (Hansen *et al.*, 1988), but are correlated with tissue damage during ischemia (Somjen 2001). Within 2 minutes of stroke onset, neurones and glia suddenly depolarize in the brain area where cerebral blood flow falls to 10% of control (Macdonald *et al.*, 1998). In these conditions, the generation of AD may contribute to the extent and severity of neuronal damage. In particular, the propagation of the AD to the hypoxic/hypoglycaemic region (penumbral area) surrounding the ischemic core may extend the damage. Consistently, it has been demonstrated that one major factor contributing to neuronal death in the penumbra is the propagation of spreading depression waves (Koroleva *et al.*, 1996). Because the penumbra constitutes potentially salvageable tissue, the molecular responses of the perifocal neurones to focal ischemia and AD are of interest (Obeidat *et al.*, 2000).

In our experiments, a substantial field depolarization was recorded for several minutes (see e.g. figures 14, 16 and 19) after the AD peak and therefore even when OGD is interrupted immediately after the AD peak, hypoxia persists for few min after AD. Indeed, in our experimental conditions the recovery of pO$_2$ to normal levels takes about 3-4 minutes (Pugliese *et al.*, 2003).

This is important for the possible therapeutic outcome during ischemia *in vivo*. It may be envisaged that the block of A$_3$ receptors may increase the resistance of the brain tissue not only in the ischemic core but also in the surrounding "penumbral" region. However, while the action of A$_3$ block is of limited effectiveness in the ischemic core (depending on the duration of the episode), more effective neuroprotection can occur in the surrounding regions, where the damage can be ascribed to the concomitant hypoxia/hypoglycaemia and appearance of AD. The observation that a statistically significant recovery of fEPSPs occurred when AD peaked concurrently or after interruption of OGD in the presence of A$_3$ antagonists but not in control slices, supports the notion that A$_3$ receptor block increases the resistance to the deleterious effect of AD in conditions of milder hypoglycaemia/hypoxia. The causal association of A$_3$ receptor block, delayed AD appearance and better recovery from ischemic episodes needs, however, further investigation.

Regardless of the exact mechanisms exerted by A_3 receptors at a cellular level, it appears that the activation of these adenosine receptor subtypes during a prolonged ischemic episode produces deleterious consequences for the survival of neuronal cells and that the block of A_3 receptors may substantially increase the resistance of brain tissue to OGD occurring in ischemia.

3.3 Role of adenosine receptor agonists in depression and disruption of CA1 hippocampal excitatory synaptic transmission during *in vitro* ischemia.

Our results show, unexpectedly, that the effects induced by Cl-IB-MECA during OGD of different duration are similar to those elicited by adenosine A_3 antagonists. In fact, Cl-IB-MECA reduces fEPSP depression induced by a 2-minute OGD episode, induces a faster recovery of fEPSPs after a 5-minute OGD and permits a full recovery of neurotransmission after severe (7-minute) OGD. A decrease in OGD-induced fEPSP depression, brought about by A_3 agonists, may be attributed to A_{2A} receptor stimulation. It was, in fact, previously demonstrated that selective stimulation of A_{2A} receptors by CGS 21680 decreases fEPSP depression induced by 2 minutes of OGD and that the effect is antagonized by the selective A_{2A} antagonist, ZM 241385 (Latini *et al.*, 1999a). However, the concentration of Cl-IB-MECA used in the present study (10 nM) is highly selective for A_3 versus A_{2A} receptors (Muller 2003) and the effect of Cl-IB-MECA is not antagonized by ZM 241385, not withstanding that Cl-IB-MECA-induced depression of fEPSPs inhibition during a 2-minute OGD insult is mediated by A_{2A} adenosine receptors. Specific involvement of A_3 receptors in the observed effects is also ensured by observation that five chemically related compounds demonstrated similar effects to those elicited by Cl-IB-MECA. Concentrations of Cl-IB-MECA and of MRS 1523 used in the present study induce maximal effects. Therefore, the observation that the effects of Cl-IB-MECA and MRS 1523 during 2 or 5 minutes of OGD are not additive indicates that the effect of both drugs on fEPSP depression evoked by OGD is mediated by the same receptor system (i.e. A_3 receptors). In addition, the hypothesis of A_3 desensitization is also supported by the fact that 15 minutes of Cl-IB-MECA pre-treatment are sufficient to allow a full recovery of fEPSP amplitude after 7 minutes of OGD.

A reducing effect of Cl-IB-MECA on fEPSPs inhibition induced by adenosine has been attributed to a desensitization of A_1 receptors(Dunwiddie *et al.*, 1997a). Our results do not support such a mechanism because: i) the selective A_3 receptor antagonist MRS 1523 not only does not potentiate fEPSP inhibition induced by 2 and 5 minutes of OGD, but it attenuates this effect; ii) Cl-IB-MECA protects against AD appearance and irreversible disruption of excitatory neurotransmission caused by severe (7 minutes) OGD episodes while the selective A_1 antagonist DPCPX impairs the recovery of neurotransmission after hypoxia (Sebastiao *et al.*, 2001). Therefore, the effects of Cl-IB MECA are likely attributable to a rapid desensitization of A_3 receptors. This adenosine receptor subtype is particularly susceptible to phosphorylation by G protein-coupled receptor kinases (Linden 2001; Palmer *et al.*, 2000). Studies using stably transfected CHO cells have demonstrated that, following a few minutes of exposure to the agonist, there is a 30-40% decrease in the A_3 high affinity binding sites (von Lubitz *et al.*, 2001) and receptor internalization (Trincavelli *et al.*, 2000). Desensitization of A_3 receptors following exposure to Cl-IB-MECA and other A_3 selective agonists is supported by the observation that when Cl-IB-MECA was applied for a shorter time, it induced a slower recovery of fEPSPs after a 5-minute OGD episode instead of shortening the recovery. Further evidence in support of A_3 desensitization is provided by the observation that

perfusion with Cl-IB-MECA 20 minutes before application of a 7-minute OGD insult still allows a significant recovery of neurotransmission.

When considering that A_3 receptors encounter desensitization after prolonged exposure to A_3 agonists, we also have to consider that, under the OGD conditions used in the present study, endogenous adenosine released by the ischemic stimulus is not sufficient to cause A_3 receptor desensitization. During hypoxic/ischemic conditions adenosine is released from hippocampal slices, reaching concentrations up to 30 μM after 5-min OGD (Latini *et al.*, 1998; Pearson *et al.*, 2006). However, the efficacy of A_3 antagonists in blocking the depression induced by OGD of different durations indicates that endogenous adenosine concentrations reached in the extracellular milieu are not sufficient to desensitize A_3 receptors. Therefore, stimulation as massive as that reached in the presence of endogenous adenosine plus A_3 agonists is necessary to carry out substantial A_3 receptor plastic adjustments.

3.5 Conclusions

In conclusion, our data indicate that the block of A_3 receptors, stimulated by adenosine released during ischemia, counteracts fEPSP depression induced by OGD of different durations. Adenosine A_3 receptors stimulated by adenosine released by brief periods of ischemia might exert A_1-like protective effects on neurotransmission. Longer periods of ischemia, implying longer A_3 receptor stimulation, would switch the A_3 receptor-mediated effects to injurious effects. Moreover our data support the notion that A_3 receptors undergo rapid desensitization.

The major outcome of the present work is that selective block of adenosine A_3 receptors, or their desensitization, during severe ischemic insults in the brain may exerts neuroprotective effects on synaptic transmission, thus opening possible therapeutic perspectives for the future.

Increased knowledge of molecular mechanisms of A_3 receptors during cerebral ischemia may increase our understanding of the utility of A_3 agonists/antagonists in ischemic and different neurodegenerative disorders.

Chapter 2
Role of P2 purinergic receptors on hippocampal CA1 neurotransmission under normoxic conditions and during OGD

1. Historical background

Both potentiating and suppressing effects of exogenously applied ATP on synaptic transmission have been reported to date in the literature, depending on varying expression and localization of purinergic receptor subtypes (Cunha *et al.*, 2000; Hugel *et al.*, 2000; Nakatsuka *et al.*, 2001). From first evidence, it was clear that ATP-excitatory effects were mediated by P2X receptor stimulation since they were blocked by selective antagonists (Edwards *et al.*, 1992a; Evans *et al.*, 1992; Khakh *et al.*, 1998; Mori *et al.*, 2001; Pankratov *et al.*, 1998). In contrast, the inhibitory action of ATP and its analogues was usually found to be blocked by the selective A_1 antagonist DPCPX, suggesting an involvement of adenosine A_1 receptors (Cunha *et al.*, 1998; Masino *et al.*, 2002). In fact, it is generally known that extracellular ATP is rapidly converted into adenosine through ecto-ATPases and ecto-nucleotidases (Zimmermann 1996), with subsequent activation of P1 adenosine receptors. This was particularly evident in the hippocampus, where adenosine A_1 receptors are highly expressed, and their inhibitory role in CA1 neurotransmission has been well described (Fredholm *et al.*, 2001). Firstly, several lines of evidence lead to the hypothesis that ATP-mediated inhibition of hippocampal synaptic activity was probably mediated by adenosine A_1 receptors after a rapid degradation (<1s) of the nucleotide by ecto-ATPases and ecto-nucleotidases. In fact, this response was theophylline-sensitive (Cunha *et al.*, 1998; Dunwiddie *et al.*, 1997b; O'Kane *et al.*, 1998) and absent in A_1 knock out mice (Masino *et al.*, 2002). On the other hand, a more detailed observation of adenine nucleotide-evoked effects and the synthesis of new pharmacological tools revealed a P2-mediated inhibition (mostly attributed to P2Y receptor activation) of synaptic transmission in the hippocampus (Luthardt *et al.*, 2003; Mendoza-Fernandez *et al.*, 2000; Rodrigues *et al.*, 2005). However, the relative contribution of P1 and P2 receptor activation to the total hippocampal neurotransmission is still to be clarified (see Masino *et al.*, 2002; Rodrigues *et al.*, 2005).

The role of P2 receptors in the hippocampus may become even more relevant during pathological conditions such as ischemia, when an increased outflow of radioactive ATP from hippocampal slices during ischemic-like conditions has been reported (Juranyi *et al.*, 1999; Melani *et al.*, 2005). Some evidence already exists about a cytotoxic role of endogenously released ATP under such pathological conditions, both *in vivo* (Kharlamov *et al.*, 2002; Lammer *et al.*, 2006; Melani *et al.*, 2006; Ryu *et al.*, 2002) and *in vitro* (Cavaliere *et al.*, 2003 and 2004), but the mechanisms by which P2 receptors exert this toxic action are still unknown.

In this work we investigated the role of P2 purinergic receptor activation in CA1 neurotransmission in rat hippocampal slices under normoxic and ischemia-like con-

ditions, through the application of different P2 purinergic receptor agonists and antagonists.

2. Results

2.1 Effects of ATP on CA1 hippocampal neurotransmission

In the first series of experiments, the effect of ATP on evoked synaptic transmission in the CA1 region of rat hippocampal slices was investigated. Figure 20A shows that a 10-minute application of ATP decreased the evoked fEPSP amplitude in a concentration-dependent manner. A partial but statistically significant inhibition was observed at a concentration of 10 μM ATP (20.3±2.5 %, $P<0.0001$, paired Student's t test) while a substantial inhibition was observed at a concentration of 100 μM ATP (77.8±3.3%). As shown in figure 20A, the effect was always reversible after a few minutes of washout. The apparent EC_{50} value of ATP on fEPSP inhibition was 59 μM (95% C.L. 17-198 μM). These data are consistent with previous results demonstrating an ATP-mediated inhibition of extracellularly recorded CA1 neurotransmission (Cunha *et al.*, 1998; Dunwiddie *et al.*, 1997b; Masino *et al.*, 2002; Mendoza-Fernandez *et al.*, 2000; O'Kane *et al.*, 1998). At the beginning of each experiment and 15 minutes after ATP washout, a stimulus-response curve was recorded to verify if there was a relatively "long lasting" potentiation of synaptic responses after ATP removal. Such an effect has previously been reported to occur in hippocampal slices (Fujii *et al.*, 1995a; 1995b; 1999; 2002; Nishimura *et al.*, 1990; O'Kane *et al.*, 1998; Wieraszko *et al.*, 1989; Yamazaki *et al.*, 2002). At concentrations of 1-10 μM we did not observe any change in fEPSP amplitude after a 15-minute application of ATP at any stimulus intensity tested (data not shown). In contrast, an increase of 6.6±3.8% and of 12.3±7.2% in fEPSP amplitude was observed at the highest stimulus intensity tested after 30 μM (upper inset of figure 20A) and 100 μM ATP superfusion, respectively.

The inhibitory effect of ATP on fEPSP amplitude was not blocked by the P2 antagonists PPADS and suramin (figure 20B). The two compounds were applied 10 minutes before, during and 5 minutes after ATP superfusion. As shown in Figure 20B, 10 μM ATP in the presence of 30 μM PPADS still elicited a fEPSP inhibition of 20±9% that is not different from that obtained with ATP alone. Similarly, 30 μM ATP in the presence of 100 μM suramin evoked a 32±3.5% fEPSP inhibition, that is not different from the 36±10.6% fEPSP reduction obtained with 30 μM ATP alone. The potentiation induced by 30 μM ATP was blocked in the presence of 100 μM suramin (lower inset of figure 20A). It should be noticed that PPADS alone, but not suramin, significantly reduced the fEPSP amplitude by 5.21± 1.6% (inset of figure 20B; $P<0.05$, paired Student's t-test; n=29) in accordance with previous data obtained in rat hippocampus

It is well known that extracellular ATP is rapidly metabolized by membrane ecto-ATPases, leading to the formation of ADP, AMP and adenosine. Adenosine A_1 receptors are widely distributed in the CA1 hippocampus and many effects of exogenous ATP have been attributed to A_1 adenosine receptor activation after ATP catabolism in this brain region. For this reason, the effect of ATP was also evaluated in the presence of the selective adenosine A_1 antagonist DPCPX. The application of 100 nM DPCPX 30 minutes before ATP superfusion significantly increased fEPSP amplitude (12.7± 5.2% vs control, n=5; $P<0.05$, paired Student's t-test, data not shown). In addition, it completely blocked the ATP-mediated reduction of fEPSP ($P<0.05$, one-way ANOVA,
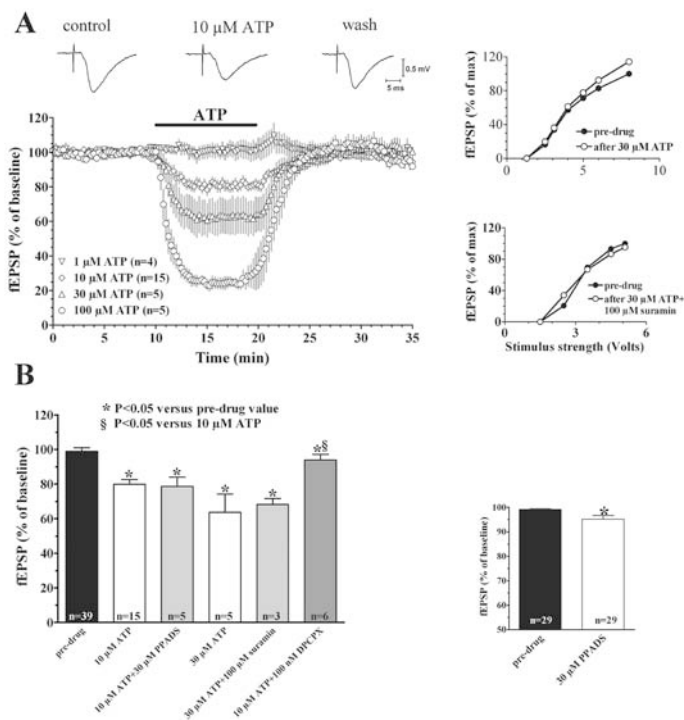
Figure 20. The inhibitory effect induced by ATP on fEPSP amplitude is not blocked by P2 purinergic antagonists. A. Time-course of fEPSP amplitude before, during and after the application of different concentrations of ATP. Each point in the graph represents the mean ± s.e. of fEPSP value measured as percent of baseline, pre-drug level. Upper panels represent single traces recorded in a typical experiment before, during and after 10 μM ATP application. Upper inset: stimulus-response curves recorded before and after 30 μM ATP application illustrate the potentiating effect of the P2 agonist on a wide range of stimulus strength in a typical experiment. fEPSP amplitude is expressed as percent of the maximal value obtained in control conditions at the highest stimulus strength. Lower inset: the potentiating effect was prevented in the presence of 100 μM suramin. B. Columns in the graph summarize the average amplitude (mean ± s.e.) of evoked fEPSP recorded from CA1 hippocampal region in control conditions, 5 minutes after superfusion of ATP alone and 5 minutes after ATP superfusion in the presence of different purinergic antagonists. Note that the inhibitory effect of ATP on fEPSP amplitude is not blocked by the P2 antagonists PPADS and suramin, but only by the A_1 adenosine antagonist, DPCPX. *$P<0.05$, one-way ANOVA followed by Newman-Keuls test versus pre-drug value. §$P<0.05$, one-way ANOVA followed by Newman-Keuls test versus 10 μM ATP. Inset: bars in the graph represent the average of fEPSP amplitude 5 minutes before and during the last 5 minutes of PPADS superfusion (30 μM). *$P<0.05$, paired Student's t test.
(Pankratov et al., 1998; Safiulina et al., 2005) and prefrontal cortex (Luthardt et al., 2003; Wirkner et al., 2002).

Newman-Keuls multiple comparison post-hoc test, figure 20B). We also investigated the effect of ATP in the presence of different ecto-ATPase inhibitors: ARL 67156, BGO 136 and PV4. As shown in figure 21A, in the presence of PV4, the inhibitory effect on fEPSP amplitude elicited by 10 μM ATP (35.2±6.1%, n=6) was significantly enhanced in comparison to that observed with 10 μM ATP alone (20.3±2.5%, $P<0.05$, one-way

ANOVA, Newman-Keuls multiple comparison post-hoc test). Similar results were obtained with all the ecto-ATPase inhibitors tested (figure 21B: $35.8 \pm 6.4\%$ in ATP+ARL 67156, n=5; $38.2 \pm 3.6\%$ in ATP+BGO 136, n=5).

The effects of ATP were also studied by recording synaptic potentials at the somatic level of CA1 region. ATP ($10\,\mu M$) induced a $66 \pm 7.1\%$ decrease in PS amplitude ($P<0.0001$; paired Student's t test, figure 22A) that was reversed after few minutes washout. The apparent EC_{50} value of ATP on PS inhibition was $7\,\mu M$ (95% C.L. 1.5-$33\,\mu M$). When the stimulus-response curve was delivered 15 minutes after drug removal, a significant increase in PS amplitude ($P<0.05$, paired Student's t-test, n=7) was observed at a stimulus intensity able to evoke a response higher than 50% of the maximum (upper inset of figure 22A). At the highest stimulus intensity tested, the increase was $14.8 \pm 3\%$ (n=7).
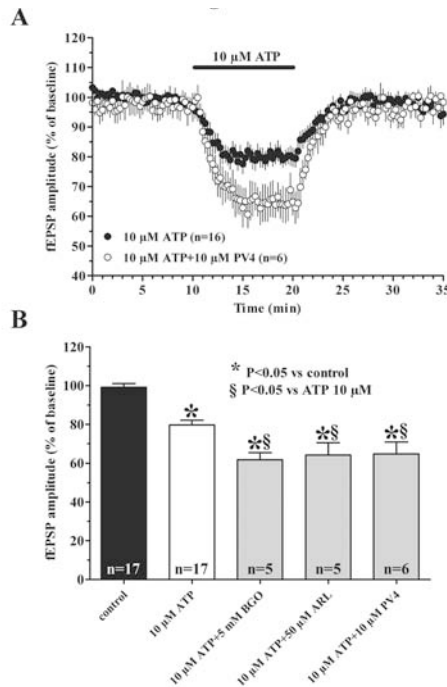
Figure 21. The inhibitory effect induced by ATP on fEPSP amplitude is potentiated in the presence of different NTPDase inhibitors. A. Time-course of fEPSP amplitude before, during and after the application of ATP in the absence or in the presence of the NTPDase1,2,3 inhibitor PV4. Each point in the graph represents the mean ± s.e. of fEPSP value measured as percent of baseline, pre-drug level. Note that fEPSP inhibition induced by $10\,\mu M$ ATP in the presence of PV4 is significantly greater than that induced by $10\,\mu M$ ATP alone ($P<0.05$, one-way ANOVA one-way ANOVA, Newman-Keuls multiple comparison post-hoc test). B. Columns in the graph summarize the average amplitude (mean ± s.e.) of evoked fEPSP recorded from CA1 hippocampal region in control conditions, 5 minutes after superfusion of ATP alone and 5 minutes after ATP superfusion in the presence of different ecto-ATPases inhibitors. Note that the inhibitory effect of ATP on fEPSP amplitude is potentiated by BGO 136, PV4 and ARL 67156. *$P<0.05$ one-way ANOVA, Newman-Keuls multiple comparison post-hoc test versus pre-drug value. §$P<0.05$, one-way ANOVA, Newman-Keuls multiple comparison post-hoc test versus $10\,\mu M$ ATP treated slices.
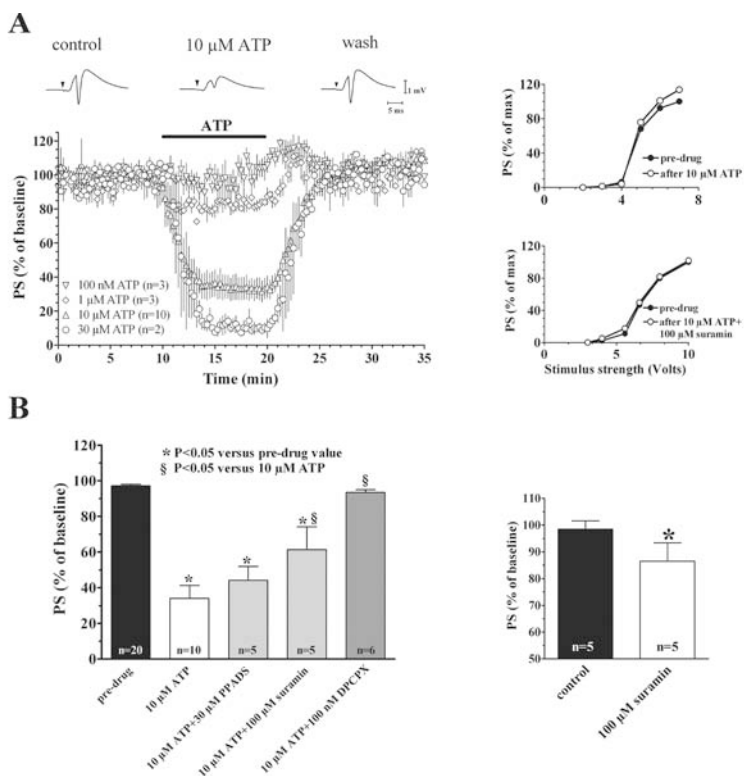
Figure 22. The inhibitory effect induced by ATP on PS amplitude is blocked by DPCPX, a selective A_1 adenosine receptor antagonist, and by suramin, an aspecific P2 antagonist. A. Time-course of PS amplitude before, during and after the application of different concentrations of ATP. Each point in the graph represents the mean ± s.e. of PS value measured as percent of baseline, pre-drug level. Upper panels represent single traces recorded in a typical experiment before, during and after 10 μM ATP application. The stimulus artefact was blanked and replaced by the arrowhead. Upper inset: stimulus-response curves recorded before and after 10 μM ATP application illustrate the potentiating effect of the P2 agonist on a wide range of stimulus strength in a typical experiment. PS amplitude is expressed as percent of the maximal value obtained in control conditions at the highest stimulus strength. Lower inset: the potentiating effect was prevented in the presence of 100 μM suramin. B. Columns in the graph summarize the average amplitude (mean ± s.e.) of evoked PS recorded from CA1 hippocampal region in control conditions, 5 minutes after superfusion of ATP alone, and 5 minutes after ATP superfusion in the presence of different purinergic antagonists. *P<0.05, one-way ANOVA, Newman-Keuls multiple comparison post-hoc test versus pre-drug value. §P<0.05, one-way ANOVA, Newman-Keuls multiple comparison post-hoc test versus 10 μM ATP. Inset: bars in the graph represent the average of PS amplitude 5 minutes before and during the last 5 minutes of 100 μM suramin application. *P<0.05, paired Student's *t* test.

No block of ATP-mediated inhibition of PS amplitude was observed in the presence of PPADS (figure 22B). In contrast, 100 μM suramin significantly blocked the ATP-mediated inhibition of the evoked potentials ($P<0.05$, one-way ANOVA, Newman-Keuls multiple comparison post-hoc test, figure 22B) and completely prevented the potentiation of stimulus-response curve (lower inset of figure 22A). In addition, it induced a significant decrease in PS amplitude (12.8±3.4%; $P<0.05$, paired Student's t-test) when applied alone (inset of figure 22B). DPCPX (100 nM) applied 30 minutes before, during and 5 minutes after ATP superfusion, antagonized the effects of 10 μM ATP on PS amplitude, as observed at dendritic level. DPCPX alone significantly increased PS amplitude (60.3±11.4% vs control PS, n=6; $P<0.05$, paired Student's t-test, data not shown).

2.2 Effects of ATPγS on CA1 hippocampal neurotransmission

ATPγS, the metabolically stable ATP analogue, evoked a concentration-dependent decrease in fEPSP amplitude (figure 23A). A statistically significant reduction was evident starting from a concentration of 3 μM ($P<0.05$, paired Student's t-test), and at 10 μM, ATPγS inhibited fEPSP amplitude by 32.6±4.2% (figure 23A). The apparent EC_{50} value estimated for ATPγS on fEPSP inhibition was 22 μM (95% C.L. 4.6-106 μM). In all the slices in which we recorded a stimulus-response curve before and 15 minutes after ATPγS application, a statistically significant potentiation of fEPSP ($P<0.05$, paired Student's t-test, n=12) was observed at intensities able to evoke a response higher than 50% of the maximum (upper inset of figure 23A).

The inhibitory effect of ATPγS on fEPSP amplitude was significantly reduced both in the presence of 30 μM PPADS and 10 μM MRS 2179. When higher concentrations of PPADS (50 μM, figure 23B) and MRS 2179 (30 μM, data not shown) were tested, no significant difference in the block of ATPγS-induced inhibition was found. Both antagonists completely prevented the potentiation of the stimulus-response curve observed after 15 minutes of ATPγS washout (lower inset of figure 23A) at dendritic level. It should be noted that the application of 10 μM MRS 2179 alone caused a modest but significant reduction in fEPSP amplitude (6.1±3.2%, $P<0.05$, paired Student's t-test, inset of figure 23B, n=15). Contrary to PPADS and MRS 2179, the nonspecific purinergic antagonist suramin (100 μM) did not significantly inhibit ATPγS effects at dendritic level (figure 23B).

Surprisingly, the effect of ATPγS on fEPSP amplitude was completely antagonized by the selective adenosine A_1 antagonist, DPCPX (figure 23B). Evidence exists that even this metabolically stable ATP analogue is partially converted to adenosine (Masino *et al.*, 2002). To verify this possibility we applied ATPγS after a 30-minute application of 50 μM ARL 67156. However, in these experimental conditions, a 10-minute application of ATPγS induced an even more pronounced effect on evoked neurotransmission (figure 23B). In fact, the reduction in fEPSP amplitude elicited by 10 μM ATPγS in the presence of ARL 67156 was of 68.2±4.6%, that is significantly greater than that observed under control conditions ($P<0.001$; one-way ANOVA, Newman-Keuls multiple comparison post-hoc test). At somatic level, we delivered a cumulative concentration-response curve (figure 24A) for ATPγS, since no desensitization was observed during single drug applications (data not shown). Also in this case, the exogenous application of ATPγS produced a concentration-dependent decrease in PS amplitude. A significant effect was observed starting from a concentration of 3 μM (17.4±8.6%, $P<0.05$, paired Student's t-test, n=4), while at a 30 μM concentration PS was completely suppressed.
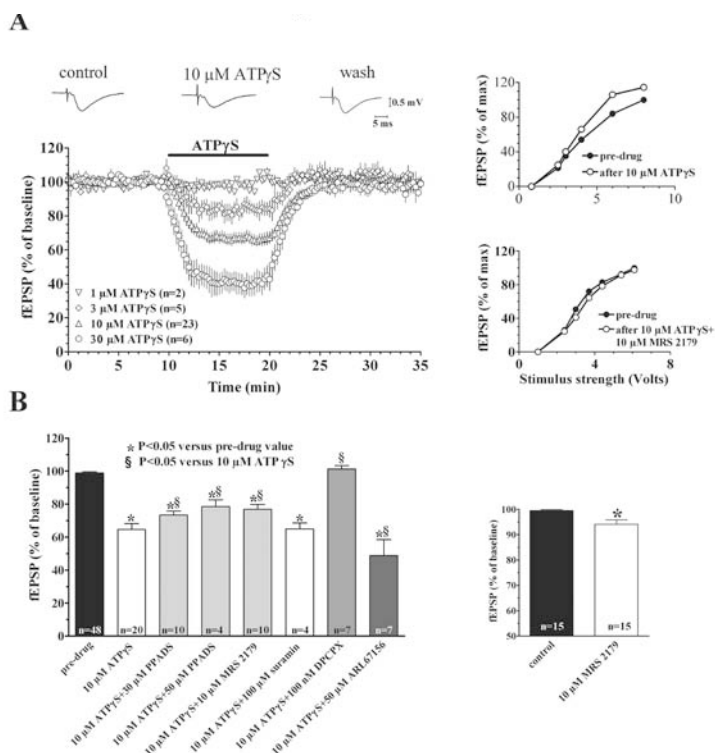
Figure 23. The inhibitory effect induced by ATPγS on fEPSP amplitude is reduced by the P2 purinergic antagonists PPADS and MRS 2179 and is enhanced by the ecto-ATPases inhibitor ARL 67156. A. Time-course of fEPSP amplitude before, during and after the application of different concentrations of ATPγS. Each point in the graph represents the mean ± s.e. of fEPSP value measured as percent of baseline, pre-drug level. Upper panels represent single traces recorded in a typical experiment before, during and after 10 μM ATPγS application. Upper inset: stimulus-response curves recorded before and after 10 μM ATPγS application illustrate the potentiating effect of the P2 agonist on a wide range of stimulus strength in a typical experiment. fEPSP amplitude is expressed as percent of the maximal value obtained in control conditions at the highest stimulus strength. Lower inset: the potentiating effect was prevented in the presence of 10 μM MRS 2179. B. Columns in the graph summarize the average amplitude (mean ± s.e.) of evoked fEPSP recorded from hippocampal slices in control conditions, 5 minutes after superfusion of ATP S alone, and 5 minutes after ATPγS superfusion in the presence of different drugs. *P<0.05, one-way ANOVA, Newman-Keuls multiple comparison post-hoc test versus pre-drug value. §P<0.05, one-way ANOVA, Newman-Keuls multiple comparison post-hoc test versus 10 μM ATPγS. Inset: bars in the graph represent the average of fEPSP amplitude recorded 5 minutes before and during the last 5 minutes of 10 μM MRS 2179 application. *P<0.05, paired Student's *t* test.

The apparent EC_{50} value for ATPγS on PS inhibition was 6 μM (95% C.L. 1.2-28 μM). In these experimental conditions, a potentiation of PS amplitude (37±12.1%) was observed after drug removal in comparison to pre-drug values (see figure 24A, trace f) even without eliciting a stimulus-response curve. The potentiation of somatic response persisted for at least 30 minutes and was also recorded during the stimulus-response curve (inset of figure 24A) after 15 minutes of washout.
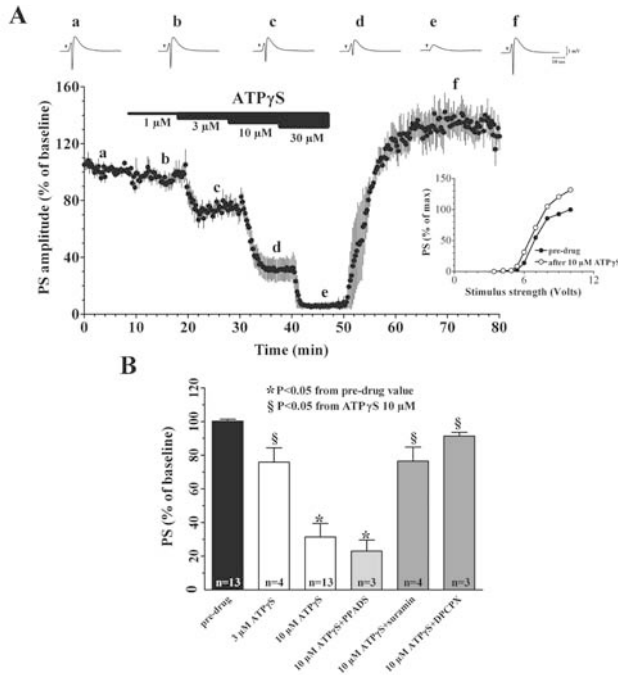
Figure 24. ATPγS induces a concentration-dependent inhibition and a subsequent potentiation of PS amplitude in the CA1 region of rat hippocampus. A. Averaged time-course (n=4) of PS amplitude before, during and after the application of different concentrations of ATPγS. PS amplitude (mean ± s.e.) is measured as percent of baseline level. Upper panels represent single traces recorded in a typical experiment before, during and after ATPγS application at different concentrations. Inset: stimulus-response curve recorded before and after 10 μM ATPγS application illustrate the potentiating effect of the P2 agonist on a wide range of stimulus strength in a typical experiment. PS amplitude is expressed as percent of the maximal value obtained in control conditions at the highest stimulus strength. B. Columns in the graph summarize the average amplitude (mean ± s.e.) of evoked PS recorded from the CA1 region in control conditions, 5 minutes after superfusion of ATP S alone, and 5 minutes after ATPγS superfusion in the presence of different purinergic antagonists (PPADS: 30 μM; suramin: 100 μM; DPCPX: 100 nM). *P<0.05, one-way ANOVA, Newman-Keuls multiple comparison post-hoc test versus pre-drug value. §P<0.05, one-way ANOVA, Newman-Keuls multiple comparison post-hoc test versus 10 μM ATPγS.

The application of 30 μM PPADS was unable to block the ATPγS-mediated inhibition of PS amplitude (figure 24B) and did not affect the potentiation of the stimulus-response curve observed 15 minutes after drug removal (data not shown). In contrast, suramin (100 μM) significantly reduced the ATPγS-mediated inhibition of PS amplitude (figure 24B), and completely prevented the potentiation of the stimulus-response curve (data not shown). As observed at the dendritic level, the effect of ATPγS on PS amplitude was completely antagonized by the adenosine A_1 selective antagonist, DPCPX (figure 24B).

Figure 25 shows the concentration-response curves obtained for ATP and ATPγS at both the dendritic and somatic level. It can be noted that lower concentrations of both P2 agonists are necessary to elicit the inhibitory effect on PS amplitude in comparison to
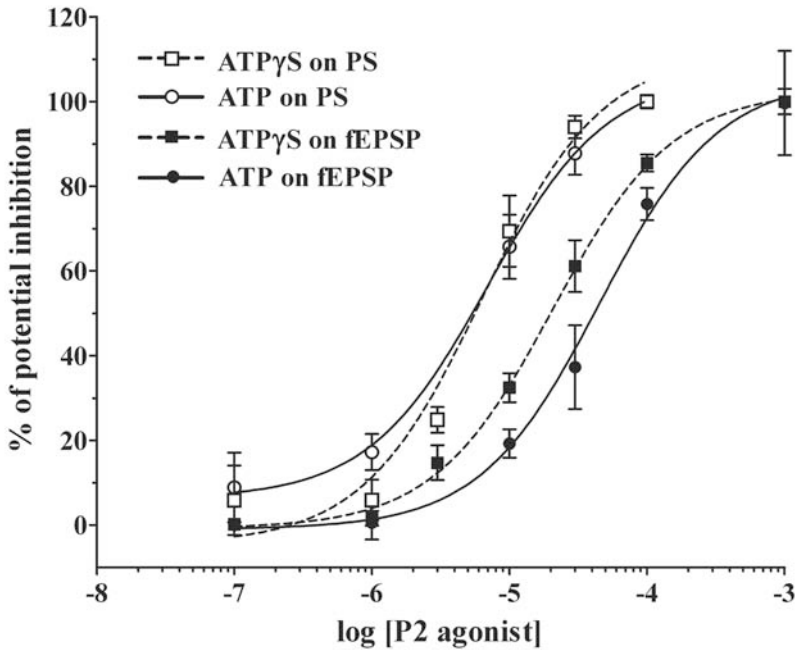
Figure 25. Concentration-response curves of ATP and ATPγS on dendritic fEPSP and somatic PS responses. The graph shows the fitting curves of concentration-dependent inhibitory effects of ATP and ATPγS on fEPSP and PS amplitude. Note that the curves obtained for both puriner-gic agonists at somatic level are shifted to the left in respect to those recorded at dendritic level. In addition, at the dendritic level, the concentration-response curve obtained in the presence of ATPγS is steeper than that obtained in the presence of ATP.

what is observed at the dendritic level. In addition, the figure shows that ATPγS is more efficient in reducing fEPSP amplitude (but not PS amplitude) in comparison to ATP.

2.3 Effects of ATP and ATPγS on PPF in the CA1 region of rat hippocampus

In order to discern if the ATP and ATPγS mediated effects on fEPSP amplitude were due to pre- or postsynaptic mechanisms, we performed a PPF protocol (see methods). As shown in table 8, a 10-minute application of 10 μM ATP increased PPF, an effect that is not statistically significant. On the other hand, at a concentration of 100 μM, a significant increase in PPF was observed ($P<0.01$; paired Student's t test). Ten minutes application of ATPγS significantly increased PPF starting from a concentration of 10 μM (table 8).

To clarify if these effects on PPF were due to P1 or P2 receptor activation, we tested different purinergic antagonists. The action elicited by ATP was tested only in the pres-ence of DPCPX, since we previously demonstrated that PPADS and suramin are not able to antagonize the ATP-inhibitory effect on fEPSP amplitude.

DPCPX (100 nM) alone decreased PPF and fully prevented the ATP-mediated ef-fect. Since the effects of ATPγS at dendritic level were blocked by both P2 and the A_1

receptor antagonists, the effect was checked in the presence of PPADS, MRS 2179 and DPCPX.

PPADS (30 μM) and MRS 2179 (10 μM), applied alone 10 and 15 minutes before agonist superfusion respectively, significantly increased, *per se*, the P2/P1 ratio, but failed to block the increase in PPF induced by 10 μM ATPγS. DPCPX (100 nM) alone decreased PPF and fully prevented ATPγS-mediated effect (table 8).

Table 8. Effects of P2 purinergic agonists and antagonists on PPF in the CA1 hippocampal region.

	n	P2/P1 ratio		n	P2/P1 ratio
Pre-drug	n=2	1.49±0.12	Pre-drug	n=4	1.32±0.02
10 μM ATP	n=2	1.59±0.13	100 nM DPCPX	n=4	1.25±0.07*
wash	n=2	1.48±0.11	100 nM DPCPX + 10 μM ATP	n=4	1.22±0.07
Pre-drug	n=5	1.54±0.06	Pre-drug	n=5	1.31±0.01
100 μM ATP	n=5	2.16±0.06*	100 nM DPCPX	n=5	1.29±0.05*
wash	n=5	1.56±0.06	100 nM DPCPX + 100 μM ATP	n=5	1.29±0.04
Pre-drug	n=9	1.48±0.08	Pre-drug	n=6	1.51±0.08
10 μM ATPγS	n=9	1.69±0.06*	30 μM PPADS	n=6	1.53±0.09*
Wash	n=8	1.47±0.09	30 μM PPADS + 10 μM ATPγS	n=6	1.90±0.12**
Pre-drug	n=4	1.49±0.03	Pre-drug	n=8	1.43±0.04
30 μM ATPγS	n=4	1.90±0.07*	10 μM MRS	n=8	1.46±0.04*
wash	n=4	1.50±0.03	10 μM MRS + 10 μM ATPγS	n=8	1.67±0.08**

* $P<0.05$ from respective pre-drug value (paired Student's *t*-test).
** $P<0.05$ from antagonist alone (paired Student's *t*-test).

2.4 Effects of different purinergic antagonists on OGD-evoked disruption of neurotransmission in the CA1 region of rat hippocampal slices

The effect of P2 purinergic receptor stimulation by endogenous ATP released during *in vitro* OGD episodes on the impairment of synaptic transmission was investigated using P2 selective antagonists.

In the first series of experiments we characterized the synaptic response of evoked fEPSPs following severe (7-minute) OGD, an ischemia-like insult that in our experimental conditions has been consistently shown to produce an irreversible loss of synaptic transmission (Pugliese *et al.*, 2003; Pugliese *et al.*, 2006). At the same time as the fEPSPs recordings, we also monitored another important parameter of brain tissue integrity, the DC shift produced by AD. It has been well described in the literature that AD is one of the major factors inducing brain damage after an ischemic episode (Somjen 2001).

One 7-minute OGD episode induced the disappearance of fEPSP, which did not recover (4.2±1.9%, n=13) after superfusion with oxygenated, glucose-containing aCSF as monitored up to 80 minutes.In addition, in all control slices, AD was recorded as a DC shift with a mean peak latency of 6.2±0.2 minutes after OGD initiation and a mean peak amplitude of 6.1±0.6 mV (table 9 and figure 26A).
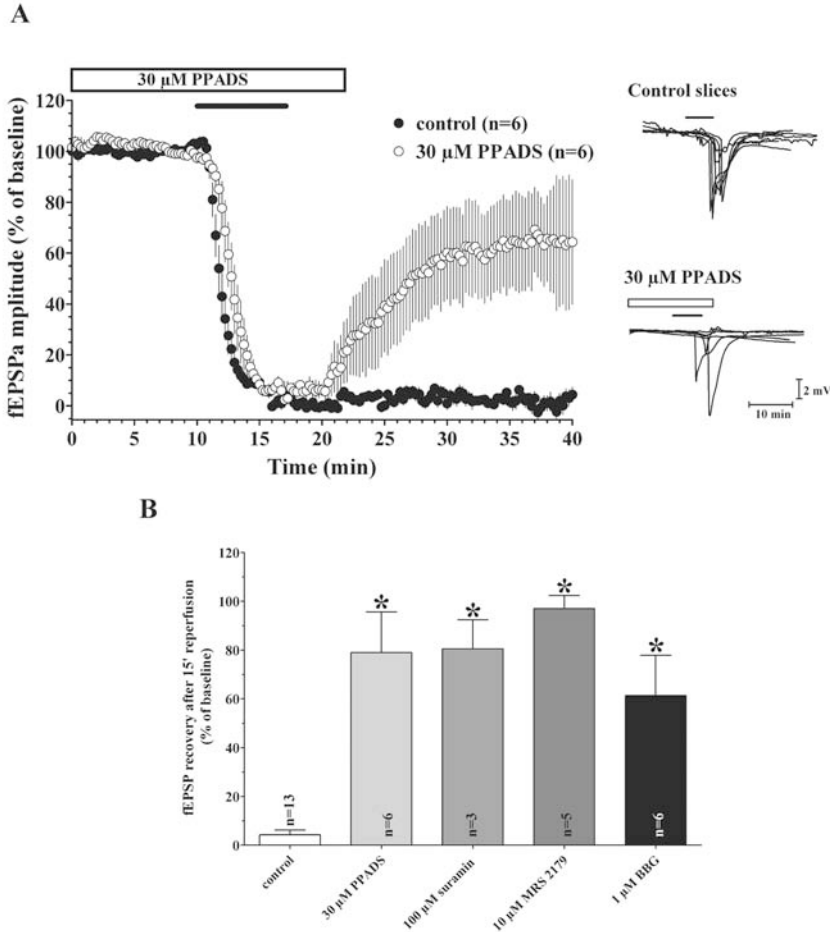
Figure 26. Different P2 antagonists prevent the irreversible loss of hippocampal CA1 neurotransmission after a 7-minute OGD. A. The graph shows the time-courses of fEPSP amplitude before, during 7 minutes of OGD, and after reperfusion in normal oxygenated aCSF in the absence and in the presence of 30 μM PPADS (open bar). Data (mean ± s.e.) are expressed as a percent of the baseline values. Right panels: in the same groups of slices, AD was recorded as a negative voltage shift in response to 7 minutes of OGD in control slices (upper panel) and in the presence of PPADS (lower panel). Solid bars indicate the time duration of OGD. B. Columns in the graph summarize the average recovery (mean ± s.e.) of fEPSP amplitude in CA1 hippocampal region after 7 minutes of OGD in control conditions or in the presence of different P2 antagonists. Only slices showing a fEPSP recovery >15% after 15 minutes of reperfusion were included in the analysis. *P<0.001, one-way ANOVA, Newman-Keuls multiple comparison post-hoc test versus control slices.

In the presence of PPADS, a non-selective P2 antagonist, the irreversible block of synaptic transmission induced by a 7-minute OGD episode was prevented in 5 of the 6 slices tested. As shown in figure 26A, 30 μM PPADS, applied 10 minutes before, during, and 5 minutes after the OGD insult, allowed a significant recovery of the fEPSP amplitude within 15-minutes reperfusion with oxygenated and glucose-containing aCSF (from 4.2±2.1% recovery in control slices to 79±16.6% in the presence of 30 μM PPADS, n=6). Figure 26B (right panels) shows that in this experimental group, only 3 out of 6 slices exposed to 7-minute OGD insults presented a sizeable AD (>1 mV) whose peak latency was delayed (7.1±1 minutes) by PPADS 30 μM. One of these three slices, in spite of the appearance of AD (2.5 mV, 30 s after oxygen and glucose restoration) recovered a significant fraction (78.5%) of the original fEPSP amplitude after 20 minutes of reperfusion.

Table 9. Effects of P2 purinergic receptors antagonists on CA1 hippocampal synaptic transmission after 7 minutes of OGD.

		AD appearance (n/n)	AD peak time (min)	AD peak amplitude (mV)	fEPSP recovery ≥ 15% (n/n)	fEPSP recovery (%) after 15 min reperfusion
Control	(n=13)	(13/13)	6.2±0.2	6.1±0.6	(1/13)	4.2±1.9
PPADS	10 μM (n=4)	(3/4)	6.4±0.3	6.2±0.3	(3/4)	34.3±18.7
	30 μM (n=6)	(3/6)	7.1±0.9	5.9±0.4	(5/6)	65.9±20*
MRS 2179	1 μM (n=3)	(2/3)	7.5±0.6	6.8±1.8	(2/3)	42.9±29.7
	10 μM (n=5)	(2/5)	7±0.3	4±1.8	(4/5)	79.2±18.2*
Suramin	10 μM (n=4)	(3/4)	7.6±0.6	6±2.3	(2/4)	53.1±29.5
	100 μM (n=3)	(2/3)	6.6±0.5	4.7±1.1	(3/3)	80.5±11.9*
BBG	500 nM (n=4)	(2/4)	6.1±0.3	7.9±0.4	(2/4)	57.6±31.6
	1 μM (n=7)	(4/7)	7.9±0.3	6.7±0.8	(4/7)	52.9±16.3*

Data are taken from slices receiving 7 minutes OGD in control conditions or in the presence of different P2 purinergic antagonists. Numbers in parentheses (n/n) indicate the number of observations out of investigated slices. Time is calculated from OGD initiation. The amplitude of the final fEPSP recovery is expressed as per cent of baseline fEPSP value recorded 5 minutes before OGD application. *$P<0.01$ from control value (one-way ANOVA, Newman-Keuls post test).

As shown in table 9, similar results were obtained in the presence of different purinergic antagonists: suramin, MRS 2179 and BBG. In all cases the effect on recovery of fEPSP amplitude (figure 26B) and AD inhibition was concentration-dependent. In addition, in 8 out of all 29 slices treated with the P2 antagonists, no AD appearance was observed. In the remaining 21 treated slices in which AD was recorded, its appearance was significantly delayed (7.1±0.2 minutes after OGD initiation). A significant recovery of fEPSP amplitude (>15% of preischemic value) was observed in 10 out of the 21 treated slices in which AD emerged.

3. Discussion

3.1 Role of P2 receptors in hippocampal neurotransmission under normoxic conditions

Our results demonstrate that ATP or its stable analogue ATPγS modulate evoked synaptic transmission in the CA1 region of the rat hippocampus. The main effect, observed within the first 2-3 minutes of drug application, is a reduction in fEPSP and PS amplitude evoked by electrical stimulation of the Schaffer collateral-commissural pathway. This effect is concentration-dependent and reversible after a few minutes of washout. Another effect elicited by both ATP and ATPγS is a significant potentiation of evoked responses, recorded after drug removal and persisting for at least 30 minutes. The inhibitory effect observed during ATP application has already been described, and attributed to P1 (Cunha *et al.*, 1998; Dunwiddie *et al.*, 1997b; Masino *et al.*, 2002) or to P2 receptor stimulation (Luthardt *et al.*, 2003; Mendoza-Fernandez *et al.*, 2000; Rodrigues *et al.*, 2005). Our observation that the selective A_1 receptor antagonist DPCPX blocks ATP-induced inhibition of synaptic responses suggests that adenosine formed from ATP catabolism and acting at A_1 receptors is responsible for synaptic depression. We would therefore expect that the ecto-ATPase inhibitors tested (ARL 67156, BGO 136 and PV4) would antagonize the ATP inhibition of synaptic responses. On the contrary, all the ecto-ATPase inhibitors potentiate the ATP inhibitory effect, suggesting that they unmask a significant ATP-mediated inhibitory action that is otherwise covered by adenosine acting on A_1 receptors. This interpretation is supported by the observation that both ATP- and ATPγS-mediated inhibitory responses are partially blocked by the nonselective P2 antagonists suramin and PPADS and the selective $P2Y_1$ antagonist MRS 2179. These observations indicate that, in addition to P1 receptor activation, a P2 component is responsible for an ATP-mediated decrease in synaptic transmission in the CA1 area of the rat hippocampus.

The block of ATPγS effects by DPCPX was unexpected because the agonist is considered a metabolically stable ATP analogue. Our result is however, consistent with previous observations that at least a fraction of ATPγS undergoes enzymatic degradation and activates A_1 adenosine receptors (Masino *et al.*, 2002). An enzymatic degradation of ATPγS is further supported by the result that ARL 67156 potentiates the inhibitory effect of this P2 agonist.

It has been suggested that, in hippocampal neurones, ATP may activate DPCPX-sensitive P2 receptors (Mendoza-Fernandez *et al.*, 2000). The existence of a heteromeric association between A_1 and $P2Y_1$ receptors was demonstrated by co-localization staining, co-immunoprecipitation and bioluminescence resonance energy transfer technology in HEK293T cells transfected with both A_1 and $P2Y_1$ receptors (Yoshioka *et al.*, 2001; Yoshioka *et al.*, 2002b) and in primary cultures of cortical hippocampal and cerebellar neurons (Yoshioka *et al.*, 2002a). Therefore, we could hypothesize that the DPCPX sensitivity of both ATP and ATPγS inhibitory effects is attributable both to their enzymatic degradation to adenosine and to the activation of the heteromeric A_1-$P2Y_1$ receptor. The fact that, in the present work, the $P2Y_1$ antagonist MRS 2179 reduces the ATPγS- inhibitory effect on fEPSP amplitude supports this notion.

Other groups have previously described a persistent ATP-induced potentiation of CA1 hippocampal neurotransmission (Fujii *et al.*, 1995a; 1995b; 1999 and 2002; Nishimura *et al.*, 1990; O'Kane *et al.*, 1998; Wieraszko *et al.*, 1989; Yamazaki *et al.*, 2002). In the present work, we clearly observed this phenomenon after a prolonged application

of ATPγS during somatic recordings. When the dendritic potential was measured, the increase in fEPSP amplitude elicited by both purinergic agonists was detectable only by evoking a stimulus-response curve 15 minutes after drug removal. The increase in fEPSP amplitude was statistically significant only at the highest stimulus intensities tested. The potentiating effect elicited by ATP and ATPγS application is completely blocked by P2 antagonists at both the dendritic and somatic level, demonstrating that it is due to P2 receptor stimulation. It has to be noted that higher stimulus strengths are needed to observe a potentiation of dendritic potentials in comparison to somatic responses and that ATP and ATPγS induce a significant potentiation of PS amplitude at lower concentrations in respect to those required at dendritic level. Altogether, these data suggest that both presynaptic P2 receptors modulating glutamate release and postsynaptic P2 receptors modulating cell excitability are involved in potentiation of CA1 hippocampal neurotransmission. The P2 antagonists PPADS and MRS 2179 applied alone significantly decrease fEPSP amplitude. At somatic level, only suramin diminishes the evoked responses. These observations demonstrate that in the CA1 region of rat hippocampal slices there is an endogenous tonic activation of P2 receptors that contributes to excitatory neurotransmission and is in agreement with those reported in the rat hippocampus (Pankratov et al., 1998; Safiulina et al., 2005) and prefrontal cortex (Luthardt et al., 2003; Wirkner et al., 2002). The varying efficacy of the P2 antagonists at the dendritic and somatic levels suggests that different subtypes of P2 receptors located in the pre- and postsynaptic compartments are involved in the excitatory effect.

The effect of P2 agonist application was also evaluated using a PPF protocol. The P2/P1 ratio was significantly increased by ATP and ATPγS application. The same effect has been described in hippocampal slices during exogenous adenosine application by other groups (Moore et al., 2003) and is attributed to an adenosine A_1 receptor-mediated decrease of glutamate release. Our data indicate that the increase in PPF elicited by ATP application is completely blocked by DPCPX, suggesting that it is effectively due to A_1 receptor stimulation after ATP conversion to adenosine. Similar results are observed for ATPγS-induced PPF increase, because it is not blocked by PPADS or MRS 2179, but only by DPCPX. These data support the hypothesis that part of ATPγS is converted to adenosine and activates A_1 receptors. It should be noted that both purinergic antagonists (PPADS and MRS 2179) applied alone induced a significant increase of PPF (P2\P1 ratio). This observation indicates that ATP contributes to excitatory neurotransmission stimulating the release of glutamate. These results are in line with those obtained by Rodrigues and colleagues (Rodrigues et al., 2005) on hippocampal synaptosomes.

3.2 Role of P2 receptors in hippocampal neurotransmission during OGD

The application of purinergic antagonists before, during and after a severe (7 minutes) OGD insult allows a significant recovery of fEPSP amplitude that is never observed in control slices. The concentration range of the drug effects falls within the Ki value estimated for all the antagonists in rat tissue (Boyer et al., 1998; Ralevic and Burnstock 1998).

The mechanism by which these drugs protect hippocampal slices from the OGD-induced irreversible loss of synaptic transmission is likely correlated to AD appearance (Pugliese et al., 2006), a phenomenon that contribute to cell damage during ischemia (for a review see Somjen 2001). In all 13 control slices, AD is recorded within the 7-minute OGD insult (mean latency of AD appearance: 6.2±0.2 minutes after OGD initiation) and the recovery of fEPSP amplitude after 15 minutes of reperfusion in oxy-

genated and glucose-containing aCSF is always less than 10% of the preischemic value. In contrast, P2 antagonists both delay or block AD appearance and allow a significant recovery of neurotransmission.

Our data suggest that hippocampal P2 receptors activated during OGD by endogenously released ATP exert a deleterious effect on CA1 neurotransmission by participating in the appearance of AD.

An increase in extracellular ATP concentration during ischemia was demonstrated in hippocampal slices by Jurani (Juranyi et al., 1999) and Frenguelli (Frenguelli et al., 2006) who report a peak in extracellular ATP concentration immediately before AD appearance during an OGD insult. In agreement with our results, the same authors show that this phenomenon is always followed by the complete loss of synaptic transmission.

Under ischemic conditions both direct and indirect actions could account for P2 receptor antagonist-mediated protection. A protective effect of P2 antagonists may be attributed to a direct inhibition of intracellular Ca^{2+} loading in neuron and glial cells (Schipke et al., 2002; Troadec et al., 1999). In fact, calcium is the main toxicity factor under ischemia (Dirnagl et al., 1999). Further possible indirect protective effects of P2 receptor antagonists may reside in the prevention of glutamate-evoked toxicity (Volontè et al., 1996; Zona et al., 2000) and in maintaining normal energy stores (Cavaliere et al., 2001b). Antagonism of P2 receptors during ischemia might also regulate intracellular pathways involved in ischemia-associated necrosis/apoptosis pathways such as expression of the glucose-regulated protein GRP75 and of the caspase-2 enzyme (Cavaliere et al., 2001a).

Among the antagonists checked in the present model, the high selectivity of BBG indicates that $P2X_7$ receptors are clearly involved in the deleterious effects induced by OGD in the CA1 hippocampal region. In addition, the participation of $P2Y_1$ receptors in this effect is supported by the efficacy of MRS 2179 in blocking AD appearance and preventing the irreversible loss of neurotransmission induced by a severe OGD.

These results are in agreement with the protective effect exerted by P2 antagonists in in vitro OGD (Cavaliere et al., 2004; Pugliese et al., 2003) and in vivo ischemic conditions (Kharlamov et al., 2002; Lammer et al., 2006; Melani et al., 2006).

3.3 Conclusions

I conclude that P2 receptors play an important role in CA1 hippocampal neurotransmission in both normoxic and ischemic conditions. Under normoxic conditions, both inhibitory and excitatory effects are observed after application of ATP or the stable analogue ATPγS. The inhibition of CA1 neurotransmission recorded during ATP application, under our experimental conditions, is mostly due to enzymatic degradation to adenosine and subsequent activation of A_1 receptors. The ATP analogue ATPγS evokes an inhibition of hippocampal neurotransmission by both P2 and A_1 adenosine receptors. A later excitatory effect, as pointed out by enhancement of fEPSP and PS amplitude, is attributable only to P2 receptors. In addition, a tonic activation of P2 receptors (likely located at a presynaptic level since their block enhances PPF) contributes to excitatory neurotransmission normally recorded in this brain area.

Under in vitro ischemic conditions (OGD), a deleterious role of ATP is suggested by the observation that P2 antagonists allow the restoration of neurotransmission after an otherwise lethal insult and block or delay the appearance of AD.

RESULTS
Section 2

STUDIES ON P2 RECEPTOR MODULATION OF MEMBRANE IONIC
CURRENTS BY PATCH CLAMP RECORDINGS

Chapter 3
Role of P2Y$_1$ receptor stimulation in medium spiny neurons of rat striatal slices

1. Historical background

Purinergic P2 receptors have been extensively investigated in recent years and growing evidence indicates their involvement in numerous cell-to-cell communication systems. Particular interest has been dedicated to the role of these membrane receptors during cerebral development, on the basis of studies underlying a possible role of extracellular ATP as a growth and trophic factor influencing neurons and glial differentiation (Abbracchio *et al.*, 1995b; Mishra *et al.*, 2006; Stevens *et al.*, 2000).

In particular, P2Y$_1$ receptors are widely distributed in the CNS, and both mRNA transcription (Moore *et al.*, 2001) and protein expression (Franke *et al.*, 2003; Moore *et al.*, 2000) has been demonstrated in human and rat striatum. On the other hand, there is conflicting evidence regarding their functional role in this brain region. Ikeuchi and Nishizaki (Ikeuchi *et al.*, 1995) demonstrated that ATP application in primary cultures of striatal neurons (from 1 day old rats) activates a sustained outward potassium current sensitive to GDPβS and PKC inhibitors but insensitive to PTX. In contrast, Scheibler and colleagues (Scheibler *et al.*, 2004) recently reported a lack of functional effects after P2X or P2Y selective activation in medium spiny neurons of 5-26 days old rat striatal slices. These discrepancies might be due to differences in postnatal development of experimental animals, in parallel with the profound electrophysiological changes of medium spiny neurones during the first 3 postnatal weeks (Tepper *et al.*, 1993). A recent paper from Rubini *et al.* (Rubini *et al.*, 2006) demonstrated that neuronally enriched striatal cell cultures from 1 day old rat give distinct responses to exogenous ATP application depending on whether they were cultured in NBM or DMEM growth medium. The same authors demonstrated that NBM-cultured striatal neurones present immature electrophysiological characteristics (wide, low amplitude action potentials, no repetitive firing, low Na$_v$ channels density on cell membrane) resembling those observed in "young" *in vivo* striatum, whereas DMEM-cultured neurones display fully-developed electrical behaviour (more hyperpolarized resting membrane potential, fast and pronounced action potential, repetitive firing) typical of adult striatal neurons. Interestingly, only "immature" NBM-cultured striatal neurones responded to extracellular ATP with an intracellular Ca^{2+} rise. These interesting results suggest that purinergic signalling in the rat striatum is related to brain development.

In the present work we investigated the role of P2Y$_1$ purinergic receptor activation in medium spiny neurons of striatal slices from neonatal (1 week old) rats using the patch clamp technique, in both voltage-clamp and current-clamp mode.

Our results show that the P2Y$_1$ agonist 2MeS-ADP can activate calcium-sensitive potassium channels during voltage-ramp depolarizations and regulate action potential firing rate in current clamp recordings.

2. Results

2.1 P2Y$_1$ receptor activation increases the outward currents elicited by a voltage ramp depolarization in striatal medium spiny neurons

In order to investigate the presence of a purinergic modulation in the striatum we recorded whole cell currents evoked by voltage ramp depolarization in medium spiny neurons of rat striatal slices in the absence and in the presence of a P2Y$_1$ selective agonist.

In the first set of experiments we measured the amplitude of currents evoked by a ramp protocol before, during and after 10 minutes application of 250 nM 2MeS-ADP, a selective P2Y$_1$ agonist. As shown in figure 27A, the current recorded in control conditions doesn't show any inward component, as expected in the presence of the Na$^+$-channel blocker TTX (100 nM), and in accordance with previous observations demonstrating that, in medium spiny neurons, voltage-dependent Ca^{2+}-currents do not normally contribute to steady-state whole cell currents (Bargas *et al.*, 1999; Hoehn *et al.*, 1993). As shown in figure 27A, voltage ramps under control conditions were dominated by outward potassium conductances. After 5 minutes superfusion of 250 nM 2MeS-ADP, the outward current elicited by the ramp depolarization was markedly increased, and the effect was reversed after drug removal. Figure 27B shows the 2MeS-ADP activated current obtained by subtraction of the ramp current recorded in the P2Y$_1$ agonist from the control trace. Inset of figure 27B shows the time course of current changes at +40 mV recorded before, during and after 2MeS-ADP application. The maximal effect is reached after 8 minutes of drug superfusion and is reversible after a few minutes of wash out. Figure 27C shows the 2MeS-ADP sensitive conductance activated in the presence of the P2Y$_1$ agonist in the same cell, assuming that the calculated reversal potential for potassium ions in our experimental conditions is -101.4 mV. The curve obtained can be fitted by the Boltzmann equation for voltage-dependent membrane conductances:

$$Y=g_{min}+(g_{max}-g_{min})/\{1+\exp[z(V_{1/2}-Vm)/(RT/F)]\}$$

where g_{min} and g_{max} are the minimum and maximum value for membrane conductance, $V_{1/2}$ is the membrane potential at which half of the maximum conductance (g_{max}) is reached, z is the equivalent charge, RT and F are the gas constant, the absolute temperature and the Faraday constant, respectively.

The values obtained by the fitting of the 2MeS-ADP activated conductance in this cell were: $V_{1/2}$ = -15.78 mV, z = 2.12 and a g_{max} = 10.86 nS.

Figure 28A shows the normalized average conductance activated by 2MeS-ADP in 29 cells investigated. The curve obtained can be fitted by a combination of a linear equation (to describe the non-voltage dependent membrane conductance at potentials ≤ -20 mV) and the Boltzmann relation for voltage-gated ion channels. The fitted parameters are shown in the lower inset. The upper inset of figure 28A shows that the average value of current amplitude elicited by the ramp protocol at a membrane potential of +40 mV is significantly increased in the presence of 2MeS-ADP (paired Student's *t*-test, P=0.0065, n=29). It is to be mentioned that 16 out of the 45 cells investigated (64.4%) didn't show any increase in the outward current during the 10 minutes superfusion of 2MeS-ADP. Figure 28C represent a population distribution of the maximal increase in membrane conductance recorded in the presence of 2MeS-ADP in all the cells investigated.
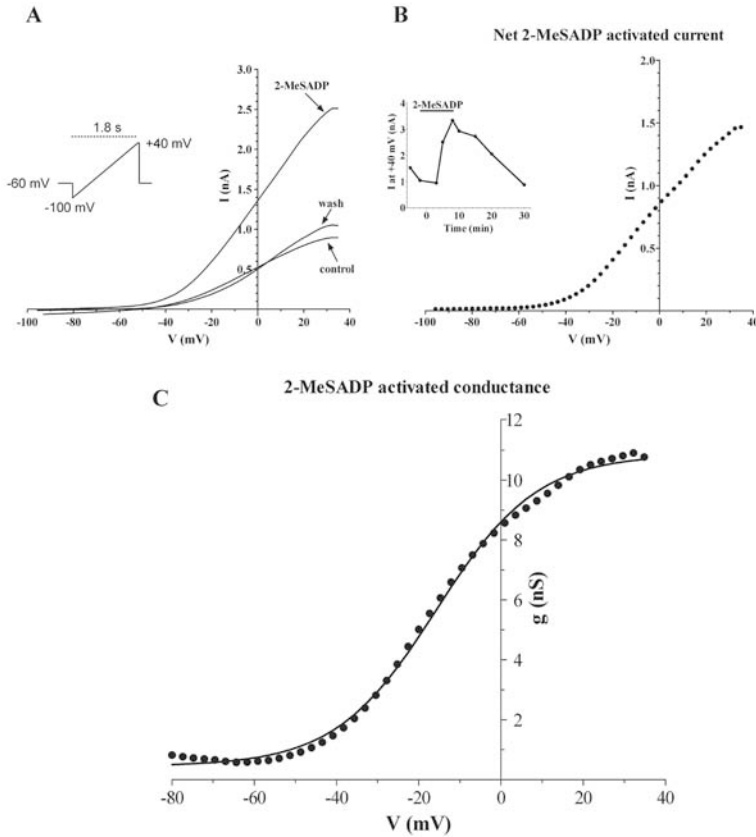
Figure 27. Effect of 2MeS-ADP on whole cell current elicited by voltage ramps in medium spiny neurons of rat striatal slices. A. The figure shows ramp protocols recorded in a typical experiment. The whole cell outward current activated by the ramp protocol is increased after 5 minutes application of 250 nM 2MeS-ADP. In this cell, the effect of 2MeS-ADP is reversed after 20 minutes of drug removal. The inset shows the ramp protocol applied. B. The graph shows the 2MeS-ADP sensitive current in the cell shown in A obtained by subtraction of the ramp current recorded in the P2Y1 agonist from the control trace. Inset: Time course of current amplitude activated by the ramp protocol at +40 mV before, during and after 2MeS-ADP application. C. The graph shows the 2MeS-ADP activated conductance in the same cell. The solid line shows the fit of the data from -80 mV to +40 mV to the Boltzmann relation giving a half-maximal voltage of -15.78 mV and equivalent charge of 2.12.

In another experimental group we recorded the ramp-evoked current before, during and after the co-application of 250 nM 2MeS-ADP and 15 μM MRS 2179, a P2Y$_1$ selective antagonist. Figure 28B shows a representative cell in which no changes in the outward current elicited by the voltage ramp were observed during the co-application of the two drugs. The inset in figure 28B shows that no significant difference was found between the current amplitude measured at +40 mV in control conditions and during the co-application of 2MeS-ADP and MRS 2179 in 16 cells investigated (paired Student's t-test, P>0.05).

These results indicate that the increase in the outward current amplitude recorded in the presence of 2MeS-ADP is due to P2Y$_1$ receptor activation.

2.2 Characterization of the P2Y$_1$-activated conductance in striatal medium spiny neurones.

In order to investigate which type/s of K-conductances are activated by the P2Y$_1$ receptor agonist in medium spiny neurones, we applied three different kinds of K-channel blockers. Since only 64.4% of the cells investigated in the previous section of experiments showed a response to the P2Y$_1$ agonist, the K-channel blocker was applied by superfusion after a marked response to 2MeS-ADP was observed. Firstly, we applied TEA at a concentration (200 μM) that is relatively selective for blocking the large conductance-Ca^{+2}-activated-K$^+$-channels (BK channels). As shown in figure 29A, the application of 200 μM TEA blocked the P2Y$_1$-activated current. The TEA-sensitive current is shown in the inset of figure 29A and is obtained by subtraction of the ramp current recorded in the presence of 2MeS-ADP minus the ramp current recorded in the presence of 2MeS-ADP + TEA. The average values obtained in 7 cells are shown in the bar graph of figure 29A (right panel). The amplitude of currents elicited by the ramp at + 40 mV is significantly increased by the application of 2MeS-ADP and this effect is blocked in the presence of TEA. The average of the TEA-sensitive conductance obtained in the 7 cells investigated is shown in figure 30A (open circles) and is well fitted by the Boltzmann equation with a g$_{max}$ value of 3.66 nS, a z value of 1.95 and a V$_{1/2}$ value of 0.67 mV.

Since TEA could also decrease the currents recorded in the presence of 2MeS-ADP by blocking K-currents already present in control conditions, we performed a series of experiment in which we superfused TEA alone for 5 minutes before applying 2MeS-ADP. In 6 out of 8 cells, an increase in conductance elicited by the P2Y$_1$ agonist was not observed, indicating that it was due to TEA-sensitive ion channels (figure 29D). It is to be noted that the application of TEA significantly reduced (paired Student's t-test, P=0.0197, n=8) the current amplitude measured at + 40 mV in control cells; in fact TEA was also able to reduce the current amplitude below the control level in the group where it was applied after 2MeS-ADP superfusion (figure 29A, left panel, paired Student's t-test, P=0.0339, n=7). In the remaining two cells, a small increase of outward current was still observed in the presence of TEA (not shown), suggesting that potassium channels other than BK could also be involved in the 2MeS-ADP mediated effect.

In a separate set of experiments we applied the selective blocker of BK channels, iberiotoxin, after the 2MeS-ADP induced effect was observed. When a significant increase of the current amplitude was elicited by the P2Y$_1$ agonist, the application of the toxin completely blocked the effect in 6 out of 7 cells (figure 29B, right and left panel). The iberiotoxin-sensitive current is shown in the inset of figure 29B, and the average

of the iberiotoxin-sensitive conductances is shown in figure 30A. It is to be mentioned that in one cell, not included in this analysis, the toxin failed to block the P2Y$_1$-mediated effect, suggesting again the implication of other K-channel subtypes in the effect observed with 2MeS-ADP.
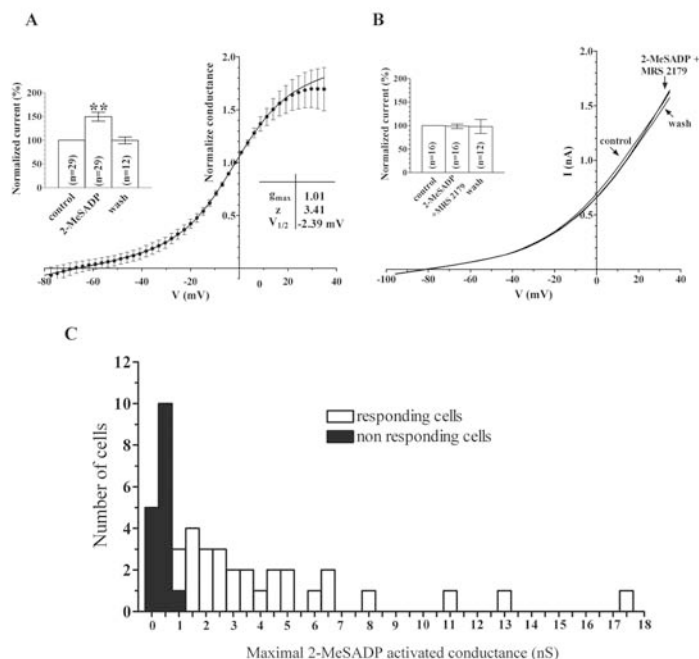
Figure 28. Averaged results showing the effect of selective P2Y$_1$ agonist or antagonist application. A. The graph shows the averaged conductance (±s.e.) normalized to the "zero voltage" value obtained in 29 cells investigated. The straight line shows the fitted curve obtained by the combination of a linear function and the Boltzmann equation, with parameter values shown in the grid. Inset: the column bars in the graph represent the average of current amplitude elicited by the ramp depolarization at +40 mV normalized to the control value in the 29 cells investigated. A significant increase was observed in the presence of 2MeS-ADP (**:P=0.0065, paired Student's t test). B. In a typical experiment, no difference was found in the outward current amplitude activated by the ramp at +40 mV in the absence or in the presence of 2MeS-ADP (250 nM) and MRS 2179 (15 μM). Inset: averaged values of current amplitude at +40 mV in 16 cells investigated. No significant difference was found during the coapplication of the P2Y1 agonist with 15 μM MRS 2179 (P>0.05, paired Student's t test). C. Population graph showing the distribution of responding and non responding cells in relation to the maximal value measured for the P2Y$_1$-activated conductance.

To better investigate the nature of this possibly non-BK-mediated effect, we also applied apamin (100 nM), a selective blocker of small conductance Ca^{2+}-activated K$^+$ channels (SK channels, figure 29B) after the 2MeS-ADP mediated effect was elicited. As shown in figure 29C, the application of apamin (10 μM) reversed the effect elicited by the P2Y$_1$ agonist in three out of four cells investigated. The apamin-sensitive current is shown in the inset of figure 29C, and the average of the apamin-sensitive conductances

is shown in figure 28B. As observed for the averaged 2MeS-ADP activated conductance (figure 28A), this curve shows a linear component at negative potentials (<-20 mV). For this reason we fitted the curve with a combination of a linear equation (to describe the non-voltage dependent membrane conductance at potentials ≤ -20 mV) and the Boltzmann relation described above. A summary of all the parameters obtained by fitting the conductances sensitive to each potassium channels blocker investigated is reported in the table of figure 30.
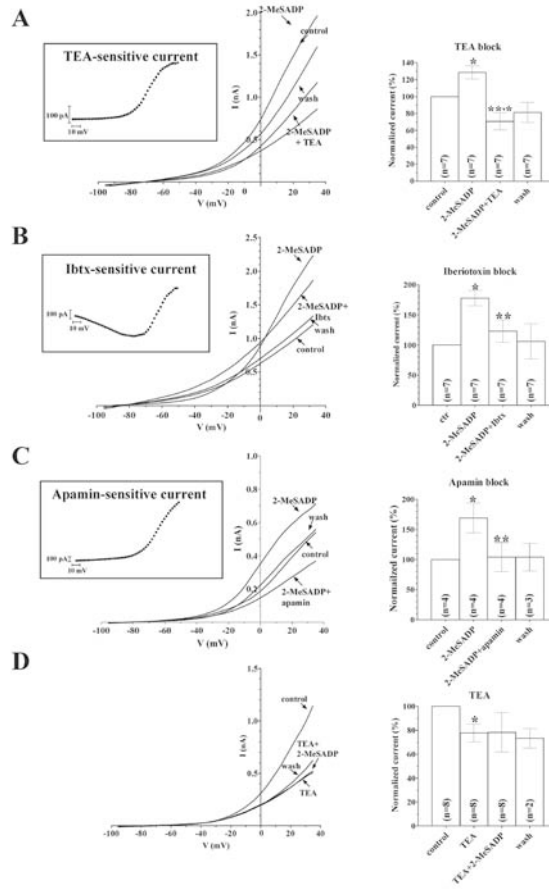
Figure 29. Effect of different potassium channel blockers on the 2MeS-ADP activated current. A. Left panel shows a single experiment where 2-MeSADP application (250 nM) was followed by the perfusion of the 2-MeSADP + 200μM TEA. The current increase observed in the presence of the P2Y$_1$ agonist was completely blocked by TEA. Inset: in the same cell, the TEA-sensitive current obtained by subtraction of the ramp current recorded in the presence of 2-MeSADP + TEA from that observed with the P2Y$_1$ agonist alone. Right panel: average current amplitudes recorded at +40 mV in each cell of this experimental group. *: P<0.05 from the control group, **: P<0.05 from 2-MeSADP group, paired Student's t test. A similar protocol was performed in the presence of 200 nM iberiotoxin (B) and 100 nM apamin (C). D. Left panel: when 200 μM TEA is applied before the P2Y$_1$ agonist, no increase in ramp-evoked outward current was observed. The right panel shows that in this group TEA applied alone significantly reduced the total outward current evoked by the voltage ramp (P=0.0197, paired Student's t test).

A

	2-MeSADP	2-MeSADP+TEA	2-MeSADP+Ibtx	2-MeSADP+apamin
gmax	2.06 nS	3.66 nS	3.02 nS	1.70 nS
z	3.98	1.95	3.08	5.30
V$_{1/2}$	-9.33 mV	0.67 mV	-4.59 mV	-10.36 mV

B
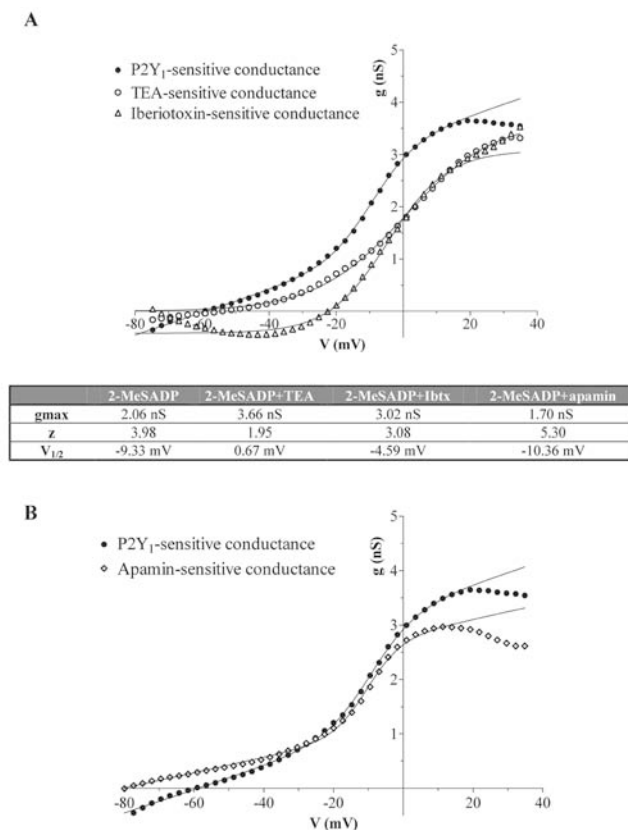
Figure 30. Averaged TEA-, iberiotoxin-, and apamin-sensitive conductances compared to the P2Y$_1$-activated conductance. A. Filled circles represent the averaged P2Y$_1$-activated conductance in 29 cells investigated. The solid line is the curve obtained by fitting the sum of a linear function and the Bolzmann equation. Open circles represent the averaged TEA-sensitive conductance after the application of 2MeS-ADP. Thick dashed line is the fitted curve of a Boltzmann equation. B. Filled squares show the iberiotoxin-sensitive conductance, thin solid line is the fitted Boltzmann equation. Open squares indicate the apamin-sensitive conductance. The table shows the Boltzmann parameters obtained by fitting each curve.

2.3 Single channel recordings show SK potassium channel opening following P2Y$_1$ receptor activation

In order to investigate further the mechanisms underlying the results obtained with voltage and current clamp experiments in whole cell configuration, we investigated the effect of 2MeS-ADP during cell-attached single channels recordings. Patch current was measured for two minutes during the imposition of different membrane potentials to the recording pipette, before and after 5 minutes application of 250 nM 2MeS-ADP. In a total of 14 patches recorded from the soma of medium spiny neurons, only 3 showed openings of SK-like potassium channels, and none of them included BK-like currents, presumably reflecting a low density of these two kinds of ionic channels at the soma level of striatal medium spiny neurons.
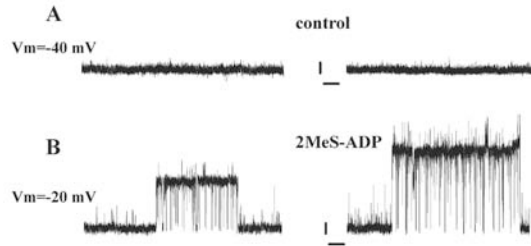
Figure 31. Single channel recordings in cell-attached configuration show the activation of SK channels in the presence of 2MeS-ADP. A. Representative recordings of 20 s duration from the same cell in control conditions (upper panels) and in the presence of 250 nM 2MeS-ADP (lower panels) at two different pipette potentials. The potential values indicated in the figure represent the membrane potential calculated assuming a resting membrane potential of – 80mV. Channel openings are shown as upward deflection of the current traces. Calibration bars: 2 s, 1 pA.

However, in some cells, the application of 2MeS-ADP revealed the presence of potassium channels in the patch pipette (figure 31). On the basis of the current-voltage relationship, the estimated conductance of such channels was 35pS, which is consistent with SK channel activity.

2.4 2MeS-ADP decreases the firing rate of medium spiny neurons recorded under the current-clamp mode in striatal slices

In order to gain insight into possible physiological effects of $P2Y_1$ receptor activation in striatal medium spiny neurones, we investigated the effects of 2MeS-ADP (250 nM) on the firing pattern of these cells in current-clamp recordings.

Ten subsequent steps of current injection (1 s duration, 10 pA each) from sub-threshold to suprathreshold potentials were performed from a resting potential of –70 mV, to establish the threshold value for spiking activity in each cell investigated. The amplitude of the first step current injection was chosen on the basis of the electrophysi-ological characteristics of each cell recorded, and varied from 2 to 50 pA.

Under control conditions, increasing current injections resulting in suprathresh-old voltages cause the cell to fire with increasing frequency (figure 32A, thin trace). Little frequency adaptation was observed during current pulses (see table 10), as pre-viously described for medium spiny neurons (Calabresi *et al.*, 1987; Kawaguchi *et al.*, 1989; Kawaguchi 1992; Kawaguchi 1993), and a medium after hyperpolarization po-tential (mAHP) was usually present after each action potential. No slow after hyperpo-larization potential (sAHP) was observed at the end of the depolarising step, as expect-ed for this kind of cell (Kawaguchi 1992; Kawaguchi 1993) particularly during the first postnatal week (Tepper *et al.*, 1993; Tepper *et al.*, 1998). The current clamp parameters measured in 11 cells investigated are shown in table 10.

In the presence of 2MeS-ADP (250 nM) the resting potential was usually more nega-tive than the control value, and the current injected was adjusted to maintain the resting membrane potential at -70 mV. After 5 minutes application of the selective $P2Y_1$ agonist, a significant decrease in the frequency of action potential firing (figure 32A, thick trace; figure 32B, open circle, thick line) was observed in all 11 cells investigated (paired Stu-dent's *t*-test, P=0.0346). We also recorded an increase of the first action potential latency during the first step of current injection (figure 32C, left panel), of the interspike-interval

(ISI) between the first and the second action potentials (figure 32C, central panel, paired Student's *t*-test, P<0.01), as well as between the second and the third (figure 32C, right panel, paired Student's *t*-test, P<0.001) in the presence of 2MeS-ADP. It has been demonstrated that calcium-dependent potassium conductances, mainly SK channels, are crucial factors in determining firing frequency and adaptation in medium spiny neurons (Pineda *et al.*, 1992), so these results are in agreement with the purinergic-mediated activation of Ca^{2+}-dependent K$^+$ currents observed during our voltage ramp experiments.

In contrast, other current-clamp parameters like action potential threshold, depolarization and hyperpolarization rate (mV/ms), amplitude and duration (the time between the threshold and the point where the membrane potential crossed the threshold value during the depolarization phase) were not significantly affected by 2MeS-ADP (table 10). Surprisingly, the mAHP amplitude, known to depend on SK channel activation, was not significantly increased by the P2Y$_1$ agonist.
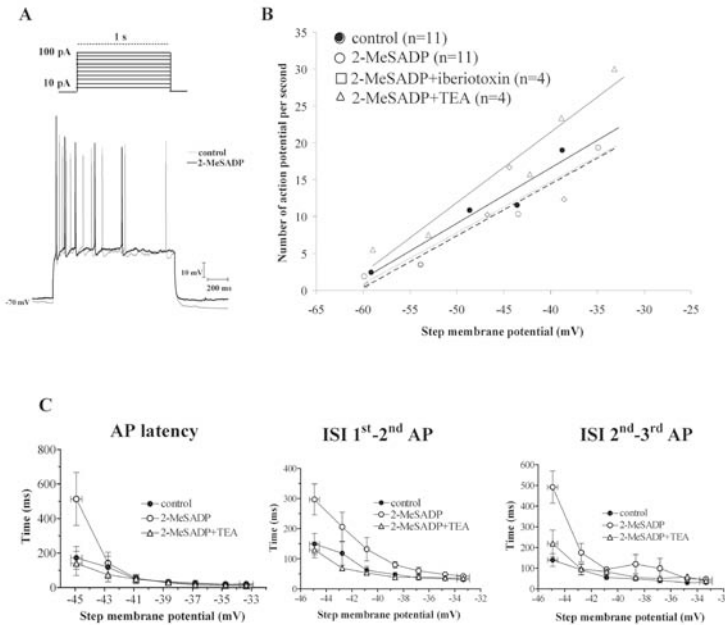
Figure 32. Effects of 2MeS-ADP application on firing activity of medium spiny neurones during current clamp recordings. A. Traces recorded in the same cell stimulated by suprathreshold current injections in control conditions (thin line) and after 5 minutes application of 250 nM 2MeS-ADP (thick line) are superimposed. Each trace shows the step depolarization in response to a 100 pA current injection. Note that in the presence of the selective P2Y$_1$ agonist the spike frequency is greatly reduced. The inset shows the stimulation protocol used. B. Average number of action potentials obtained in each group investigated as a function of the membrane potential reached by the current injection (X axis), assuming an imposed resting potential of -70 mV in all cells. For each group of cells the trend line of action potential frequency as a function of the membrane potential reached by the step pulse is shown. Note that iberiotoxin does not modify the firing frequency recorded in the presence of 2MeS-ADP. C. A significant difference in the latency of the first action potential (left panel) was found in the presence of 2MeS-ADP. The latency between the first and the second spike (inter-spike interval: ISI 1st-2nd: central panel) and between the second and the third spike (ISI 2nd-3rd: right panel) is increased in the presence of the P2Y$_1$ agonist (in particular during the first suprathreshold stimulation).

In a group of 4 cells in current clamp, 2MeS-ADP application was followed by co-application of the P2Y$_1$ agonist + TEA (200 μM). In this case, the effects of P2Y$_1$ receptor activation described before were reversed. Indeed, the frequency of action potential firing was even higher than the control value (figure 32B, open triangles, thin line).

When the same protocol was applied with iberiotoxin (200 nM) instead of TEA, no blockade of the effect elicited by 2MeS-ADP on action potential frequency was observed (figure 32B, open squares, dotted line).

Table 10. Current clamp parameters

	Control (n=11)	2MeS-ADP (n=11)
1st action potential amplitude (mV)	107 ± 2.41	111 ± 2.58
Action potential threshold (mV)	-36.3 ± 0.71	-35.6 ± 0.76
Action potential depolarization rate (mV/ms)	134 ± 3.94	127 ± 4.46
Action potential hyperpolarization rate (mV/ms)	-103 ± 3.36	-96.4 ± 3.41
Action potential width (ms)	3.50 ± 0.14	3.44 ± 0.13
Action potential latency (ms)	83.5 ± 13.9	135 ± 31.8*
mAHP amplitude (mV)	10.1 ± 0.76	10.6 ± 0.98
ISI 1st-2nd (ms)	87.8 ± 12.7	126 ± 16.8*
ISI 2nd-3rd (ms)	89.5 ± 22.4	138 ± 23.9*
Spike-frequency adaptation	1.15±0.19	0.96±0.16
Action potential frequency (Hz)	9.63 ± 1.26	6.11 ± 0.90*

The table reports the values of different current clamp parameters recorded in 11 medium spiny neurons investigated. Each value is the average of values obtained by suprathreshold current injection. *: $P<0.05$ from control values, paired t-test.

2.5 Spontaneous miniature synaptic currents are increased in amplitude during the application of 2meS-ADP.

Finally, in order to investigate a possible role of P2Y$_1$ receptors in regulating synaptic strength in the striatum, we recorded spontaneously occurring miniature synaptic currents (mEPSCs) in the presence of extracellular TTX. In control conditions the average frequency of such events was 0.21 ± 0.07 Hz and their amplitude was 4.18 ± 0.39 pA (n=19). During the superfusion of 2MeS-ADP (250 nM) the mEPSCs amplitude was increased to a value of 4.9 ± 0.5 pA (figure 33A, left panel), and this effect was statistically significant in 19 cells investigated (figure 33A, inset in left panel). When the P2Y$_1$ agonist was applied in the presence of the selective antagonist MRS 2179, no difference was found in the amplitude of mEPSCs (figure 33A, right panel and respective inset). The other parameters of mEPSCs analyzed (frequency, rise time and time constant of decay) were not significantly affected by the application of the 2MeS-ADP (figure 33B and table in the figure) or its co-application with MRS 2179 (data not shown).
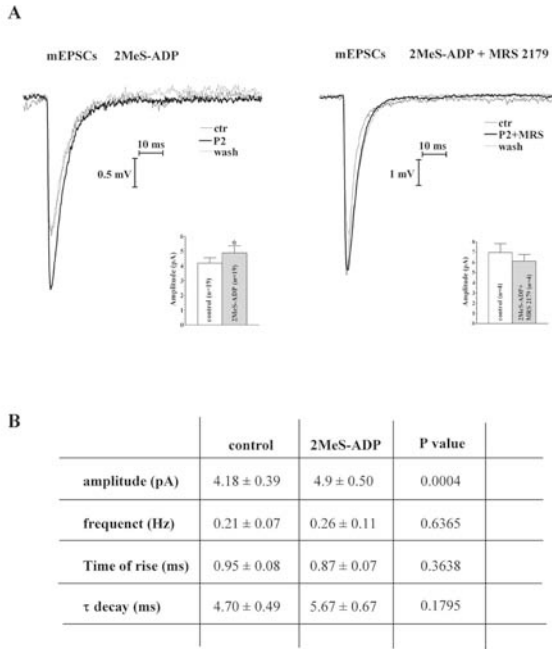
Figure 33. Effect of 2MeS-ADP on spontaneous mEPSCs in medium spiny neurons. A. Left panel: the three traces superimposed represent the average of mEPSCs recorded in a single cell before, during and 5 minutes after the application of 2MeS-ADP. The average mEPSCs obtained in the presence of the P2Y$_1$ agonist is increased (solid line). The inset shows that a significant increase in mEPSCs amplitude was observed in 19 cells investigated (*: P<0.05 versus control, paired Student's t test). Right panel: in another cell, no difference was found between the average of mEPSCs measured in control conditions (thin line) and during the coapplication of 2MeS-ADP + MRS 2179 (solid line). B. mEPSCs parameters are summarizad in the table, with respective P values from a paired Student's t test.

3. Discussion

There is clear evidence in the literature that P2Y purinergic receptors are expressed in the striatum. In fact, mRNA for P2Y$_{1,2,4,6,11}$ (Moore et $al.$, 2001) and P2Y$_1$ protein expression (Franke et $al.$, 2003; Moore et $al.$, 2000) have been found in human and rat striatum. However, there are conflicting reports of whether these physiologically expressed receptors have a functional role in this brain area (Ikeuchi et $al.$, 1995; Scheibler et $al.$, 2004).

In the present work we found that the activation of P2Y$_1$ receptors by a selective agonist induces an increase in the outward potassium currents in medium spiny neurons of rat striatal slices in 64.4% of cells. The P2Y$_1$-activated conductance shows a linear I-V relationship at potentials more negative than -20 mV, and a sigmoidal I-V curve at more positive potentials. In fact, the averaged P2Y$_1$-activated conductance recorded in 29 cells investigated is well fitted by the combination of a linear equation and the Boltzmann relation for voltage-gated ion channels, as shown in figure 26A. We conclude

that the ion carrying that current is K^+, since the reversal potential for the 2MeS-ADP activated current is around –100 mV (see figure 27A), close to the Nernst-calculated potassium equilibrium in our experimental conditions (E_k=-101 mV). Another candidate for the outward current observed in the presence of 2MeS-ADP could be chloride, since in our recording conditions the internal and external solutions contain 12 mM and 132.5 mM chloride ions respectively. However chloride is unlikely to carry the current observed in the presence of 2MeS-ADP, since the current reverses at potentials around -100 mV, whereas the calculated chloride equilibrium potential in our experimental conditions is E_{Cl}=-61.4 mV.

A relatively high percentage (35.6%) of medium spiny neurons didn't respond to the $P2Y_1$ agonist application with an increase in outward current. A possible explanation for this phenomenon is the presence of different cell populations of striatal medium spiny neurons presenting different expression patterns of purinergic receptors. In fact, in the last few years, emerging evidence demonstrates that medium spiny neurons are not such an homogeneous cell population as they were considered in the past. For example, it has been demonstrated that medium spiny neurons can be divided into enkephalin and P-substance expressing neurons, on the basis of different staining for these two histological markers (Gerfen *et al.*, 1988; Izzo *et al.*, 1987). It is reasonable that these two different subpopulations of cells (not distinguishable in our experimental conditions) express distinct pathways of P2 purinergic receptors. This hypothesis is consistent with recent results from Scheibler and colleagues (Scheibler *et al.*, 2004) showing that only 50% of striatal medium spiny neurons from 10-14 day old rats express the $P2Y_1$ purinergic receptor.

The half maximal activation potential of the 2MeS-ADP activated conductance is -9 mV, and the maximal value of conductance is reached at about +20 mV, whereas at more positive potentials the total outward conductance tends to decrease. This characteristic is typical of Ca^{2+}-activated K^+ channels, where a component of the calcium increase is from voltage dependent calcium channels that would be expected to reach a maximum around 0 mV.

Three different kinds of calcium-activated potassium channels have been described: the big conductance (BK), the intermediate conductance (IK) and the small conductance (SK) calcium-activated potassium channels. Both BK and SK channels are found in mammalian brain, whereas IK channels are present only in a few non-neuronal cell types, such as epithelial and red blood cells (Gardos 1958; Ishii *et al.*, 1997). In particular, BK and SK channels have been histochemically and functionally described in striatal neurones (Knaus *et al.*, 1996; Pineda *et al.*, 1992), and are shown to represent more that 50% of outward currents in acutely dissociated medium spiny neurones (Bargas *et al.*, 1999). BK channels are known to be voltage-sensitive, in fact intracellular calcium rise and membrane depolarizations both enhance the channel open probability (Bargas *et al.*, 1999; Horrigan *et al.*, 2002). In contrast, SK channels are voltage-independent; therefore we hypothesize that $P2Y_1$-mediated activation of SK channel could be responsible of the linear region of 2MeS-ADP activated conductance, whereas BK channel activation could determine the sigmoid region at positive potential values.

These conclusions were confirmed in the present study by the use of selective blockers. BK channels are the most likely K-channels blocked by sub-millimolar concentrations of TEA (Blatz *et al.*, 1986), by iberiotoxin (except for BK channels containing the β4 subunit, see: Faber *et al.*, 2003; Meera *et al.*, 2000) and by charybdotoxin (Galvez *et al.*, 1990). IK channels are blocked by charybdotoxin but not iberiotoxin or apamin (Ishii *et al.*, 1997), whereas mammalian SK channels are very sensitive to block

by apamin, with IC$_{50}$ values found in the pM range (Kohler *et al.*, 1996). In voltage clamp experiments of the present study either TEA at micromolar concentration, iberiotoxin or apamin were able to significantly block the current activated by 2MeS-ADP, confirming the involvement of both BK and SK channels in the P2Y$_1$-mediated effect. It should be noticed that the blockade of outward currents elicited by TEA was greater than that observed with iberiotoxin or apamin, even though the concentrations of both toxins (iberiotoxin: 200 nM; apamin: 100nM) were largely saturating (complete blockade at 10 nM for both toxins has been demonstrated in striatal neurons: (Bargas *et al.*, 1999; Nisenbaum *et al.*, 1996). It is interesting that the application of 200 μM TEA after the P2Y$_1$ agonist caused a significant reduction of the total outward current even in comparison to control values (figure 29A), whereas iberiotoxin and apamin did not. In addition, TEA was also able to significantly reduce the whole cell current in the absence of the P2Y$_1$ agonist (figure 29D). This may be due to some other potassium channels, not blocked by iberiotoxin or apamin but blocked by low TEA concentrations, already activated in control conditions, such as IK channels. In fact, Bargas and colleagues (Bargas *et al.*, 1999) demonstrated that in medium spiny neurones there is a residual outward current (sensitive to extracellular cadmium application) not blocked in the presence of both apamin and iberiotoxin at saturating concentrations.

The voltage-dependence of K-blocker-sensitive conductances found in the present work was well described by a Boltzmann relationship. This result was expected for TEA and iberiotoxin-sensitive conductances, if these reflect blockade of voltage-dependent BK channels. Surprisingly, the apamin-sensitive conductance obtained in the present work and shown in figure 28B presents a linear g-V relationship at potentials negative to -20 mV but also a voltage-sensitive component at higher potentials, which is fitted by the Boltzmann relationship. This is probably a consequence of the voltage-sensitivity of calcium influx through voltage-activated calcium channels that activates the SK conductance. In fact, in cholinergic interneurones of rat striatum it has been demonstrated that SK channels are activated by calcium influx from N-type calcium channels, as well as from the classical calcium release from intracellular stores (Goldberg *et al.*, 2005).

In current clamp experiments under control conditions, we recorded the typical electrophysiological characteristics previously described for medium spiny neurons at this maturational stage (Kawaguchi 1992; Kawaguchi 1993; Tepper *et al.*, 1993): a resting membrane potential around -80 mV, little spike frequency adaptation, little AHP, high threshold for action potential firing and no visible sAHP after the current step (see table 10). In the presence of 2MeS-ADP, we found a significant reduction of firing frequency induced by positive current injections, as well as an increase in the first spike latency and an increased adaptation between the first three action potentials in comparison to control values. This data is consistent with the idea of SK channel activation by the P2Y$_1$ agonist. It has been shown that the frequency of action potential firing in striatal medium spiny neurones is finely tuned by SK channels, which play an important role during the interspike period because they shape the AHP amplitude. This is probably due to their high calcium-sensitivity at hyperpolarized potentials (not observed for BK channels) that leads to more long-lasting currents than those mediated by BK channels. In contrast, BK channels are mostly implicated in shaping action potential repolarization since they are characterized by fast activation and inactivation kinetics. In fact, iberiotoxin was unable to reverse the spike frequency decrease caused by P2Y$_1$ receptor activation, confirming that BK channels are not involved in determining action potential frequency. Surprisingly, micromolar concentrations of TEA (that are not expected to block SK channels) markedly reverse the P2Y$_1$-mediated effect, caus-

ing an increase in firing frequency even in comparison to control conditions. We may hypothesise that, in this case, the action of TEA is due to the blockage of calcium-dependent potassium channels other than BK, such as the IK subtype. Alternatively, it can be hypothesised that TEA is blocking other potassium currents tonically activated in medium spiny neurons but not related to the $P2Y_1$ effect (for example the M-current, since KCNQ2 formed M-channels are blocked by submillimolar concentrations of TEA, see (Robbins 2001; Shapiro et al., 2000). From these data we conclude that, in current clamp mode, SK channel activation elicited by the $P2Y_1$ agonist predominates over the BK channel-mediated actions in determining the firing rate of medium spiny neurones. The lack of increase in AHP amplitude during 2MeS-ADP application is surprising if we expect that $P2Y_1$ receptors activate SK channels. A possible explanation is that a long-lasting hyperpolarization after thalamic or cortical stimulation in vivo is recorded in medium spiny neurons only after the third postnatal week (Tepper et al., 1993; Tepper et al., 1998), when the electrophysiological characteristics of these cells reach their mature phenotype. It could be that the lack of AHP increase in our experiments reflects some immature characteristic of this cell type.

The results obtained during the recordings of mEPSCs also confirm that $P2Y_1$ receptors may influence striatal neurotransmission. As application of 2MeS-ADP caused a significant increase in the amplitude, but not in the frequency, or time course of such events, it may be that P2Y receptor activation can modulate the strength of synaptic inputs in these neonatal neurones.

An increase in mEPSC amplitude is usually associated with increased strength of the synaptic circuitry, since the synapse efficacy is potentiated. This phenomenon is usually explained by an increase in the number of postsynaptic receptors, in this case glutamate AMPA receptors, and is also described as "chemical potentiation" (chemical LTP).

In vivo (but not in vitro) medium spiny neurons show some spontaneous oscillations of membrane potential in the subthreshold range, and different kinds of potassium channels play an important role in determining such phenomenon. These membrane potential oscillations, known as "up" and "down" states (Wilson et al., 1981; Wilson 1993), reflect a similar behaviour in corticostriatal projecting neurons (medial and lateral agranular layers: Stern et al., 1997; infragranular layer: (Plenz and Kitai 1998). During the "up" state the medium spiny neuron can show spontaneous spiking activity, with bursting events rarely observed, whereas during the "down" state no firing is recorded. On the basis of data obtained in the present work, we hypothesise that $P2Y_1$ receptors, by modulating SK and BK channels, may play an important role in determining the pattern of such oscillations in neonatal animals and influence the spontaneous firing activity of medium spiny neurones in vivo.

Finally, it is important to note that this study has been performed on 7 day old rats, so the observed effect of $P2Y_1$ receptors activation may be relevant to this time window of striatal development. It has been extensively described that the electrophysiological characteristics of 7 day old rat medium spiny neurons are profoundly different from the adult phenotype (Sharpe et al., 1998; Tepper et al., 1993; Tepper et al., 1998). These results are in agreement with the fact that Ikeuchi and Nishizaki reported an ATP-mediated increase in outward K^+ conductances in cultured medium spiny neurones from 1-day old rats (Ikeuchi et al., 1995), whereas Scheibler and colleagues demonstrated a lack of P2Y-mediated effects in striatal medium spiny neurons from older rats (Scheibler et al., 2004). Further support for this idea comes from a recently published paper by Rubini and co-workers (Rubini et al., 2006). In that work the authors demonstrated

that neuronally enriched striatal cell cultures from 1 day old rats respond to extracellularly applied ATP with a transient increase in intracellular Ca^{2+} concentration only if they are grown in NBM medium, which allows the maintenance of an "immature" electrophysiological profile (no repetitive firing, depolarized resting membrane potential, low density of I$_{Na}$) that is lost in normal DMEM cultured neurones.

The selective expression-activation of P2Y$_1$ receptors during early developmental stages of postnatal life could be correlated with particularly interesting ATP effects on cell development and proliferation recently reported by different authors. For example, an increased proliferation and migration of neuronal (Hogg *et al.*, 2004; Ryu *et al.*, 2003; Scemes *et al.*, 2003) and glial (Agresti *et al.*, 2005; Weissman *et al.*, 2004) progenitor cells has been linked to the stimulation of purinergic P2 receptors. On this basis, it can be envisaged that there is an important role for ATP during ontogenesis in the striatum.

Chapter 4
Role of purine nucleotides in cultured hMSCs: release of ATP and activation of P2 receptors

1. Historical background

In the last few years, several studies have demonstrated an interesting trophic role exerted by P2 receptor activation in various lineages of differentiated (Arthur *et al.*, 2005 and 2006) and undifferentiated cells. Haematopoietic stem cells (Lemoli *et al.*, 2004; Sak *et al.*, 2003), neuronal progenitor stem cells (Hogg *et al.*, 2004; Ryu *et al.*, 2003) and oligodendrocyte progenitors (Agresti *et al.*, 2005) respond to extracellular ATP with increased proliferation, differentiation and/or migration by intracellular signalling cascades that are similar or synergistic to those activated by numerous growth factors. In different cell systems, the trophic role of extracellular ATP is correlated with the occurrence of spontaneous intracellular Ca^{2+} waves, a self-renewing mechanism promoting periodic oscillation of intracellular Ca^{2+} levels that plays a crucial role in cellular proliferation and differentiation (Clapham 1995). It has been demonstrated that a number of cultured cells (Gerasimovskaya *et al.*, 2002; Gomes *et al.*, 2005b; Henriksen *et al.*, 2006; Scemes *et al.*, 2003) can release ATP that, in an autocrine/paracrine manner, propagate Ca^{2+} waves. It was demonstrated that ATP-mediated propagation of Ca^{2+} waves through radial glial cells modulates neurogenesis in the embryonic rat neocortex (Weissman *et al.*, 2004).

There has been great interest lately in human mesenchymal stem cells (hMSCs), a population of undifferentiated stromal stem cells derived from human adult bone marrow (Caplan *et al.*, 2001; Pittenger *et al.*, 1999; Reyes *et al.*, 2001 and 2002) that can be isolated, expanded in culture, and stimulated to differentiate into a variety of cell lineages (bone, cartilage, muscle, marrow stroma, tendon, fat) including neurones (Jiang *et al.*, 2002). Because large numbers of MSCs can be generated in culture, tissue-engineered constructs principally composed of these cells may be re-introduced into the in vivo setting. It has been recently demonstrated that *in vivo* transplantations of hMSCs into the post-ischemic brain (Zhao *et al.*, 2002) or infarcted myocardium (Min *et al.*, 2002; Shake *et al.*, 2002) of experimental animals significantly improved tissue functions, suggesting a possible role of these cells in the therapy of degenerating pathologies (Benvenuti *et al.*, 2006; Schwarz *et al.*, 1999). In spite of the huge employment of hMSCs in experimental cell transplantation in the last few years, the precise mechanisms determining *in vivo* migration and differentiation of engrafted hMSCs into the host tissue are still unclear.
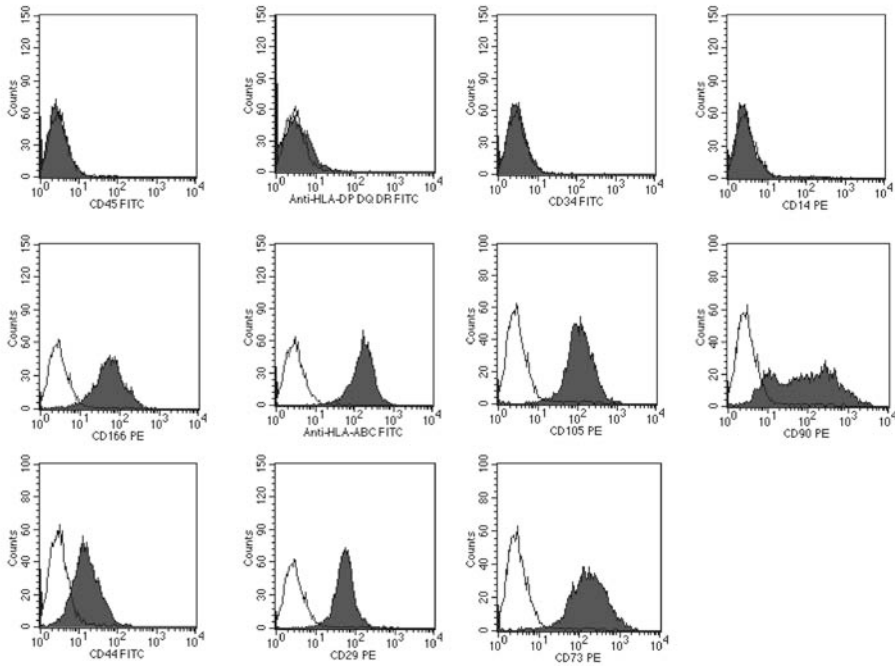
Figure 34. Flow cytometric analysis of surface adhesion molecules on human mesenchymal stem cells. Cells were labeled with monoclonal antibodies specific for molecules indicated in each flow cytometric histogram (negative for CD45, HLA-DP DQ DR, CD34, and CD14 and positive for CD166, HLA-ABC, CD105, CD90, CD44, CD29, and CD73). Abbreviations: FITC, fluorescein isothiocyanate; HLA, human leucocyte antigen; PE, phycoerythrin.

2.Results

Experiments were conducted on successfully culture-expanded hMSCs. A morphologically homogeneous population of fibroblast-like cells with more than 90% confluence was seen after 14 days. Thereafter, primary cultured (P0) cells were trypsinized and re-plated and, after the first passage in culture (P1), the cells grew exponentially, requiring weekly passages.

Flow cytometric analysis was used to assess the purity of hMSC cultures, which appeared uniformly positive for CD29, CD44, CD166, CD90, CD73, HLA-ABC and CD105. HLA-DPQR was expressed in less than 2% of the population. There was no detectable contamination of haematopoietic cells: in fact, markers of haematopoietic lineage, CD14, CD34 and CD45, were not detectable (figure 34). This pattern of cellular markers was stably expressed till P9 (data not shown).

Once a stable hMSC line was obtained (figure 35A), we investigated whether it tonically released ATP into the culture medium. As shown in figure 35B, the extracellular ATP concentration measured in the medium containing hMSCs, 24 h after a medium change, was 7.6 ± 0.57 nM. This value was significantly higher than that measured in the medium without cells, which was 0.3 ± 0.11 nM ($P<0.0001$, unpaired Students't test; n=11). Since no difference in ATP concentration was found at different cell passages in culture (P0-P5), all the results were plotted together.

Unfortunately, in our study, we could not determine ATP concentration in the presence of the ecto-ATPase inhibitor, ARL 67156, that prevents degradation of ATP, because the drug interfered with the luciferin/luciferase assay (Melani *et al.*, 2005).

2.1 Electrophysiological experiments

To investigate the presence and role of P2 receptors in hMSCs we used the patch-clamp technique to record whole-cell currents before and after the application of purinergic agonists and antagonists. The present work was carried out on 36 cells with a mean membrane resistance of 408.9± 78.6 MΩ, a mean membrane capacitance of 47± 5.9 pF and a mean membrane potential of -19.6± 3.2 mV. All the experiments were carried out at room temperature on cells from P0 to P5 passage in culture.

Exogenous ATP application modulates ionic membrane currents in hMSCs in culture.

In a first group of cells we studied the effects of ATP (10 μM, 5 minutes application, n=19) on hMSCs on the overall currents elicited by a voltage ramp protocol (inset figure 36A). In these experimental conditions, ATP elicited two different responses, shown in figures 36A-B and 36C-D, respectively.
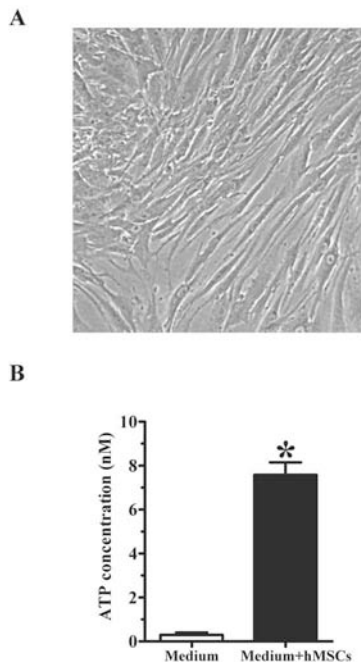
Figure 35. hMSCs in culture tonically release ATP. A. The figure shows adherent hMSCs as they appear in a primary culture (P0) 14 days after plating. B. Extracellular concentrations of ATP were measured with the luciferine/luciferase bioluminescence assay method in the medium containing hMSCs (50.000 cells/well) and in control medium not containing cells. Data are expressed as mean ± s.e., n=11. Unpaired Student's *t* test: *P<0.0001 vs medium alone.

In figure 36A, we reported that ATP enhanced the outward currents at membrane potentials more positive than -20 mV, with a modest increase in the inward component at more negative voltages. The ATP-sensitive current, obtained by subtraction of the control ramp from the trace recorded in the presence of ATP, showed a reversal potential of -30.8 mV (figure 36B). Similar results were obtained in 9 cells, that presented a mean resting membrane potential of -33.3±5.9 mV in control conditions and of -33.4±5.8 mV during ATP application (P>0.05, paired Student's t-test). The effect induced by the P2 purinergic agonist was maximal since no difference was found when ATP was applied at a higher concentration (30 μM, n=3, not shown). The maximal increase in the outward currents was reached after 5 minutes of ATP application and was reversible after drug washout (inset of figure 36B). In this group of cells, the average current amplitude at +40 mV was 639.6±129.8 pA in control conditions and 1021± 235.4 pA after 5 minutes of ATP application (P<0.05, paired Student's t-test).

Figure 36C shows the other response elicited by ATP in hMSCs on overall membrane currents evoked by the ramp protocol. In this case, the effect produced by 10 μM ATP was an increase in inward currents without significant changes in outward currents. The ATP-sensitive current presented a reversal potential of 0.5 mV (figure 36D). A similar response was obtained in 6 cells that presented a mean resting membrane potential of -15.27±3.2 mV in control conditions. The mean resting membrane potential measured at the peak of ATP effect was of -10.31±2.8 mV, indicating a significant depolarization induced by ATP (P<0.01, paired Student's t-test). The maximal effect was reached after 3 minutes of ATP application and it desensitised before the end of drug superfusion (inset of figure 36D). The average current amplitude at -90 mV was -162.2±76.8 pA in control and -292.5±149.2 pA after 3 minutes of ATP superfusion (P<0.01, paired Student's t-test).

In 4 out of 19 cells investigated in this experimental section no effects of ATP on membrane currents were observed.

From this first set of experiments we conclude that 79% of hMSCs respond to the application of exogenous ATP. These ATP-responding cells can be divided into two subgroups. One group presented a negative membrane potential (-33.3±5.9 mV) and responded to exogenous ATP superfusion with the activation of an outwardly rectifying ATP-sensitive current, with a reversal potential of -45.9±2.5 mV. The other group of hMSCs presented a more depolarized membrane potential (-15.27±3.2 mV) and responded to exogenous ATP with the activation of an inwardly rectifying ATP-sensitive current. This effect was accompanied by membrane depolarization. Cell capacitance, as a measure of cell size, was not different in both subgroups. Similarly, cell passage in culture (P0 and P5) did not influence ATP-mediated responses, and cells from P0 to P5 were pooled together.

In order to investigate the properties of the outward currents activated by ATP, we studied the effects of ATP on membrane currents elicited by a voltage step protocol.

As shown in figure 37A, a consistent increase in outward currents evoked by the step protocol was induced in a typical cell by 10 μM ATP starting from membrane potentials of +40 mV. The ATP-sensitive current showed a more evident increase in the transient early phase followed by a moderate but significant enhancement in the late sustained current. Figure 37B showed the averaged I-V plot of ATP-sensitive current obtained in this group of cells (n=3). To isolate the late sustained currents activated by ATP, we used another step protocol starting from a holding potential of -40 mV (inset of figure 37C) that inactivated transient conductances. As expected, in this case only slowly-activating, sustained currents were evoked by this protocol, and their amplitude

was increased in the presence of 10 μM ATP (figure 37C). Figure 37D shows the averaged I-V plot of ATP-sensitive current obtained in this group of cells (n=5).

The effects of ATP were further investigated in the presence of different P2 purinergic antagonists. In the presence of a selective P2Y$_1$ receptor antagonist, MRS2179 (10 μM), ATP (10 μM) did not induce any effect on ionic currents, evoked either by the ramp (figure 38A) or by the step protocol (figure 38B), and on resting membrane potential. Figure 38C shows that the mean effects of ATP on both inward and outward currents, measured at -90 mV and +40 mV respectively, were blocked in the presence of MRS2179 (figure 38C). In contrast, the other P2 antagonist tested, the non-selective PPADS, was efficacious in blocking only the ATP-induced increase in inward conductances, also revealing a membrane hyperpolarization during ATP application of from -16.3±3.7 mV to -23.9±2.6 mV.
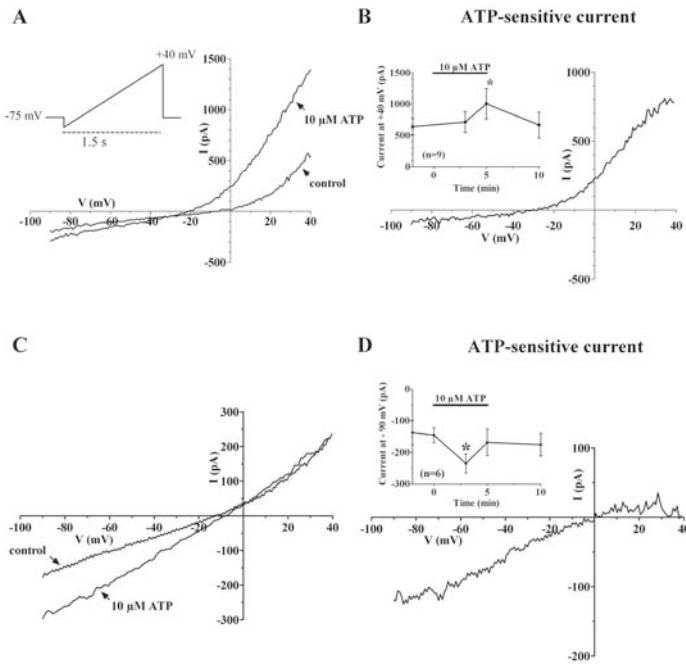
Figure 36. Exogenous ATP increases non-desensitising outward currents and/or desensitising inward currents in hMSCs in the whole-cell patch-clamp configuration. A. Typical experiment in which ATP evoked the increase of outward currents in an isolated hMSC. Inset: voltage ramps (inset: from -90 to +40 mV, ms duration) were applied before and during 10 μM ATP superfusion. B. ATP-sensitive current recorded in the same cells and obtained by subtraction of the current recorded at the maximal peak of effect (after 5 minutes of ATP application) from the control trace. Inset: time course of current amplitude activated by the ramp protocol at +40 mV before, during and after 10 μM ATP application. Each point in the graph represents the mean ± s.e. of 9 experiments in which ATP increased outward currents. C. Typical experiment in which ATP evoked the increase in inward currents in an isolated hMSC. Inset: voltage ramps were applied before and during 10 μM ATP superfusion. D. ATP-sensitive current recorded in the same cells and obtained by subtraction of the current recorded at the maximal peak of effect (after 3 minutes of ATP application) from the control trace. Inset: time course of current amplitude activated by the ramp protocol at -90 mV before, during and after 10 μM ATP application. Each point in the graph represents the mean ± s.e. of 6 experiments in which ATP enhanced inward currents.

2.2 Effects of exogenous ATP in potassium-free conditions

To better clarify the nature of the ATP-sensitive currents in hMSCs, we investigated the effect of ATP under K^+-free conditions by substituting all the K^+ ions of the intracellular and extracellular solution with equimolar Cs^+. In this experimental condition cells showed a mean resting membrane potential of -5.9±2.8 mV. As shown in figure 39A, 10 μM ATP increased the overall currents evoked by the ramp protocol, mainly affecting inward currents, as indicated also by the ATP-sensitive current (figure 39A, right panel). The same effect was recorded in all 6 cells tested. The maximal increase in inward current was reached after 3 minutes of ATP superfusion, and it desensitised after 5 minutes of agonist application (figure 39B). The averaged ATP-sensitive current showed a reversal potential of -6.5±0.6 mV, indicating the non-specific nature of the ATP-activated conductance (figure 39C). It should be mentioned that this effect resembles that observed in the presence of ATP in a group of cells, and shown in figure 36C. The fact that in K^+-free conditions ATP affected mainly inward current, suggests that the ATP-sensitive outward currents, also shown in figures 36A and 37, are carried by K^+ ions.
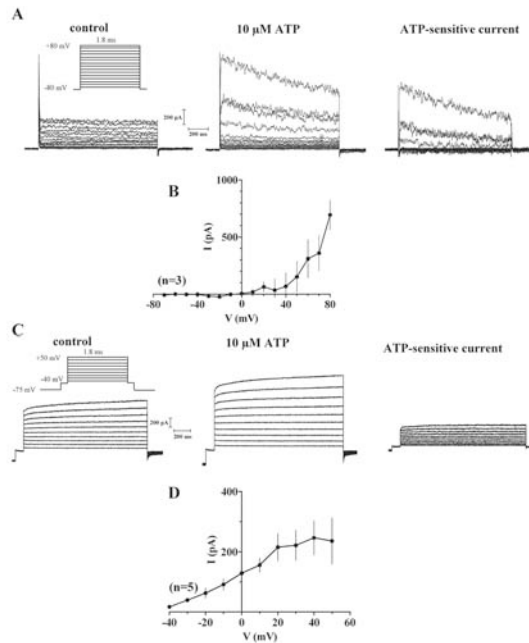
Figure 37. Exogenous ATP increases both early and late phase of outward currents in hMSCs. A. Representative current traces recorded in a hMSC by using the voltage step protocol (inset) in the absence (left panel) and in the presence of 10 μM ATP (5 minutes application: middle panel). The right panel shows the ATP-sensitive current obtained in the same cell by subtraction of the two precedent traces. B. Current-voltage relationship of ATP-sensitive current amplitude (measured at the peak) evoked with the protocol described in A and obtained by averaging the results recorded in 3 cells. C. Representative current traces recorded in a hMSC by using the voltage step protocol (inset) in the absence (left panel) and in the presence of 10 μM ATP (5 minutes application: central panel). The right panel shows the ATP-sensitive current obtained in the same cell by subtraction of the two precedent traces. D. Current-voltage relationship of ATP-sensitive currents (measured at the steady state) evoked with the protocol described in C and obtained by averaging the results recorded in 5 cells.
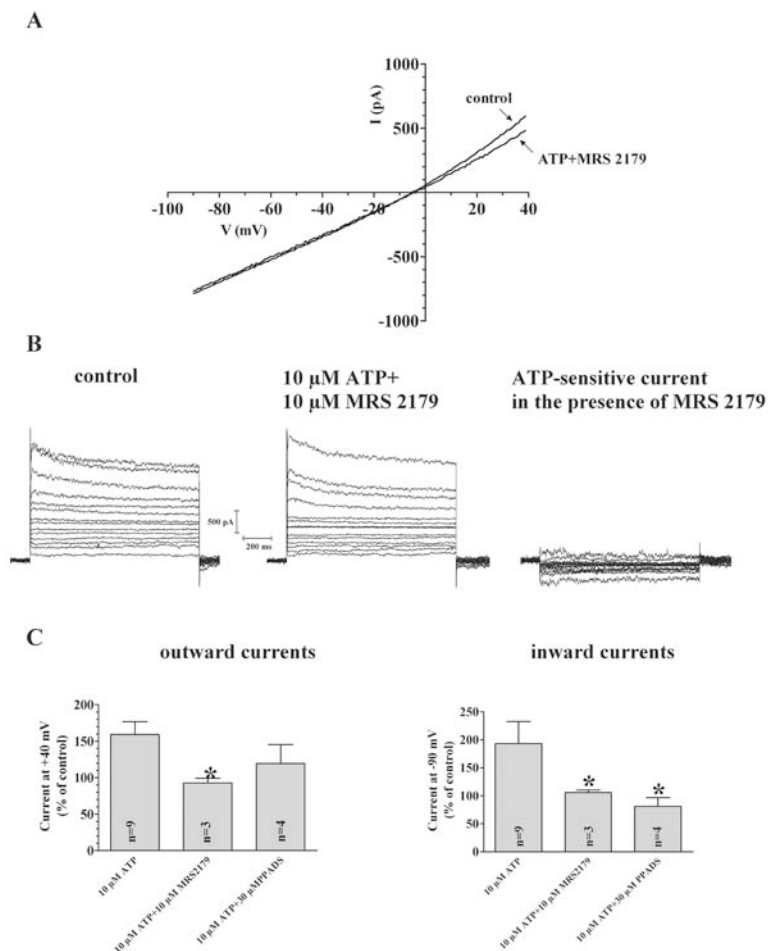
Figure 38. Effects of different P2 receptor antagonists on ATP-evoked currents. A. Typical experiment in which the application of MRS 2179 (10 μM) prevents the increase of both inward and outward currents evoked by the ramp protocol in the presence of 10 μM ATP. B. Representative current traces recorded in a hMSC by using the voltage step protocol (from -70 to +80 mV, 1800 ms duration, -80 mV holding potential) in the absence (left panel) and in the presence of ATP+MRS 2179 (middle panel). The right panel shows that no ATP-sensitive currents are evoked in this cell in the presence of MRS 2179. C. The bar graphs report the average current values at +40mV (left panel) and at -90 mV (right panel) evoked by the ramp protocol in the presence of ATP alone or in combination with different P2 antagonists. *: P<0.05 from 10 μM ATP alone (One-way ANOVA, Newman-Keuls post test).
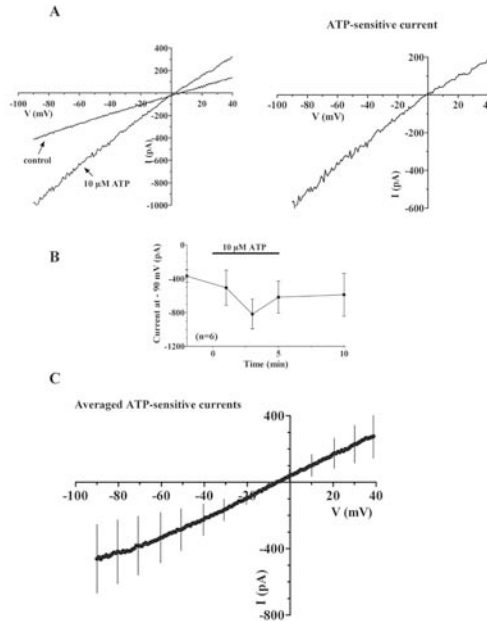
Figure 39. In K^{+}-free conditions only the increase in inward currents was elicited by ATP. A. Left panel: Representative experiment recorded in K^{+}-free conditions obtained by substitution with equimolar Cs^{+}. Right panel: ATP-sensitive current recorded in the same cell. B. Time course of current amplitude recorded at -90 mV before, during and after 10 μM ATP application. Each point in the graph represents the mean ± s.e. of 6 experiments. C. Averaged ATP-sensitive current amplitude elicited by the ramp protocol and recorded in the 6 cells investigated in K^{+}-free conditions.

2.3 Effects of ATP in hMSCs in the perforated patch-clamp configuration

Since it has been described that ATP promotes an intracellular increase in Ca^{2+} concentration in hMSCs, we performed perforated patch-clamp experiments to better investigate the effects of ATP on Ca^{2+}-dependent ionic conductances.

Also in these conditions ATP elicited two different responses. In 3 out of 5 cells investigated, ATP (10 μM, 5 minutes application) induced a consistent increase in outward currents and a modest enhancement in the inward currents evoked by the ramp protocol. The mean ATP-sensitive current (figure 40A, filled circles) showed a reversal potential of -38.7±1.2 mV. In the remaining 2 cells, 10 μM ATP increased inward currents, producing an ATP-sensitive current with a reversal potential of -5.6 mV, as shown in figure 40A (open circles). By comparing the ATP-sensitive currents recorded in the perforated-patch configuration (figure 40A) and that observed in the whole-cell configuration, shown in a typical experiment in figure 40A and 36C and averaged in figure 40B, it can be noted that in both experimental conditions ATP elicited comparable effects. In both cases, we can distinguish two groups of responding cells: cell responding to ATP with an increase in outward currents (filled circles) and cells responding to ATP with an increase in inward currents (open circles). It appears that in the perforated patch configuration the magnitude of ATP effects was greater, suggesting the involvement of a diffusible messenger (probably Ca^{2+} ions).

A summary of membrane properties measured in the different experimental groups is shown in table 11.

Table 11. Electrophysiological membrane properties of hMSCs.

		(n/n)	Rm (MΩ)	Cm (pF)	Vm (mV)
	ATP outward	(9/19)	363± 66	41.1± 10.2	-36.9± 7.2
Whole-cell (n=19)	ATP inward	(6/19)	375.7± 76.4	45± 11.6	-12.5 ±3.3
	ATP no effect	(4/19)	258.3± 61.3	46.1± 18.7	-17.5± 2.9
Whole-cell Cs$^+$ (n=6)	ATP inward	(6/6)	212.7± 46.4	40.3±5.2	-2.9± 1.7
Perforated patch (n=5)	ATP outward	(3/5)	330.5± 218.2	/	-28.2± 11.7
	ATP inward	(2/5)	302.0±58.2	/	-11.6±4.3

Data are taken from a total of 30 hMSCs investigated with the patch clamp technique in different experimental conditions. Numbers in parentheses (n/n) indicate the number of observations out of investigated cells.
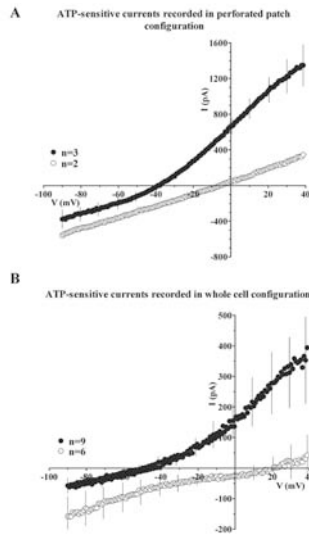
Figure 40. The same dual pattern of responses to exogenous ATP is observed in the perforated patch and whole-cell configurations. A. The graph shows the ATP-sensitive currents evoked by the ramp protocol in the perforated patch configuration. Filled circles: in 3 out of 5 cells the ATP-sensitive current presented a marked outward component with a minor effect on inward currents and a reversal potential of about -40 mV. Open circles: in the remaining two cells the ATP-sensitive current shows a prevalent inward component, with a reversal potential around 0 mV. B. The graph shows the ATP-sensitive currents evoked by the ramp protocol in the whole-cell configuration (K$^+$-containing solutions: experimental section described in figure 36). Filled circles: in 9 cells the ATP-sensitive current presents a marked outward component with a minor inward current and a reversal potential around -40 mV. Open circles: in 6 cells the ATP-sensitive current shows a marked inward rectification, with a reversal potential around 0 mV. Note that mean current amplitudes in the perforated patch configuration are greater than that recorded in the whole-cell patch-clamp.

3. Discussion

In this work we demonstrate for the first time that hMSCs in culture, from P0 to P5, tonically release ATP and express functional P2 purinergic receptors which modulate ionic conductances.

Our result that cultured hMSCs tonically release ATP is in agreement with Kawano and co-workers (Kawano *et al.*, 2006). The tiny difference between the value of ATP concentration reported by these authors (~3 nM) and that shown in the present work (~7.5 nM) might be due to the earlier culture passages (P0-P5) of cells used in the present study compared to those used by Kawano and colleagues (P6-P19). A decrease in ATP release during culture passages together with the observation of Kawano (Kawano *et al.*, 2006) that ATP-induced Ca^{2+}-waves in hMSCs gradually decrease during cell differentiation until they disappear in the fully-differentiated adipogenic phenotype, suggests a prevalent role of ATP in the earlier, undifferentiated, cell culture steps.

Our data demonstrate that exogenous ATP modulates ionic conductances in hMSCs by inducing two different responses. By imposing voltage ramp protocols to evoke overall currents at a wide range of membrane potentials, we observed that a population of cells responded to exogenous ATP with a marked increase in the outward currents that reached a maximum at the end of drug application (5 minutes); this effect was accompanied by a small enhancement of the inward component. In the other group of cells, exogenous ATP enhanced only the inward conductances that reached a maximum at 3 minutes and decayed at the end of the 5-minute agonist superfusion, indicating a desensitising response. The same dual pattern of ATP responses was observed when the cells were recorded in the perforated patch-clamp configuration. When K^+ ions were replaced by equimolar Cs^+, ATP elicited only one type of response, i.e. an increase in the inward currents, demonstrating that the outward ATP-sensitive currents are carried by K^+ ions.

The increase in outward K^+ currents observed in the presence of ATP is abolished in the presence of the selective $P2Y_1$ receptor antagonist MRS2179, suggesting that such currents are modulated by $P2Y_1$ receptor activation. Conversely, in the presence of PPADS, a non-selective P2X-P2Y antagonist, an increase in outward currents was still elicited in the presence of ATP. This fact could be due to the expression and activation in hMSCs of PPADS-insensitive P2Y receptors (such as the human $P2Y_2$ and $P2Y_{11}$ receptors: Charlton *et al.*, 1996; Communi *et al.*, 1999). An involvement of a metabotropic receptor in the modulation of outward K^+ currents is also supported by the observation that the maximal effect is reached at the end of ATP application (5 minutes). Since P2Y receptors ($P2Y_{1,2,4,6,11}$) stimulate PLC, with subsequent IP_3 formation and Ca^{2+} release from intracellular stores (von Kugelgen 2006), it is likely that this signalling cascade activates the K^+ conductances (I_{KCa}) in hMSCs, similarly to what is observed in other cell cultures (Hafting *et al.*, 2000; Mule *et al.*, 2003; Zizzo *et al.*, 2006). In agreement with a metabotropic-mediated effect, our results show that the amplitude of ATP-sensitive currents is greater in the perforated patch- clamp configuration that avoids dilution of intracellular constituents (second messengers) with the internal pipette solution.

Previous electrophysiological experiments conducted in hMSCs in culture report the presence of three distinct K^+ currents with different activation and inactivation kinetics (Heubach *et al.*, 2004; Li *et al.*, 2005). In these works, 94% of tested cells present a rapidly activating and noise-like current, identified as the Ca^{2+}-activated K^+ current (I_{KCa}); 48% of cells show a typical delayed rectified K^+ current (IK_{DR}) and a small fraction of cells (8%) presents a rapidly inactivating transient outward current, similar to

the cardiac and neuronal I_{to}. Almost all cells investigated express a combination of the three K^+ currents that is not correlated to cell diameter or passage in culture. In our experiments, the ATP-sensitive outward K^+ conductances were studied in isolation by applying a voltage step protocol. Our results indicate that at least two different types of K^+ conductances are involved in ATP effects. When the holding potential is clamped at -80 mV, the effect observed in the presence of ATP is the enhancement of both the transient early currents and the late sustained currents. The ATP-sensitive conductance obtained in these cells shows a highly noisy trace, suggesting the involvement of high conductances Ca^{2+}-dependent K^+ channels (BK channels). However, when we inactivate transient conductances by setting the holding potential at -40 mV, ATP still enhances outward currents, demonstrating that late sustained K^+ conductances, most likely represented by IK_{DR}, are also positively modulated by the P2 purinergic agonist. Both currents are activated by $P2Y_1$ receptors since they are completely blocked in the presence of the selective $P2Y_1$ antagonist MRS 2179.

The inward ATP-sensitive current presents the typical features of a non-selective cationic conductance, as expected after P2X receptor activation. It shows a reversal potential of 0 mV and a weak inward rectification, as determined by the I-V relationship. The observation that the response desensitises before drug removal is evidence of a P2X-like receptor-mediating ATP-sensitive inward current. In agreement with the involvement of a P2X-like receptor is the observation that ATP-induced inward current is associated with a concomitant membrane depolarization, as already demonstrated (Zemkova *et al.*, 2006). The increase in inward currents and membrane depolarization induced by ATP were prevented by PPADS, a non selective P2 purinergic antagonist, and by MR S2179, that mainly affects $P2Y_1$ receptors. PPADS is known to block $P2Y_{1,2,4,6}$ receptors and recombinant homomeric $P2X_{1,2,3,5}$, as well as heteromeric $P2X_{2/3}$ and $P2X_{1/5}$ receptor subtypes (Ralevic and Burnstock 1998). On these bases, we suggest that ATP-sensitive inward currents are mediated by the activation of P2X receptors, but we rule out the involvement of $P2X_1$ and $P2X_3$ subunits, at least in homomeric structures, since their inactivation takes place within 200-300 ms (Rettinger *et al.*, 2003; Werner *et al.*, 1996). Even if MRS 2179 is generally reported as a $P2Y_1$ antagonist, it must be considered that it also blocks some P2X receptors in transfected cells (Nandanan *et al.*, 2000). In agreement with this observation, we envisage that a native system such as immature stem cells at early stages in culture can express peculiar assemblies of heteromeric P2X receptors that are blocked by MRS 2179, in addition to the classical MRS 2179-sensitive $P2Y_1$ subtype. Alternatively, in an attempt to explain the MRS 2179-sensitivity of the ATP-sensitive inward current, we can ascribe this effect to a $P2Y_1$-mediated activation of "transient receptor potential" (TRP) channels, a family of non-selective cation channels specifically activated by G_q protein-coupled receptors (Zuker 1996). There is no evidence, to date, for TRP channels expression in hMSCs. Anyway, we cannot rule out the hypothesis that, in hMSCs, exogenous ATP stimulates $P2Y_1$ receptors that leads to TRP channels opening with a consequent influx of cations in the cell, as demonstrated in megakaryocytes (Tolhurst *et al.*, 2005).

When voltages ramps were recorded in Cs^+ containing solutions, even if all K^+ conductances are blocked by Cs^+ replacement in these conditions, the inward ATP-sensitive current also shows a small outward component. We hypothesize that in this case the outward current is carried by Cs^+ ions themselves, permeating through P2X channels, since it has been demonstrated that some P2X receptors expressed in native systems are also partially permeable to Cs^+ ions (Ikeda 2006; Liu *et al.*, 2001; Ma *et al.*, 2006), given the large size of the pore diameter (North 2002).

Finally, it should be noted that the effects of ATP on inward currents are always present in hMSCs, even in cells where ATP mainly induces an increase in outward currents. This is confirmed by the observation that the reversal potential of the ATP-sensitive outward current is -40 mV, that is different from the Nernst-calculated K^+ equilibrium potential in our experimental conditions (E_K=-81.7 mV). These results suggest that all hMSCs can potentially respond to ATP with an increase in inward currents, but, when K^+ channels or $P2Y_1$ receptors are present, the outward current activation overlaps the effect on inward currents.

Accordingly, in the latter case, no change in membrane potential was observed during ATP superfusion. This observation suggests that the depolarization due to the increase in inward currents elicited by ATP is counterbalanced by the outward current increase. In fact, when ATP is applied in the presence of PPADS, that only blocks the ATP-sensitive inward currents, an hyperpolarization is revealed, reasonably due to the ATP-induced activation of K^+ channels.

The absence of the outward ATP-sensitive current in some cells may be justified in several ways. For example, it is possible that not all the cells tested express the same subtype/s of P2X and/or P2Y receptors. Consequently, one possibility is that hMSCs responding to exogenous ATP with an increase in outward currents, are provided with $P2Y_1$ receptors, whereas cells that do not show this effect are not. Alternatively, since not all hMSCs express the same subtypes of K^+ channels (Heubach *et al.*, 2004; Li *et al.*, 2005). the lack of outward current increase in some hMSCs could be due to the absence of the particular subtype/s of K^+ channels activated by ATP, even in cells expressing $P2Y_1$ receptors. In agreement with the last assumption is the fact that cells in which ATP increases outward currents present a more negative resting membrane potential in comparison to cells in which ATP enhances inward currents, in both perforated and whole-cell configurations (see table 11). The question arises as to whether the two populations of hMSCs, showing distinct responses to exogenous ATP, also present some differences in morphological parameters. However, we reported that cell capacitance, as a measure of cell size, is not different in hMSCs responding to ATP with the increase of inward or outward currents (see table 11) and that the passage in culture from P0 to P5 does not affect the characteristics of ATP-sensitive currents.

3.1 Conclusion

In summary, ATP released from hMSCs, by producing two different responses, reveals two separate populations of these cells with distinct electrophysiological and pharmacological characteristics. It is possible that these characteristics correlate with different developmental potential of hMSCs. The precise mechanisms by which hMSCs may spontaneously differentiate into osteogenic, adipogenic or chondrogenic phenotypes are still unclear, and we can hypothesize that ATP may act as one of the early factors determining cell fate.

Chapter 5
Pharmacological characterization of the recently deorphanized GPR17 receptor transfected in 1321N1 astrocytoma cells.

1. Historical background

The human genome comprises several hundred orphan GPCRs (Fredriksson *et al.*, 2003), which are molecularly identified and cloned receptors that still lack a defined physiologically relevant ligand. The "deorphanization" of these receptors consists in detection of their pharmacological profiles and, eventually, their physiological roles.
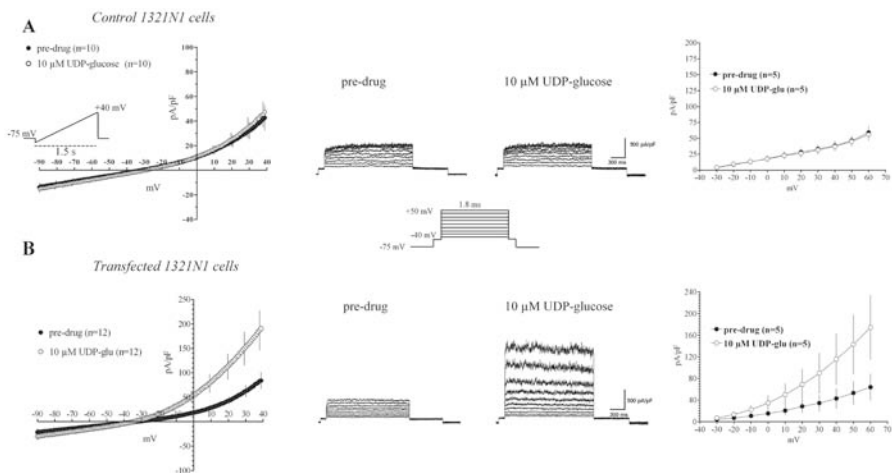
Figure 41. UDP-glucose elicited a significant increase in outward currents only in transfected 1321N1 cells. A. Left panel: Each point in the graph represents the current (mean ± s.e.) evoked by ramp protocol (inset: from -90 to +40 mV, 1500 ms duration, -75 mV holding potential) in the absence (pre-drug) and in the presence of 10 μM UDP-glucose. Middle panel: representative current traces recorded at voltage steps (inset: from -30 to +60 mV, -80 mV holding potential) in the absence (pre-drug) and in the presence of 10 μM UDP-glucose. Right panel: The I-V plot in the absence and in the presence of 10 μM UDP-glucose is superimposed. The values in the graph were obtained at the steady-state (1.7 s from episode start) of each current elicited by voltage steps (central panel). B. Left panel: Each point in the graph represents the current (mean ± s.e.) evoked by ramp protocol (inset: from -90 to +40 mV, 1500 ms duration, -75 mV holding potential) in the absence (pre-drug) and in the presence of 10 μM UDP-glucose. Middle panel: Representative current traces recorded at voltage steps (inset: from -30 to +60 mV, -80 mV holding potential) in the absence (pre-drug) and in the presence of 10 μM UDP-glucose. Right panel: The I-V plot in the absence and in the presence of 10 μM UDP-glucose shows the increase in outward currents induced by the P2 purinergic agonist. The values in the graph were obtained at the steady-state (1.7 s from episode start) of each current elicited by voltage steps.

The purinergic receptor family is growing by addition of newly deorphanized receptors that are found to bind purinergic-related compounds. The last one has been GPR17, whose recent deorphanization by Abbracchio and colleagues demonstrated a dual ligand binding profile. In fact, this receptor is activated by both sugar uridine nucleotides (UDP-glucose and UDP-galactose) and cysteinil-leukotrienes (CysLTs, such as LTD$_4$ and LTC$_4$). In addition, it is also blocked by purinergic antagonists (MRS 2179, AR-C-69931) and CysLT blockers (Montelukast and Pranlukast). This paper helped clarifying the already reported functional cross-talk between purinergic and leukotriene signalling (Ballerini *et al.*, 2005; Capra *et al.*, 2005; Mamedova *et al.*, 2005), mainly during inflammatory responses (Capra *et al.*, 2005; Mellor *et al.*, 2001). In fact, CysLTs are inflammatory lipid mediators generated by 5-lipoxygenase metabolism of arachidonic acid {Samuelsson, 2000 590 /id} that, by activating two different subtypes of G-protein-coupled receptors (CysLT$_1$ and CysLT$_2$) participate in inflammatory processes implicated, for instance, in bronchial asthma (Drazen 2003), stroke (Ciceri *et al.*, 2001) and cardiovascular diseases (Brink *et al.*, 2003). Similarly, dysfunctions of nucleotides and their receptors have been associated to various human diseases, including immune and ischemic/inflammatory conditions (Abbracchio *et al.*, 2003; Burnstock *et al.*, 2004). At molecular levels, GPR17 is coupled to G$_i$ protein, but either a reduction in cAMP and an increase in intracellular Ca^{2+} concentration has been reported upon stimulation (Ciana *et al.*, 2006).

In the present work we performed an electrophysiological study on 1321N1 astrocytoma cells stably transfected with GRP17. By investigating its role in modulating membrane ionic currents, we confirmed its dual pharmacological profile with such functional studies. This cell line has been chosen because it does not endogenously express other P2 receptors (excluded a tiny fraction of P2Y$_1$ subtype) but present several kind of K$^+$ channels subjected to GPCR modulation.

2. Results

This study was carried out on 113 cells, 22 control cells which were transfected with pcDNA and 91 cells transfected with the GPR17 receptor (Ciana *et al.*, 2006). Control 1321N1 cells presented a mean Cm of 14.7± 2.7 pF, and a mean membrane potential of -35.8± 2.7 mV̄ Transfected 1321N1 cells presented a mean Cm of 11± 0.67 pF and a mean membrane potential of -37.1 ± 3.4 mV.

2.1 Exogenously applied UDP-glucose and UDP-galactose activate outward potassium currents in 1321N1 astrocytoma cell stably transfected with GPR17.

As shown in figure 41A (left panel), the application of 10 μM UDP-glucose did not modify the overall currents evoked by the ramp protocol (inset) in control 1321N1 cells (n=10). In addition, no changes in outward potassium currents amplitude were observed (middle and right panels, figure 41A) when different voltage steps (step protocol: central panel) were applied. In contrast, UDP-glucose induced a significant increase in overall currents in transfected 1321N1 cells (figure 41B, left panel). This effect was evident in 12 out of 17 cells examined. The effect was evident starting from a membrane potential of -30 mV. At +40 mV the amplitude of outward currents increased from +84.1±16.6 pA/pF in control to +190.4±41.3 pA/pF in UDP-glucose (n=12, P<0.05, paired Student's *t*-test). The effect of UDP-glucose was reversible after
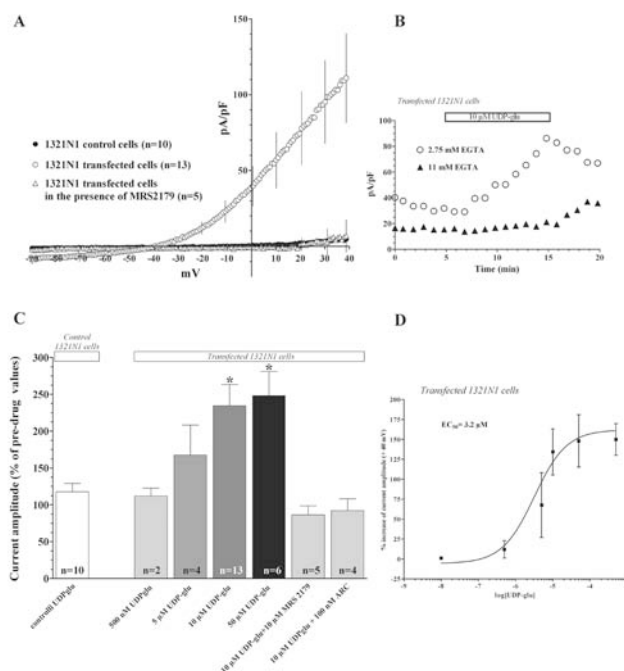
Figure 42. The effect of UDP-glucose in transfected 1321N1 cells was delayed in the presence of 11 mM EGTA and blocked by two different P2Y antagonists. A. UDP-glucose sensitive currents recorded from 1321N1 cells in different experimental conditions. Each value (mean ± s.e.) was obtained by subtraction of the current recorded at the maximal peak of effect from the respective control, pre-drug traces. B. Time course of current amplitude evoked by ramp protocol and recorded at +40 mV in the presence of different concentration of EGTA in the intracellular pipette solution. The two graphs are taken from two different cells. Note that 10 μM UDP-glucose induces a significant increase in current in both the conditions reaching the maximal peak within the 4 minutes washout, in the presence of 11 mM EGTA. C. Summary of the effects elicited by different concentrations of UDP-glucose on current amplitude in the absence or in the presence of two P2 purinergic antagonists in transfected 1321N1 cells. Values (mean ± s.e.) are expressed as percent of respective pre-drug responses. * P< 0.05 vs control cells: one-way ANOVA, Neuman-Keuls post test. D. Fitting curve of concentration-dependent increase in outward currents elicited by of UDP-glucose in 1321N1 transfected cells and recorded at +40 mV.

10-15 minutes washout (data not shown). UDP-glucose (10 μM; n=5) also significantly increased outward potassium currents amplitude induced by step protocol (figure 41B middle and right panels). No significant change in membrane potential at the end of 10 μM UDP-glucose superfusion (from 34.75±5.2 mV in control, pre-drug conditions, n=11 to 36±3 mV in the presence of the agonist, n=11) was found. The UDP-glucose sensitive currents, obtained by subtraction of the respective control ramps from the traces recorded in the presence of 10 μM UDP-glucose, are shown in figure 42A. In 1321N1 transfected cells, UDP-glucose elicited a current with a mean reversal potential of -43.6±4.9 mV (figure 42A). No UDP-glucose sensitive currents were recorded when the compound was applied in control 1321N1 cells or when the P2 agonist was applied in transfected 1321N1 cells in the presence of 1 μM MRS 2179, a P2Y purinergic antagonist (figure 42A).

Evidence in the literature indicates that the principal effect observed after P2Y purinergic receptor activation is an increase in the intracellular concentration of calcium ions (Ikeuchi and Nishizaki, 1996a; Ikeuchi *et al.*, 1996b; Koizumi *et al.*, 2002). To investigate a possible calcium dependency of currents elicited by GPR17 receptor stimulation, we increased EGTA concentration. The presence of 11 mM EGTA in the pipette solution decreased the overall current amplitude, both in transfected (from a value of +115.8±31 pA/pF, n=12, to a value of +33.7±10.8 pA/pF in EGTA, n=7) and control 1321N1 cells (from +93±47.2 pA/pF, n=7, to 40±4.8 pA/pF in EGTA, n=3) (data not shown). In these experimental conditions, 10 µM UDP-glucose did not change the amplitude of currents evoked by the ramp protocol in control 1321N1 cells (n=5, data not shown). In transfected 1321N1 cells, 10 µM UDP-glucose still elicited an increase in outward currents but with a slower time-course. As shown by two typical experiments in figure 42B, in fact, while the maximal increase in 2.75 mM EGTA is reached at the end of drug superfusion, in 11 mM EGTA the maximal increase of current amplitude induced by UDP-glucose was reached during the 4 minutes washout. The mean increase in outward current induced by 10 µM UDP-glucose in transfected 1321N1 cells in the presence of 11 mM EGTA was of 52±19% (P<0.05 vs respective control, paired Student's *t* test, n=7).

As shown in figure 42C, in transfected 1321N1 cells, the effect of UDP-glucose in the presence of 2.75 mM EGTA was evident starting from a concentration of 5 µM and the apparent EC_{50} value estimated for UDP-glucose effect on outward currents (figure 42D) was 3.2 µM (95% C.L. 0.36-38 µM). As shown in figure 42A and C, MRS 2179 completely prevents the increase in outward currents elicited by 10 µM UDP-glucose. In fact, in the presence of 1 µM MRS 2179, no effect of the P2 agonist on ionic currents evoked by the ramp (figure 42A and C) or by the step protocol (n=4, not shown) was recorded. Similarly, 100 nM AR-C69931MX (n=4), another P2 purinergic antagonists, completely prevented the effect of 10 µM UDP-glucose (figure 42C).

On the basis of previous results obtained in studies on GRP17 (Ciana *et al.*, 2006) we also tested the effects of UDP-galactose and UDP. In agreement with Ciana and colleagues, both compounds presented an agonistic activity on GRP17 transfected in 1321N1 cells. Figure 43A shows that the UDP-galactose sensitive current is superimposed to that evoked by UDP-glucose. In fact, it shows a similar current-voltage relationship and membrane reversal potential (-39±3 mV).

Conversely, UDP sensitive current was smaller in amplitude and presented a membrane reversal potential of -23.6±8.3 mV. As illustrated in figure 43B, the effect of both UDP-galactose and UDP on outward currents was completely blocked in the presence of 1 µM MRS 2179 in 1321N1 transfected cells.

2.2 GPR17 receptor, stably transfected1321N1 astrocytoma cells, is also sensitive to leukotriene-related compounds

In a set of experiments we also evaluated the effects of leucotrieneD4 (LTD4) both on transfected and control 1321N1 cells. LTD4 (10 nM) increased the amplitude of outward currents evoked either by the ramp protocol (figure 44A) or by the step protocol (middle and right panels, figure 44B) in transfected 1321N1 cells. No significant difference in membrane potential at the end of 10 nM LTD4 superfusion was found (from -47.23±8.5 mV pre-drug value, n=6, to -45.8±7.4 mV in the presence of the agonist, n=6, data not shown). The LTD4 sensitive currents, obtained by subtraction of the respective control ramps from the traces recorded in the presence of 10 nM LTD4 are shown
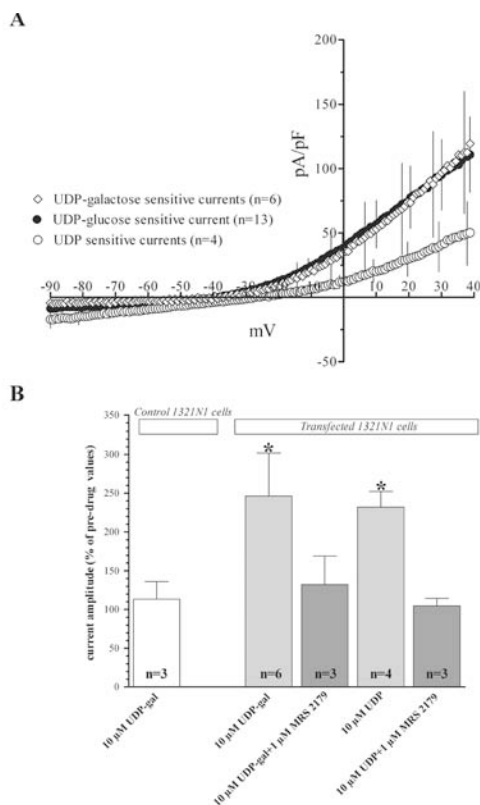
Figure 43. UDP-galactose elicited a significant increase in outward currents in transfected 1321N1 cells. A. Left panel: Each point in the graph represents the current (mean ± s.e.) evoked by the ramp protocol. Either UDP and UDP-galactose (10 μM both) increase outward currents. The UDP-glucose sensitive current is reported for comparison. B. Summary of UDP and UDP-galactose effects, alone or in combination with MRS 2179, on outward currents recorded at +40 mV either in control or in transfected 1321N1 cells. Values (mean ± s.e.) are expressed as percent of the respective pre-drug responses. * P< 0.05 vs control cells: one-way ANOVA, Neuman-Keuls post test.

in figure 44C. In transfected 1321N1 cells LTD4 elicited currents with a mean reversalpotential of -46.5±3.6 mV (figure 44C). No LTD4 sensitive currents were recorded in control 1321N1 cells (figure 44C,D). In transfected 1321N1 cells the compound was tested at different concentrations and the percentage increase in outward currents was of 4±8% (n=3) at 0.05 nM, of 59±42% (n=3) at 5 nM; of 111±34% (P<0.05 vs respective pre-drug value, paired Student's t test, n=6) at 10 nM and of 85±22 (P<0.05 vs respective pre-drug value, paired Student's t test, n=6) at 50 nM (figure 44D). The apparent EC_{50} value estimated for LTD4 effect on outward currents (figure 44E) was 0.92 nM. The effect of 10 nM LTD4 was significantly reduced either by MRS 2179 (figure 44C,D) or Montelukast (figure 44D), a P2Y purinergic antagonist and a CysLT receptor antagonist, respectively. We also tested the effects of LTD4 in the presence of Pranlukast, an-
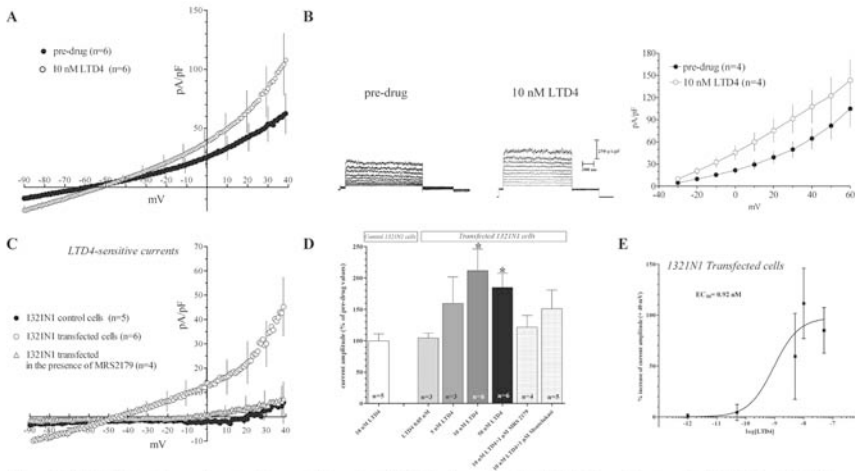
Figure 44. LTD4 elicits an increase in outward currents in transfected 1321N1 cells, an effect that is blocked by a P2 antagonist, MRS 2179, and a CysLT antagonist, montelukast. A. Each point in the graph represents the current (mean ± s.e.m.) evoked by the ramp protocol. LTD4 (10 nM) increases outward currents starting from -20 to +40 mV. B. Representative current traces recorded with the voltage step protocol in the absence (pre-drug) and in the presence of 10 nM LTD4. Right panel: The I-V plot of the step protocol-evoked currents recorded in 4 cells in the absence and in the presence of 10 nM LTD4 (current amplitude is measured at the steady-state). C. LTD4 sensitive currents recorded from control and transfected 1321N1 cells in different experimental conditions. Each value (mean ± s.e.) was obtained by subtraction of the currents recorded at the maximal peak of effect from the respective control, pre-drug traces. D. Summary of the effect of LTD4, applied at different concentrations, on the amplitude of outward currents evoked by the ramp pulse at a voltage of +40 mV both in control and transfected 1321N1 cells. Values (mean ± s.e.) are expressed as percent of the respective pre-drug responses. Cell number of each experimental group is shown on the corresponding bar. * P< 0.05 vs control cells: one-way ANOVA, Neuman-Keuls post test. E. Fitting curve of the concentration-dependent increase in outward currents elicited by LTD4 in 1321N1 transfected cells and recorded at +40 mV.

other leukotriene antagonist. Differently from Pranlukast, this compound, *per se*, elicited a significant increase in outward currents evoked by the ramp protocol (n=3, data not shown). No effect of 10 nM LTD4 in control 1321N1 cells (10 nM, n=5) was observed. (figure 44C,D).

In a group of experiments UDP-glucose and LTD4 were co-applied at the submaximal and maximal concentrations in transfected 1321N1 cells to verify if the effects elicited by the two agonists were additive or occlusive. As shown in figure 45A, when the two drugs were co-applied at submaximal concentrations (5 μM UDP-glucose and 5 nM LTD4, n=4) no additive effect was found. In fact, the value of current amplitude recorded at +40 mV in the presence of both compounds was not significantly different from the pre-drug level obtained in control conditions (P>0.05, paired Student's *t*-test). Furthermore, no significant difference was found between current values measured in this group of cells and that previously recorded in the presence of each drug alone, confirming that 5 μM UDP-glucose and 5 nM LTD4, applied alone or in combination, are ineffective (P>0.05, one-way ANOVA, Neumann-Keuls post test). An occlusive effect was observed when the two drugs were co-applied at maximal concentrations (50 μM UDP-glucose and 50 nM LTD4). In these experimental conditions, 8 out of 10 cells in-

A

B
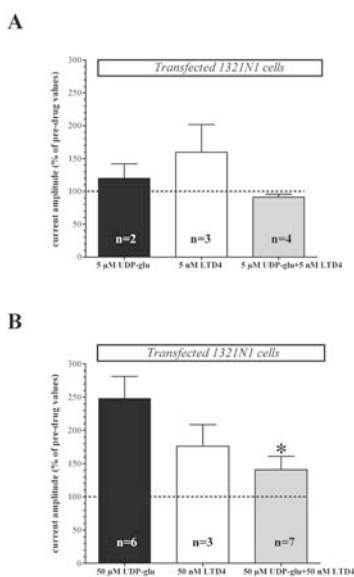
Figure 45. Summary of the effects of UDP-glucose and of LTD4, applied alone or in combination, on the amplitude of outward currents evoked by the ramp protocol at a voltage of +40 mV in transfected 1321N1 cells. Each column bar represents the mean ± s.e. of current amplitude measured at + 40 mV. Values are expressed as percent of the respective pre-drug responses. A. Effect of 5 μM UDP-glucose applied in combination with 5 nM LTD4 (submaximal concentrations). No significant difference was found among all experimental groups. B. Effect of 50 μM UDP-glucose applied in combination with 50 nM LTD4 (maximal concentrations). *: P<0.05, one-way ANOVA, Neuman-Keuls post test.

vestigated responded with an enhancement in outward conductances activated by the ramp protocol. The averaged increase in current amplitude measured at + 40 mV in the presence of 50 μM UDP-glucose and 50 nM LTD4 was of 154.3±36.1% in respect to pre-drug responses (n=8). This result is not significantly different from that obtained in the presence of each drug applied alone. Finally, in order to investigate which class of G protein coupled to GPR17 is involved in the effect elicited by UDP-glucose or LTD4 in 1321N1 transfected cells, we studied the effect of both agonists, applied separately, in PTX-treated cells. Figure 46A shows that in 5 out of 8 cells, the increase in outward currents produced by 10 μM UDP-glucose was blocked by the toxin. However, in the remaining 3 cells, an increase in outward currents was found. This latter effect is not different from that elicited by UDP-glucose in 1321N1 transfected cells without PTX pre-treatment. In all the 5 cells investigated, 10 nM LTD4 was able to increase outward currents in PTX-pre-treated 1321N1 transfected cells, similarly to what observed in the absence of the toxin.

3. Discussion

Our data demonstrate that the GPR17 receptor transfected in 1321N1 astrocytoma cell line is a functional receptor whose activation, by micromolar concentrations of UDP-glucose, UDP-galactose and UDP lead to a significant increase of outward potassium
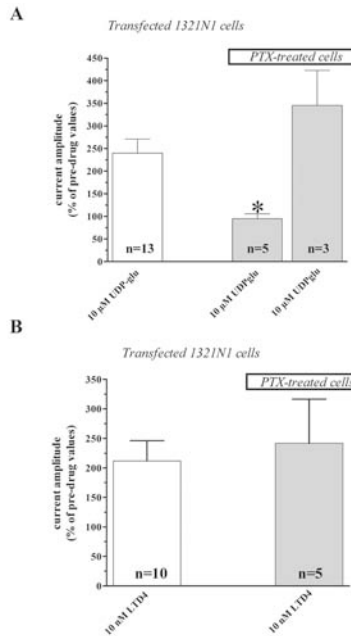
Figure 46. Pertussis toxin (PTX) sensitivity of UDP-glucose and LTD4 elicited effects in 1321N1 transfected cells. Each column bar represents the mean ± s.e. of current amplitude measured at + 40 Mv. Values are expressed as percent of the respective pre-drug responses. A. Effect of 10 μM UDP-glucose in 1321N1 transfected cells in the absence and in the presence of PTX pre-treatment. In three out of 8 cells PTX was unable to block the UDP-glucose elicited effect. * P<0.05 vs UDP-glucose alone in transfected cells: one-way ANOVA, Neuman-Keuls post test. B. Effect of 10 nM LTD4 in 1321N1 transfected cells in the absence or in the presence of PTX pretreatment. No significant difference was found between the two groups (P>0.05, unpaired Student's *t* test.

currents. In particular, micromolar concentrations of both the agonists bring to a significant increase in outward potassium currents. In control 1321N1 cells, UDP-glucose and UDP-galactose do not have any effect. It's worth noticing that P2Y receptors are able to regulate potassium currents in different cultured cells (Ikeuchi and Nishizaki 1996a; Ikeuchi *et al.*, 1996b; Hede *et al.*, 2005; Von Kugelgen *et al.*, 2005). Since the increase of potassium currents was observed only in transfected 1321N1 cells and it was blocked by a specific purinergic antagonist, MRS 2179, we can assume that the effects of both UDP-glucose and UDP-galactose are mediated by the GPR17 receptor.

The relatively slow time-course of current changes (8-10 minutes to reach the maximum peak value) indicates that the receptor acts by a typical metabotropic mechanism, mediated by intracellular second messengers. In our experiments, the increase of EGTA (from 2.75 to 11 mM) in the pipette solution delays and reduces the magnitude of UDP-glucose-mediated effect (an increase of 140±31%, in 2.75 mM EGTA at a concentration of 10 μM vs 52±19% in 11 mM EGTA). This result confirms that the potassium currents activated by UDP-glucose are calcium dependent. Since EGTA is a slight calcium chelator, presumably it does not completely block the intracellular calcium rise evoked after the receptor stimulation bringing to only a transient delay or reduction of the response.

It has been demonstrated that the effects of cysteinyl leukotriene LTD_4 are mediated by a specific interaction with cell surface receptors belonging to the rhodopsin family of the G protein-coupled receptor. Until now, two receptor subtypes have been cloned, namely $CysLT_1$ and $CysLT_2$ (Brink *et al.*, 2003). CysLT receptors have been detected in astrocytes (Ciccarelli *et al.*, 2004), and $CysLT_2$ receptors (Mamedova *et al.*, 2005). GPR17, a recently deorphanized receptor, is at intermediate phylogenetic position between P2Y and CysLT receptors and it is specifically activated by both families of endogenous ligands, P2 agonists and cysteinyl leukotriene, respectively (Ciana *et al.*, 2006).

An important finding of the present work is that LTD4, at nanomolar concentrations, is able to increase outward potassium currents evoked by a ramp protocol in transfected, but not in control, 1321N1 cells. In addition, we demonstrate that the effect of LTD4 on ionic currents was blocked by the purinergic antagonist MRS 2179. Therefore, we assume that LTD4 exerts its action by activating the GPR17 receptor. However, we found that the effect of LTD4 was also significantly reduced in the presence of the CysLT antagonist Montelukast. Recently, Mamedova et al., (2005) demonstrated that Montelukast inhibits the effects of nucleotides acting at P2Y receptors in 1321N1 cells stably expressing human $P2Y_{1,2,4,6}$ receptors. Therefore, UDP glucose, UDP galactose, UDP and LTD4 reasonably act on the same receptor as already demonstrated by Ciana *et al.* (2006). This conclusion is supported by the observation that the effects of UDP-glucose and LTD4 co-application at submaximal concentrations are not additive.

In conclusions, our data indicate that both UDP-glucose and LTD4 increase outward potassium currents in transfected 1321N1 cells through activation of the GPR17 receptor.

Final remarks

On the basis of the present results, it can be summarized that purinergic signalling actually plays important roles in cell functions either under physiological or pathological circumstances, in different tissues and at various developmental stages of living animals. What emerges in most cases is that both nucleosides (adenosine) and nucleotides (ADP, ATP, UDP, UTP), by activating specific membrane receptors (P1 and P2, respectively), are strictly correlated in orchestrating such responses. However, the respective contribution of each single element is hard to discern from the total outcome, due to the rapid and ubiquitous enzymatic interconvertion of these molecules into one another.

Regarding the CNS, adenosine and ATP share a modulatory role on synaptic transmission but, if adenosine only acts as a neuromodulator by activation of specific metabotropic receptors (A_1 A_{2A}, A_{2B} and A_3), ATP presents a more complex profile. In fact, it may act either as a neuromodulator or as a neurotransmitter itself. Under physiological conditions, both compounds are likely to play a role in neuronal activity, and the inhibitory action of endogenous adenosine in excitatory neurotransmission (mainly due to A_1 receptor activation) is well documented. Conversely, the present results, in line with previous observations in the literature, suggest a prevalent excitatory action of endogenous ATP under physiological conditions. This effect is modest, and probably restricted to certain brain regions (such as the hippocampus), but it is unmasked by the application of P2 purinergic antagonists that enhances evoked synaptic responses. However, the plurality of P2 receptors present in the brain (seven P2X subunits and eight P2Y subtypes) complicates the *scenario*. In fact, the application of exogenous ATP elicits opposite effects to that described for the endogenous agonist, mainly exerting an inhibitory effect on synaptic transmission. The discrepancy between the endogenously released and the exogenously applied agonist effect could be due to the stimulation of distinct P2 receptor subtypes in each situation. The inhibitory effect elicited by exogenous ATP application has long been ascribed to adenosine formation from ATP catabolism and subsequent activation of P1 receptors. However, the present work demonstrates that ATP itself may inhibit hippocampal synaptic transmission since an even more pronounced effect is observed when enzymatic ATP degradation is blocked. At a single cell level, the inhibitory role of ATP in synaptic responses can be ascribed to the activation of K^+ conductances, as already described for other neurotransmitters. This hypothesis is supported by the results obtained in this thesis on striatal slices, where $P2Y_1$ selective activation enhances Ca^{2+}-dependent K^+ currents (BK and SK channels) and decrease the firing frequency of medium spiny neurons in response to certain depolarizing inputs. However, the fact that the two effects elicited by ATP and reported in the present work (inhibition of synaptic transmission and activation of K^+ currents)

have been observed in different brain regions and in animals at distinct developmental stages should be considered (1 week old rats for striatal slices and 3 weeks-1 month old rats for hippocampal slices) and might not be correlated.

Within the CNS, ATP seems to be also involved in synaptic plasticity phenomenona. In fact evidence in the literature confirms the results shown in the present work in demonstrating that ATP application not only induces short lasting effects terminated by drug removal, but it also elicits long lasting responses. For example, an ATP-induced LTP has been described by Fuji and colleagues in different works (Fuji *et al.*, 1995, 1999 and 2002). In the present research, in the hippocampus, a potentiation of neurotransmission develops few minutes after the inhibitory effect has been washed out, and it persists up to 45'-1 h. In addition, experiments on rat striatal slices (presented in section 2, chapter 1) revealed an intriguing effect of P2 receptor stimulation in enhancing the amplitude of spontaneous mEPSCs recorded in the absence of synaptic activity (TTX in the extracellular milieu). This phenomenon is ascribed to an increased "synaptic strength", *i.e.* an enhanced response capability at certain synaptic inputs (due, for example, to an enhancement in membrane receptor expression), and is generally called "chemical LTP". Summarising hippocampal potentiating effects and striatal "chemical LTP" induced by P2 receptor stimulation, it can be argued that ATP could be an important mediator of long lasting effects in synaptic plasticity.

Either adenosine or ATP seem to become particularly important signalling molecules under pathological conditions, such as ischemia, when the extracellular concentration of both compounds drastically rises. It is well known that adenosine exerts important neuroprotective effects during brain ischemic insults by activating adenosine A_1 receptors which profoundly inhibits synaptic transmission and in particular the release of glutamate, that is known to contribute to ischemic damage. On the basis of the present results we propose that, during brief ischemic insults, adenosine A_1 and A_3 receptors share a common inhibitory effect on synaptic transmission. However, under severe ischemia, a prolonged stimulation of A_3 receptors causes a switch to deleterious effects, as demonstrated by the fact that a number of A_3 selective antagonists protect hippocampal slices from AD appearance and neurotransmission impairment after a severe OGD. The role of endogenously released ATP during cerebral ischemia is mainly deleterious, as found in the present work and in the literature, since the application of P2 antagonists always results in a reduction of ischemic damage. The mechanisms underlying these effects are still unknown, but they can be correlated to the tonic excitatory action of endogenous ATP found in many brain regions (for example in the hippocampus and prefrontal cortex).

Concerning developmental processes, growing evidence indicates an ancient phylogenetic origin of purinergic signalling. The expression of P2 receptors on cell membrane and a responses to extracellular ATP and are found in primitive prokaryotic species up to evolved animals and plants, suggesting an important and highly conserved role of extracellular purine nucleotides through the evolution. Similarly, ontogenetic development in several species seems to involve purinergic signalling especially during its first stages. In fact, in the present work, we describe an effect elicited by extracellular ATP in hMSCs, an undifferentiated line of human stem cells derived from stromal bone marrow able to originate a number of different cell lineages (adipocytes, condrocytes, osteoblasts,….). hMSCs in culture are shown to spontaneously release ATP in the extracellular space and to express functional purinergic P2 receptors which modulates different kinds (either inward Na^+-Ca^{2+} and/or outward K^+) of membrane currents. These results suggest an authocrine/paracrine mechanism of action for extracellular

purines in modulating cell functions of undifferentiated stem cells at early developmental stages.

Regarding the future of the purine field, new perspectives of investigation come from the still large area of orphan receptors, whose characterization is providing new members of the P2 receptor family. One example is GPR17, which has been recently deorphanized. In the present work we provide a pharmacological characterization of this receptor transfected in astrocytoma cells, that is sensitive to both uridine and leukotrienes compounds, solving the puzzling interrelation between these two systems already described in the literature. Our data demonstrate that the activation of GPR17, transfected in 1321N1 astrocytoma cells, leads to an increase in outward K^+ currents, an effect similar to that described after stimulation of $P2Y_1$ receptors endogenously expressed in striatal medium spiny neurons.

References

Abbracchio MP, Boeynaems JM, Barnard EA, Boyer JL, Kennedy C, Miras-Portugal MT, King BF, Gachet C, Jacobson KA, Weisman GA and BURNSTOCK G (2003). Characterization of the UDP-glucose receptor (re-named here the P2Y14 receptor) adds diversity to the P2Y receptor family. *Trends Pharmacol Sci* 24(2), 52-55.

Abbracchio MP, Brambilla R, Ceruti S, Kim HO, von Lubitz DK, Jacobson KA and Cattabeni F (1995a). G protein-dependent activation of phospholipase C by adenosine A3 receptors in rat brain. *Mol Pharmacol* 48(6), 1038-1045.

Abbracchio MP and Burnstock G (1994). Purinoceptors: are there families of P2X and P2Y purinoceptors? *Pharmacol Ther* 64(3), 445-475.

Abbracchio MP, Burnstock G, Boeynaems JM, Barnard EA, Boyer JL, Kennedy C, Knight GE, Fumagalli M, Gachet C, Jacobson KA and Weisman GA (2006). International Union of Pharmacology LVIII: update on the P2Y G protein-coupled nucleotide receptors: from molecular mechanisms and pathophysiology to therapy. *Pharmacol Rev* 58(3), 281-341.

Abbracchio MP and Cattabeni F (1999). Brain adenosine receptors as targets for therapeutic intervention in neurodegenerative diseases. *Ann N Y Acad Sci* 890, 79-92.

Abbracchio MP, Ceruti S, Langfelder R, Cattabeni F, Saffrey MJ and Burnstock G (1995b). Effects of ATP analogues and basic fibroblast growth factor on astroglial cell differentiation in primary cultures of rat striatum. *Int J Dev Neurosci* 13(7), 685-693.

Adams PR, Brown DA and Constanti A (1982). Pharmacological inhibition of the M-current. *J Physiol* 332,223-262.

Agresti C, Meomartini ME, Amadio S, Ambrosini E, Volonte C, Aloisi F and Visentin S (2005). ATP regulates oligodendrocyte progenitor migration, proliferation, and differentiation: involvement of metabotropic P2 receptors. *Brain Res Brain Res Rev* 48(2), 157-165.

Aitken PG, Fayuk D, Somjen GG and Turner DA (1999). Use of intrinsic optical signals to monitor physiological changes in brain tissue slices. *Methods* 18(2), 91-103.

Aitken PG, Tombaugh GC, Turner DA and Somjen GG (1998). Similar propagation of SD and hypoxic SD-like depolarization in rat hippocampus recorded optically and electrically. *J Neurophysiol* 80(3), 1514-1521.

Akasu T, Hirai K and Koketsu K (1983). Modulatory actions of ATP on membrane potentials of bullfrog sympathetic ganglion cells. *Brain Res* 258(2), 313-317.

Anderson CM, Bergher JP and Swanson RA (2004). ATP-induced ATP release from astrocytes. *J Neurochem* 88(1), 246-256.

Aono K, Nakanishi N and Yamada S (1990). Increase in intracellular Ca2+ level and modulation of nerve growth factor action on pheochromocytoma PC12h cells by extracellular ATP. *Meikai Daigaku Shigaku Zasshi* 19(2), 221-229.

Arthur DB, Akassoglou K and Insel PA (2005). P2Y2 receptor activates nerve growth factor/TrkA signaling to enhance neuronal differentiation. *Proc Natl Acad Sci U S A* 102(52), 19138-19143.

Arthur DB, Georgi S, Akassoglou K and Insel PA (2006). Inhibition of apoptosis by P2Y2 receptor activation: novel pathways for neuronal survival. *J Neurosci* 26(14), 3798-3804.

Ascherio A, Zhang SM, Hernan MA, Kawachi I, Colditz GA, Speizer FE and Willett WC (2001). Prospective study of caffeine consumption and risk of Parkinson's disease in men and women. *Ann Neurol* 50(1), 56-63.

King BF and Burnstock G (2002). Purinergic receptors. M.Pangalos and C.Davies. *Understanding G Protein-coupled Receptors and their Role in the CNS*. 422-438. Oxford University Press . Ref Type: Book Chapter

Baldwin SA, Beal PR, Yao SY, King AE, Cass CE and Young JD (2004). The equilibrative nucleoside transporter family, SLC29. *Pflugers Arch* 447(5), 735-743.

Ballerini P, Di Iorio P, Ciccarelli R, Caciagli F, Poli A, Beraudi A, Buccella S, D'Alimonte I, D'Auro M, Nargi E, Patricelli P, Visini D and Traversa U (2005). P2Y1 and cysteinyl leukotriene receptors mediate purine and cysteinyl leukotriene co-release in primary cultures of rat microglia. *Int J Immunopathol Pharmacol* 18(2), 255-268.

Baraldi PG, Cacciari B, Romagnoli R, Merighi S, Varani K, Borea PA and Spalluto G (2000). A(3) adenosine receptor ligands: history and perspectives. *Med Res Rev* 20(2), 103-128.

Barer R, Ross Kf and Tkaczyk S (1953). Refractometry of living cells. *Nature* 171(4356), 720-724.

Bardoni R., Goldstein PA, Lee CJ, Gu JG and MacDermott AB. (1997). ATP P2X receptors mediate fast synaptic transmission in the dorsal horn of the rat spinal cord. *J.Neurosci.* 17(14), 5297-5304.

Bargas J, Ayala GX, Vilchis C, Pineda JC and Galarraga E (1999). Ca2+-activated outward currents in neostriatal neurons. *Neuroscience* 88(2), 479-488.

Barnard EA, Burnstock G and Webb TE (1994). G protein-coupled receptors for ATP and other nucleotides: a new receptor family. *Trends Pharmacol Sci* 15(3), 67-70.

Barrera NP, Ormond SJ, Henderson RM, Murrell-Lagnado RD and Edwardson JM (2005). Atomic force microscopy imaging demonstrates that P2X2 receptors are trimers but that P2X6 receptor subunits do not oligomerize. *J Biol Chem* 280(11), 10759-10765.

Baurand A, Raboisson P, Freund M, Leon C, Cazenave JP, Bourguignon JJ and Gachet C (2001). Inhibition of platelet function by administration of MRS2179, a P2Y1 receptor antagonist. *Eur J Pharmacol* 412(3), 213-221.

Bean BP (1990). ATP-activated channels in rat and bullfrog sensory neurons: concentration dependence and kinetics. *J Neurosci* 10(1), 1-10.

Bean BP, Williams CA and Ceelen PW (1990). ATP-activated channels in rat and bullfrog sensory neurons: current-voltage relation and single-channel behavior. *J Neurosci* 10(1), 11-19.

Benvenuti S, Saccardi R, Luciani P, Urbani S, Deledda C, Cellai I, Francini F, Squecco R, Rosati F, Danza G, Gelmini S, Greeve I, Rossi M, Maggi R, Serio M and Peri A (2006). Neuronal differentiation of human mesenchymal stem cells: changes in the expression of the Alzheimer's disease-related gene seladin-1. *Exp Cell Res* 312(13), 2592-2604.

Bergner A and Sanderson MJ (2002). ATP stimulates Ca2+ oscillations and contraction in airway smooth muscle cells of mouse lung slices. *Am J Physiol Lung Cell Mol Physiol* 283(6), L1271-L1279.

Beukers MW, Chang LC, von Frijtag Drabbe Kunzel JK, Mulder-Krieger T, Spanjersberg RF, Brussee J and IJzerman AP (2004). New, non-adenosine, high-potency agonists for the human adenosine A2B receptor with an improved selectivity profile compared to the reference agonist N-ethylcarboxamidoadenosine. *J Med Chem* 47(15), 3707-3709.

Biber K, Fiebich BL, Gebicke-Harter P and van Calker D (1999). Carbamazepine-induced upregulation of adenosine A1-receptors in astrocyte cultures affects coupling to the phosphoinositol signaling pathway. *Neuropsychopharmacology* 20(3), 271-278.

Blatz AL and Magleby KL (1984). Ion conductance and selectivity of single calcium-activated potassium channels in cultured rat muscle. *J Gen Physiol* 84(1), 1-23.

Blatz AL and Magleby KL (1986). Single apamin-blocked Ca-activated K+ channels of small conductance in cultured rat skeletal muscle. *Nature* 323(6090), 718-720.

Bo X, Kim M, Nori SL, Schoepfer R, Burnstock G and North RA (2003). Tissue distribution of

P2X4 receptors studied with an ectodomain antibody. *Cell Tissue Res* 313(2), 159-165.

Bodin P and Burnstock G (2001). Purinergic signalling: ATP release. *Neurochem Res* 26(8-9), 959-969.

Boehm S (1998). Selective inhibition of M-type potassium channels in rat sympathetic neurons by uridine nucleotide preferring receptors. *Br J Pharmacol* 124(6), 1261-1269.

Bofill-Cardona E, Vartian N, Nanoff C, Freissmuth M and Boehm S (2000). Two different signaling mechanisms involved in the excitation of rat sympathetic neurons by uridine nucleotides. *Mol Pharmacol* 57(6), 1165-1172.

Bogdanov Y, Rubino A and BURNSTOCK G (1998). Characterisation of subtypes of the P2X and P2Y families of ATP receptors in the foetal human heart. *Life Sci* 62(8), 697-703.

Bona E, Aden U, Gilland E, Fredholm BB and Hagberg H (1997). Neonatal cerebral hypoxia-ischemia: the effect of adenosine receptor antagonists. *Neuropharmacology* 36(9), 1327-1338.

Borowiec A, Lechward K, Tkacz-Stachowska K and Skladanowski AC (2006). Adenosine as a metabolic regulator of tissue function: production of adenosine by cytoplasmic 5'-nucleotidases. *Acta Biochim Pol* 53(2), 269-278.

Bowler JW, Bailey RJ, North RA and Surprenant A (2003). P2X4, P2Y1 and P2Y2 receptors on rat alveolar macrophages. *Br J Pharmacol* 140(3), 567-575.

Bowser DN and Khakh BS (2004). ATP excites interneurons and astrocytes to increase synaptic inhibition in neuronal networks. *J Neurosci* 24(39), 8606-8620.

Boyer JL, Adams M, Ravi RG, Jacobson KA and Harden TK (2002). 2-Chloro N(6)-methyl-(N)-methanocarba-2'-deoxyadenosine-3',5'-bisphosphate is a selective high affinity P2Y(1) receptor antagonist. *Br J Pharmacol* 135(8), 2004-2010.

Boyer JL, Mohanram A, Camaioni E, Jacobson KA and Harden TK (1998). Competitive and selective antagonism of P2Y1 receptors by N6-methyl 2'-deoxyadenosine 3',5'-bisphosphate. *Br J Pharmacol* 124(1), 1-3.

Brake AJ, Wagenbach MJ and Julius D (1994). New structural motif for ligand-gated ion channels defined by an ionotropic ATP receptor. *Nature* 371(6497), 519-523.

Brand A, Vissiennon Z, Eschke D and Nieber K (2001). Adenosine A(1) and A(3) receptors mediate inhibition of synaptic transmission in rat cortical neurons. *Neuropharmacology* 40(1), 85-95.

Brandle U, Kohler K and Wheeler-Schilling TH (1998). Expression of the P2X7-receptor subunit in neurons of the rat retina. *Brain Res Mol Brain Res* 62(1), 106-109.

Brandle U, Zenner HP and Ruppersberg JP (1999). Gene expression of P2X-receptors in the developing inner ear of the rat. *Neurosci Lett* 273(2), 105-108.

Bringmann A, Pannicke T, Weick M, Biedermann B, Uhlmann S, Kohen L, Wiedemann P and Reichenbach A (2002). Activation of P2Y receptors stimulates potassium and cation currents in acutely isolated human Muller (glial) cells. *Glia* 37(2), 139-152.

Brink C, Dahlen SE, Drazen J, Evans JF, Hay DW, Nicosia S, Serhan CN, Shimizu T and Yokomizo T (2003). International Union of Pharmacology XXXVII. Nomenclature for leukotriene and lipoxin receptors. *Pharmacol Rev* 55(1), 195-227.

Brinley YFJ Jr., Kandel ER. and Marshall WH. (1960). Potassium outflux from rabbit cortex during spreading depression. *J Neurophysiol* 23, 246-256.

Broch OJ and Ueland PM (1980). Regional and subcellular distribution of S-adenosylhomocysteine hydrolase in the adult rat brain. *J Neurochem* 35(2), 484-488.

Brown DA and Adams PR (1980). Muscarinic suppression of a novel voltage-sensitive K+ current in a vertebrate neurone. *Nature* 283(5748), 673-676.

Brown J and Brown CA (2002a). Evaluation of reactive blue 2 derivatives as selective antagonists for P2Y receptors. *Vascul Pharmacol* 39(6), 309-315.

Brown SG, King BF, Kim YC, Burnstock G and Jacobson KA (2000). Activity of novel adenine nucleotide derivatives as agonists and antagonists at recombinant rat P2X receptors. *Drug Dev Res* 49, 253-259.

Brown SG, Townsend-Nicholson A, Jacobson KA, Burnstock G and King BF (2002b). Heterom-

ultimeric P2X(1/2) receptors show a novel sensitivity to extracellular pH. *J Pharmacol Exp Ther* 300(2), 673-680.

Bruns RF and Fergus JH (1990). Allosteric enhancement of adenosine A1 receptor binding and function by 2-amino-3-benzoylthiophenes. *Mol Pharmacol* 38(6), 939-949.

Buell G, Lewis C, Collo G, North RA and Surprenant A (1996). An antagonist-insensitive P2X receptor expressed in epithelia and brain. *EMBO J* 15(1), 55-62.

Burke SP and Nadler JV (1988). Regulation of glutamate and aspartate release from slices of the hippocampal CA1 area: effects of adenosine and baclofen. *J Neurochem* 51(5), 1541-1551.

Burnstock G (1972). Purinergic nerves. *Pharmacol Rev* 24(3), 509-581.

Burnstock G (1976). Do some nerve cells release more than one transmitter? *Neuroscience* 1(4), 239-248.

Burnstock G (1978). A basis for distinguishing two types of purinergic receptor. R.W.Straub and L.Bolis. *Cell Membrane Receptors for Drugs and Hormones: A Multidisciplinary Approach*. 107-118. *Raven Press* .Ref Type: Book Chapter

Burnstock G, Campbell G, Bennett M and Holman Me (1963). Inhibition of the smooth muscle on the taenia coli. *Nature* 200, 581-582.

Burnstock G, Campbell G, Satchell D and Smythe A (1970). Evidence that adenosine triphosphate or a related nucleotide is the transmitter substance released by non-adrenergic inhibitory nerves in the gut. *Br J Pharmacol* 40(4), 668-688.

Burnstock G, Cocks T, Kasakov L and Wong HK (1978). Direct evidence for ATP release from non-adrenergic, non-cholinergic ("purinergic") nerves in the guinea-pig taenia coli and bladder. *Eur J Pharmacol* 49(2), 145-149.

Burnstock G and Knight GE (2004). Cellular distribution and functions of P2 receptor subtypes in different systems. *Int Rev Cytol* 240, 31-304.

Calabresi P, Centonze D and Bernardi G (2000). Cellular factors controlling neuronal vulnerability in the brain: a lesson from the striatum. *Neurology* 55(9), 1249-1255.

Calabresi P, Misgeld U and Dodt HU (1987). Intrinsic membrane properties of neostriatal neurons can account for their low level of spontaneous activity. *Neuroscience* 20(1), 293-303.

Camaioni E, Boyer JL, Mohanram A, Harden TK and Jacobson KA (1998). Deoxyadenosine bisphosphate derivatives as potent antagonists at P2Y1 receptors. *J Med Chem* 41(2), 183-190.

Cantiello HF, Jackson GR, Jr., Grosman CF, Prat AG, Borkan SC, Wang Y, Reisin IL, O'Riordan CR and Ausiello DA (1998). Electrodiffusional ATP movement through the cystic fibrosis transmembrane conductance regulator. *Am J Physiol* 274(3 Pt 1), C799-C809.

Caplan AI and Bruder SP (2001). Mesenchymal stem cells: building blocks for molecular medicine in the 21st century. *Trends Mol Med* 7(6), 259-264.

Caplan LR (1998). Stroke treatment: promising but still struggling. *JAMA* 279(16), 1304-1306.

Capra V, Ravasi S, Accomazzo MR, Citro S, Grimoldi M, Abbracchio MP and Rovati GE (2005). CysLT1 receptor is a target for extracellular nucleotide-induced heterologous desensitization: a possible feedback mechanism in inflammation. *J Cell Sci* 118(Pt 23), 5625-5636.

Castell DO (1975). The lower esophageal sphincter. Physiologic and clinical aspects. *Ann Intern Med* 83(3), 390-401.

Catterall WA, Striessnig J, Snutch TP and Perez-Reyes E (2003). International Union of Pharmacology. XL. Compendium of voltage-gated ion channels: calcium channels. *Pharmacol Rev* 55(4), 579-581.

Cavaliere F, Amadio S, Sancesario G, Bernardi G and Volonte C (2004). Synaptic P2X7 and oxygen/glucose deprivation in organotypic hippocampal cultures. *J Cereb Blood Flow Metab* 24(4), 392-398.

Cavaliere F, D'Ambrosi N, Ciotti MT, Mancino G, Sancesario G, Bernardi G and Volonte C (2001a). Glucose deprivation and chemical hypoxia: neuroprotection by P2 receptor antagonists. *Neurochem Int* 38(3), 189-197.

Cavaliere F, D'Ambrosi N, Sancesario G, Bernardi G and Volonte C (2001b). Hypoglycaemia-

induced cell death: features of neuroprotection by the P2 receptor antagonist basilen blue. *Neurochem Int* 38(3), 199-207.

Cavaliere F, Florenzano F, Amadio S, Fusco FR, Viscomi MT, D'Ambrosi N, Vacca F, Sancesario G, Bernardi G, Molinari M and Volonte C (2003). Up-regulation of P2X2, P2X4 receptor and ischemic cell death: prevention by P2 antagonists. *Neuroscience* 120(1), 85-98.

Charles AC, Merrill JE, Dirksen ER and Sanderson MJ (1991). Intercellular signaling in glial cells: calcium waves and oscillations in response to mechanical stimulation and glutamate. *Neuron* 6(6), 983-992.

Charles AC, Naus CC, Zhu D, Kidder GM, Dirksen ER and Sanderson MJ (1992). Intercellular calcium signaling via gap junctions in glioma cells. *J Cell Biol* 118(1), 195-201.

Charlton SJ, Brown CA, Weisman GA, Turner JT, Erb L and Boarder MR (1996). PPADS and suramin as antagonists at cloned P2Y- and P2U-purinoceptors. *Br J Pharmacol* 118(3), 704-710.

Chaudry IH (1982). Does ATP cross the cell plasma membrane. *Yale J Biol Med* 55(1), 1-10.

Chen BC, Lee CM and Lin WW (1996). Inhibition of ecto-ATPase by PPADS, suramin and reactive blue in endothelial cells, C6 glioma cells and RAW 264.7 macrophages. *Br J Pharmacol* 119(8), 1628-1634.

Chen CC, Akopian AN, Sivilotti L, Colquhoun D, BURNSTOCK G and Wood JN (1995). A P2X purinoceptor expressed by a subset of sensory neurons. *Nature* 377(6548), 428-431.

Chen JF, Huang Z, Ma J, Zhu J, Moratalla R, Standaert D, Moskowitz MA, Fink JS and Schwarzschild MA (1999). A(2A) adenosine receptor deficiency attenuates brain injury induced by transient focal ischemia in mice. *J Neurosci* 19(21), 9192-9200.

Chessell IP, Simon J, Hibell AD, Michel AD, Barnard EA and Humphrey PP (1998). Cloning and functional characterisation of the mouse P2X7 receptor. *FEBS Lett* 439(1-2), 26-30.

Chhatriwala M, Ravi RG, Patel RI, Boyer JL, Jacobson KA and Harden TK (2004). Induction of novel agonist selectivity for the ADP-activated P2Y1 receptor versus the ADP-activated P2Y12 and P2Y13 receptors by conformational constraint of an ADP analog. *J Pharmacol Exp Ther* 311(3), 1038-1043.

Choi DW (1990). Possible mechanisms limiting N-methyl-D-aspartate receptor overactivation and the therapeutic efficacy of N-methyl-D-aspartate antagonists. *Stroke* 21(11 Suppl), III20-III22.

Ciana P, Fumagalli M, Trincavelli ML, Verderio C, Rosa P, Lecca D, Ferrario S, Parravicini C, Capra V, Gelosa P, Guerrini U, Belcredito S, Cimino M, Sironi L, Tremoli E, Rovati GE, Martini C and Abbracchio MP (2006). The orphan receptor GPR17 identified as a new dual uracil nucleotides/cysteinyl-leukotrienes receptor. *EMBO J*

Ciccarelli R, D'Alimonte I, Santavenere C, D'Auro M, Ballerini P, Nargi E, Buccella S, NicosiaFolco S, Caciagli F and Di Iorio P (2004). Cysteinyl-leukotrienes are released from astrocytes and increase astrocyte proliferation and glial fibrillary acidic protein via cys-LT1 receptors and mitogen-activated protein kinase pathway. *Eur J Neurosci* 20(6), 1514-1524.

Ciceri P, Rabuffetti M, Monopoli A and Nicosia S (2001). Production of leukotrienes in a model of focal cerebral ischaemia in the rat. *Br J Pharmacol* 133(8), 1323-1329.

Clapham DE (1995). Calcium signaling. *Cell* 80(2), 259-268.

Cloues R. (1995). Properties of ATP-gated channels recorded from rat sympathetic neurons: voltage dependence and regulation by Zn2+ ions. *J. Neurophysiol.* 73(1), 312- 319.

Collewijn H and Harreveld AV (1966). Membrane potential of cerebral cortical cells during reading depression and asphyxia. *Exp Neurol* 15(4), 425-436.

Collo G, Neidhart S, Kawashima E, Kosco-Vilbois M, North RA and Buell G (1997). Tissue distribution of the P2X7 receptor. *Neuropharmacology* 36(9), 1277-1283.

Collo G, North RA, Kawashima E, Merlo-Pich E, Neidhart S, Surprenant A and Buell G (1996). Cloning OF P2X5 and P2X6 receptors and the distribution and properties of an extended family of ATP-gated ion channels. *J Neurosci* 16(8), 2495-2507.

Communi D, Gonzalez NS, Detheux M, Brezillon S, Lannoy V, Parmentier M and Boeynaems JM (2001). Identification of a novel human ADP receptor coupled to G(i). *J Biol Chem*

276(44), 41479-41485.

Communi D, Robaye B and Boeynaems JM (1999). Pharmacological characterization of the human P2Y11 receptor. *Br J Pharmacol* 128(6), 1199-1206.

Corradetti R, Lo CG, Moroni F, Passani MB and Pepeu G (1984). Adenosine decreases aspartate and glutamate release from rat hippocampal slices. *Eur J Pharmacol* 104(1-2), 19-26.

Corsi C, Melani A, Bianchi L and Pedata F (2000). Striatal A2A adenosine receptor antagonism differentially modifies striatal glutamate outflow in vivo in young and aged rats. *Neuroreport* 11(11), 2591-2595.

Corsi C, Melani A, Bianchi L, Pepeu G and Pedata F (1999). Striatal A2A adenosine receptors differentially regulate spontaneous and K+-evoked glutamate release in vivo in young and aged rats. *Neuroreport* 10(4), 687-691.

Costenla AR, Lopes LV, de Mendonca A and Ribeiro JA (2001). A functional role for adenosine A3 receptors: modulation of synaptic plasticity in the rat hippocampus. *Neurosci Lett* 302(1), 53-57.

Crack BE, Pollard CE, Beukers MW, Roberts SM, Hunt SF, Ingall AH, McKechnie KC, IJzerman AP and Leff P (1995). Pharmacological and biochemical analysis of FPL 67156, a novel, selective inhibitor of ecto-ATPase. *Br J Pharmacol* 114(2), 475-481.

Cunha RA, Johansson B, Fredholm BB, Ribeiro JA and Sebastiao AM (1995). Adenosine A2A receptors stimulate acetylcholine release from nerve terminals of the rat hippocampus. *Neurosci Lett* 196(1-2), 41-44.

Cunha RA, Johansson B, van dP, I, Sebastiao AM, Ribeiro JA and Fredholm BB (1994). Evidence for functionally important adenosine A2a receptors in the rat hippocampus. *Brain Res* 649(1-2), 208-216.

Cunha RA and Ribeiro JA (2000a). ATP as a presynaptic modulator. *Life Sci* 68(2), 119-137.

Cunha RA, Sebastiao AM and Ribeiro JA (1998). Inhibition by ATP of hippocampal synaptic transmission requires localized extracellular catabolism by ecto-nucleotidases into adenosine and channeling to adenosine A(1) receptors. *Journal of Neuroscience* 18(6), 1987-1995.

Cunha RA, Vizi ES, Ribeiro JA and Sebastiao AM (1996). Preferential release of ATP and its extracellular catabolism as a source of adenosine upon high- but not low-frequency stimulation of rat hippocampal slices. *J Neurochem* 67(5), 2180-2187.

Curro D and Preziosi P (1998). Non-adrenergic non-cholinergic relaxation of the rat stomach. *Gen Pharmacol* 31(5), 697-703.

D'Ambrosi N, Cavaliere F, Merlo D, Milazzo L, Mercanti D and Volonte C (2000). Antagonists of P2 receptor prevent NGF-dependent neuritogenesis in PC12 cells. *Neuropharmacology* 39(6), 1083-1094.

D'Ambrosi N, Murra B, Cavaliere F, Amadio S, Bernardi G, BURNSTOCK G and Volonte C (2001). Interaction between ATP and nerve growth factor signalling in the survival and neuritic outgrowth from PC12 cells. *Neuroscience* 108(3), 527-534.

D'Ambrosi N, Murra B, Vacca F and Volonte C (2004). Pathways of survival induced by NGF and extracellular ATP after growth factor deprivation. *Prog Brain Res* 146, 93-100.

Dal Ben D, Lambertucci C, Taffi S, Vttori S, Volpini R, Klotz KN, and Cristalli G (2006). Molecular modeling study of 2-phenylethynyladenosine (PEAdo) derivatives as highly selective A$_3$ adenosine receptor ligands. Purinergic Signalling 2, 589-594.

Daval JL and Nicolas F (1994). Opposite effects of cyclohexyladenosine and theophylline on hypoxic damage in cultured neurons. *Neurosci Lett* 175(1-2), 114-116.

Dave S and Mogul DJ (1996). ATP receptor activation potentiates a voltage-dependent Ca channel in hippocampal neurons. *Brain Res* 715(1-2), 208-216.

Davies JA, Annels SJ, Dickie BG, Ellis Y and Knott NJ (1995). A comparison between the stimulated and paroxysmal release of endogenous amino acids from rat cerebellar, striatal and hippocampal slices: a manifestation of spreading depression? *J Neurol Sci* 131(1), 8-14.

Davis CW, Dowell ML, Lethem M and Van Scott M (1992). Goblet cell degranulation in isolated canine tracheal epithelium: response to exogenous ATP, ADP, and adenosine. *Am J Physiol*

262(5 Pt 1), C1313-C1323.

De Keyser J, Sulter G and Luiten PG (1999). Clinical trials with neuroprotective drugs in acute ischaemic stroke: are we doing the right thing? *Trends Neurosci* 22(12), 535-540.

De M, Austin KF, and Dudley MW (1993). Differential distribution of A3 receptors in rat brain. *Society of Neuroscience*. Ref Type: Abstract.

Deckert J and Jorgensen MB (1988). Evidence for pre- and postsynaptic localization of adenosine A1 receptors in the CA1 region of rat hippocampus: a quantitative autoradiographic study. *Brain Res* 446(1), 161-164.

Deshpande JK, Siesjo BK and Wieloch T (1987). Calcium accumulation and neuronal damage in the rat hippocampus following cerebral ischemia. *J Cereb Blood Flow Metab* 7(1), 89-95.

Deuchars SA, Atkinson L, Brooke RE, Musa H, Milligan CJ, Batten TF, Buckley NJ, Parson SH and Deuchars J (2001). Neuronal P2X7 receptors are targeted to presynaptic terminals in the central and peripheral nervous systems. *J Neurosci* 21(18), 7143-7152.

Deussen A (2000). Metabolic flux rates of adenosine in the heart. *Naunyn Schmiedebergs Arch Pharmacol* 362(4-5), 351-363.

Di Virgilio F, Ferrari D, Falzoni S, Chiozzi P, Munerati M, Steinberg TH and Baricordi OR (1996). P2 purinoceptors in the immune system. *Ciba Found Symp* 198, 290-302.

Ding S and Sachs F (1999). Single channel properties of P2X2 purinoceptors. *J Gen Physiol* 113(5), 695-720.

Dirnagl U, Iadecola C and Moskowitz MA (1999). Pathobiology of ischaemic stroke: an integrated view. *Trends Neurosci* 22(9), 391-397.

Diverse-Pierluissi M, Dunlap K and Westhead EW (1991). Multiple actions of extracellular ATP on calcium currents in cultured bovine chromaffin cells. *Proc Natl Acad Sci U S A* 88(4), 1261-1265.

Dixon AK, Gubitz AK, Sirinathsinghji DJ, Richardson PJ and Freeman TC (1996). Tissue distribution of adenosine receptor mRNAs in the rat. *Br J Pharmacol* 118(6), 1461-1468.

Dixon AK, Widdowson L and Richardson PJ (1997). Desensitisation of the adenosine A1 receptor by the A2A receptor in the rat striatum. *J Neurochem* 69(1), 315-321.

Douglas WW and Poisner AM (1966). Evidence that the secreting adrenal chromaffin cell releases catecholamines directly from ATP-rich granules. *J Physiol* 183(1), 236-248.

Dowdall MJ, Boyne AF and Whittaker VP (1974). Adenosine triphosphate. A constituent of cholinergic synaptic vesicles. *Biochem J* 140(1), 1-12.

Drakulich DA, Spellmon C and Hexum TD (2004). Effect of the ecto-ATPase inhibitor, ARL 67156, on the bovine chromaffin cell response to ATP. *Eur J Pharmacol* 485(1-3), 137-140.

Drazen JM (2003). Leukotrienes in asthma. *Adv Exp Med Biol* 525, 1-5.

Drury AN and Szent-Gyorgyi A (1929). The physiological activity of adenine compounds with especial reference to their action upon the mammalian heart. *J Physiol* 68(3), 213-237.

Duan S, Anderson CM, Keung EC, Chen Y, Chen Y and Swanson RA (2003). P2X7 receptor-mediated release of excitatory amino acids from astrocytes. *J Neurosci* 23(4), 1320-1328.

Dunwiddie TV and Diao L (2000). Regulation of extracellular adenosine in rat hippocampal slices is temperature dependent: role of adenosine transporters. *Neuroscience* 95(1), 81-88.

Dunwiddie TV, Diao L, Kim HO, Jiang JL and Jacobson KA (1997a). Activation of hippocampal adenosine A3 receptors produces a desensitization of A1 receptor-mediated responses in rat hippocampus. *J Neurosci* 17(2), 607-614.

Dunwiddie TV, Diao L and Proctor WR (1997b). Adenine nucleotides undergo rapid, quantitative conversion to adenosine in the extracellular space in rat hippocampus. *J Neurosci* 17(20), 7673-7682.

Duval M, Beaudoin AR, Bkaily G, Gendron FP and Orleans-Juste P (2003). Characterization of the NTPDase activities in the mesentery pre- and post-capillary circuits of the guinea pig. *Can J Physiol Pharmacol* 81(3), 212-219.

Dux E, Fastbom J, Ungerstedt U, Rudolphi K and Fredholm BB (1990). Protective effect of adenosine and a novel xanthine derivative propentofylline on the cell damage after bilateral

carotid occlusion in the gerbil hippocampus. *Brain Res* 516(2), 248-256.

Dux E, Schubert P and Kreutzberg GW (1992). Ultrastructural localization of calcium in ischemic hippocampal slices: the influence of adenosine and theophylline. *J Cereb Blood Flow Metab* 12(3), 520-524.

Edwards FA, Konnerth A, Sakmann B and Takahashi T (1989). A thin slice preparation for patch clamp recordings from neurones of the mammalian central nervous system. *Pflugers Arch.* 414(5), 600-612.

Edwards FA, Gibb AJ and Colquhoun D (1992a). ATP receptor-mediated synaptic currents in the central nervous system. *Nature* 359(6391), 144-147.

Edwards FA and Konnerth A (1992b). Patch-clamping cells in sliced tissue preparations. *Methods Enzymol* 207, 208-222.

Ellenbogen KA, O'Neill G, Prystowsky EN, Camm JA, Meng L, Lieu HD, Jerling M, Shreeniwas R, Belardinelli L and Wolff AA (2005). Trial to evaluate the management of paroxysmal supraventricular tachycardia during an electrophysiology study with tecadenoson. *Circulation* 111(24), 3202-3208.

Eltzschig HK, Abdulla P, Hoffman E, Hamilton KE, Daniels D, Schonfeld C, Loffler M, Reyes G, Duszenko M, Karhausen J, Robinson A, Westerman KA, Coe IR and Colgan SP (2005). HIF-1-dependent repression of equilibrative nucleoside transporter (ENT) in hypoxia. *J Exp Med* 202(11), 1493-1505.

Ennion SJ and Evans RJ (2002). Conserved cysteine residues in the extracellular loop of the human P2X(1) receptor form disulfide bonds and are involved in receptor trafficking to the cell surface. *Mol Pharmacol* 61(2), 303-311.

Erb L, Garrad R, Wang Y, Quinn T, Turner JT and Weisman GA (1995). Site-directed mutagenesis of P2U purinoceptors. Positively charged amino acids in transmembrane helices 6 and 7 affect agonist potency and specificity. *J Biol Chem* 270(9), 4185-4188.

Erb L, Liao Z, Seye CI and Weisman GA (2006). P2 receptors: intracellular signaling. *Pflugers Arch* 452(5), 552-562.

Erdmann AA, Gao ZG, Jung U, Foley J, Borenstein T, Jacobson KA and Fowler DH (2005). Activation of Th1 and Tc1 cell adenosine A2A receptors directly inhibits IL-2 secretion in vitro and IL-2-driven expansion in vivo. *Blood* 105(12), 4707-4714.

Etherington LA and Frenguelli BG (2004). Endogenous adenosine modulates epileptiform activity in rat hippocampus in a receptor subtype-dependent manner. *Eur J Neurosci* 19(9), 2539-2550.

Evans RJ, Derkach V and Surprenant A (1992). ATP mediates fast synaptic transmission in mammalian neurons. *Nature* 357(6378), 503-505.

Evans RJ, Lewis C, Virginio C, Lundstrom K, Buell G, Surprenant A and North RA (1996). Ionic permeability of, and divalent cation effects on, two ATP-gated cation channels (P2X receptors) expressed in mammalian cells. *J Physiol* 497 (Pt 2)(413-422.

Faber ES and Sah P (2003). Calcium-activated potassium channels: multiple contributions to neuronal function. *Neuroscientist* 9(3), 181-194.

Falzoni S, Munerati M, Ferrari D, Spisani S, Moretti S and Di Virgilio F (1995). The purinergic P2Z receptor of human macrophage cells. Characterization and possible physiological role. *J Clin Invest* 95(3), 1207-1216.

Fedorova IM, Jacobson MA, Basile A and Jacobson KA (2003). Behavioral characterization of mice lacking the A3 adenosine receptor: sensitivity to hypoxic neurodegeneration. *Cell Mol Neurobiol* 23(3), 431-447.

Feoktistov I and Biaggioni I (1997). Adenosine A2B receptors. *Pharmacol Rev* 49(4), 381-402.

Ferguson DR (1999). Urothelial function. *BJU Int* 84(3), 235-242.

Ferguson G, Watterson KR and Palmer TM (2000). Subtype-specific kinetics of inhibitory adenosine receptor internalization are determined by sensitivity to phosphorylation by G protein-coupled receptor kinases. *Mol Pharmacol* 57(3), 546-552.

Fernandez-Fernandez JM, Abogadie FC, Milligan G, Delmas P and Brown DA (2001). Multiple pertussis toxin-sensitive G-proteins can couple receptors to GIRK channels in rat sympa-

thetic neurons when expressed heterologously, but only native G(i)-proteins do so in situ. *Eur J Neurosci* 14(2), 283-292.

Ferrari D, Chiozzi P, Falzoni S, Hanau S and Di Virgilio F (1997). Purinergic modulation of interleukin-1 beta release from microglial cells stimulated with bacterial endotoxin. *J Exp Med* 185(3), 579-582.

Ferrè S, von Euler G, Johansson B, Fredholm BB and Fuxe K (1991). Stimulation of high-affinity adenosine A2 receptors decreases the affinity of dopamine D2 receptors in rat striatal membranes. *Proc Natl Acad Sci U S A* 88(16), 7238-7241.

Fieber LA and Adams DJ (1991). Adenosine triphosphate-evoked currents in cultured neurones dissociated from rat parasympathetic cardiac ganglia. *J Physiol* 434, 239-256.

Fiebich BL, Biber K, Lieb K, van Calker D, Berger M, Bauer J and Gebicke-Haerter PJ (1996). Cyclooxygenase-2 expression in rat microglia is induced by adenosine A2a-receptors. *Glia* 18(2), 152-160.

Filippov AK and Brown DA (1996). Activation of nucleotide receptors inhibits high-threshold calcium currents in NG108-15 neuronal hybrid cells. *Eur J Neurosci* 8(6), 1149-1155.

Filippov AK, Fernandez-Fernandez JM, Marsh SJ, Simon J, Barnard EA and Brown DA (2004). Activation and inhibition of neuronal G protein-gated inwardly rectifying K(+) channels by P2Y nucleotide receptors. *Mol Pharmacol* 66(3), 468-477.

Filippov AK, Selyanko AA, Robbins J and Brown DA (1994). Activation of nucleotide receptors inhibits M-type K current [IK(M)] in neuroblastoma x glioma hybrid cells. *Pflugers Arch* 429(2), 223-230.

Filippov AK, Simon J, Barnard EA and Brown DA (2003). Coupling of the nucleotide P2Y4 receptor to neuronal ion channels. *Br J Pharmacol* 138(2), 400-406.

Filippov AK, Webb TE, Barnard EA and Brown DA (1998). P2Y2 nucleotide receptors expressed heterologously in sympathetic neurons inhibit both N-type Ca2+ and M-type K+ currents. *J Neurosci* 18(14), 5170-5179.

Filippov AK, Webb TE, Barnard EA and Brown DA (1999). Dual coupling of heterologously-expressed rat P2Y6 nucleotide receptors to N-type Ca2+ and M-type K+ currents in rat sympathetic neurones. *Br J Pharmacol* 126(4), 1009-1017.

Fleming KM and Mogul DJ (1997). Adenosine A3 receptors potentiate hippocampal calcium current by a PKA-dependent/PKC-independent pathway. *Neuropharmacology* 36(3), 353-362.

Flores RV, Hernandez-Perez MG, Aquino E, Garrad RC, Weisman GA and Gonzalez FA (2005). Agonist-induced phosphorylation and desensitization of the P2Y2 nucleotide receptor. *Mol Cell Biochem* 280(1-2), 35-45.

Florio C, Prezioso A, Papaioannou A and Vertua R (1998b). Adenosine A1 receptors modulate anxiety in CD1 mice. *Psychopharmacology (Berl)* 136(4), 311-319.

Florio C, Prezioso A, Papaioannou A and Vertua R (1998a). Adenosine A1 receptors modulate anxiety in CD1 mice. *Psychopharmacology (Berl)* 136(4), 311-319.

Fowler JC (1990). Adenosine antagonists alter the synaptic response to in vitro ischemia in the rat hippocampus. *Brain Res* 509(2), 331-334.

Franke H and Illes P (2006). Involvement of P2 receptors in the growth and survival of neurons in the CNS. *Pharmacol Ther* 109(3), 297-324.

Franke H, Kittner H, Grosche J and Illes P (2003). Enhanced P2Y1 receptor expression in the brain after sensitisation with d-amphetamine. *Psychopharmacology (Berl)* 167(2), 187-194.

Fraser H, Gao Z, Ozeck MJ and Belardinelli L (2003). N-[3-(R)-tetrahydrofuranyl]-6-aminopurine riboside, an A1 adenosine receptor agonist, antagonizes catecholamine-induced lipolysis without cardiovascular effects in awake rats. *J Pharmacol Exp Ther* 305(1), 225-231.

Fredholm BB (1995). Purinoceptors in the nervous system. *Pharmacol Toxicol* 76(4), 228-239.

Fredholm BB, Arslan G, Halldner L, Kull B, Schulte G and Wasserman W (2000). Structure and function of adenosine receptors and their genes. *Naunyn Schmiedebergs Arch Pharmacol* 362(4-5), 364-374.

Fredholm BB, Chen JF, Masino SA and Vaugeois JM (2005). Actions of adenosine at its receptors

in the CNS: insights from knockouts and drugs. *Annu Rev Pharmacol Toxicol* 45, 385-412.

Fredholm BB and Dunwiddie TV (1988). How does adenosine inhibit transmitter release? *Trends Pharmacol Sci* 9(4), 130-134.

Fredholm BB, IJzerman AP, Jacobson KA, Klotz KN and Linden J (2001). International Union of Pharmacology. XXV. Nomenclature and classification of adenosine receptors. *Pharmacol Rev* 53(4), 527-552.

Fredholm BB and Svenningsson P (2003). Adenosine-dopamine interactions: development of a concept and some comments on therapeutic possibilities. *Neurology* 61(11 Suppl 6), S5-S9.

Fredriksson R, Lagerstrom MC, Lundin LG and Schioth HB (2003). The G-protein-coupled receptors in the human genome form five main families. Phylogenetic analysis, paralogon groups, and fingerprints. *Mol Pharmacol* 63(6), 1256-1272.

Frenguelli BG, Llaudet E and Dale N (2006). Real-time measurements of ATP and adenosine release during oxygen-glucose deprivation in area CA1 of rat hippocampal slices. 24-5-2006. Paper presented at the 8th International Symposium on Adenosine and Adenine Nucleotides, Univesity of Ferrara, Ferrara, Italy, 24-28 May 2006. 24-5-2006. Ref Type: Conference Proceeding

Fugate SE and Cudd LA (2006). Cangrelor for treatment of coronary thrombosis. *Ann Pharmacother* 40(5), 925-930.

Fujii S (2004). ATP- and adenosine-mediated signaling in the central nervous system: the role of extracellular ATP in hippocampal long-term potentiation. *J Pharmacol Sci* 94(2), 103-106.

Fujii S, Ito K, Osada H, Hamaguchi T, Kuroda Y and Kato H (1995a). Extracellular phosphorylation of membrane protein modifies theta burst-induced long-term potentiation in CA1 neurons of guinea-pig hippocampal slices. *Neurosci Lett* 187(2), 133-136.

Fujii S, Kato H, Furuse H, Ito K, Osada H, Hamaguchi T and Kuroda Y (1995b). The mechanism of ATP-induced long-term potentiation involves extracellular phosphorylation of membrane proteins in guinea-pig hippocampal CA1 neurons. *Neurosci Lett* 187(2), 130-132.

Fujii S, Kato H and Kuroda Y (1999). Extracellular adenosine 5'-triphosphate plus activation of glutamatergic receptors induces long-term potentiation in CA1 neurons of guinea pig hippocampal slices. *Neurosci Lett* 276(1), 21-24.

Fujii S, Kato H and Kuroda Y (2002). Cooperativity between extracellular adenosine 5'-triphosphate and activation of N-methyl-D-aspartate receptors in long-term potentiation induction in hippocampal CA1 neurons. *Neuroscience* 113(3), 617-628.

Fulgenzi A, Dell'Antonio G, Foglieni C, Dal Cin E, Ticozzi P, Franzone JS and Ferrero ME (2005). Inhibition of chemokine expression in rat inflamed paws by systemic use of the antihyperalgesic oxidized ATP. *BMC Immunol* 6, 18-25

Fumagalli M, Brambilla R, D'Ambrosi N, Volonte C, Matteoli M, Verderio C and Abbracchio MP (2003). Nucleotide-mediated calcium signaling in rat cortical astrocytes: Role of P2X and P2Y receptors. *Glia* 43(3), 218-03.

Gaarder A, Jonsen J, Laland S, Hellem A and Owren Pa (1961). Adenosine diphosphate in red cells as a factor in the adhesiveness of human blood platelets. *Nature* 192, 531-532.

Gachet C (2005). The platelet P2 receptors as molecular targets for old and new antiplatelet drugs. *Pharmacol Ther* 108(2), 180-192.

Galietta LJ, Falzoni S, Di Virgilio F, Romeo G and Zegarra-Moran O (1997). Characterization of volume-sensitive taurine- and Cl(-)-permeable channels. *Am J Physiol* 273(1 Pt 1), C57-C66.

Galvez A, Gimenez-Gallego G, Reuben JP, Roy-Contancin L, Feigenbaum P, Kaczorowski GJ and Garcia ML (1990). Purification and characterization of a unique, potent, peptidyl probe for the high conductance calcium-activated potassium channel from venom of the scorpion Buthus tamulus. *J Biol Chem* 265(19), 11083-11090.

Gamper N, Reznikov V., Yamada Y. Yang J. and Shapiro MS. (2004). Phosphatidylinositol [correction] 4,5-bisphosphate signals underlie receptor-specific Gq/11-mediated modulation of N-type Ca2+ channels. *J Neurosci* 24(48), 10980-10992.

Gandia L, Garcia AG and Morad M (1993). ATP modulation of calcium channels in chromaffin cells. *J Physiol* 470, 55-72.

Gao Y and Phillis JW (1994). CGS 15943, an adenosine A2 receptor antagonist, reduces cerebral ischemic injury in the Mongolian gerbil. *Life Sci* 55(3), L61-L65.

Gao ZG, Mamedova L, Tchilibon S, Gross AS and Jacobson KA (2004). 2,2'-Pyridylisatogen tosylate antagonizes P2Y1 receptor signaling without affecting nucleotide binding. *Biochem Pharmacol* 68(2), 231-237.

Gardos G (1958). The function of calcium in the potassium permeability of human erythrocytes. *Biochim Biophys Acta* 30(3), 653-654.

Gendron FP, Chalimoniuk M, Strosznajder J, Shen S, Gonzalez FA, Weisman GA and Sun GY (2003). P2X7 nucleotide receptor activation enhances IFN gamma-induced type II nitric oxide synthase activity in BV-2 microglial cells. *J Neurochem* 87(2), 344-352.

Gerasimovskaya EV, Ahmad S, White CW, Jones PL, Carpenter TC and Stenmark KR (2002). Extracellular ATP is an autocrine/paracrine regulator of hypoxia-induced adventitial fibroblast growth. Signaling through extracellular signal-regulated kinase-1/2 and the Egr-1 transcription factor. *J Biol Chem* 277(47), 44638-44650.

Gerfen CR and Young WS, III (1988). Distribution of striatonigral and striatopallidal peptidergic neurons in both patch and matrix compartments: an in situ hybridization histochemistry and fluorescent retrograde tracing study. *Brain Res* 460(1), 161-167.

Glynn IM (1968). Membrane adenosine triphosphatase and cation transport. *Br Med Bull* 24(2), 165-169.

Goldberg JA and Wilson CJ (2005). Control of spontaneous firing patterns by the selective coupling of calcium currents to calcium-activated potassium currents in striatal cholinergic interneurons. *J Neurosci* 25(44), 10230-10238.

Gomes P, Srinivas SP, Van Driessche W, Vereecke J and Himpens B (2005a). ATP release through connexin hemichannels in corneal endothelial cells. *Invest Ophthalmol Vis Sci* 46(4), 1208-1218.

Gomes P, Srinivas SP, Vereecke J and Himpens B (2005b). ATP-dependent paracrine intercellular communication in cultured bovine corneal endothelial cells. *Invest Ophthalmol Vis Sci* 46(1), 104-113.

Gordon JL (1986). Extracellular ATP: effects, sources and fate. *Biochem J* 233(2), 309-319.

Gotz T, Kraushaar U, Geiger J, Lubke J, Berger T and Jonas P (1997). Functional properties of AMPA and NMDA receptors expressed in identified types of basal ganglia neurons. *J Neurosci* 17(1), 204-215.

Gourine AV, Dale N, Gourine VN and Spyer KM (2004). Fever in systemic inflammation: roles of purines. *Front Biosci* 9, 1011-1022.

Grafstein B (1956). Mechanism of spreading cortical depression. *J Neurophysiol* 19(2), 154-171.

Greco NJ, Tonon G, Chen W, Luo X, Dalal R and Jamieson GA (2001). Novel structurally altered P(2X1) receptor is preferentially activated by adenosine diphosphate in platelets and megakaryocytic cells. *Blood* 98(1), 100-107.

Green HN and Stoner HB (1950). Biological Actions of theAdenine Nucleotides. H.K. Lewis and Co., London.. Ref Type: Book.

Gribkoff VK, Bauman LA and VanderMaelen CP (1990). The adenosine antagonist 8-cyclopentyltheophylline reduces the depression of hippocampal neuronal responses during hypoxia. *Brain Res* 512(2), 353-357.

Griffith and Jarvis. Nucleoside and nucleobase transport systems in mammalian cells. 1286. 1996. *Biochem Biophys Acta*.

Grygorczyk R, Tabcharani JA and Hanrahan JW (1996). CFTR channels expressed in CHO cells do not have detectable ATP conductance. *J Membr Biol* 151(2), 139-148.

Hafting T and Sand O (2000). Purinergic activation of BK channels in clonal kidney cells (Vero cells). *Acta Physiol Scand* 170(2), 99-109.

Hagberg H, Andersson P, Lacarewicz J, Jacobson I, Butcher S and Sandberg M (1987). Extracellular adenosine, inosine, hypoxanthine, and xanthine in relation to tissue nucleotides and purines in rat striatum during transient ischemia. *J Neurochem* 49(1), 227-231.

Hamill OP, Marty A, Neher E, Sakmann B and Sigworth FJ (1981). Improved patch-clamp techniques for high-resolution current recording from cells and cell-free membrane patches. *Pflugers Arch* 391(2), 85-100.

Hansen AJ and Nedergaard M (1988). Brain ion homeostasis in cerebral ischemia. *Neurochem Pathol* 9, 195-209.

Hansen MA, Bennett MR and Barden JA (1999a). Distribution of purinergic P2X receptors in the rat heart. *J Auton Nerv Syst* 78(1), 1-9.

Hansen MA, Dutton JL, Balcar VJ, Barden JA and Bennett MR (1999b). P2X (purinergic) receptor distributions in rat blood vessels. *J Auton Nerv Syst* 75(2-3), 147-155.

Hardy AR, Conley PB, Luo J, Benovic JL, Poole AW and Mundell SJ (2005). P2Y1 and P2Y12 receptors for ADP desensitize by distinct kinase-dependent mechanisms. *Blood* 105(9), 3552-3560.

Hauser RA, Hubble JP and Truong DD (2003). Randomized trial of the adenosine A(2A) receptor antagonist istradefylline in advanced PD. *Neurology* 61(3), 297-303.

He ML, Zemkova H, Koshimizu TA, Tomic M and Stojilkovic SS (2003). Intracellular calcium measurements as a method in studies on activity of purinergic P2X receptor channels. *Am J Physiol Cell Physiol* 285(2), C467-C479.

Hechler B, Toselli P, Ravanat C, Gachet C and Ravid K (2001). Mpl ligand increases P2Y1 receptor gene expression in megakaryocytes with no concomitant change in platelet response to ADP. *Mol Pharmacol* 60(5), 1112-1120.

Hede SE, Amstrup J, Klaerke DA and Novak I (2005). P2Y2 and P2Y4 receptors regulate pancreatic Ca(2+)-activated K+ channels differently. *Pflugers Arch.*, 450(6), 429-436.

Heine C, Heimrich B, Vogt J, Wegner A, Illes P and Franke H (2006). P2 receptor-stimulation influences axonal outgrowth in the developing hippocampus in vitro. *Neuroscience* 138(1), 303-311.

Henriksen Z, Hiken JF, Steinberg TH and Jorgensen NR (2006). The predominant mechanism of intercellular calcium wave propagation changes during long-term culture of human osteoblast-like cells. *Cell Calcium* 39(5), 435-444.

Hentschel S, Lewerenz A and Nieber K (2003). Activation of A(3) receptors by endogenous adenosine inhibits synaptic transmission during hypoxia in rat cortical neurons. *Restor Neurol Neurosci* 21(1-2), 55-63.

Herold CL, Qi AD, Harden TK and Nicholas RA (2004). Agonist versus antagonist action of ATP at the P2Y4 receptor is determined by the second extracellular loop. *J Biol Chem* 279(12), 11456-11464.

Herreras O and Jing J (1993a). Blockade of antidromic invasion of CA1 pyramidal cells during synaptic activation of NMDA receptors. *Brain Res* 616(1-2), 330-334.

Herreras O and Somjen GG (1993b). Effects of prolonged elevation of potassium on hippocampus of anesthetized rats. *Brain Res* 617(2), 194-204.

Herreras O and Somjen GG (1993c). Propagation of spreading depression among dendrites and somata of the same cell population. *Brain Res* 610(2), 276-282.

Hettinger BD, Lee A, Linden J and Rosin DL (2001). Ultrastructural localization of adenosine A2A receptors suggests multiple cellular sites for modulation of GABAergic neurons in rat striatum. *J Comp Neurol* 431(3), 331-346.

Heubach JF, Graf EM, Leutheuser J, Bock M, Balana B, Zahanich I, Christ T, Boxberger S, Wettwer E and Ravens U (2004). Electrophysiological properties of human mesenchymal stem cells. *J Physiol* 554(Pt 3), 659-672.

Hillion J, Canals M, Torvinen M, Casado V, Scott R, Terasmaa A, Hansson A, Watson S, Olah ME, Mallol J, Canela EI, Zoli M, Agnati LF, Ibanez CF, Lluis C, Franco R, Ferre S and Fuxe K (2002). Coaggregation, cointernalization, and codesensitization of adenosine A2A recep-

tors and dopamine D2 receptors. *J Biol Chem* 277(20), 18091-18097.

Hoehn K, Watson TW and MacVicar BA (1993). Multiple types of calcium channels in acutely isolated rat neostriatal neurons. *J Neurosci* 13(3), 1244-1257.

Hofer A and Dermietzel R (1998). Visualization and functional blocking of gap junction hemichannels (connexons) with antibodies against external loop domains in astrocytes. *Glia* 24(1), 141-154.

Hoffman CJ, Clark FJ and Ochs S (1973). Intracortical impedance changes during spreading depression. *J Neurobiol* 4(5), 471-486.

Hogg RC, Chipperfield H, Whyte KA, Stafford MR, Hansen MA, Cool SM, Nurcombe V and Adams DJ (2004). Functional maturation of isolated neural progenitor cells from the adult rat hippocampus. *Eur J Neurosci* 19(9), 2410-2420.

Holgate ST (2005). The Quintiles Prize Lecture 2004. The identification of the adenosine A2B receptor as a novel therapeutic target in asthma. *Br J Pharmacol* 145(8), 1009-1015.

Hollopeter G, Jantzen HM, Vincent D, Li G, England L, Ramakrishnan V, Yang RB, Nurden P, Nurden A, Julius D and Conley PB (2001). Identification of the platelet ADP receptor targeted by antithrombotic drugs. *Nature* 409(6817), 202-207.

Horrigan FT and Aldrich RW (2002). Coupling between voltage sensor activation, Ca2+ binding and channel opening in large conductance (BK) potassium channels. *J Gen Physiol* 120(3), 267-305.

Houston D, Ohno M, Nicholas RA, Jacobson KA and Harden TK (2006). [32P]2-iodo-N6-methyl-(N)-methanocarba-2'-deoxyadenosine-3',5'-bisphosphat e ([32P]MRS2500), a novel radioligand for quantification of native P2Y1 receptors. *Br J Pharmacol* 147(5), 459-467.

Hu GY, Hvalby O, Walaas SI, Albert KA, Skjeflo P, Andersen P and Greengard P (1987). Protein kinase C injection into hippocampal pyramidal cells elicits features of long term potentiation. *Nature* 328(6129), 426-429.

Hu HZ, Gao N, Zhu MX, Liu S, Ren J, Gao C, Xia Y and Wood JD (2003). Slow excitatory synaptic transmission mediated by P2Y1 receptors in the guinea-pig enteric nervous system. *J Physiol* 550(Pt 2), 493-504.

Huang CM and Kao LS (1996). Nerve growth factor, epidermal growth factor, and insulin differentially potentiate ATP-induced [Ca2+]i rise and dopamine secretion in PC12 cells. *J Neurochem* 66(1), 124-130.

Hugel S and Schlichter R (2000). Presynaptic P2X receptors facilitate inhibitory GABAergic transmission between cultured rat spinal cord dorsal horn neurons. *J Neurosci* 20(6), 2121-2130.

Hussl S and Boehm S (2006). Functions of neuronal P2Y receptors. *Pflugers Arch* 452(5), 538-551.

Hutchison AJ, Webb RL, Oei HH, Ghai GR, Zimmerman MB and Williams M (1989). CGS 21680C, an A2 selective adenosine receptor agonist with preferential hypotensive activity. *J Pharmacol Exp Ther* 251(1), 47-55.

Ikeda M (2006). Characterization of functional P2X(1) receptors in mouse megakaryocytes. *Thromb Res*

Ikeuchi Y and Nishizaki T (1995). ATP-evoked potassium currents in rat striatal neurons are mediated by a P2 purinergic receptor. *Neurosci Lett* 190(2), 89-92.

Ikeuchi Y and Nishizaki T (1996a). P2 purinoceptor-operated potassium channel in rat cerebellar neurons. *Biochem Biophys Res Commun* 218(1), 67-71.

Ikeuchi Y, Nishizaki T, Mori M and Okada Y (1996b). Regulation of the potassium current and cytosolic Ca2+ release induced by 2-methylthio ATP in hippocampal neurons. *Biochem Biophys Res Commun* 218(2), 428-433.

Iqbal J, Vollmayer P, Braun N, Zimmermann H and Muller CE (2005). A capillary electrophoresis method for the characterization of ecto-nucleoside triphosphate diphosphohydrolases (NTPDases) and the analysis of inhibitors by in-capillary enzymatic microreaction. *Purinergic Signalling* 1, 349-358.

Ishii TM, Silvia C, Hirschberg B, Bond CT, Adelman JP and Maylie J (1997). A human interme-

diate conductance calcium-activated potassium channel. *Proc Natl Acad Sci U S A* 94(21), 11651-11656.

Izzo PN, Graybiel AM and Bolam JP (1987). Characterization of substance P- and [Met]enkephalin-immunoreactive neurons in the caudate nucleus of cat and ferret by a single section Golgi procedure. *Neuroscience* 20(2), 577-587.

Jacobson KA, Jarvis MF and Williams M (2002). Purine and pyrimidine (P2) receptors as drug targets. *J Med Chem* 45(19), 4057-4093.

Jacobson KA, Park KS, Jiang JL, Kim YC, Olah ME, Stiles GL and Ji XD (1997). Pharmacological characterization of novel A3 adenosine receptor-selective antagonists. *Neuropharmacology* 36(9), 1157-1165.

Jain M, Armstrong RJ, Barker RA and Rosser AE (2001). Cellular and molecular aspects of striatal development. *Brain Res Bull* 55(4), 533-540.

James S and Richardson PJ (1993). Production of adenosine from extracellular ATP at the striatal cholinergic synapse. *J Neurochem* 60(1), 219-227.

Jarvis MF, Bianchi B, Uchic JT, Cartmell J, Lee CH, Williams M and Faltynek C (2004). [3H]A-317491, a novel high-affinity non-nucleotide antagonist that specifically labels human P2X2/3 and P2X3 receptors. *J Pharmacol Exp Ther* 310(1), 407-416.

Jarvis MF and Williams M (1989). Direct autoradiographic localization of adenosine A2 receptors in the rat brain using the A2-selective agonist, [3H]CGS 21680. *Eur J Pharmacol* 168(2), 243-246.

Jenkinson KM and Reid JJ (2000). The P(2)-purinoceptor antagonist suramin is a competitive antagonist at vasoactive intestinal peptide receptors in the rat gastric fundus. *Br J Pharmacol* 130(7), 1632-1638.

Jeong LS, Jin DZ, Kim HO, Shin DH, Moon HR, Gunaga P, Chun MW, Kim YC, Melman N, Gao ZG and Jacobson KA (2003). N6-substituted D-4'-thioadenosine-5'-methyluronamides: potent and selective agonists at the human A3 adenosine receptor. *J Med Chem* 46(18), 3775-3777.

Ji X, Kim YC, Ahern DG, Linden J and Jacobson KA (2001). [3H]MRS 1754, a selective antagonist radioligand for A(2B) adenosine receptors. *Biochem Pharmacol* 61(6), 657-663.

Ji XD, Gallo-Rodriguez C and Jacobson KA (1994). A selective agonist affinity label for A3 adenosine receptors. *Biochem Biophys Res Commun* 203(1), 570-576.

Jiang LH, Mackenzie AB, North RA and Surprenant A (2000a). Brilliant blue G selectively blocks ATP-gated rat P2X(7) receptors. *Mol Pharmacol* 58(1), 82-88.

Jiang LH, Rassendren F, Surprenant A and North RA (2000b). Identification of amino acid residues contributing to the ATP-binding site of a purinergic P2X receptor. *J Biol Chem* 275(44), 34190-34196.

Jiang Q, Guo D, Lee BX, Van Rhee AM, Kim YC, Nicholas RA, Schachter JB, Harden TK and Jacobson KA (1997). A mutational analysis of residues essential for ligand recognition at the human P2Y1 receptor. *Mol Pharmacol* 52(3), 499-507.

Jiang Y, Jahagirdar BN, Reinhardt RL, Schwartz RE, Keene CD, Ortiz-Gonzalez XR, Reyes M, Lenvik T, Lund T, Blackstad M, Du J, Aldrich S, Lisberg A, Low WC, Largaespada DA and Verfaillie CM (2002). Pluripotency of mesenchymal stem cells derived from adult marrow. *Nature* 418(6893), 41-49.

Jin J, Dasari VR, Sistare FD and Kunapuli SP (1998). Distribution of P2Y receptor subtypes on haematopoietic cells. *Br J Pharmacol* 123(5), 789-794.

Johansson B, Halldner L, Dunwiddie TV, Masino SA, Poelchen W, Gimenez-Llort L, Escorihuela RM, Fernandez-Teruel A, Wiesenfeld-Hallin Z, Xu XJ, Hardemark A, Betsholtz C, Herlenius E and Fredholm BB (2001). Hyperalgesia, anxiety, and decreased hypoxic neuroprotection in mice lacking the adenosine A1 receptor. *Proc Natl Acad Sci U S A* 98(16), 9407-9412.

Johnson RG, Jr. (1987). Proton pumps and chemiosmotic coupling as a generalized mechanism for neurotransmitter and hormone transport. *Ann N Y Acad Sci* 493, 162-177.

Juranyi Z, Sperlagh B and Vizi ES (1999). Involvement of P2 purinoceptors and the nitric oxide

pathway in [3H]purine outflow evoked by short-term hypoxia and hypoglycemia in rat hippocampal slices. *Brain Res* 823(1-2), 183-190.

Kaku T, Hada J and Hayashi Y (1994). Endogenous adenosine exerts inhibitory effects upon the development of spreading depression and glutamate release induced by microdialysis with high K+ in rat hippocampus. *Brain Res* 658(1-2), 39-48.

Kalckar HM. Biological phosphorylations: development of concepts. 1969. Englewood Cliffs, NJ: Prentice Hall. Ref Type: Conference Proceeding

Kasakov L, Ellis J, Kirkpatrick K, Milner P and Burnstock G (1988). Direct evidence for concomitant release of noradrenaline, adenosine 5'-triphosphate and neuropeptide Y from sympathetic nerve supplying the guinea-pig vas deferens. *J Auton Nerv Syst* 22(1), 75-82.

Kawaguchi Y (1992). Large aspiny cells in the matrix of the rat neostriatum in vitro: physiological identification, relation to the compartments and excitatory postsynaptic currents. *J Neurophysiol* 67(6), 1669-1682.

Kawaguchi Y (1993). Physiological, morphological, and histochemical characterization of three classes of interneurons in rat neostriatum. *J Neurosci* 13(11), 4908-4923.

Kawaguchi Y, Wilson CJ and Emson PC (1989). Intracellular recording of identified neostriatal patch and matrix spiny cells in a slice preparation preserving cortical inputs. *J Neurophysiol* 62(5), 1052-1068.

Kawamura M, Gachet C, Inoue K and Kato F (2004). Direct excitation of inhibitory interneurons by extracellular ATP mediated by P2Y1 receptors in the hippocampal slice. *J Neurosci* 24(48), 10835-10845.

Kawano S, Otsu K, Kuruma A, Shoji S, Yanagida E, Muto Y, Yoshikawa F, Hirayama Y, Mikoshiba K and Furuichi T (2006). ATP autocrine/paracrine signaling induces calcium oscillations and NFAT activation in human mesenchymal stem cells. *Cell Calcium* 39(4), 313-324.

Kawasaki K, Czeh G and Somjen GG (1988). Prolonged exposure to high potassium concentration results in irreversible loss of synaptic transmission in hippocampal tissue slices. *Brain Res* 457(2), 322-329.

Kennedy C, Qi AD, Herold CL, Harden TK and Nicholas RA (2000). ATP, an agonist at the rat P2Y(4) receptor, is an antagonist at the human P2Y(4) receptor. *Mol Pharmacol* 57(5), 926-931.

Khakh BS. (2001). Molecular physiology of P2X receptors and ATP signalling at synapses. *Nat. Rev.Neurosci.* 2(3), 165-174.

Khakh BS, Burnstock G, Kennedy C, King BF, North RA, Seguela P, Voigt M and Humphrey PP (2001). International union of pharmacology. XXIV. Current status of the nomenclature and properties of P2X receptors and their subunits. *Pharmacol Rev* 53(1), 107-118.

Khakh BS and Henderson G (1998). ATP receptor-mediated enhancement of fast excitatory neurotransmitter release in the brain. *Mol Pharmacol* 54(2), 372-378.

Khakh BS, Humphrey PP and Henderson G (1997). ATP-gated cation channels (P2X purinoceptors) in trigeminal mesencephalic nucleus neurons of the rat. *J Physiol* 498 (Pt 3)(709-715.

Kharlamov A, Jones SC and Kim DK (2002). Suramin reduces infarct volume in a model of focal brain ischemia in rats. *Exp Brain Res* 147(3), 353-359.

Kidd EJ, Grahames CB, Simon J, Michel AD, Barnard EA and Humphrey PP (1995). Localization of P2X purinoceptor transcripts in the rat nervous system. *Mol Pharmacol* 48(4), 569-573.

Kim M, Spelta V, Sim J, North RA and Surprenant A (2001). Differential assembly of rat purinergic P2X7 receptor in immune cells of the brain and periphery. *J Biol Chem* 276(26), 23262-23267.

Kim YC, Ji X, Melman N, Linden J and Jacobson KA (2000). Anilide derivatives of an 8-phenylxanthine carboxylic congener are highly potent and selective antagonists at human A(2B) adenosine receptors. *J Med Chem* 43(6), 1165-1172.

Kim YC, Ji XD and Jacobson KA (1996). Derivatives of the triazoloquinazoline adenosine antagonist (CGS15943) are selective for the human A3 receptor subtype. *J Med Chem* 39(21),

4142-4148.

King BF (1998). Cardiovascular biology of purines. Molecular biology of P2X purinoceptors.
Ref Type: Book Chapter

King BF, Townsend-Nicholson A, Wildman SS, Thomas T, Spyer KM and BURNSTOCK G (2000). Coexpression of rat P2X2 and P2X6 subunits in Xenopus oocytes. *J Neurosci* 20(13), 4871-4877.

Kishore BK, Ginns SM, Krane CM, Nielsen S and Knepper MA (2000). Cellular localization of P2Y(2) purinoceptor in rat renal inner medulla and lung. *Am J Physiol Renal Physiol* 278(1), F43-F51.

Kitagawa H, Mori A, Shimada J, Mitsumoto Y and Kikuchi T (2002). Intracerebral adenosine infusion improves neurological outcome after transient focal ischemia in rats. *Neurol Res* 24(3), 317-323.

Klapperstuck M, Buttner C, Nickel P, Schmalzing G, Lambrecht G and Markwardt F (2000). Antagonism by the suramin analogue NF279 on human P2X(1) and P2X(7) receptors. *Eur J Pharmacol* 387(3), 245-252.

Knaus HG, Schwarzer C, Koch RO, Eberhart A, Kaczorowski GJ, Glossmann H, Wunder F, Pongs O, Garcia ML and Sperk G (1996). Distribution of high-conductance Ca(2+)-activated K+ channels in rat brain: targeting to axons and nerve terminals. *J Neurosci* 16(3), 955-963.

Koh SD, Dick GM and Sanders KM (1997). Small-conductance Ca(2+)-dependent K+ channels activated by ATP in murine colonic smooth muscle. *Am J Physiol* 273(6 Pt 1), C2010-C2021.

Kohler M, Hirschberg B, Bond CT, Kinzie JM, Marrion NV, Maylie J and Adelman JP (1996). Small-conductance, calcium-activated potassium channels from mammalian brain. *Science* 273(5282), 1709-1714.

Koizumi S, Saito Y, Nakazawa K, Nakajima K, Sawada JI, Kohsaka S, Illes P and Inoue K (2002). Spatial and temporal aspects of Ca2+ signaling mediated by P2Y receptors in cultured rat hippocampal astrocytes*. Life Sci.*; 72(4-5), 431-442.

Kong W, Engel K and Wang J (2004). Mammalian nucleoside transporters. *Curr Drug Metab* 5(1), 63-84.

Koroleva VI and Bures J (1996). The use of spreading depression waves for acute and long-term monitoring of the penumbra zone of focal ischemic damage in rats. *Proc Natl Acad Sci U S A* 93(8), 3710-3714.

Koshimizu TA, Van Goor F, Tomic M, Wong AO, Tanoue A, Tsujimoto G and Stojilkovic SS (2000). Characterization of calcium signaling by purinergic receptor-channels expressed in excitable cells. *Mol Pharmacol* 58(5), 936-945.

Kow LM and Van Harreveld A (1972). Ion and water movements in isolated chicken retinas during spreading depression. *Neurobiology* 2(2), 61-69.

Krishtal OA, Marchenko SM and Obukhov AG (1988). Cationic channels activated by extracellular ATP in rat sensory neurons. *Neuroscience* 27(3), 995-1000.

Kukulski F and Komoszynski M (2003). Purification and characterization of NTPDase1 (ecto-apyrase) and NTPDase2 (ecto-ATPase) from porcine brain cortex synaptosomes. *Eur J Biochem* 270(16), 3447-3454.

Kull B, Arslan G, Nilsson C, Owman C, Lorenzen A, Schwabe U and Fredholm BB (1999). Differences in the order of potency for agonists but not antagonists at human and rat adenosine A2A receptors. *Biochem Pharmacol* 57(1), 65-75.

Labasi JM, Petrushova N, Donovan C, McCurdy S, Lira P, Payette MM, Brissette W, Wicks JR, Audoly L and Gabel CA (2002). Absence of the P2X7 receptor alters leukocyte function and attenuates an inflammatory response. *J Immunol* 168(12), 6436-6445.

Lambrecht G, Braun K, Damer M, Ganso M, Hildebrandt C, Ullmann H, Kassack MU and Nikkel P (2002). Structure-activity relationships of suramin and pyridoxal-5'-phosphate derivatives as P2 receptor antagonists. *Curr Pharm Des* 8(26), 2371-2399.

Lammer A, Gunther A, Beck A, Krugel U, Kittner H, Schneider D, Illes P and Franke H (2006).

Neuroprotective effects of the P2 receptor antagonist PPADS on focal cerebral ischaemia-induced injury in rats. *Eur J Neurosci* 23(10), 2824-2828.

Lappas CM, Rieger JM and Linden J (2005). A2A adenosine receptor induction inhibits IFN-gamma production in murine CD4+ T cells. *J Immunol* 174(2), 1073-1080.

Latini S, Bordoni F, Corradetti R, Pepeu G and Pedata F (1998). Temporal correlation between adenosine outflow and synaptic potential inhibition in rat hippocampal slices during ischemia-like conditions. *Brain Res* 794(2), 325-328.

Latini S, Bordoni F, Corradetti R, Pepeu G and Pedata F (1999a). Effect of A2A adenosine receptor stimulation and antagonism on synaptic depression induced by in vitro ischaemia in rat hippocampal slices. *Br J Pharmacol* 128(5), 1035-1044.

Latini S, Bordoni F, Pedata F and Corradetti R (1999b). Extracellular adenosine concentrations during in vitro ischaemia in rat hippocampal slices. *Br J Pharmacol* 127(3), 729-739.

Latini S, Corsi C, Pedata F and Pepeu G (1995). The source of brain adenosine outflow during ischemia and electrical stimulation. *Neurochem Int* 27(3), 239-244.

Latini S, Pazzagli M, Pepeu G and Pedata F (1996). A2 adenosine receptors: their presence and neuromodulatory role in the central nervous system. *Gen Pharmacol* 27(6), 925-933.

Latini S and Pedata F (2001). Adenosine in the central nervous system: release mechanisms and extracellular concentrations. *J Neurochem* 79(3), 463-484.

Laudadio MA and Psarropoulou C (2004). The A3 adenosine receptor agonist 2-Cl-IB-MECA facilitates epileptiform discharges in the CA3 area of immature rat hippocampal slices. *Epilepsy Res* 59(2-3), 83-94.

Lazarowski ER, Boucher RC and Harden TK (2000). Constitutive release of ATP and evidence for major contribution of ecto-nucleotide pyrophosphatase and nucleoside diphosphokinase to extracellular nucleotide concentrations. *J Biol Chem* 275(40), 31061-31068.

Leão AAP (1944). Spreading depression of activity in the cerebral cortex. *J Neurophysiol* 7, 359-390.

Leão AAP (1947). Further observations on the spreading depression of activity in the cerebral cortex. *J Neurophysiol* 10, 409-414.

Leão AAP and Martin-Ferreira H. (1953). Alteraçao de impedancia electrica no decurso de depressão alastrante da atividade do córtex cerebral. *Ann Acad Brasil Cienc* 25, 259-266.

Lechner SG, Dorostkar MM, Mayer M, Edelbauer H, Pankevych H and Boehm S (2004). Autoinhibition of transmitter release from PC12 cells and sympathetic neurons through a P2Y receptor-mediated inhibition of voltage-gated Ca2+ channels. *Eur J Neurosci* 20(11), 2917-2928.

Lechner SG, Hussl S, Schicker KW, Drobny H and Boehm S. (2005). Presynaptic inhibition via a phospholipase C- and phosphatidylinositol bisphosphate-dependent regulation of neuronal Ca2+ channels. *Mol Pharmacol* 68(5), 1387-1396.

Lee HY, Bardini M and BURNSTOCK G (2000). P2X receptor immunoreactivity in the male genital organs of the rat. *Cell Tissue Res* 300(2), 321-330.

Lee JM, Zipfel GJ and Choi DW (1999). The changing landscape of ischaemic brain injury mechanisms. *Nature* 399(6738 Suppl), A7-14.

Lee YC, Chien CL, Sun CN, Huang CL, Huang NK, Chiang MC, Lai HL, Lin YS, Chou SY, Wang CK, Tai MH, Liao WL, Lin TN, Liu FC and Chern Y (2003). Characterization of the rat A2A adenosine receptor gene: a 4.8-kb promoter-proximal DNA fragment confers selective expression in the central nervous system. *Eur J Neurosci* 18(7), 1786-1796.

Lemoli RM, Ferrari D, Fogli M, Rossi L, Pizzirani C, Forchap S, Chiozzi P, Vaselli D, Bertolini F, Foutz T, Aluigi M, Baccarani M and Di Virgilio F (2004). Extracellular nucleotides are potent stimulators of human hematopoietic stem cells in vitro and in vivo. *Blood* 104(6), 1662-1670.

Leon C, Hechler B, Vial C, Leray C, Cazenave JP and Gachet C (1997). The P2Y1 receptor is an ADP receptor antagonized by ATP and expressed in platelets and megakaryoblastic cells. *FEBS Lett* 403(1), 26-30.

Lewis C, Neidhart S, Holy C, North RA, Buell G and Surprenant A (1995). Coexpression of P2X2

and P2X3 receptor subunits can account for ATP-gated currents in sensory neurons. *Nature* 377(6548), 432-435.

Li AH, Moro S, Melman N, Ji XD and Jacobson KA (1998). Structure-activity relationships and molecular modeling of 3, 5-diacyl-2,4-dialkylpyridine derivatives as selective A3 adenosine receptor antagonists. *J Med Chem* 41(17), 3186-3201.

Li C, Ramjeesingh M and Bear CE (1996). Purified cystic fibrosis transmembrane conductance regulator (CFTR) does not function as an ATP channel. *J Biol Chem* 271(20), 11623-11626.

Li CM, Campbell SJ, Kumararatne DS, Hill AV and Lammas DA (2002). Response heterogeneity of human macrophages to ATP is associated with P2X7 receptor expression but not to polymorphisms in the P2RX7 promoter. *FEBS Lett* 531(2), 127-131.

Li GR, Sun H, Deng X and Lau CP (2005). Characterization of ionic currents in human mesenchymal stem cells from bone marrow. *Stem Cells* 23(3), 371-382.

Liang BT (1998). Protein kinase C-dependent activation of KATP channel enhances adenosine-induced cardioprotection. *Biochem J* 336 (Pt 2)(337-343.

Lim W, Kim SJ, Yan HD and Kim J (1997). Ca2+-channel-dependent and -independent inhibition of exocytosis by extracellular ATP in voltage-clamped rat adrenal chromaffin cells. *Pflugers Arch* 435(1), 34-42.

Lin Y and Phillis JW (1992). Deoxycoformycin and oxypurinol: protection against focal ischemic brain injury in the rat. *Brain Res* 571(2), 272-280.

Linden J (2001). Molecular approach to adenosine receptors: receptor-mediated mechanisms of tissue protection. *Annu Rev Pharmacol Toxicol* 41, 775-787.

Linden J, Taylor HE, Robeva AS, Tucker AL, Stehle JH, Rivkees SA, Fink JS and Reppert SM (1993). Molecular cloning and functional expression of a sheep A3 adenosine receptor with widespread tissue distribution. *Mol Pharmacol* 44(3), 524-532.

Lipton P (1999). Ischemic cell death in brain neurons. *Physiol Rev* 79(4), 1431-1568.

Liu DM and Adams DJ (2001). Ionic selectivity of native ATP-activated (P2X) receptor channels in dissociated neurones from rat parasympathetic ganglia. *J Physiol* 534(Pt. 2), 423-435.

Liu SF, McCormack DG, Evans TW and Barnes PJ (1989a). Characterization and distribution of P2-purinoceptor subtypes in rat pulmonary vessels. *J Pharmacol Exp Ther* 251(3), 1204-1210.

Liu SF, McCormack DG, Evans TW and Barnes PJ (1989b). Evidence for two P2-purinoceptor subtypes in human small pulmonary arteries. *Br J Pharmacol* 98(3), 1014-1020.

Lopes LV, Rebola N, Pinheiro PC, Richardson PJ, Oliveira CR and Cunha RA (2003). Adenosine A3 receptors are located in neurons of the rat hippocampus. *Neuroreport* 14(12), 1645-1648.

Lopez HS and Adams PR (1989). A G Protein Mediates the Inhibition of the Voltage-Dependent Potassium M Current by Muscarine, LHRH, Substance P and UTP in Bullfrog Sympathetic Neurons. *Eur J Neurosci* 1(5), 529-542.

Lupica CR, Proctor WR and Dunwiddie TV (1992). Presynaptic inhibition of excitatory synaptic transmission by adenosine in rat hippocampus: analysis of unitary EPSP variance measured by whole-cell recording. *J Neurosci* 12(10), 3753-3764.

Luthardt J, Borvendeg SJ, Sperlagh B, Poelchen W, Wirkner K and Illes P (2003a). P2Y(1) receptor activation inhibits NMDA receptor-channels in layer V pyramidal neurons of the rat prefrontal and parietal cortex. *Neurochem Int* 42(2), 161-172.

Ma W, Korngreen A, Weil S, Cohen EB, Priel A, Kuzin L and Silberberg SD (2006). Pore properties and pharmacological features of the P2X receptor channel in airway ciliated cells. *J Physiol* 571(Pt 3), 503-517.

Macdonald RL and Stoodley M (1998). Pathophysiology of cerebral ischemia. *Neurol Med Chir (Tokyo)* 38(1), 1-11.

Macek TA, Schaffhauser H and Conn PJ (1998). Protein kinase C and A3 adenosine receptor activation inhibit presynaptic metabotropic glutamate receptor (mGluR) function and uncouple mGluRs from GTP-binding proteins. *J Neurosci* 18(16), 6138-6146.

Maconi A, Pastorin G, Da Ros T, Spalluto G, Gao ZG, Jacobson KA, Baraldi PG, Cacciari B, Varani K, Moro S and Borea PA (2002). Synthesis, biological properties, and molecular modeling investigation of the first potent, selective, and water-soluble human A(3) adenosine receptor antagonist. *J Med Chem* 45(17), 3579-3582.

Malmsjo M, Adner M, Harden TK, Pendergast W, Edvinsson L and Erlinge D (2000). The stable pyrimidines UDPbetaS and UTPgammaS discriminate between the P2 receptors that mediate vascular contraction and relaxation of the rat mesenteric artery. *Br J Pharmacol* 131(1), 51-56.

Mamedova L, Capra V, Accomazzo MR, Gao ZG, Ferrario S, Fumagalli M, Abbracchio MP, Rovati GE and Jacobson KA (2005). CysLT1 leukotriene receptor antagonists inhibit the effects of nucleotides acting at P2Y receptors. *Biochem Pharmacol* 71(1-2), 115-125.

Marcoli M, Raiteri L, Bonfanti A, Monopoli A, Ongini E, Raiteri M and Maura G (2003). Sensitivity to selective adenosine A1 and A2A receptor antagonists of the release of glutamate induced by ischemia in rat cerebrocortical slices. *Neuropharmacology* 45(2), 201-210.

Mark MD, Ruppersberg JP and Herlitze S (2000). Regulation of GIRK channel deactivation by Galpha(q) and Galpha(i/o) pathways. *Neuropharmacology* 39(12), 2360-2373.

Marteau F, Le Poul E, Communi D, Communi D, Labouret C, Savi P, Boeynaems JM and Gonzalez NS (2003). Pharmacological characterization of the human P2Y13 receptor. *Mol Pharmacol* 64(1), 104-112.

Martinson J (1965). The effect of graded vagal stimulation on gastric motility, secretion and blood flow in the cat. *Acta Physiol Scand* 65(4), 300-309.

Masino SA, Diao L, Illes P, Zahniser NR, Larson GA, Johansson B, Fredholm BB and Dunwiddie TV (2002a). Modulation of hippocampal glutamatergic transmission by ATP is dependent on adenosine a(1) receptors. *J Pharmacol Exp Ther* 303(1), 356-363.

Meera P, Wallner M and Toro L (2000). A neuronal beta subunit (KCNMB4) makes the large conductance, voltage- and Ca2+-activated K+ channel resistant to charybdotoxin and iberiotoxin. *Proc Natl Acad Sci U S A* 97(10), 5562-5567.

Meghji P, Skladanowski AC, Newby AC, Slakey LL and Pearson JD (1993). Effect of 5'-deoxy-5'-isobutylthioadenosine on formation and release of adenosine from neonatal and adult rat ventricular myocytes. *Biochem J* 291 (Pt 3)(833-839.

Melani A, Amadio S, Gianfriddo M, Vannucchi MG, Volonte C, Bernardi G, Pedata F and Sancesario G (2006). P2X7 receptor modulation on microglial cells and reduction of brain infarct caused by middle cerebral artery occlusion in rat. *J Cereb Blood Flow Metab* 26(7), 974-982.

Melani A, Pantoni L, Bordoni F, Gianfriddo M, Bianchi L, Vannucchi MG, Bertorelli R, Monopoli A and Pedata F (2003). The selective A2A receptor antagonist SCH 58261 reduces striatal transmitter outflow, turning behavior and ischemic brain damage induced by permanent focal ischemia in the rat. *Brain Res* 959(2), 243-250.

Melani A, Pantoni L, Corsi C, Bianchi L, Monopoli A, Bertorelli R, Pepeu G and Pedata F (1999). Striatal outflow of adenosine, excitatory amino acids, gamma-aminobutyric acid, and taurine in awake freely moving rats after middle cerebral artery occlusion: correlations with neurological deficit and histopathological damage. *Stroke* 30(11), 2448-2454.

Melani A, Turchi D, Vannucchi MG, Cipriani S, Gianfriddo M and Pedata F (2005). ATP extracellular concentrations are increased in the rat striatum during in vivo ischemia. *Neurochem Int* 47(6), 442-448.

Mellor EA, Maekawa A, Austen KF and Boyce JA (2001). Cysteinyl leukotriene receptor 1 is also a pyrimidinergic receptor and is expressed by human mast cells. *Proc Natl Acad Sci U S A* 98(14), 7964-7969.

Mendoza-Fernandez V, Andrew RD and Barajas-Lopez C (2000). ATP inhibits glutamate synaptic release by acting at P2Y receptors in pyramidal neurons of hippocampal slices. *J Pharmacol Exp Ther* 293(1), 172-179.

Meng H, Sakakibara M, Nakazawa H and Tokimasa T (2003). Pyridoxalphosphate-6-azophenyl-2',4'-disulfonic acid can antagonize the purinoceptor-mediated inhibition of M-current in

bullfrog sympathetic neurons. *Neurosci Lett* 337(2), 93-96.

Meyer PT, Elmenhorst D, Bier D, Holschbach MH, Matusch A, Coenen HH, Zilles K and Bauer A (2005). Quantification of cerebral A1 adenosine receptors in humans using [18F]CPFPX and PET: an equilibrium approach. *Neuroimage* 24(4), 1192-1204.

Meyerhof W, Muller-Brechlin R and Richter D (1991). Molecular cloning of a novel putative G-protein coupled receptor expressed during rat spermiogenesis. *FEBS Lett* 284(2), 155-160.

Min JY, Sullivan MF, Yang Y, Zhang JP, Converso KL, Morgan JP and Xiao YF (2002). Significant improvement of heart function by cotransplantation of human mesenchymal stem cells and fetal cardiomyocytes in postinfarcted pigs. *Ann Thorac Surg* 74(5), 1568-1575.

Mio K, Kubo Y, Ogura T, Yamamoto T and Sato C (2005). Visualization of the trimeric P2X2 receptor with a crown-capped extracellular domain. *Biochem Biophys Res Commun* 337(3), 998-1005.

Mishra SK, Braun N, Shukla V, Fullgrabe M, Schomerus C, Korf HW, Gachet C, Ikehara Y, Sevigny J, Robson SC and Zimmermann H (2006). Extracellular nucleotide signaling in adult neural stem cells: synergism with growth factor-mediated cellular proliferation. *Development* 133(4), 675-684.

Mohanty JG, Raible DG, McDermott LJ, Pelleg A and Schulman ES (2001). Effects of purine and pyrimidine nucleotides on intracellular Ca2+ in human eosinophils: activation of purinergic P2Y receptors. *J Allergy Clin Immunol* 107(5), 849-855.

Monopoli A, Lozza G, Forlani A, Mattavelli A and Ongini E (1998). Blockade of adenosine A2A receptors by SCH 58261 results in neuroprotective effects in cerebral ischaemia in rats. *Neuroreport* 9(17), 3955-3959.

Moore D, Chambers J, Waldvogel H, Faull R and Emson P (2000). Regional and cellular distribution of the P2Y(1) purinergic receptor in the human brain: striking neuronal localisation. *J Comp Neurol* 421(3), 374-384.

Moore DJ, Chambers JK, Wahlin JP, Tan KB, Moore GB, Jenkins O, Emson PC and Murdock PR (2001). Expression pattern of human P2Y receptor subtypes: a quantitative reverse transcription-polymerase chain reaction study. *Biochim Biophys Acta* 1521(1-3), 107-119.

Moore KA, Nicoll RA and Schmitz D (2003). Adenosine gates synaptic plasticity at hippocampal mossy fiber synapses. *Proc Natl Acad Sci U S A* 100(24), 14397-14402.

Mori M, Heuss C, Gahwiler BH and Gerber U (2001). Fast synaptic transmission mediated by P2X receptors in CA3 pyramidal cells of rat hippocampal slice cultures. *J Physiol* 535(Pt 1), 115-123.

Mori M, Nishizaki T and Okada Y (1992). Protective effect of adenosine on the anoxic damage of hippocampal slice. *Neuroscience* 46(2), 301-307.

Moriyama T, Iida T, Kobayashi K, Higashi T, Fukuoka T, Tsumura H, Leon C, Suzuki N, Inoue K, Gachet C, Noguchi K and Tominaga M (2003). Possible involvement of P2Y2 metabotropic receptors in ATP-induced transient receptor potential vanilloid receptor 1-mediated thermal hypersensitivity. *J Neurosci* 23(14), 6058-6062.

Morley P, Hogan MJ and Hakim AM (1994). Calcium-mediated mechanisms of ischemic injury and protection. *Brain Pathol* 4(1), 37-47.

Moro S, Guo D, Camaioni E, Boyer JL, Harden TK and Jacobson KA (1998). Human P2Y1 receptor: molecular modeling and site-directed mutagenesis as tools to identify agonist and antagonist recognition sites. *J Med Chem* 41(9), 1456-1466.

Muijlwijk-Koezen JE, Timmerman H, van der GH, Menge WM, Frijtag Von Drabbe KJ, de Groote M and IJzerman AP (2000). Isoquinoline and quinazoline urea analogues as antagonists for the human adenosine A(3) receptor. *J Med Chem* 43(11), 2227-2238.

Mule F and Serio R (2003). NANC inhibitory neurotransmission in mouse isolated stomach: involvement of nitric oxide, ATP and vasoactive intestinal polypeptide. *Br J Pharmacol* 140(2), 431-437.

Muller CE (2002). P2-pyrimidinergic receptors and their ligands. *Curr Pharm Des* 8(26), 2353-2369.

Muller CE (2003). Medicinal chemistry of adenosine A3 receptor ligands. *Curr Top Med Chem*

3(4), 445-462.

Muller CE, Iqbal J, Baqi Y, Zimmermann H, Rollich A and Stephan H (2006). Polyoxometalates-a new class of potent ecto-nucleoside triphosphate diphosphohydrolase (NTPDase) inhibitors. *Bioorg Med Chem Lett* 16(23), 5943-5947.

Muller M and Somjen GG (1999). Intrinsic optical signals in rat hippocampal slices during hypoxia-induced spreading depression-like depolarization. *J Neurophysiol* 82(4), 1818-1831.

Muller M and Somjen GG (2000). Na(+) and K(+) concentrations, extra- and intracellular voltages, and the effect of TTX in hypoxic rat hippocampal slices. *J Neurophysiol* 83(2), 735-745.

Nakata H, Yoshioka K and Kamiya T (2004). Purinergic-receptor oligomerization: implications for neural functions in the central nervous system. *Neurotox Res* 6(4), 291-297.

Nakata H, Yoshioka K, Kamiya T, Tsuga H and Oyanagi K (2005). Functions of heteromeric association between adenosine and P2Y receptors. *J Mol Neurosci* 26(2-3), 233-238.

Nakatsuka T and Gu JG (2001). ATP P2X receptor-mediated enhancement of glutamate release and evoked EPSCs in dorsal horn neurons of the rat spinal cord. *J Neurosci* 21(17), 6522-6531.

Nakazawa K, Inoue K, Ito K, Koizumi S and Inoue K (1995). Inhibition by suramin and reactive blue 2 of GABA and glutamate receptor channels in rat hippocampal neurons. *Naunyn Schmiedebergs Arch Pharmacol* 351(2), 202-208.

Nandanan E, Camaioni E, Jang SY, Kim YC, Cristalli G, Herdewijn P, Secrist JA, III, Tiwari KN, Mohanram A, Harden TK, Boyer JL and Jacobson KA (1999). Structure-activity relationships of bisphosphate nucleotide derivatives as P2Y1 receptor antagonists and partial agonists. *J Med Chem* 42(9), 1625-1638.

Nandanan E, Jang SY, Moro S, Kim HO, Siddiqui MA, Russ P, Marquez VE, Busson R, Herdewijn P, Harden TK, Boyer JL and Jacobson KA (2000). Synthesis, biological activity, and molecular modeling of ribose-modified deoxyadenosine bisphosphate analogues as P2Y(1) receptor ligands. *J Med Chem* 43(5), 829-842.

Newman GC, Hospod FE, Trowbridge SD, Motwani S and Liu Y (1998). Restoring adenine nucleotides in a brain slice model of cerebral reperfusion. *J Cereb Blood Flow Metab* 18(6), 675-685.

Nicke A, Kerschensteiner D and Soto F (2005). Biochemical and functional evidence for heteromeric assembly of P2X1 and P2X4 subunits. *J Neurochem* 92(4), 925-933.

Nieber K and Hentschel S (2006). Signalling pathways of the adenosine A3 receptors in rat cortical neurons. 2006. Paper presented at the 8th International Symposium on Adenosine and Adenine Nucleotides,Univesity of Ferrara,Ferrara,Italy,24-28 May 2006. Ref Type: Conference Proceeding

Nieber K, Poelchen W and Illes P (1997). Role of ATP in fast excitatory synaptic potentials in locus coeruleus neurones of the rat. *Br J Pharmacol* 122(3), 423-430.

Nisenbaum ES, Wilson CJ, Foehring RC and Surmeier DJ (1996). Isolation and characterization of a persistent potassium current in neostriatal neurons. *J Neurophysiol* 76(2), 1180-1194.

Nishimura S, Mohri M, Okada Y and Mori M (1990). Excitatory and inhibitory effects of adenosine on the neurotransmission in the hippocampal slices of guinea pig. *Brain Res* 525(1), 165-169.

Norenberg W and Illes P (2000a). Neuronal P2X receptors: localisation and functional properties. *Naunyn Schmiedebergs Arch Pharmacol* 362(4-5), 324-339.

Norenberg W, von K, I, Meyer A, Illes P and Starke K (2000b). M-type K+ currents in rat cultured thoracolumbar sympathetic neurones and their role in uracil nucleotide-evoked noradrenaline release. *Br J Pharmacol* 129(4), 709-723.

Nori S, Fumagalli L, Bo X, Bogdanov Y and BURNSTOCK G (1998). Coexpression of mRNAs for P2X1, P2X2 and P2X4 receptors in rat vascular smooth muscle: an in situ hybridization and RT-PCR study. *J Vasc Res* 35(3), 179-185.

North RA (2002). Molecular physiology of P2X receptors. *Physiol Rev* 82(4), 1013-1067.

North RA and Surprenant A (2000). Pharmacology of cloned P2X receptors. *Annu Rev Pharmacol Toxicol* 40(563-580.

O'Connor SE, Dainty IA and Leff P (1991). Further subclassification of ATP receptors based on agonist studies. *Trends Pharmacol Sci* 12(4), 137-141.

O'Kane EM and Stone TW (1998). Interaction between adenosine A1 and A2 receptor-mediated responses in the rat hippocampus in vitro. *Eur J Pharmacol* 362(1), 17-25.

O'Regan MH, Simpson RE, Perkins LM and Phillis JW (1992). The selective A2 adenosine receptor agonist CGS 21680 enhances excitatory transmitter amino acid release from the ischemic rat cerebral cortex. *Neurosci Lett* 138(1), 169-172.

Obara K, Lepor H and Walden PD (1998). Localization of P2Y1 purinoceptor transcripts in the rat penis and urinary bladder. *J Urol* 160(2), 587-591.

Obeidat AS and Andrew RD (1998). Spreading depression determines acute cellular damage in the hippocampal slice during oxygen/glucose deprivation. *Eur J Neurosci* 10(11), 3451-3461.

Obeidat AS, Jarvis CR and Andrew RD (2000). Glutamate does not mediate acute neuronal damage after spreading depression induced by O2/glucose deprivation in the hippocampal slice. *J Cereb Blood Flow Metab* 20(2), 412-422.

Ochs S and Van Harreveld A (1956). Cerebral impedance changes after circulatory arrest. *Am J Physiol* 187(1), 180-192.

Ohno M, Costanzi S, Kim HS, Kempeneers V, Vastmans K, Herdewijn P, Maddileti S, Gao ZG, Harden TK and Jacobson KA (2004). Nucleotide analogues containing 2-oxa-bicyclo[2.2.1]heptane and l-alpha-threofuranosyl ring systems: interactions with P2Y receptors. *Bioorg Med Chem* 12(21), 5619-5630.

Ortinau S, Laube B and Zimmermann H (2003). ATP inhibits NMDA receptors after heterologous expression and in cultured hippocampal neurons and attenuates NMDA-mediated neurotoxicity. *J Neurosci* 23(12), 4996-5003.

Ota S, Yoshiura K, Takahashi M, Hata Y, Kohmoto O, Kawabe T, Shimada T, Hiraishi H, Mutoh H, Terano A and . (1994). P2 purinergic receptor regulation of mucus glycoprotein secretion by rabbit gastric mucous cells in a primary culture. *Gastroenterology* 106(6), 1485-1492.

Otsuguro K, Ito S, Ohta T and Nakazato Y (1996). Influence of purines and pyrimidines on circular muscle of the rat proximal stomach. *Eur J Pharmacol* 317(1), 97-105.

Palmer RK, Boyer JL, Schachter JB, Nicholas RA and Harden TK (1998). Agonist action of adenosine triphosphates at the human P2Y1 receptor. *Mol Pharmacol* 54(6), 1118-1123.

Palmer TM, Benovic JL and Stiles GL (1995). Agonist-dependent phosphorylation and desensitization of the rat A3 adenosine receptor. Evidence for a G-protein-coupled receptor kinase-mediated mechanism. *J Biol Chem* 270(49), 29607-29613.

Palmer TM and Stiles GL (2000). Identification of threonine residues controlling the agonist-dependent phosphorylation and desensitization of the rat A(3) adenosine receptor. *Mol Pharmacol* 57(3), 539-545.

Pankratov Y, Castro E, Miras-Portugal MT and Krishtal O (1998). A purinergic component of the excitatory postsynaptic current mediated by P2X receptors in the CA1 neurons of the rat hippocampus. *Eur J Neurosci* 10(12), 3898-3902.

Pankratov Y, Lalo U, Krishtal O and Verkhratsky A (2002). Ionotropic P2X purinoreceptors mediate synaptic transmission in rat pyramidal neurones of layer II/III of somato-sensory cortex. *J Physiol* 542(Pt 2), 529-536.

Pankratov Y, Lalo U, Verkhratsky A and North RA. (2006). Vesicular release of ATP at central synapses. *Pflugers Arch.* 452(5), 589-597.

Pascual O, Casper KB, Kubera C, Zhang J, Revilla-Sanchez R, Sul JY, Takano H, Moss SJ, McCarthy K and Haydon PG (2005). Astrocytic purinergic signaling coordinates synaptic networks. *Science* 310(5745), 113-116.

Pearson RA, Dale N, Llaudet E and Mobbs P (2005). ATP released via gap junction hemichannels from the pigment epithelium regulates neural retinal progenitor proliferation. *Neuron* 46(5), 731-744.

Pearson T, Damian K, Lynas RE and Frenguelli BG (2006). Sustained elevation of extracellular adenosine and activation of A1 receptors underlie the post-ischaemic inhibition of neuronal function in rat hippocampus in vitro. *J Neurochem* 97(5), 1357-1368.

Pedata F, Corsi C, Melani A, Bordoni F and Latini S (2001). Adenosine extracellular brain concentrations and role of A2A receptors in ischemia. *Ann N Y Acad Sci* 939(74-84.

Pedata F, Latini S, Pugliese AM and Pepeu G (1993). Investigations into the adenosine outflow from hippocampal slices evoked by ischemia-like conditions. *J Neurochem* 61(1), 284-289.

Pedata F, Pepeu G and Spignoli G (1984). Biphasic effect of methylxanthines on acetylcholine release from electrically-stimulated brain slices. *Br J Pharmacol* 83(1), 69-73.

Peoples RW and Li C (1998). Inhibition of NMDA-gated ion channels by the P2 purinoceptor antagonists suramin and reactive blue 2 in mouse hippocampal neurones. *Br J Pharmacol* 124(2), 400-408.

Phillis JW (1995). The effects of selective A1 and A2a adenosine receptor antagonists on cerebral ischemic injury in the gerbil. *Brain Res* 705(1-2), 79-84.

Phillis JW (2004). Adenosine and adenine nucleotides as regulators of cerebral blood flow: roles of acidosis, cell swelling, and KATP channels. *Crit Rev Neurobiol* 16(4), 237-270.

Phillis JW, Edstrom JP, Kostopoulos GK and Kirkpatrick JR (1979). Effects of adenosine and adenine nucleotides on synaptic transmission in the cerebral cortex. *Can J Physiol Pharmacol* 57(11), 1289-1312.

Phillis JW, O'Regan MH and Perkins LM (1993). Adenosine 5'-triphosphate release from the normoxic and hypoxic in vivo rat cerebral cortex. *Neurosci Lett* 151(1), 94-96.

Picher M and Boucher RC (2003). Human airway ecto-adenylate kinase. A mechanism to propagate ATP signaling on airway surfaces. *J Biol Chem* 278(13), 11256-11264.

Pineda JC, Galarraga E, Bargas J, Cristancho M and Aceves J (1992). Charybdotoxin and apamin sensitivity of the calcium-dependent repolarization and the afterhyperpolarization in neostriatal neurons. *J Neurophysiol* 68(1), 287-294.

Pittenger MF, Mackay AM, Beck SC, Jaiswal RK, Douglas R, Mosca JD, Moorman MA, Simonetti DW, Craig S and Marshak DR (1999). Multilineage potential of adult human mesenchymal stem cells. *Science* 284(5411), 143-147.

Plenz D and Kitai ST (1998). Up and down states in striatal medium spiny neurons simultaneously recorded with spontaneous activity in fast-spiking interneurons studied in cortex-striatum-substantia nigra organotypic cultures. *J Neurosci* 18(1), 266-283.

Plum F (2001). Neuroprotection in acute ischemic stroke. *JAMA* 285(13), 1760-1761.

Poletto Chaves LA, Pontelli EP and Varanda WA (2006). P2X receptors in mouse Leydig cells. *Am J Physiol Cell Physiol* 290(4), C1009-C1017.

Pooler AM, Guez DH, Benedictus R and Wurtman RJ (2005). Uridine enhances neurite outgrowth in nerve growth factor-differentiated PC12 [corrected]. *Neuroscience* 134(1), 207-214.

Popoli P, Betto P, Reggio R and Ricciarello G (1995). Adenosine A2A receptor stimulation enhances striatal extracellular glutamate levels in rats. *Eur J Pharmacol* 287(2), 215-217.

Poucher SM, Keddie JR, Singh P, Stoggall SM, Caulkett PW, Jones G and Coll MG (1995). The in vitro pharmacology of ZM 241385, a potent, non-xanthine A2a selective adenosine receptor antagonist. *Br J Pharmacol* 115(6), 1096-1102.

Powell AD, Teschemacher AG and Seward EP (2000). P2Y purinoceptors inhibit exocytosis in adrenal chromaffin cells via modulation of voltage-operated calcium channels. *J Neurosci* 20(2), 606-616.

Press NJ, Taylor RJ, Fullerton JD, Tranter P, McCarthy C, Keller TH, Brown L, Cheung R, Christie J, Haberthuer S, Hatto JD, Keenan M, Mercer MK, Press NE, Sahri H, Tuffnell AR, Tweed M and Fozard JR (2005). A new orally bioavailable dual adenosine A2B/A3 receptor antagonist with therapeutic potential. *Bioorg Med Chem Lett* 15(12), 3081-3085.

Prince DA and Stevens CF (1992). Adenosine decreases neurotransmitter release at central synapses. *Proc Natl Acad Sci U S A* 89(18), 8586-8590.

Pugliese AM, Coppi E, Spalluto G, Corradetti R and Pedata F (2006). A3 adenosine receptor an-

tagonists delay irreversible synaptic failure caused by oxygen and glucose deprivation in the rat CA1 hippocampus in vitro. *Br J Pharmacol* 147(5), 524-532.

Pugliese AM, Latini S, Corradetti R and Pedata F (2003). Brief, repeated, oxygen-glucose deprivation episodes protect neurotransmission from a longer ischemic episode in the in vitro hippocampus: role of adenosine receptors. *Br J Pharmacol* 140(2), 305-314.

Rae J, Cooper K, Gates P and Watsky M (1991). Low access resistance perforated patch recordings using amphotericin B. *J Neurosci Methods* 37(1), 15-26.

Ralevic V and Burnstock G (1998). Receptors for purines and pyrimidines. *Pharmacol Rev* 50(3), 413-492.

Ramkumar V, Stiles GL, Beaven MA and Ali H (1993). The A3 adenosine receptor is the unique adenosine receptor which facilitates release of allergic mediators in mast cells. *J Biol Chem* 268(23), 16887-16890.

Rebola N, Pinheiro PC, Oliveira CR, Malva JO and Cunha RA (2003). Subcellular localization of adenosine A(1) receptors in nerve terminals and synapses of the rat hippocampus. *Brain Res* 987(1), 49-58.

Reisin IL, Prat AG, Abraham EH, Amara JF, Gregory RJ, Ausiello DA and Cantiello HF (1994). The cystic fibrosis transmembrane conductance regulator is a dual ATP and chloride channel. *J Biol Chem* 269(32), 20584-20591.

Rettinger J, Braun K, Hochmann H, Kassack MU, Ullmann H, Nickel P, Schmalzing G and Lambrecht G (2005). Profiling at recombinant homomeric and heteromeric rat P2X receptors identifies the suramin analogue NF449 as a highly potent P2X1 receptor antagonist. *Neuropharmacology* 48(3), 461-468.

Rettinger J and Schmalzing G (2003). Activation and desensitization of the recombinant P2X1 receptor at nanomolar ATP concentrations. *J Gen Physiol* 121(5), 451-461.

Reyes M, Dudek A, Jahagirdar B, Koodie L, Marker PH and Verfaillie CM (2002). Origin of endothelial progenitors in human postnatal bone marrow. *J Clin Invest* 109(3), 337-346.

Reyes M, Lund T, Lenvik T, Aguiar D, Koodie L and Verfaillie CM (2001). Purification and ex vivo expansion of postnatal human marrow mesodermal progenitor cells. *Blood* 98(9), 2615-2625.

Rieger JM, Brown ML, Sullivan GW, Linden J and Macdonald TL (2001). Design, synthesis, and evaluation of novel A2A adenosine receptor agonists. *J Med Chem* 44(4), 531-539.

Rivkees SA, Price SL and Zhou FC (1995). Immunohistochemical detection of A1 adenosine receptors in rat brain with emphasis on localization in the hippocampal formation, cerebral cortex, cerebellum, and basal ganglia. *Brain Res* 677(2), 193-203.

Robbins J (2001). KCNQ potassium channels: physiology, pathophysiology, and pharmacology. *Pharmacol Ther* 90(1), 1-19.

Roberts JA, Vial C, Digby HR, Agboh KC, Wen H, Atterbury-Thomas A and Evans RJ (2006). Molecular properties of P2X receptors. *Pflugers Arch* 452(5), 486-500.

Rodrigues RJ, Almeida T, Richardson PJ, Oliveira CR and Cunha RA (2005). Dual presynaptic control by ATP of glutamate release via facilitatory P2X1, P2X2/3, and P2X3 and inhibitory P2Y1, P2Y2, and/or P2Y4 receptors in the rat hippocampus. *J Neurosci* 25(27), 6286-6295.

Romagnoli R, Baraldi PG, Pavani MG, Tabrizi MA, Moorman AR, Di Virgilio F, Cattabriga E, Pancaldi C, Gessi S and Borea PA (2004). Synthesis, radiolabeling, and preliminary biological evaluation of [3H]-1-[(S)-N,O-bis-(isoquinolinesulfonyl)-N-methyl-tyrosyl]-4-(o-tolyl)-p iperazine, a potent antagonist radioligand for the P2X7 receptor. *Bioorg Med Chem Lett* 14(22), 5709-5712.

Rosenblueth A and Garcia RJ (1966). Some phenomena usually associated with spreading depression. *Acta Physiol Lat Am* 16(2), 141-179.

Rosin DL, Hettinger BD, Lee A and Linden J (2003). Anatomy of adenosine A2A receptors in brain: morphological substrates for integration of striatal function. *Neurology* 61(11 Suppl 6), S12-S18.

Rosin DL, Robeva A, Woodard RL, Guyenet PG and Linden J (1998). Immunohistochemical localization of adenosine A2A receptors in the rat central nervous system. *J Comp Neurol*

401(2), 163-186.

Ross GW, Abbott RD, Petrovitch H, Morens DM, Grandinetti A, Tung KH, Tanner CM, Masaki KH, Blanchette PL, Curb JD, Popper JS and White LR (2000). Association of coffee and caffeine intake with the risk of Parkinson disease. *JAMA* 283(20), 2674-2679.

Ruan HZ, Birder LA, Xiang Z, Chopra B, Buffington T, Tai C, Roppolo JR, de Groat WC and Burnstock G (2006). Expression of P2X and P2Y receptors in the intramural parasympathetic ganglia of the cat urinary bladder. *Am J Physiol Renal Physiol* 290(5), F1143-F1152.

Ruan HZ and BURNSTOCK G (2003). Localisation of P2Y1 and P2Y4 receptors in dorsal root, nodose and trigeminal ganglia of the rat. *Histochem Cell Biol* 120(5), 415-426.

Rubini P, Pinkwart C, Franke H, Gerevich Z, Norenberg W and Illes P (2006). Regulation of intracellular Ca2+ by P2Y1 receptors may depend on the developmental stage of cultured rat striatal neurons. *J Cell Physiol* 209(1), 81-93.

Ryu JK, Choi HB, Hatori K, Heisel RL, Pelech SL, McLarnon JG and Kim SU (2003). Adenosine triphosphate induces proliferation of human neural stem cells: Role of calcium and p70 ribosomal protein S6 kinase. *J Neurosci Res* 72(3), 352-362.

Ryu JK, Kim J, Choi SH, Oh YJ, Lee YB, Kim SU and Jin BK (2002). ATP-induced in vivo neurotoxicity in the rat striatum via P2 receptors. *Neuroreport* 13(13), 1611-1615.

Sabirov RZ, Dutta AK and Okada Y (2001). Volume-dependent ATP-conductive large-conductance anion channel as a pathway for swelling-induced ATP release. *J Gen Physiol* 118(3), 251-266.

Safiulina VF, Kasyanov AM, Sokolova E, Cherubini E and Giniatullin R (2005). ATP contributes to the generation of network-driven giant depolarizing potentials in the neonatal rat hippocampus. *J Physiol* 565(Pt 3), 981-992.

Sak K, Boeynaems JM and Everaus H (2003). Involvement of P2Y receptors in the differentiation of haematopoietic cells. *J Leukoc Biol* 73(4), 442-447.

Salvatore CA, Jacobson MA, Taylor HE, Linden J and Johnson RG (1993). Molecular cloning and characterization of the human A3 adenosine receptor. *Proc Natl Acad Sci U S A* 90(21), 10365-10369.

Salvatore CA, Tilley SL, Latour AM, Fletcher DS, Koller BH and Jacobson MA (2000). Disruption of the A(3) adenosine receptor gene in mice and its effect on stimulated inflammatory cells. *J Biol Chem* 275(6), 4429-4434.

Sasaki Y, Hoshi M, Akazawa C, Nakamura Y, Tsuzuki H, Inoue K and Kohsaka S (2003). Selective expression of Gi/o-coupled ATP receptor P2Y12 in microglia in rat brain. *Glia* 44(3), 242-250.

Saurin W, Hofnung M and Dassa E (1999). Getting in or out: early segregation between importers and exporters in the evolution of ATP-binding cassette (ABC) transporters. *J Mol Evol* 48(1), 22-41.

Scamps F and Vassort G (1994). Pharmacological profile of the ATP-mediated increase in L-type calcium current amplitude and activation of a non-specific cationic current in rat ventricular cells. *Br J Pharmacol* 113(3), 982-986.

Scemes E, Duval N and Meda P (2003). Reduced expression of P2Y1 receptors in connexin43-null mice alters calcium signaling and migration of neural progenitor cells. *J Neurosci* 23(36), 11444-11452.

Scheibler P, Pesic M, Franke H, Reinhardt R, Wirkner K, Illes P and Norenberg W (2004). P2X2 and P2Y1 immunofluorescence in rat neostriatal medium-spiny projection neurones and cholinergic interneurones is not linked to respective purinergic receptor function. *Br J Pharmacol* 143(1), 119-131.

Schindler CW, Karcz-Kubicha M, Thorndike EB, Muller CE, Tella SR, Ferre S and Goldberg SR (2005). Role of central and peripheral adenosine receptors in the cardiovascular responses to intraperitoneal injections of adenosine A1 and A2A subtype receptor agonists. *Br J Pharmacol* 144(5), 642-650.

Schindler M, Harris CA, Hayes B, Papotti M and Humphrey PP (2001). Immunohistochemical localization of adenosine A1 receptors in human brain regions. *Neurosci Lett* 297(3),

211-215.

Schipke CG, Boucsein C, Ohlemeyer C, Kirchhoff F and Kettenmann H (2002). Astrocyte Ca2+ waves trigger responses in microglial cells in brain slices. *FASEB J* 16(2), 255-257.

Schubert P, Komp W and Kreutzberg GW (1979). Correlation of 5'-nucleotidase activity and selective transneuronal transfer of adenosine in the hippocampus. *Brain Res* 168(2), 419-424.

Schwarz EJ, Alexander GM, Prockop DJ and Azizi SA (1999). Multipotential marrow stromal cells transduced to produce L-DOPA: engraftment in a rat model of Parkinson disease. *Hum Gene Ther* 10(15), 2539-2549.

Sebastiao AM, de Mendonca A, Moreira T and Ribeiro JA (2001). Activation of synaptic NMDA receptors by action potential-dependent release of transmitter during hypoxia impairs recovery of synaptic transmission on reoxygenation. *J Neurosci* 21(21), 8564-8571.

Sebastiao AM and Ribeiro JA (1996). Adenosine A2 receptor-mediated excitatory actions on the nervous system. *Prog Neurobiol* 48(3), 167-189.

Sesti C, Koyama M, Broekman MJ, Marcus AJ and Levi R (2003). Ectonucleotidase in sympathetic nerve endings modulates ATP and norepinephrine exocytosis in myocardial ischemia. *J Pharmacol Exp Ther* 306(1), 238-244.

Shake JG, Gruber PJ, Baumgartner WA, Senechal G, Meyers J, Redmond JM, Pittenger MF and Martin BJ (2002). Mesenchymal stem cell implantation in a swine myocardial infarct model: engraftment and functional effects. *Ann Thorac Surg* 73(6), 1919-1925.

Shapiro MS, Roche JP, Kaftan EJ, Cruzblanca H, Mackie K and Hille B (2000). Reconstitution of muscarinic modulation of the KCNQ2/KCNQ3 K(+) channels that underlie the neuronal M current. *J Neurosci* 20(5), 1710-1721.

Sharpe NA and Tepper JM (1998). Postnatal development of excitatory synaptic input to the rat neostriatum: an electron microscopic study. *Neuroscience* 84(4), 1163-1175.

Shibuya I, Tanaka K, Hattori Y, Uezono Y, Harayama N, Noguchi J, Ueta Y, Izumi F and Yamashita H (1999). Evidence that multiple P2X purinoceptors are functionally expressed in rat supraoptic neurones. *J Physiol* 514 (Pt 2)(351-367.

Sick TJ, Solow EL and Roberts EL, Jr. (1987). Extracellular potassium ion activity and electrophysiology in the hippocampal slice: paradoxical recovery of synaptic transmission during anoxia. *Brain Res* 418(2), 227-234.

Siesjo BK (1989). Calcium and cell death. *Magnesium* 8(5-6), 223-237.

Silinsky EM (1975). On the association between transmitter secretion and the release of adenine nucleotides from mammalian motor nerve terminals. *J Physiol* 247(1), 145-162.

Silinsky EM and Redman RS (1996). Synchronous release of ATP and neurotransmitter within milliseconds of a motor nerve impulse in the frog. *J Physiol* 492 (Pt 3)(815-822.

Sim JA, Young MT, Sung HY, North RA and Surprenant A. (2004). Reanalysis of P2X7 receptor expression in rodent brain. J Neurosci. 24(28), 6307-6314.

Simon J, Filippov AK, Goransson S, Wong YH, Frelin C, Michel AD, Brown DA and Barnard EA (2002). Characterization and channel coupling of the P2Y(12) nucleotide receptor of brain capillary endothelial cells. *J Biol Chem* 277(35), 31390-31400.

Simpson RE, O'Regan MH, Perkins LM and Phillis JW (1992). Excitatory transmitter amino acid release from the ischemic rat cerebral cortex: effects of adenosine receptor agonists and antagonists. *J Neurochem* 58(5), 1683-1690.

Skladchikova G, Ronn LC, Berezin V and Bock E (1999). Extracellular adenosine triphosphate affects neural cell adhesion molecule (NCAM)-mediated cell adhesion and neurite outgrowth. *J Neurosci Res* 57(2), 207-218.

Smart ML, Panchal RG, Bowser DN, Williams DA and Petrou S (2002). Pore formation is not associated with macroscopic redistribution of P2X7 receptors. *Am J Physiol Cell Physiol* 283(1), C77-C84.

Snow RW, Taylor CP and Dudek FE (1983). Electrophysiological and optical changes in slices of rat hippocampus during spreading depression. *J Neurophysiol* 50(3), 561-572.

Solle M, Labasi J, Perregaux DG, Stam E, Petrushova N, Koller BH, Griffiths RJ and Gabel CA (2001). Altered cytokine production in mice lacking P2X(7) receptors. *J Biol Chem* 276(1),

125-132.

Somjen GG (2001). Mechanisms of spreading depression and hypoxic spreading depression-like depolarization. *Physiol Rev* 81(3), 1065-1096.

Soto F, Garcia-Guzman M, Karschin C and Stuhmer W (1996). Cloning and tissue distribution of a novel P2X receptor from rat brain. *Biochem Biophys Res Commun* 223(2), 456-460.

Soulet C, Sauzeau V, Plantavid M, Herbert JM, Pacaud P, Payrastre B and Savi P (2004). Gi-dependent and -independent mechanisms downstream of the P2Y12 ADP-receptor. *J Thromb Haemost* 2(1), 135-146.

Sperlagh B, Kofalvi A, Deuchars J, Atkinson L, Milligan CJ, Buckley NJ and Vizi ES (2002). Involvement of P2X7 receptors in the regulation of neurotransmitter release in the rat hippocampus. *J Neurochem* 81(6), 1196-1211.

Spignoli G, Pedata F and Pepeu G (1984). A1 and A2 adenosine receptors modulate acetylcholine release from brain slices. *Eur J Pharmacol* 97(3-4), 341-342.

Stern EA, Kincaid AE and Wilson CJ (1997). Spontaneous subthreshold membrane potential fluctuations and action potential variability of rat corticostriatal and striatal neurons in vivo. *J Neurophysiol* 77(4), 1697-1715.

Stevens B and Fields RD (2000). Response of Schwann cells to action potentials in development. *Science* 287(5461), 2267-2271.

Stojilkovic SS, Tomic M, He ML, Yan Z, Koshimizu TA and Zemkova H (2005). Molecular dissection of purinergic P2X receptor channels. *Ann N Y Acad Sci* 1048(116-130.

Stone TW, Nikbakht MR and O'Kane EM (2004). From messengers to molecules: memories are made of these. Eurekah.com and Kluwer Academic. *Plenum Publishers.* Ref Type: Book Chapter.

Stout CE, Costantin JL, Naus CC and Charles AC (2002). Intercellular calcium signaling in astrocytes via ATP release through connexin hemichannels. *J Biol Chem* 277(12), 10482-10488.

Strange K, Emma F and Jackson PS (1996). Cellular and molecular physiology of volume-sensitive anion channels. *Am J Physiol* 270(3 Pt 1), C711-C730.

Su C, Bevan JA and Burnstock G (1971). [3H]adenosine triphosphate: release during stimulation of enteric nerves. *Science* 173(994), 336-338.

Surprenant A, Rassendren F, Kawashima E, North RA and Buell G (1996). The cytolytic P2Z receptor for extracellular ATP identified as a P2X receptor (P2X7). *Science* 272(5262), 735-738.

Swanson TH, Drazba JA and Rivkees SA (1995). Adenosine A1 receptors are located predominantly on axons in the rat hippocampal formation. *J Comp Neurol* 363(4), 517-531.

Takahashi T (1978). Intracellular recording from visually identified motoneurons in rat spinal cord slices. *Proc.R.Soc.Lond B Biol.Sci.* 202(1148), 417-421.

Takigawa T and Alzheimer C (1999). G protein-activated inwardly rectifying K+ (GIRK) currents in dendrites of rat neocortical pyramidal cells. *J Physiol* 517 (Pt 2)(385-390.

Takigawa T and Alzheimer C (2002). Phasic and tonic attenuation of EPSPs by inward rectifier K+ channels in rat hippocampal pyramidal cells. *J Physiol* 539(Pt 1), 67-75.

Tanaka E, Yamamoto S, Kudo Y, Mihara S and Higashi H (1997). Mechanisms underlying the rapid depolarization produced by deprivation of oxygen and glucose in rat hippocampal CA1 neurons in vitro. *J Neurophysiol* 78(2), 891-902.

Tepper JM, Sharpe NA, Koos TZ and Trent F (1998). Postnatal development of the rat neostriatum: electrophysiological, light- and electron-microscopic studies. *Dev Neurosci* 20(2-3), 125-145.

Tepper JM and Trent F (1993). In vivo studies of the postnatal development of rat neostriatal neurons. *Prog Brain Res* 99, 35-50.

Tokimasa T and Akasu T (1990). ATP regulates muscarine-sensitive potassium current in dissociated bull-frog primary afferent neurones. *J Physiol* 426, 241-264.

Tolhurst G, Vial C, Leon C, Gachet C, Evans RJ and Mahaut-Smith MP (2005). Interplay between P2Y(1), P2Y(12), and P2X(1) receptors in the activation of megakaryocyte cation

influx currents by ADP: evidence that the primary megakaryocyte represents a fully functional model of platelet P2 receptor signaling. *Blood* 106(5), 1644-1651.

Tominaga K, Shibata S and Watanabe S (1992). A neuroprotective effect of adenosine A1-receptor agonists on ischemia-induced decrease in 2-deoxyglucose uptake in rat hippocampal slices. *Neurosci Lett* 145(1), 67-70.

Tominaga M, Wada M and Masu M (2001). Potentiation of capsaicin receptor activity by metabotropic ATP receptors as a possible mechanism for ATP-evoked pain and hyperalgesia. *Proc Natl Acad Sci U S A* 98(12), 6951-6956.

Torres GE, Egan TM and Voigt MM (1998a). N-Linked glycosylation is essential for the functional expression of the recombinant P2X2 receptor. *Biochemistry* 37(42), 14845-14851.

Torres GE, Egan TM and Voigt MM (1998b). Topological analysis of the ATP-gated ionotropic [correction of ionotrophic] P2X2 receptor subunit. *FEBS Lett* 425(1), 19-23.

Torres GE, Egan TM and Voigt MM (1999). Hetero-oligomeric assembly of P2X receptor subunits. Specificities exist with regard to possible partners. *J Biol Chem* 274(10), 6653-6659.

Torres M, Pintor J and Miras-Portugal MT (1990). Presence of ectonucleotidases in cultured chromaffin cells: hydrolysis of extracellular adenine nucleotides. *Arch Biochem Biophys* 279(1), 37-44.

Touzani O, Roussel S and MacKenzie ET (2001). The ischaemic penumbra. *Curr Opin Neurol* 14(1), 83-88.

Townsend-Nicholson A, King BF, Wildman SS and Burnstock G (1999). Molecular cloning, functional characterization and possible cooperativity between the murine P2X4 and P2X4a receptors. *Brain Res Mol Brain Res* 64(2), 246-254.

Trincavelli ML, Marroni M, Tuscano D, Ceruti S, Mazzola A, Mitro N, Abbracchio MP and Martini C (2004). Regulation of A2B adenosine receptor functioning by tumour necrosis factor a in human astroglial cells. *J Neurochem* 91(5), 1180-1190.

Trincavelli ML, Tuscano D, Cecchetti P, Falleni A, Benzi L, Klotz KN, Gremigni V, Cattabeni F, Lucacchini A and Martini C (2000). Agonist-induced internalization and recycling of the human A(3) adenosine receptors: role in receptor desensitization and resensitization. *J Neurochem* 75(4), 1493-1501.

Trincavelli ML, Tuscano D, Marroni M, Falleni A, Gremigni V, Ceruti S, Abbracchio MP, Jacobson KA, Cattabeni F and Martini C (2002a). A3 adenosine receptors in human astrocytoma cells: agonist-mediated desensitization, internalization, and down-regulation. *Mol Pharmacol* 62(6), 1373-1384.

Trincavelli ML, Tuscano D, Marroni M, Klotz KN, Lucacchini A and Martini C (2002b). Involvement of mitogen protein kinase cascade in agonist-mediated human A(3) adenosine receptor regulation. *Biochim Biophys Acta* 1591(1-3), 55-62.

Troadec JD, Thirion S, Petturiti D, Bohn MT and Poujeol P (1999). ATP acting on P2Y receptors triggers calcium mobilization in primary cultures of rat neurohypophysial astrocytes (pituicytes). *Pflugers Arch* 437(5), 745-753.

Urbani S, Caporale R, Lombardini L, Bosi A and Saccardi R (2006). Use of CFDA-SE for evaluating the in vitro proliferation pattern of human mesenchymal stem cells. *Cytotherapy* 8(3), 243-253.

Valera S, Hussy N, Evans RJ, Adami N, North RA, Surprenant A and Buell G (1994). A new class of ligand-gated ion channel defined by P2x receptor for extracellular ATP. *Nature* 371(6497), 516-519.

van Calker D, Muller M and Hamprecht B (1979). Adenosine regulates via two different types of receptors, the accumulation of cyclic AMP in cultured brain cells. *J Neurochem* 33(5), 999-1005.

van der Klein PA, Kourounakis AP and IJzerman AP (1999). Allosteric modulation of the adenosine A(1) receptor. Synthesis and biological evaluation of novel 2-amino-3-benzoylthiophenes as allosteric enhancers of agonist binding. *J Med Chem* 42(18), 3629-3635.

van Giezen JJ and Humphries RG (2005). Preclinical and clinical studies with selective reversible direct P2Y12 antagonists. *Semin Thromb Hemost* 31(2), 195-204.

Van Harreveld A (1959). Compounds in brain extracts causing spreading depression of cerebral cortical activity and contraction of crustacean muscle. *J Neurochem* 3(4), 300-315.

Van Harreveld A and SCHADE JP (1959). Chloride movements in cerebral cortex after circulatory arrest and during spreading depression. *J Cell Comp Physiol* 54, 65-84.

Van Harreveld A and Stamm JS (1953). Spreading cortical convulsions and depressions. *J Neurophysiol* 16(4), 352-366.

Varani K, Gessi S, Merighi S, Vincenzi F, Cattabriga E, Benini A, Klotz KN, Baraldi PG, Tabrizi MA, Lennan SM, Leung E and Borea PA (2005). Pharmacological characterization of novel adenosine ligands in recombinant and native human A2B receptors. *Biochem Pharmacol* 70(11), 1601-1612.

Varani K, Portaluppi F, Gessi S, Merighi S, Ongini E, Belardinelli L and Borea PA (2000). Dose and time effects of caffeine intake on human platelet adenosine A(2A) receptors : functional and biochemical aspects. *Circulation* 102(3), 285-289.

Virginio C, MacKenzie A, Rassendren FA, North RA and Surprenant A (1999). Pore dilation of neuronal P2X receptor channels. *Nat Neurosci* 2(4), 315-321.

Virginio C, North RA and Surprenant A (1998). Calcium permeability and block at homomeric and heteromeric P2X2 and P2X3 receptors, and P2X receptors in rat nodose neurones. *J Physiol* 510 (Pt 1)(27-35.

Volonte C and Merlo D (1996). Selected P2 purinoceptor modulators prevent glutamate-evoked cytotoxicity in cultured cerebellar granule neurons. *J Neurosci Res* 45(2), 183-193.

Volpini R, Costanzi S, Lambertucci C, Taffi S, Vittori S, Klotz KN and Cristalli G (2002). N(6)-alkyl-2-alkynyl derivatives of adenosine as potent and selective agonists at the human adenosine A(3) receptor and a starting point for searching A(2B) ligands. *J Med Chem* 45(15), 3271-3279.

Volpini R, Dal Ben D, Lambertucci C, Vittori S, Klotz KN and Cristalli G (2006). Trisubstituted adenosines as potent and selective agonists for the A$_3$ adenosine receptor subtype. 10-9-2006. XXII Congresso Nazionale della Società Chimica Italiana, Florence, Italy, 10-15 september 2006. 10-9-2007. Ref Type: Conference Proceeding.

Volpini R, Lambertucci C, Taffi S, Vttori S, Klotz KN and Cristalli G (2005). A$_3$ adenosine receptors: synthesis and biological evaluation of new potent and selective ligands. 7, 297-300. Collection Symposium Series. Ref Type: Conference Proceeding.

von Kugelgen I (2006). Pharmacological profiles of cloned mammalian P2Y-receptor subtypes. *Pharmacol Ther* 110(3), 415-432.

von Kugelgen I, Koch H and Starke K (1997). P2-receptor-mediated inhibition of serotonin release in the rat brain cortex. *Neuropharmacology* 36(9), 1221-1227.

von Kugelgen I, Spath L and Starke K (1994). Evidence for P2-purinoceptor-mediated inhibition of noradrenaline release in rat brain cortex. *Br J Pharmacol* 113(3), 815-822.

von Lubitz DK (1999). Adenosine and cerebral ischemia: therapeutic future or death of a brave concept? *Eur J Pharmacol* 371(1), 85-102.

von Lubitz DK, Lin RC and Jacobson KA (1995). Cerebral ischemia in gerbils: effects of acute and chronic treatment with adenosine A2A receptor agonist and antagonist. *Eur J Pharmacol* 287(3), 295-302.

von Lubitz DK, Lin RC, Popik P, Carter MF and Jacobson KA (1994). Adenosine A3 receptor stimulation and cerebral ischemia. *Eur J Pharmacol* 263(1-2), 59-67.

von Lubitz DK, Simpson KL and Lin RC (2001). Right thing at a wrong time? Adenosine A3 receptors and cerebroprotection in stroke. *Ann N Y Acad Sci* 939, 85-96.

Vranic II, Matic M, Perunicic J, Simic T, Soskic L and Milic N (2006). Adenosine cardioprotection study in clinical setting of paroxysmal supraventricular tachycardia. *Prostaglandins Leukot Essent Fatty Acids* 74(6), 365-371.

Vulchanova L, Arvidsson U, Riedl M, Wang J, Buell G, Surprenant A, North RA and Elde R (1996). Differential distribution of two ATP-gated channels (P2X receptors) determined by

immunocytochemistry. *Proc Natl Acad Sci U S A* 93(15), 8063-8067.

Vulchanova L, Riedl MS, Shuster SJ, Buell G, Surprenant A, North RA and Elde R (1997). Immunohistochemical study of the P2X2 and P2X3 receptor subunits in rat and monkey sensory neurons and their central terminals. *Neuropharmacology* 36(9), 1229-1242.

Vyskocil F, Kritz N and Bures J (1972). Potassium-selective microelectrodes used for measuring the extracellular brain potassium during spreading depression and anoxic depolarization in rats. *Brain Res* 39(1), 255-259.

Waldo GL, Corbitt J, Boyer JL, Ravi G, Kim HS, Ji XD, Lacy J, Jacobson KA and Harden TK (2002). Quantitation of the P2Y(1) receptor with a high affinity radiolabeled antagonist. *Mol Pharmacol* 62(5), 1249-1257.

Wang CZ, Namba N, Gonoi T, Inagaki N and Seino S (1996). Cloning and pharmacological characterization of a fourth P2X receptor subtype widely expressed in brain and peripheral tissues including various endocrine tissues. *Biochem Biophys Res Commun* 220(1), 196-202.

Wang J, Chambers G, Cottrell JE and Kass IS (2000). Differential fall in ATP accounts for effects of temperature on hypoxic damage in rat hippocampal slices. *J Neurophysiol* 83(6), 3462-3472.

Wang L, Jacobsen SE, Bengtsson A and Erlinge D (2004). P2 receptor mRNA expression profiles in human lymphocytes, monocytes and CD34+ stem and progenitor cells. *BMC Immunol* 5, 16-22.

Wang L, Karlsson L, Moses S, Hultgardh-Nilsson A, Andersson M, Borna C, Gudbjartsson T, Jern S and Erlinge D (2002). P2 receptor expression profiles in human vascular smooth muscle and endothelial cells. *J Cardiovasc Pharmacol* 40(6), 841-853.

Webb TE, Boluyt MO and Barnard EA (1996). Molecular biology of P2Y purinoceptors: expression in rat heart. *J Auton Pharmacol* 16(6), 303-307.

Weiss SM, Benwell K, Cliffe IA, Gillespie RJ, Knight AR, Lerpiniere J, Misra A, Pratt RM, Revell D, Upton R and Dourish CT (2003). Discovery of nonxanthine adenosine A2A receptor antagonists for the treatment of Parkinson's disease. *Neurology* 61(11 Suppl 6), S101-S106.

Weissman TA, Riquelme PA, Ivic L, Flint AC and Kriegstein AR (2004). Calcium waves propagate through radial glial cells and modulate proliferation in the developing neocortex. *Neuron* 43(5), 647-661.

Werner P, Seward EP, Buell GN and North RA (1996). Domains of P2X receptors involved in desensitization. *Proc Natl Acad Sci U S A* 93(26), 15485-15490.

Westfall DP, Stitzel RE and Rowe JN (1978). The postjunctional effects and neural release of purine compounds in the guinea-pig vas deferens. *Eur J Pharmacol* 50(1), 27-38.

White PJ, Rose'Meyer RB and Hope W (1996). Functional characterization of adenosine receptors in the nucleus tractus solitarius mediating hypotensive responses in the rat. *Br J Pharmacol* 117(2), 305-308.

White PJ, Webb TE and Boarder MR (2003). Characterization of a Ca2+ response to both UTP and ATP at human P2Y11 receptors: evidence for agonist-specific signaling. *Mol Pharmacol* 63(6), 1356-1363.

White TD (1978). Release of ATP from a synaptosomal preparation by elevated extracellular K+ and by veratridine. *J Neurochem* 30(2), 329-336.

White TD and Leslie RA (1982). Depolarization-induced release of adenosine 5'-triphosphate from isolated varicosities derived from the myenteric plexus of the guinea pig small intestine. *J Neurosci* 2(2), 206-215.

Wieraszko A (1996). Extracellular ATP as a neurotransmitter: its role in synaptic plasticity in the hippocampus. *Acta Neurobiol Exp (Wars)* 56(2), 637-648.

Wieraszko A and Seyfried TN (1989). ATP-induced synaptic potentiation in hippocampal slices. *Brain Res* 491(2), 356-359.

Wilson CJ (1993). The generation of natural firing patterns in neostriatal neurons. *Prog Brain Res* 99, 277-297.

Wilson CJ and Groves PM (1981). Spontaneous firing patterns of identified spiny neurons in the rat neostriatum. *Brain Res* 220(1), 67-80.

Wirkner K, Gunther A, Weber M, Guzman SJ, Krause T, Fuchs J, Koles L, Norenberg W and Illes P (2006). Modulation of NMDA Receptor Current in Layer V Pyramidal Neurons of the Rat Prefrontal Cortex by P2Y Receptor Activation. *Cereb Cortex*

Wirkner K, Koles L, Thummler S, Luthardt J, Poelchen W, Franke H, Furst S and Illes P (2002). Interaction between P2Y and NMDA receptors in layer V pyramidal neurons of the rat prefrontal cortex. *Neuropharmacology* 42(4), 476-488.

Wu LG and Saggau P (1994). Adenosine inhibits evoked synaptic transmission primarily by reducing presynaptic calcium influx in area CA1 of hippocampus. *Neuron* 12(5), 1139-1148.

Xiang Z, Bo X and Burnstock G (1998). Localization of ATP-gated P2X receptor immunoreactivity in rat sensory and sympathetic ganglia. *Neurosci Lett* 256(2), 105-108.

Xiang Z, Bo X and Burnstock G (1999). P2X receptor immunoreactivity in the rat cochlea, vestibular ganglion and cochlear nucleus. *Hear Res* 128(1-2), 190-196.

Xiang Z and Burnstock G (2005). Distribution of P2Y2 receptors in the guinea pig enteric nervous system and its coexistence with P2X2 and P2X3 receptors, neuropeptide Y, nitric oxide synthase and calretinin. *Histochem Cell Biol* 124(5), 379-390.

Xiang Z and Burnstock G (2006a). Distribution of P2Y(6) and P2Y(12) receptor: their colocalization with calbindin, calretinin and nitric oxide synthase in the guinea pig enteric nervous system. *Histochem Cell Biol* 125(4), 327-336.

Xiang Z, Lv J, Jiang P, Chen C, Jiang B and BURNSTOCK G (2006b). Expression of P2X receptors on immune cells in the rat liver during postnatal development. *Histochem Cell Biol* 126(4), 453-463.

Xu K, Bastia E and Schwarzschild M (2005). Therapeutic potential of adenosine A(2A) receptor antagonists in Parkinson's disease. *Pharmacol Ther* 105(3), 267-310.

Yamamoto C (1975). Recording of electrical activity from microscopically identified neurons of the mammalian brain. *Experientia* 31(3), 309-311.

Yamamoto S, Tanaka E, Shoji Y, Kudo Y, Inokuchi H and Higashi H (1997). Factors that reverse the persistent depolarization produced by deprivation of oxygen and glucose in rat hippocampal CA1 neurons in vitro. *J Neurophysiol* 78(2), 903-911.

Yamazaki Y, Fujii S, Nakamura T, Miyakawa H, Kudo Y, Kato H and Ito K (2002). Changes in [Ca2+](i) during adenosine triphosphate-induced synaptic plasticity in hippocampal CA1 neurons of the guinea pig. *Neurosci Lett* 324(1), 65-68.

Yan L, Bertarelli DC, Hayallah AM, Meyer H, Klotz KN and Muller CE (2006). A new synthesis of sulfonamides by aminolysis of p-nitrophenylsulfonates yielding potent and selective adenosine A2B receptor antagonists. *J Med Chem* 49(14), 4384-4391.

Yawo H and Chuhma N (1993). Preferential inhibition of omega-conotoxin-sensitive presynaptic Ca2+ channels by adenosine autoreceptors. *Nature* 365(6443), 256-258.

Yoshioka K, Hosoda R, Kuroda Y and Nakata H (2002a). Hetero-oligomerization of adenosine A1 receptors with P2Y1 receptors in rat brains. *FEBS Lett* 531(2), 299-303.

Yoshioka K, Saitoh O and Nakata H (2001). Heteromeric association creates a P2Y-like adenosine receptor. *Proc Natl Acad Sci U S A* 98(13), 7617-7622.

Yoshioka K, Saitoh O and Nakata H (2002b). Agonist-promoted heteromeric oligomerization between adenosine A(1) and P2Y(1) receptors in living cells. *FEBS Lett* 523(1-3), 147-151.

Yu L, Huang Z, Mariani J, Wang Y, Moskowitz M and Chen JF (2004). Selective inactivation or reconstitution of adenosine A2A receptors in bone marrow cells reveals their significant contribution to the development of ischemic brain injury. *Nat Med* 10(10), 1081-1087.

Zablocki JA, Wu L, Shryock J and Belardinelli L (2004). Partial A(1) adenosine receptor agonists from a molecular perspective and their potential use as chronic ventricular rate control agents during atrial fibrillation (AF). *Curr Top Med Chem* 4(8), 839-854.

Zampighi GA, Loo DD, Kreman M, Eskandari S and Wright EM (1999). Functional and morphological correlates of connexin50 expressed in Xenopus laevis oocytes. *J Gen Physiol* 113(4), 507-524.

Zemkova H, Balik A, Jiang Y, Kretschmannova K and Stojilkovic SS (2006). Roles of purinergic P2X receptors as pacemaking channels and modulators of calcium-mobilizing pathway in

pituitary gonadotrophs. *Mol Endocrinol* 20(6), 1423-1436.

Zetterstrom T and Fillenz M (1990). Adenosine agonists can both inhibit and enhance in vivo striatal dopamine release. *Eur J Pharmacol* 180(1), 137-143.

Zhang L and Sanderson MJ (2003). Oscillations in ciliary beat frequency and intracellular calcium concentration in rabbit tracheal epithelial cells induced by ATP. *J Physiol* 546(Pt 3), 733-749.

Zhao HB, Yu N and Fleming CR (2005). Gap junctional hemichannel-mediated ATP release and hearing controls in the inner ear. *Proc Natl Acad Sci U S A* 102(51), 18724-18729.

Zhao LR, Duan WM, Reyes M, Keene CD, Verfaillie CM and Low WC (2002). Human bone marrow stem cells exhibit neural phenotypes and ameliorate neurological deficits after grafting into the ischemic brain of rats. *Exp Neurol* 174(1), 11-20.

Zhao Z, Francis CE and Ravid K (1997). An A3-subtype adenosine receptor is highly expressed in rat vascular smooth muscle cells: its role in attenuating adenosine-induced increase in cAMP. *Microvasc Res* 54(3), 243-252.

Zhou AM, Li WB, Li QJ, Liu HQ, Feng RF and Zhao HG (2004). A short cerebral ischemic preconditioning up-regulates adenosine receptors in the hippocampal CA1 region of rats. *Neurosci Res* 48(4), 397-404.

Zhou QY, Li C, Olah ME, Johnson RA, Stiles GL and Civelli O (1992). Molecular cloning and characterization of an adenosine receptor: the A3 adenosine receptor. *Proc Natl Acad Sci U S A* 89(16), 7432-7436.

Zimmermann H (1986). Hydrolysis of ATP and formation of adenosine at the surface of cholinergic nerve endings. *Cellular biology of ectoenzymes*. Ref Type: Book Chapter.

Zimmermann H (1996). Biochemistry, localization and functional roles of ecto-nucleotidases in the nervous system. *Prog Neurobiol* 49(6), 589-618.

Zimmermann H (2000). Extracellular metabolism of ATP and other nucleotides. *Naunyn Schmiedebergs Arch Pharmacol* 362(4-5), 299-309.

Zimmermann H, Braun N, Kegel B and Heine P (1998). New insights into molecular structure and function of ectonucleotidases in the nervous system. *Neurochem Int* 32(5-6), 421-425.

Zimmermann H and Denston CR (1976). Adenosine triphosphate in cholinergic vesicles isolated from the electric organ of Electrophorus electricus. *Brain Res* 111(2), 365-376.

Zimmermann H. (2006). Nucleotide signaling in nervous system development. *Pflugers Arch.* 452(5), 573-588.

Zizzo MG, Mule F and Serio R (2006). Mechanisms underlying hyperpolarization evoked by P2Y receptor activation in mouse distal colon. *Eur J Pharmacol* 544(1-3), 174-180.

Zona C, Marchetti C, Volonte C, Mercuri NB and Bernardi G (2000). Effect of P2 purinoceptor antagonists on kainate-induced currents in rat cultured neurons. *Brain Res* 882(1-2), 26-35.

Zuker CS (1996). The biology of vision of Drosophila. *Proc Natl Acad Sci U S A* 93(2), 571-576.

PREMIO FIRENZE UNIVERSITY PRESS
TESI DI DOTTORATO

Coppi E., *Purines as Transmitter Molecules. Electrophysiological Studies on Purinergic Signalling in Different Cell Systems*, 2007

Natali I., *The Ur-Portrait.* Stephen Hero *ed il processo di creazione artistica in* A Portrait of the Artist as a Young Man, 2007

Petretto L., *Imprenditore ed Università nello start-up di impresa. Ruoli e relazioni critiche*, 2007

Mannini M., *Molecular Magnetic Materials on Solid Surfaces*, 2007

Bracardi M., *La Materia e lo Spirito. Mario Ridolfi nel paesaggio umbro*, 2007